Durham E-Theses

Computer simulations of cosmic ray extensive air showers

Dixon, M. E.

How to cite:

Dixon, M. E. (1974) *Computer simulations of cosmic ray extensive air showers*, Durham theses, Durham University. Available at Durham E-Theses Online: http://etheses.dur.ac.uk/8169/

Use policy

COMPUTER SIMULATIONS

OF

COSMIC RAY EXTENSIVE AIR SHOWERS

by

H.E. Dixon, B.Sc.

A thesis submitted to the University of

Durham in accordance with the regulations

for admittance to the degree of

Doctor of Philosophy

Department of Physics   July 1974.
University of Durham

C O N T E N T S

CHAPTER FIVE: Fragmentation of Primary Heavy Nuclei

CHAPTER SIX: Fluctuations in Shower Development

A B S T R A C T

This thesis describes the results of computer simulations of cosmic ray extensive air showers with primary energy in the range $10^{14} - 10^{19}$ eV.

A brief review of simulations made by other authors is presented after which models for high energy nuclear interactions are discussed. The parameters choosen for the preferred model employed here are stated and some more recent data from accelerator experiments are mentioned.

The predictions from the preferred model for proton initiated air showers are compared with experimental data and the results of previous simulations; the consequences of including trends seen from recent accelerator experiments in the model for interactions are also discussed.

The break-up of energetic particles with atomic mass number as high as 56 as they traverse the atmosphere is discussed and a model to reconstruct this process at cosmic ray energies is described. The predictions from the preferred model for interactions assuming iron primary particles are given. It is concluded that a study of the average shower characteristics will not lead to a reliable determination of the mass composition of the primary radiation.

Predictions for the fluctuations of measurable parameters in air showers are presented; it is shown that on the basis of these studies it is likely that comment may be made upon the primary composition.

The results of these simulations are particularly relevant to the Haverah Park Extensive Air Shower Array; the improvements to

the array presently being implemented should, according to the present results, enable an estimation of the primary composition at energies $\geqslant 10^{17}$eV to be made. In particular the presence or otherwise of protons in the primary beam should be estimated.

The feasibility of the cluster analysis of experimental data is investigated and it is shown on the basis of the clustering of simulation data that to a limited extent the separation of air showers into groups according to the atomic mass number of the primary particle is possible.

C H A P T E R   O N E

INTRODUCTION

1-1   The Cosmic Radiation

The first suggestion that there existed a form of radiation
of extra-terrestrial origin came in 1900. C.T.R. Wilson, the
originator of the Wilson Cloud Chamber,and also Elster and Geitel
noticed that a carefully insulated gold leaf electroscope lost its
charge even when the greatest care was taken with its insulation
(Wilson(1901)). This was deduced to be due to some form of radiation
which ionized the gas in the electroscope and resulted in its discharge.
For some time it was thought that this radiation could be of terrestrial
origin (eg. from the natural radioactivity of the earth's rocks) but a
series of balloon flights by Hess (1912) and Kolhorster (1914) proved
that the radiation was extra terrestrial since the intensity increased
to ten times the value at sea level at a height of 9200m. Since this
early work the investigation of the cosmic radiation has lead to
many major discoveries in physics. For example the positron was
discovered in 1932 by Anderson and later the μ-meson and π-meson
were discovered.

The amount of effort that has been expended over the years on
detailed improvements in measurements of the arrival direction,
energy spectra and composition of primary cosmic radiation may at first
glance seem surprising. However, the radiation is so complex that
the details potentially contain much information.

The radiation provides a powerful tool for gathering experimental
evidence relevant to the fields of astrophysics and cosmology and of
particle physics. Energetic cosmic rays provide us with a direct
sample of matter originating outside our solar system. They bring

with them information on their source regions (the state of matter and
acceleration mechanisms) and also on the radiation and matter which
they have traversed. The particles of greatest potential interest are
those of very high energy ($> 10^{18}$eV) which may be extragalactic in
origin.

The integral energy spectrum up to the energy of $\sim 10^{20}$eV/nucleus
is now relatively well known; it can be represented by a simple
power law. In the energy range 10^{11}-10^{15}eV the exponent of the power
law is 1.6 to 1.7 (eg.Grigorov et al.(1971)). Above this energy the
exponent increases to ~ 2.1 (Edge (1974)) and continues with this
slope to energies in excess of 10^{19}eV.

The distribution in atomic mass number of the high energy
primary cosmic radiation is still unknown and this thesis is primarily
concerned with the determination of this aspect of the radiation.

1-2 Extensive Air Showers

At primary energies $> 10^{14}$eV the direct observation of cosmic
radiation is made impossible by the small   flux : of particles
falling (for example, at energies greater than 10^{16}eV the flux of
primary cosmic ray particles falls to less than a particle $m^{-2}yr^{-1}$).
For tunately a study can be made of these high energy primary
particles by indirect methods.

When a primary cosmic ray reaches the top of the earth's atmosphere
it is presented with ~ 1030 g.cm.$^{-2}$ of material through which it must
pass before reaching sea level. (We will for simplicity consider
sea level to be the observational level). Since the interaction
length for protons with air nuclei is ~ 80 g cm^{-2} (and the corresponding
quantity is shorter for heavier particles) the primary particle will
undergo many collisions with air nuclei as it traverses the atmosphere

which will result in laterally extensive cascades of secondary particles observable at sea level. This phenomenon is known as an 'extensive air shower' (EAS).

The primary nucleon of an EAS (we will consider here a nucleon initiated EAS although, as we shall consider later, the primary particles could be heavier) interacts with an air nucleus and produces many secondary particles most of which are pions. The incident nucleon proceeds through the atmosphere to its next interaction with about half of its initial energy. The charged pions that were created in the nucleon interaction either interact catastrophically with air nuclei to produce more pions (the interaction mean free path of such interactions being ~ 120 g cm^{-2}) or decay to muons ($\pi^{\pm} \rightarrow \mu^{\pm} + \nu$) with a lifetime of 2.6×10^{-8}s. Once muons are created they either survive until they reach the level of observation or they decay to electrons or positrons. The transverse momentum with which the pions are produced causes the cascade of particles to spread laterally. The neutral pions produced in interactions decay almost instantaneously to two gamma rays ($\tau \sim 10^{-16}$s) which in turn produce electron positron pairs. These particles radiate by bremsstrahlung to produce more photons and thus the electron-photon cascade is formed. The electron-photon cascade grows by superposition of many individual cascades with energy being continually fed from the nuclear component.

1-3 Primary Composition

Very little is known about the mass composition of the primary cosmic radiation above energies of a few hundred GeV. At low energies the composition has been investigated directly using emulsion stacks flown in balloons and the information that can be extracted from these

TABLE 1-1

Energy	Total Number of events	Percentage of protons (and neutrons)	Percentage of α-particles	Percentage of heavier particles	Reference
$>3.7 \times 10^{11}$eV	46	80%	13%	7%	Malhotra et al (1966)
$>10^{12}$eV	112	46%	16%	38%	McCusker (1967)

experiments is shown in Table 1-1. There have been isolated cases of identified interactions of high energy being reported - a proton of 2×10^{14} eV, an oxygen nucleus of 2×10^{14} eV and a calcium nucleus of $\sim 4 \times 10^{14}$ eV. Therefore direct observations with nuclear emulsion stacks confirm that heavy nuclei are present up to energies of the order of 4×10^{14} eV, although the relative abundances remain undetermined.

The results from the Proton Satellite experiment (Grigorov et al. (1971)) indicate that while the 'all particle' energy spectrum continues with a slope of 1.6 up to 10^{15} eV, the spectrum for protons alone suddenly steepens at 10^{12} eV. This implies that there is an increasing proportion of heavy primary particles in the energy range $10^{12} - 10^{15}$ eV. However, this steepening of the proton spectrum at 10^{12} eV is not supported by the results of the balloon experiments of Ryan et al. (1971).

The chemical composition of the primaries in the air shower region of the energy spectrum is still unknown. In the forseeable future it seems unlikely that much detail will become available on the exact mass composition of the primary cosmic radiation at energies $>10^{16}$ eV/nucleus but it may well be possible to determine the proportion of protons (if any) present at these energies. A review of the data available on primary composition in the energy range $10^{10} - 10^{19}$ eV together with the interpretations with which they were presented has been made by Sreekantan (1972), and the result is inconclusive. As an example of the confusion that exists on this subject we will consider two of the experiments included in this review. The Sydney group (McCusker et al.(1969)) have made investigations of the proportion of 'multiple core' events as a function of energy using the matrix of 64 scintillators located in the centre of their EAS array.

They compared their observations with model calculations for various primary masses and concluded that the primary cosmic ray beam has a mixed chemical composition at energies around 10^{15}eV which becomes progressively richer in heavy nuclei up to 10^{17}eV where the ratio of multiple core to single core events is greater.

The Kiel results (Samorski et al.(1969), (1971)) are in direct conflict with the Sydney results. Samorski et al. interpret their results as meaning that the primary cosmic ray beam at energies $3 \times 10^{15}-10^{16}$eV has either a pure proton or a mixed composition but not all heavy primaries.

The confusion existing on this subject underlines the importance of making a reliable estimate of the mass composition in the energy range $10^{17}-10^{18}$eV which is covered by the Haverah Park EAS array (see §1-5).

1-4 Computer simulation of EAS

In order to interpret the observations of EAS made by air shower arrays it is necessary to construct a model describing as far as possible the development of the cascade of secondary particles through the atmosphere. This task is complicated by the fact that no information regarding proton-nucleus or nucleus-nucleus interactions is available at the energies under consideration. It is therefore necessary to make extrapolations to air showers energies from information gained from accelerator experiments ($\leftarrow$ 1500 GeV). Even at these energies the information available concerns proton-proton interactions and it is necessary to make assumptions in order to make the information relevant to proton-nucleus interactions.

In order to calculate the hadronic and muonic components of air showers values must be assigned to the following parameters:

(i)   the interaction mean free path of protons

(ii) the interaction mean free path of pions

(iii) the inelasticity of protons and of pions in interactions with

        air nuclei,

(iv) the multiplicity, momentum distribution, and composition of

        particles produced in proton-nucleus and pion-nucleus

        interactions,

(v)   the decay time of pions and muons.

The values of (v) are well known; however, the remaining information

required is not available at air shower energies and must be obtained

by extrapolation from accelerator energies.

The processes contributing to the electron-photon cascade are well

understood and a number of solutions have been made to the diffusion

equations of the problem, (Snyder (1949)). The interactions involved

are pair production, bremsstralung, Compton effect and ionization loss;

the last two of these are usually neglected for solutions of the

diffusion equations which are valid only for high energy electrons

and photons (Rossi (1965)). With the advent of powerful computers

it has been possible to use Monte Carlo techniques to follow each

particle in the three dimensional electron-photon cascade resulting

from a low energy electron or photon ($\lesssim 100$ GeV) and results from this

type of calculation are often combined with the analytical solutions

for the high energy particles (as in the case of the present work).

The possibility that the primary particle may not necessarily

be a proton adds an additional complication to the construction of a

simulation model. One must adopt a model for the way in which heavy

nuclei interact with air-nuclei. The model chosen for the present work

is described in Chapter 5.

The responses of the detectors to the particles passing through them must be known and included in the model.

The completed simulation model must produce predictions which are consistent with experimental observations. For instance, the ratio of muons to electrons at particular distances from the shower core and the shape of the muon lateral distribution must agree with experiment.

Having tested the model for inconsistences with experimental data it may then be used to make predictions about the primary mass and energy of particles recorded by the array.

Another use for EAS simulations could be in the determination of the parameters of high energy interactions which cannot be studied directly. This possibility has been investigated as a part of the present work.

1-5 The Haverah Park Array

The Haverah Park Extensive Air Shower Array, as it was at the commencement of this work, consisted of 32 deep water Cerenkov detectors arranged as shown in Fig. 1-1 over an area of approximately 12 km^2. This array developed from the original array described by Tennant (1967). Each detector consists of a number of galvanised steel tanks filled to a depth of 1.2m with water and covering an area 2.25 m^2. The tanks are lined with a white plastic material (Darvic) and filled with clear water. The relativistic particles comprising the air shower produce Cerenkov light as they pass through the water. This light is diffused by the Darvic lining of the tank and a small proportion (0.05%) of the diffused radiation is detected by a photomultiplier which dips into the water at the top of the tank. For each detector the responses from the individual tanks are added together and the resulting pulse is sent to the array recording and

The Haverah Park EAS Array

Fig.1·1
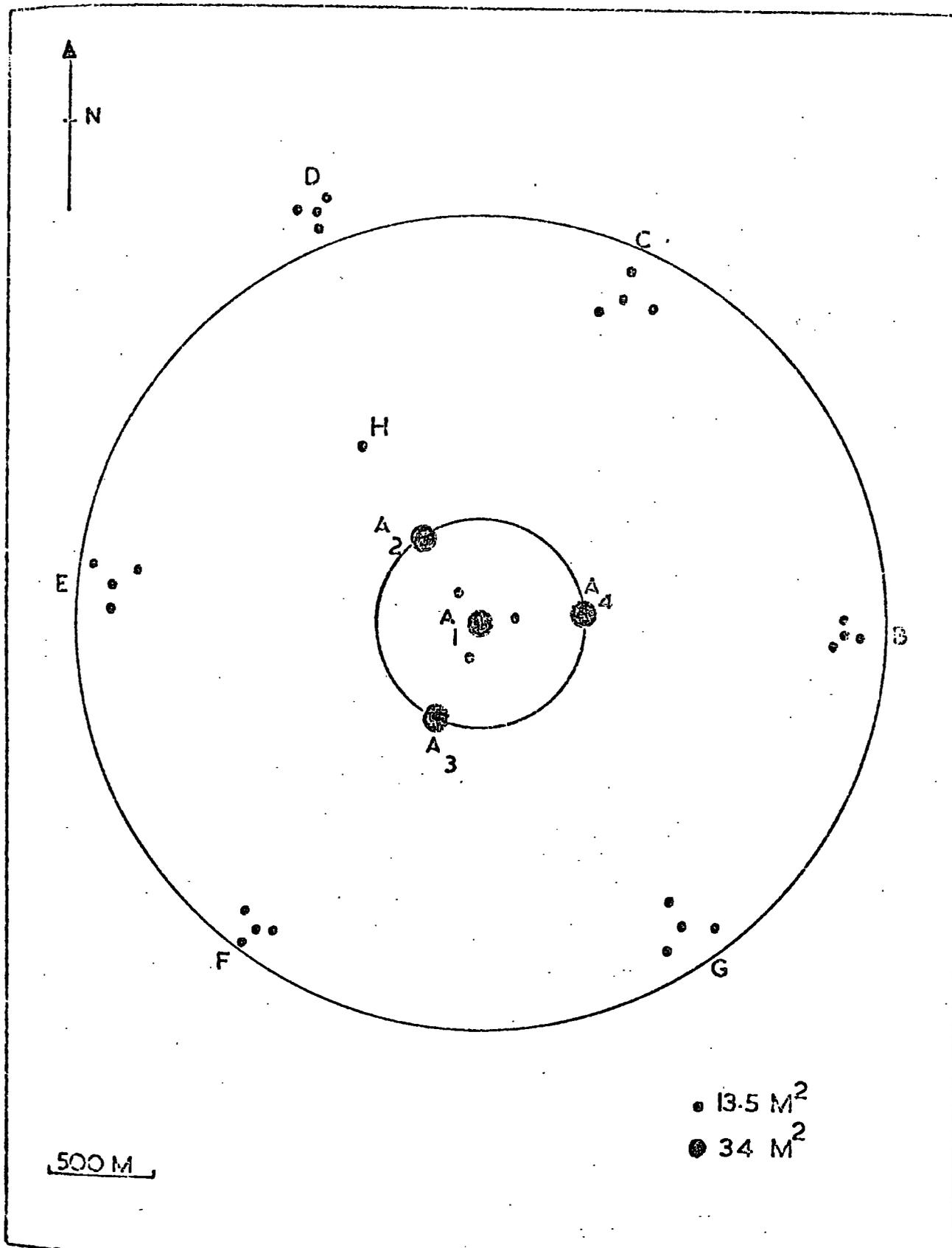
coincidence detecting system. The response of the tanks to air

showers has been described previously (Turver (1963), Hollows (1968)).

The Cerenkov tanks are calibrated in terms of vertically incident

relativistic muons ($\dot{v} \cdot e \cdot \mu$) ie. the energy deposited by one relativistic

vertical muon passing through the tank.

1-6   The Present Work

The main purposes of the present work are twofold:

(i)   to aid the design of improvements for the Haverah Park Air

shower array with the aim of increasing its sensitivity

to the nature of the primary particles of showers:

(ii)   to consider the feasability of using EAS for the determination

of parameters in high energy nucleon-nucleus interactions.

The work also provides predictions for a very broad range of

EAS parameters which are relevant to other EAS detecting arrays as

well as to the Haverah Park array.

Chapter 2 provides a historical review of the air shower

simulation studies which have been made to the present time.

Chapter 3 summarises the various models for high energy

interactions and a data survey of parameters involved in these

interactions is presented with the aim of justifying the choice

of values used in the 'normal' model. More recent data are also

given here as an indication of changes that might be included in

the model for interactions.

The results of the 'normal' model for proton initiated air

showers are presented in Chapter 4 and comparison is made with

experimental data and the results of other simulations. Also

included in this chapter are the results of changes in the model

for nuclear interactions. Comment is made upon the likely validity

of the models used.

Chapter 5 describes the model adopted for the fragmentation of heavy primary nuclei as they traverse the atmosphere. This is considered by the author to be a more realistic approach than has previously been used in simulation studies.

The fluctuations in shower parameters are described in Chapter 6 and, on the grounds of these results, suggestions are made as to which parameters will be useful in the measurement of both primary mass andprimary energy.

Chapter 7 reviews the modifications presently being implemented at Haverah Park and considers the feasability of the use of cluster analysis for the classification of experimental data in categories typical of primary particles of different mass number.

CHAPTER TWO-

A REVIEW OF PREVIOUS AIR SHOWER SIMULATIONS

2-1 Introduction

Later in this thesis the results of the simulations of EAS made by other authors will be compared with those from the present work. It is useful therefore to summarise the development of the work in this field.

The detail and refinement of the air shower simulations used at present to interpret the experimental results from the EAS arrays are possible only as a result of the increases in computing facilities in recent years. The earliest simulations (pre-1956) were confined to following the most energetic particles produced in relatively low energy showers. These simulations frequently involved a solution of the diffusion equations and gave a reasonable estimate of the populous electron-photon cascade together with predictions for the energetic pions and muons. No information was available from these models concerning the many low energy pions and muons.

The advent of more powerful computers in the mid-1960s lead many physicists to apply the Monte-Carlo technique to predict the detailed development of EAS. Each particle was followed from its point of creation until it disappeared (eg. a pion might decay to a muon or interact with an air nucleus). This method can now be used to simulate fully EAS initiated by primary particles with energy greater than 10^{15} eV.

The so called 'step-by-step' procedure, which enables predictions to be made about the average characteristics of, for example, low energy muons in large showers was developed independently by Dedenko (1966) and Hillas (1966). In this

procedure the average distribution in energy and depth of production in the atmosphere of all pions are obtained from numerical evaluations of the appropriate analytical formulae.

There have also been developments using the Monte-Carlo technique combined with an analytical approach which have enabled realistic values for the fluctuations of EAS initiated by primaries with energies up to 10^{19}eV to be predicted. This is one of the approaches used in the present simulations.

2-2 A Survey of Earlier Simulations

The earliest work that will be considered here is that of Oda (1956) who produced results based upon two interaction models. The first model assumed Fermi's theory of meson production was applicable (Fermi (1951)) and the second employed a Landau-type theory of meson production (Landau (1953)) in which there is a stronger concentration of emitted energy in the forward direction. The results produced by both models were in agreement with the data for energetic muons of Barrett et al (1952). Ueda and Ogita (1957), following suggestions by Rozental (1952), produced a one-dimensional treatment and predicted pion and muon numbers in excess of two different energy thresholds at two observational levels in EAS initiated by primaries in the energy range 10^4 - 10^6 GeV. This model was extended by Fukuda, Ueda and Ogita (1957) who made it three-dimensional and introduced the concept of the 'forward and backward cones' in the spatial distribution of produced pions.

The 'step-by-step' method of simulating air showers was introduced independently by Dedenko (1966) and Hillas (1966). This model differed from the method used until that date - often known as the successive generation method - in that the diffusion equation was simplified and as a result the number of low energy muons and

pions in the showers could be calculated. This simplification is described in detail by Dedenko (1966). Hillas constructed a model based upon data from accelerator experiments which was similar in many aspects to the representation of data on proton-light-nuclei interactions suggested by Cocconi, Koester and Perkins (1961). This is referred to as the CKP model which has subsequently been used in many models. This work allowed the prediction of the lateral distributions of muons with energy as low as 300 MeV in the range of core distance 20-2000 m in showers with primary energy up to 10^{17} eV. Hillas considered the problem of the heights of production of muons in air showers in order to find the relative importance of muons produced at particular heights for the densities predicted at various lateral distances.

In the same year Cowsik (1966) produced a one dimensional diffusion equation model which incorporated the production of iso-bars (following suggestions by Pal and Peters (1962)) and copious nucleon-antinucleon production in the nucleon interactions. The model used a multiplicity law for the numbers of both pions and nucleons produced which increased as the square root of the radiated energy. The calculations were carried out for primary energies in the range $10^4 - 10^7$ GeV. In an attempt to identify a satisfactory representation of energetic interactions Lal (1966) carried out simulations using a semi-Monte Carlo method in one dimension only. This model incorporated nine variations of the values for the coefficient of inelasticity and multiplicity of produced particles, all based on the CKP model.

Comprehensive simulations were made by de Beer et al. (1966) for showers with electron size at sea level of 10^6 particles (this corresponds to an energy for a primary proton of $\sim 8 \times 10^{15}$ eV).

The aim of the work was to throw light on the primary particle mass composition and to examine those characteristics of high energy collisions which are not accessible to scrutiny by other means. The model was used to make predictions for the characteristics of heavy primary nucleus initiated EAS as well as for proton initiated showers. In order to do this, what has come to be termed the 'super-position' model for the break-up of heavy nuclei was used. This model implies that the observations resulting from an air shower initiated by a primary of atomic mass number A and energy E_p will be equivalent to the sum of A showers each initiated by a proton of energy (E_p/A). de Beer et al studied three models for nuclear interactions in detail. Two of those used a relation for the multiplicity of pions produced which increased as the quarter root of the radiated energy, E_r, and the third had a law which was proportional to $E_r^{\frac{1}{4}}$ until E_r reached 2.10^3 GeV and increased as $E_r^{\frac{1}{2}}$ for higher energies. Fluctuations to be expected in shower parameters were considered by these authors and estimates were made of the expected fluctuations if the following three spectra of mass of primaries were used:-

(a) All primaries were protons.

(b) There was a constant composition throughout the energy range considered which was consistent with that found at 10^{12}eV.

(c) There was variable composition with an enhanced contribution from heavy nuclei above 10^{15}eV and re-appearance of protons from assumed extra galactic sources above 10^{17}eV.

The predictions of this model were subsequently used in studies aimed at deriving the mean transverse momentum of pions

produced in high energy interactions (de Beer et al.(1968)) and in
many other applications up to the present date.

In 1967 Bradt and Rappaport produced a complete three-dimensional
Monte-Carlo model which followed each particle produced either to sea
level or until it disappeared. Predictions were made for two levels
of observation, 530 g cm^{-2} (corresponding to the depth of the
Mt. Chacaltaya experiment) and 970 g cm^{-2}. A very clear and
detailed description of this type of model is given by these authors.
The simulations were carried out in the range of primary energy, E_p,
of 10^{14}-10^{16}eV but the predictions were limited to characteristics
of nucleons, pions and muons with energy greater than $(E_p \times 10^{-4})$.
Three models were used to represent the nuclear interactions, one was
a two centre model, one an isobar model and one a passive baryon
model. An attempt at solving the problem of accurate predictions
for heavy primary nucleus initiated EAS was made during the study.
As a result of studying emulsion data the authors decided that the
'super-position' model did not realistically describe the break-up
of a heavy nucleus as it traversed the atmosphere and instead they
opted for a 'partial fragmentation model'. They allowed between
30% and 50% of the mass of the primary to be detached in the form
of alpha particles when the heavy nucleus interacted with an air
nucleus. The alpha particles went on to interact with air nuclei
releasing all four constituent nucleons. The 'sub-heavy' (that
portion of the heavy primary particle which remained bound) was
then treated as the primary nucleus had been. The mean free paths
used were those found from emulsion data. One short coming of this
model for the break-up of heavy nuclei was the fact that no pions
were produced during the fragmentation of either the primary
nucleus, its fragments, or the alpha particles; pions were produced

only when individual nucleons interacted with air nuclei.

Murthy et al, (1968) produced a semi Monte Carlo model for proton and heavy primary initiated EAS - again using the 'super-position' model for the latter. Eight different interaction models were used and, as a result of comparing the results of these models with experimental data, it was concluded that nucleon-anti--nucleon production was necessary in order to make shower absorption lengths agree with those found experimentally.

The prediction of the characteristics of the smaller EAS has been of great interest in recent years. Castagnoli (1969) produced a three dimensional model, incorporating the production of isobars, with the aim of explaining data for the muon lateral distribution in small showers at sea level and then applying the model to studies of multiple penetrating particles underground. Suschenko and Fomin (1968) concerned themselves with interpreting data from smaller air showers for which they used a three-dimensional Monte-Carlo model. They produced predictions for four observation levels (20^0, 500, 70^0 and 1030 g cm^{-2}). Greider ((1970, 1971)) has developed a very refined model which contains structure in the description of the nuclear reactions. Theilheim and Beiersdorf (1970) produced a three-dimensional Monte-Carlo calculation based upon a CKP model for interactions and used it to study the nuclear active component in proton and heavy nucleus induced showers in the energy range 10^{12} - 10^{15}eV. They used a model similar to that of Bradt and Rappaport to describe the fragmentation of the heavy primary nuclei.

In recent years calculations have been made (eg by Hillas ((1970), (1972)) which are aimed at predicting the response of a specific type of particle detector to an EAS of prescribed primary

energy falling with its core at a known distance. For example, Hillas has calculated the responses at various core distances of the 120 cm deep water Cerenkov detectors used in the Haverah Park experiment and for the plastic scintillation counters (thickness 8 g cm^{-2}) used in the Volcano Ranch experiment. Using a range of interaction models (labelled A→K) he predicted the deep water Cerenkov detector responses to EAS of energies up to 10^{20}eV with cores falling at distances between 100 - 1300m from the detectors. These calculations showed that at the Haverah Park array, in the region of core distances around 400-500m, the detector response was particularly insensitive to the choice of either the model for interactions or the mass of the primary. Marsden (1971) described in detail the results of calculations based on one of the models used by Hillas (Model A) and he considered the detailed temporal and spatial development of the electron photon cascade. Model E used by Hillas is the most similar to the model taken as the 'normal' model in the calculations to be discussed later in this thesis. This interaction model differs from the 'normal' model only in that the coefficient of inelasticity is assumed to be 0.44 and the mean free path for pion interactions as 100 g cm^{-2} (compared with 0.5 and 120 g cm^{-2} in the 'normal' model).

Capdevielle et al. (1970) made simulations of large EAS using the step-by-step method. Their calculations covered a range of energies between 10^{16} and 10^{20} eV. The three parameters that were varied in their interaction model were the multiplicity of produced pions, the inelasticity assumed for p-N collisions, K, and the mean free path of the nucleon, λ_p. The relation governing the multiplicity of produced pions considered were of the forms $n_s = BE_o^{\frac{1}{4}}$ and $n_s = B \log E_o$ where the value of B was changed

with different combinations of K and λ_p. The production of nucleon-anti-nucleon pairs was also taken into account for some combinations of these variables. These authors also considered EAS produced by heavy nuclei using a 'superposition' model but taking into account the mean free path of heavy particles.

2-3 Results Obtained in Previous Simulation Studies

2-3.1 The Electron Component

The electron component of EAS was one of the earliest features to be studied experimentally. The growth and decay of the electron shower through the atmosphere can give a good indication, when combined with other observations, of the primary energy of the EAS.

The two main methods of calculating the electron shower, given the production spectrum for neutral pions through the atmosphere are:-

(i) a solution of the diffusion equations for the electron photon cascade under certain simplifying assumptions. Only brems-strahlung, pair production and ionization loss are considered; the Compton effect is ignored. This treatment is known as Approximation B (Snyder and Serber (1938)) and produces the number of electrons effectively above zero energy produced by initial Y-rays; and

(ii) a solution of the diffusion equations for the electron photon cascade leaving out the ionization loss as well as the Compton effect, (Rossi (1965)). This is known as Approximation A and reliably predicts the number of high energy photons and electrons which may then be combined with the results of rigorous Monte-Carlo calculations (eg those of Messel and Crawford (1969)) for the lower energy particles.

Both of these methods have been used in the present calculations and they are described fully in Appendix 3. Fig. 2.1 shows the one-dimensional longitudinal development of the electron cascade for showers initiated by protons of energy 10^8 GeV according to Hillas (1972).

Many authors have considered the dependence of electron shower size at sea level and the depth of maximum development of the electron cascade upon the primary energy. Fig. 2.2 gives a comparison of the results of various authors and it can be seen that there is satisfactory agreement between the data from most studies; many of the small differences occur because of minor differences in the assumed interaction models.

2-3.2 The Muon Component

The total muon energy spectrum produced by EAS at a particular observation level is a parameter which is not easily measured unless very many detectors of considerable area are used. However, several of the calculations that have been mentioned in this chapter produce predictions for the muon energy spectrum at sea level for particular primary energies. Fig. 4-5 shows a comparison of the predictions for this parameter from various studies; also shown are the experimental data summarized by Gaisser and Maurer (1972). The lateral distribution of muons above particular threshold energies is a more readily measured quantity (eg for the Haverah Park experiment both the Durham Spectrograph (Dixon et al.(1973(a)) and the Nottingham muon detectors (Armitage (1973)) can measure this quantity) Fig. 2.3 compares the lateral distributions of muons derived from some simulations with the experimental data of Armitage. The results shown in this figure from the present work have been calculated with the inclusion of geomagnetic and Coulomb scattering.
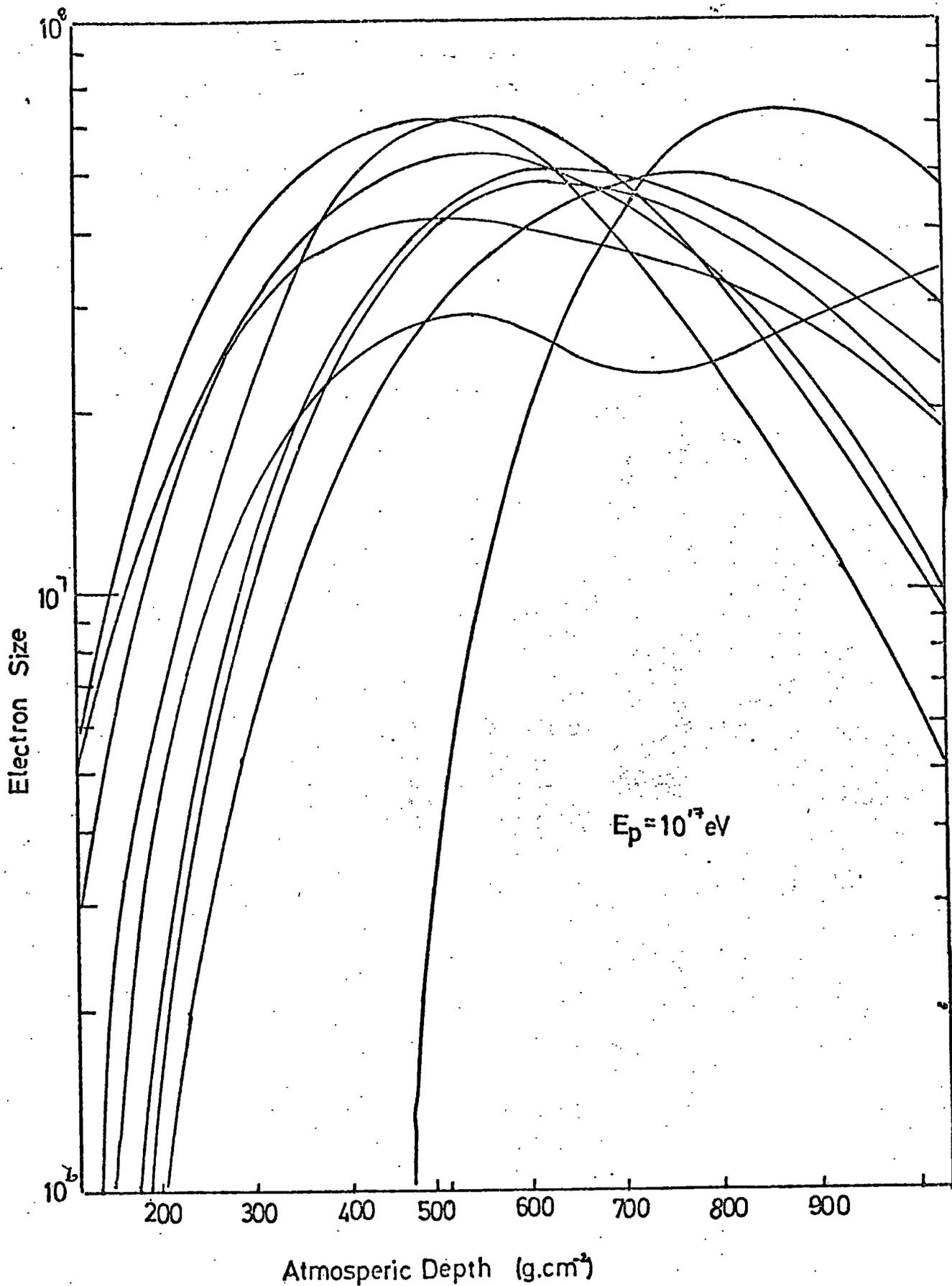
Figure 2-1

Longitudinal development of the electron cascades from 10^{17}eV proton initiated EAS.
(After Hillas (1972)).
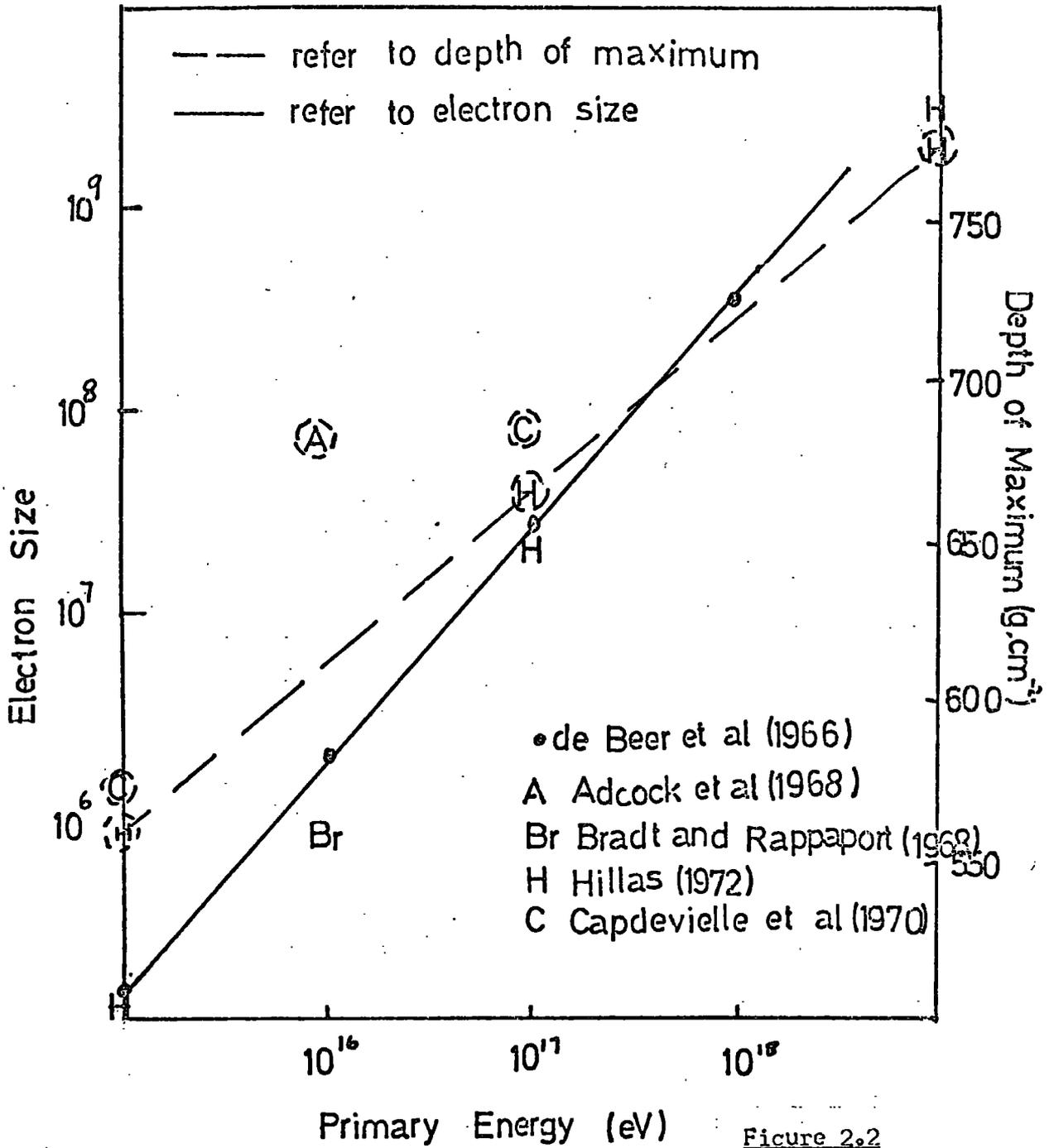
Figure 2.2

The variation of depth of maximum and electron size for proton initiated EAS with primary energy.
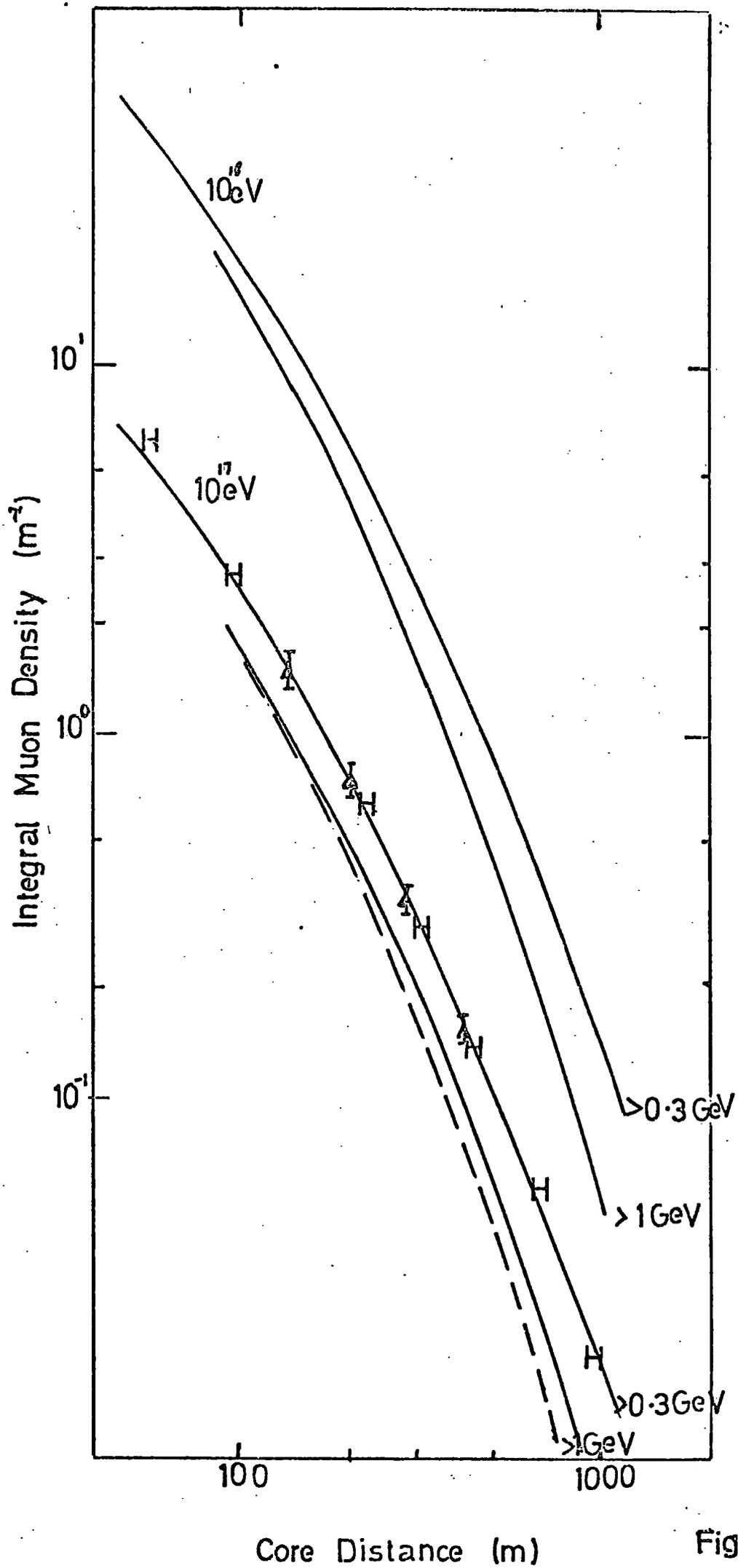
Fig. 2·3

2-3.3 The Nuclear Active Component

Fig. 2.4 shows a comparison of the pion spectra at sea level produced by proton primaries of energy 10^6 GeV from several calculations. It can be seen that there are wide differences in the results and the comparison with experimental data (eg Tanahashi (1970)) indicates that there is good agreement achieved by one of Grieders model (Grieder (1970); the model refered to is the IDFB which is basically a double fire ball model with a leading pion (isobar) produced).

2-4 Summary

The aim of this chapter has been to give a broad indication of the evolution of the techniques of extensive air shower simulation. The comparisons which have been made are brief because it is intended to compare those aspects which are appropriate to the present study in detail in later chapters. Table 2-1 gives a summary of the characteristics of many of the models surveyed in this section together with the main points of interest concerning each model.
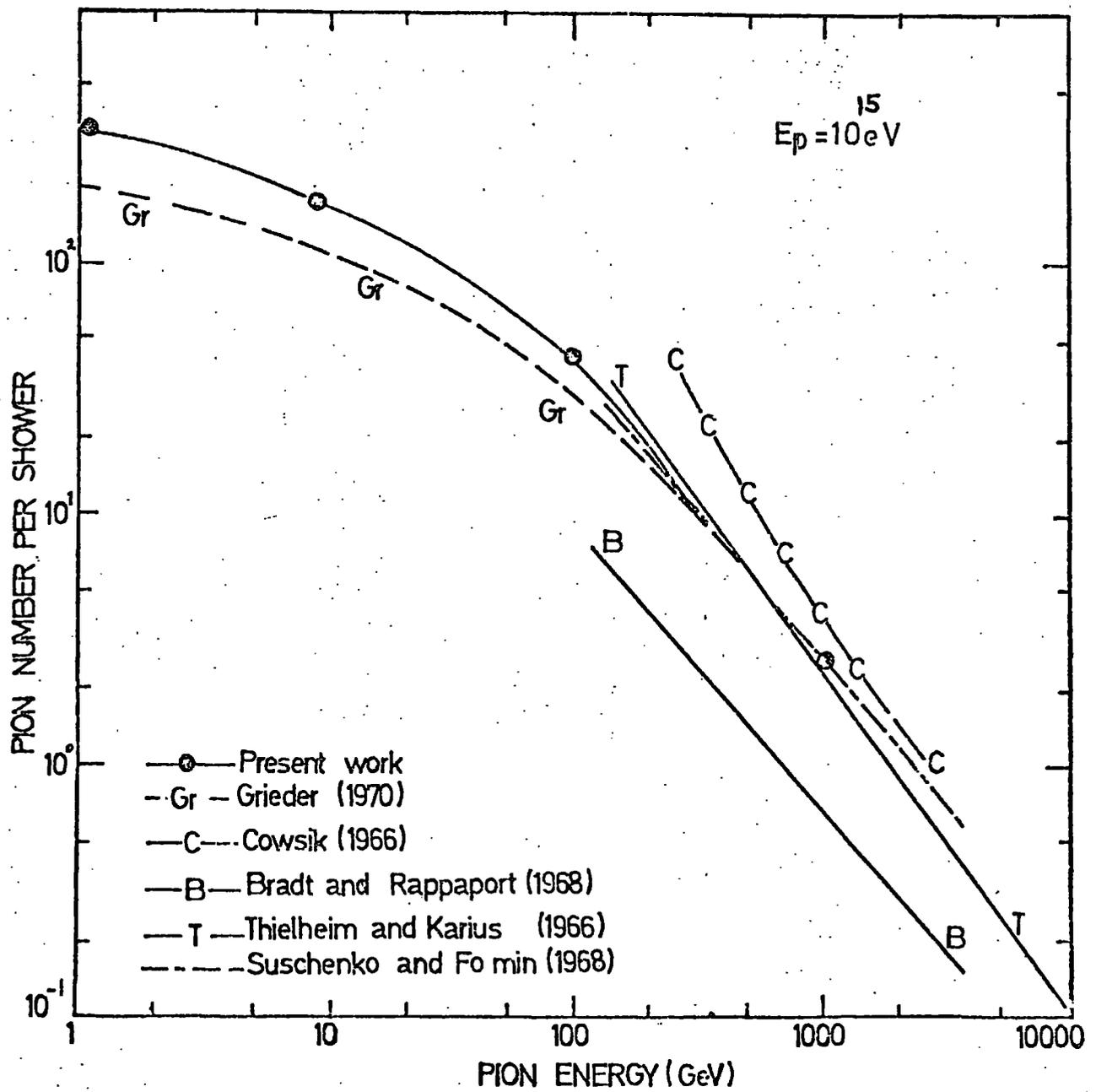
Figure 2.4

Integral Pion Energy Spectra

TABLE 2.1

Author(s)	Scope of Simulations	Model for Interactions				Comments
		Multiplicity Law	Mean Free Path of Protons λ_p	Inelasticity	Transverse Momentum (p_t)	
Oda (1956)	Fermi Theory of meson production. Landau-type theory	$n = 1.3\, E^{\frac{1}{4}}$	70g cm^{-2}	-	-	-
Ueda & Ogita (1957)	1-dimensional calculations	$E_p^{\frac{1}{4}}$	constant	variable	-	Primary energy range 10^{13}–10^{15}eV. The importance of early interactions in the cascade was emphasised
Fukuda, Ueda & Ogita (1957)	Extension to 3-dimensions	$E_p^{\frac{1}{4}}$	constant	0.5 fixed	$<p_t> = 0.4$GeV/c	The concept of 'backward and forward cone' was introduced into the model for pionization.
Hillas (1966)	"Step-by-step" Technique: CKP model for interactions	$E_p^{\frac{1}{4}}$ for10^{12}eV $E_p^{\frac{1}{2}}$ for $>10^{13}$eV	λ_p=100gcm^{-2} =100gcm^{-2}	-	$<p_t> = 0.35$GeV/c	Predicted the lateral distribution of muons between 20–2000m for E > 0.3 Primary energy $\sim 10^{17}$eV
Dedenko (1966)	Step-by-step technique. 4 models for interactions including single fireball, double fireball and multiple fire-ball.	-	-	-	-	The aim of the work was a study of the altitude variations of EAS. Observation levels considered were (12, 9, 5.2, 3.3, 2.8) km.
Cowsik (1966)	1-dimensional diffusion equation model including the isobar model of Pal & Peters (1962)	$E_p^{\frac{1}{2}}$	λ_p=75 g cm^{-2} λ_π=120g cm^{-2}	0.35→0.7		The energy range was 10^{13}–10^{16}eV. Copious nucleon-antinucleon production included.
Lal (1967)	Semi-Monte Carlo model. 1-dimensional	$E_p^{\frac{1}{4}}$ $E_p^{\frac{1}{2}}$ and Log (E_p)	λ_p=80 g cm^{-2} λ_π=120g cm^{-2}	0.5		
de Beer et al. (1966) de Beer et al. (1968) Adcock et al. (1968)	Proton and iron initiated EAS (super-position used)	$3.2(E_p)^{\frac{1}{4}}$; also a model with $E_p^{\frac{1}{2}}$ law.	80 g cm^{-2}	mean of 0.5	$<p_t> = 0.4$ GeV/c	A comprehensive study paying particular attention to those showers recorded at large zenith angles. Prime interest in estimating the mean p_t of pions produced in high energy interactions. Size of showers investigated $\sim 10^6$ particles. Aimed at determining the nature of the primary cosmic rays from fluctuation measurements
Bradt and Rappaport (1967)	3-dimensional full Monte-Carlo computation. Proton and Iron nucleus initiated showers. A partial fragmentation model adopted for break-up of heavy particle.	$5.5(KE_p)^{0.28}$ and $5.5(KE_p)^{0.22}$	λ_p=λ_π= 80.g.cm^{-2}	.25 .75 (uniform distribution)	$f(p_t) \propto p_t \exp\left(\frac{-p_t^2}{P_o^2}\right)$ $<p_t> = 0.35$GeV/c	Simulations made in the energy range 10^{14} – 10^{16} eV.

Table 2-1 Continued

Author(s)	Scope of Simulations	Multiplicity Law	Mean Free Path of protons p	Inelasticity	Transverse Momentum (p_t)	Comments
Murthy et al (1968)	3-dimensional Monte-Carlo for lower energies following up with 1-dimensional diffusion equation model for higher primary energies.	8 models Mult. laws include $\log(E_p), E_p^{\frac{1}{4}}, E_p^{\frac{1}{2}}$	$\lambda_p = 80g\ cm^{-2}$ $\lambda_\pi = 120gcm^{-2}$	0.5	$<p_t> = 0.4GeV/c$	No 'backward cone' was considered in the distribution of pion energies Copious $n\bar{n}$ production included. The energy range considered was $10^{13}-10^{16}eV$
Castagnoli et al (1969)	3-dimensional full Monte-Carlo simulations	$n_s \alpha E_p^{0.3}$	$\lambda_p = 80g\ cm^{-2}$ $\lambda_\pi = 120g\ cm^{-2}$	0.4	$f(p_t) \alpha\ p_t$ $\exp\left[-\frac{p_t}{p_o}\right]$ $p_t = 0.35GeV/c$	These simulations were designed to make predictions for low energy showers $(E_p < 10^{16}eV)$
Suschenko & Fomin (1968)	3-dimensional Monte-Carlo simulations. Normal CKP model used plus isobars	$n_s = 2 \times (KE_p)^{\frac{1}{4}}$	$\lambda_p = 80g\ cm^{-2}$	0.45	$<p_t> = 0.3$ GeV/c	Calculations aimed at making predictions for energetic muons and pions in small showers $(10^{14}-10^{15}eV)$
Capdevielle et al (1970)	Step-by-step model	$n_s = bE_p^{\frac{1}{4}}$ (b=1.3,2,3)	$\lambda_p = 90g\ cm^{-2}$	0.3, 0.5, 0.7	$f(p_t) \alpha\ p_t$ $\exp\left[-\frac{p_t}{p_o}\right]$	$E_p \sim 10^{15}eV$
Hillas (1969-1972)	Wide range of models. Mainly step-by-step techniques employed. 'Super position' used for iron nucleus induced EAS	$E_p^{\frac{1}{4}}$	$\lambda_p = 80g\ cm^{-2}$ $\lambda_\pi = 100g\ cm^{-2}$	0.44	$f(p_t) \alpha\ p_t$ $\cdot\exp\left(\frac{-p_t}{p_o}\right)$	Energy range considered $10^{15}-10^{20}eV$. The work of this author has been used as a starting point for detailed calculations of the electron-photon cascade (eg Marsden(1971)). The model labelled E is the one most similar to the preferred model of the present work.
Grieder (1969-1972)	3-dimensional Monte-Carlo simulations	$E_p^{\frac{1}{4}}$ $E_p^{3/8}$ $E_p^{\frac{1}{2}}$	$\lambda_p = 75g\ cm^{-2}$ $\lambda_\pi = 120gcm^{-2}$		$f(p_t)\ \alpha p_t \exp\left(\frac{p_t}{p_o}\right)$ $<p_t>$ ranging from 0.25-1.0 GeV/c	Predictions made for primary energy $\sim10^{16}eV$ at observational levels of 3km and 5km.
Theilheim and Beiresdorf (1970)	3-dimensional model. Monte-Carlo technique. Incorporating isobars combined with CKP model Partial fragmentation model was used for heavy primary initiated showers.	$2.3E_p^{\frac{1}{4}}$	$\lambda_p = 80\ g\ cm^{-2}$ $\lambda_\pi = 100g\ cm^{-2}$		$f(p_t) \alpha p_t \exp$ $\left[-\frac{p_t}{p_o}\right]$ $<p_t> = 0.55,$ 0.42	The calculations were made for primary energies $10^{12}-10^{15}eV$

C H A P T E R   T H R E E

MODELS FOR INTERACTIONS AND COMPUTATIONAL TECHNIQUES

3-1   The Aim of the Simulations

The present work was commenced in October 1971 with the specific aim of aiding the design of improvements for the EAS experiment at Haverah Park. The Durham group had hitherto been involved in computer simulations of the muon component of air showers to a small extent (Orford and Turver (1968)); this work was used as a starting point for the present study.

The Haverah Park experiment is briefly described in Chapter 1 as it was at the time of commencement of this work. Since the rate of detection of very high energy particles is governed by the collection area of the array (the flux of particles with energy greater than 10^{20} eV is probably not much above 1 per 100 km^2 per year) it seemed unlikely that the array could be modified in such a way as to detect even higher energy particles at a useful rate. However, a problem of equal importance, the determination of the atomic mass number of the primaries was amenable to solution and so it seemed reasonable to consider improvements that would make the array more sensitive to the primary particle mass. The simulations were developed to provide as broad a variety of measurable (or possibly measurable) parameters as possible in attempts to identify the optimum parameters for measurement. To this end such aspects of the shower as the optical Cerenkov radiation, not hitherto considered either theoretically or experimentally in the Haverah Park experiment, were calculated for each EAS.

A secondary aim of this work, which assumed more importance after the improvements of the Haverah Park array had been specified, was to identify models for the nuclear interactions involved in the

propagation of EAS through the Earth's atmosphere i.e. characteristics of p-N and possibly N-N interactions at ultra-high energies. It was hoped that on the grounds, of these simulations, at the least, some values of the parameters for these interactions which cannot be ruled out at accelerator energies might be positively eliminated at air shower energies. For example, at accelerator energies the dependence of the multiplicities of mesons produced in nucleon-nucleon interactions upon the interaction energy E_r can be fitted equally well with a law of the form $E_r^{\frac{1}{4}}$ or $\log_e E_r$, but at air shower energies the values of multiplicities derived from extrapolation of these laws differ greatly.

The calculations have been undertaken by, the author, Dr. K.E. Turver, Dr. J. Hough and G.J. Smith, the work on the radio signal from EAS was done by J.H. and the optical Cerenkov signal was largely the responsibility of GJS.

The Haverah Park experiment is now being improved, as will be described in Chapter 7, in such a way as to increase the sensitivity to the atomic mass number of the primary particle.

3-2 The Requirement for a Single Model for High Energy Interactions

To use the results of a computer model for EAS to make predictions about the sensitivity of an array to the primary particle mass one must first establish the correctness of the assumptions used in the model. Since the available data are normally at energies several orders of magnitude lower than those applicable to EAS, the best that can be done is to fit this data at low energies and then extrapolate to higher energies. Thus the first requirement for assumptions used in EAS models is that they are a good fit to data from accelerator experiments. This is not the only criterion; the results obtained from the given simulation must also represent well our present knowledge of many aspects of EAS. For example, certain equations

relating the multiplicity of mesons produced in p-N interactions

to the interaction energy can be discarded because they produce

EAS incompatible with those observed in spite of the fact that they

appear to agree with the accelerator data reasonably well (see

§ ·3-4.1 and Fig. 3-2).

In addition to these requirements for a preferred model, the

computation for fluctuation studies (Chapter 6) would be prohibitive

if a single preferred model could not be chosen.

After a brief survey of the main theories of nucleon-nucleon

ultra-relativistic interactions, the data available from the accelerator

experiments is reviewed leading to the choice of the parameters for

the 'normal' model.

3-3 Models for High Energy Interactions

In the last twenty-five years, during which major advances

have been made in elementary particle physics, there have been

many different models proposed to describe ultra-relativistic

nucleon-nucleon interactions.

The simplest approach is to assume that the nucleon-nucleon

interaction is so strong that the projectile. and target stop

each other in the centre of mass system. As all the kinetic energy

is now dissipated it might be reasonably expected that the number

of produced particles be directly proportional to the centre of

mass energy, $E_c \alpha E_L^{\frac{1}{2}}$ (E_L being the laboratory energy) but this is

false. Fermi (1950) neglected the interactions among the produced

particles and assumed the probability that the collision produced some

final state which was proportional to the phase space available

inside a contracted nuclear volume, $V = \frac{4}{3} \pi (\frac{1}{m})^3 (\frac{2M_N}{E})$; the

multiplicity was predicted to increase as $(E_c^\pi)^{\frac{1}{2}} \alpha E_L^{\frac{1}{4}}$ which is

not inconsistent with present experimental evidence.

A weak point in this type of theory is a composition for the produced particles differing from that observed. At high energy the relative particle abundance is determined only by their internal (charge and spin) degrees of freedom. Therefore the ratio of average numbers of nucleons $(p, \bar{p}, n, \bar{n})$ each having two spin states, kaons $(K^+, K^-, K^0, \bar{K})$ and pions (π^+, π^-, π^0) should be

$$\langle n_N \rangle : \langle n_K \rangle : \langle n_\pi \rangle = 8 : 4 : 3 \text{ compared with experimental}$$

values $\langle n_N \rangle : \langle n_K \rangle ; \langle n_\pi \rangle = 1 : 20 : 1000$. This may be remedied by assuming that the 'temperature' of the statistical hadron system cannot exceed some bound $T_0 \sim m_\pi$ (Hagedorn (1965)). A further difficulty of the model is that transverse and longitudinal momentum are treated symmetrically and so the observed transverse momentum cut off is not reproduced.

The simplest way of achieving dominance of longitudinal momentum over transverse momentum is to assume that both the target and the projectile each produce a Fermi statistical 'fireball' either diffractively or by pion exchange. The two fireball model was proposed about fifteen years ago as a phenomenological description of multiple meson production at high energy. The model was suggested by the fact that in high energy interactions observed in photographic plates the secondaries are emitted isotropically from two centres (Cocconi (1958)). It was proposed that in nucleon-nucleon interactions two fireballs are formed and move in opposite directions with respect to the centre of momentum of the system and that each fireball emits in its own system of reference about half the total number of secondaries (See Fig. 3-1(a)). It is also possible to include diffractive excitation of the leading particles. The multiplicity is predicted to increase as $E_L^{\frac{1}{4}}$ treating the fireballs in analogy to the Fermi statistical model; however the observed transverse momentum cut-off is now reproduced. The CKP momentum distribution (Cocconi, Koester and

The Two Fireball Model .

(a)

projectile

Leading particle

(and isobar production possibly)

fireball

fireball

target

(b)
projectile

Multiperipheral Production of
Several Fireballs

target
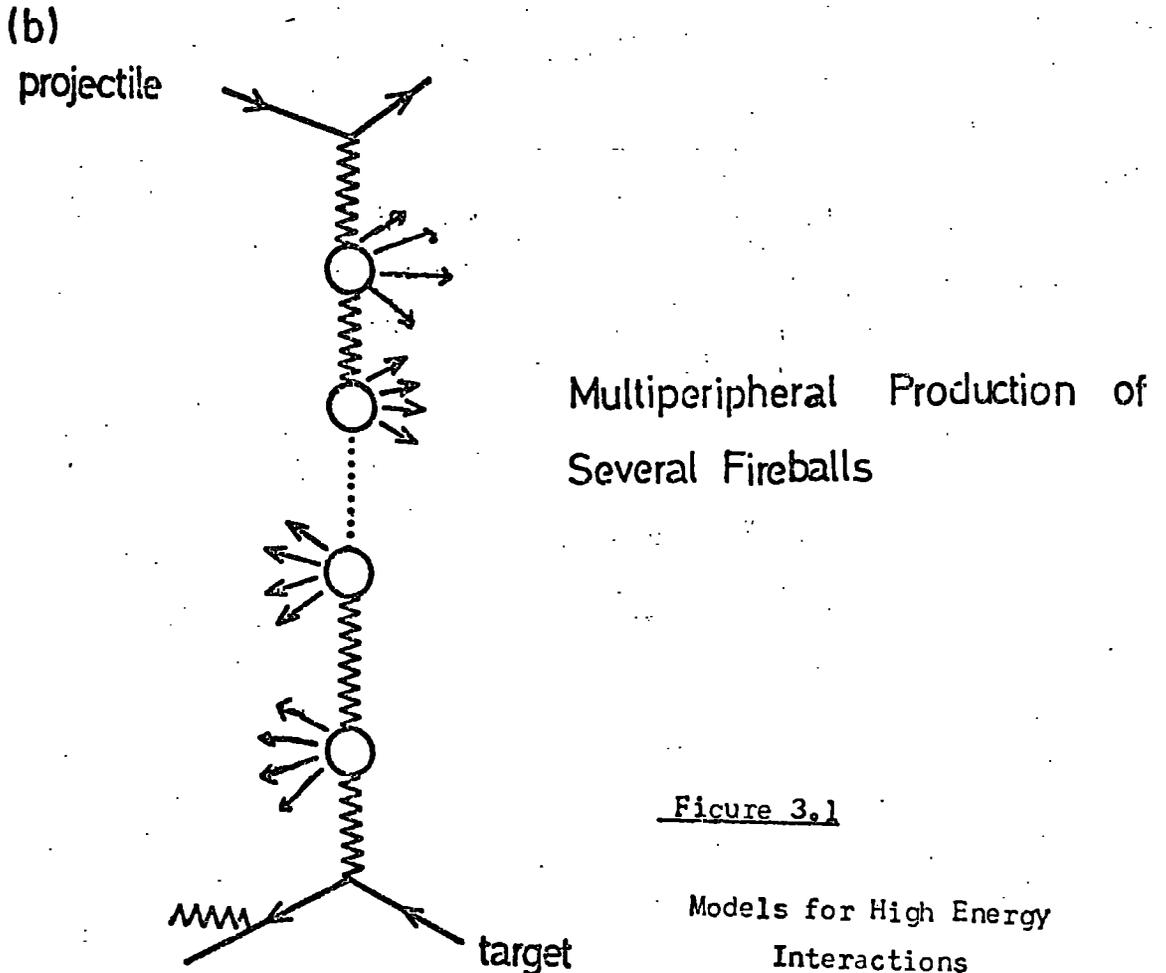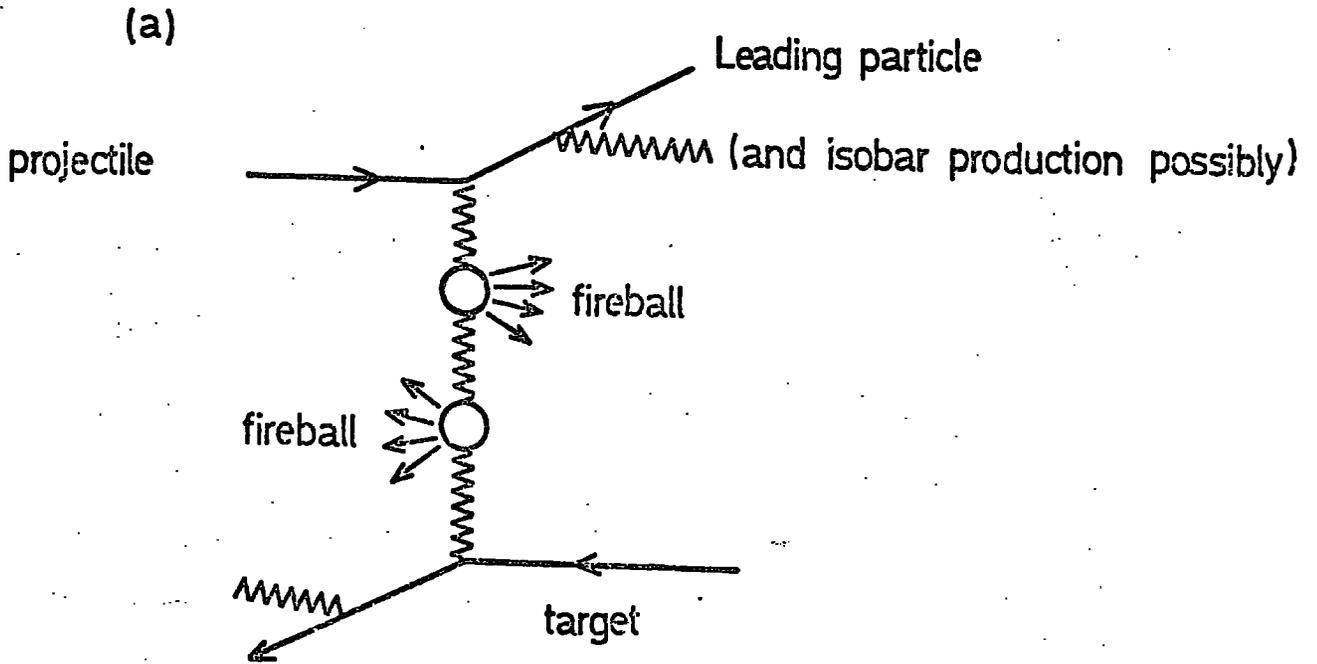
Figure 3.1

Models for High Energy
Interactions

Perkins (1961)) is based on data for p-light nucleus interaction frcm

accelerators up to 1961 and is consistent with the two fireball model.

At high energies, however, the assumption of isotropic decay

of the fireball is very dubious as can be seen by consideration

of the collision ep →eX. Only one fireball is produced in this

interaction but the momentum distribution is found to be not

isotropic at high energy (Benecke et al.(1969)).

Once the condition of isotropy is relaxed the leading particles

need no longer be considered separately from the 'pionization' products

and a picture where the projectile and target pass through each other

becoming excited and subsequently fragmenting becomes reasonable.

This is the approach of the limiting fragmentation hypothesis

(Benecke et al.(1969)); scaling is predicted since the distribution

of target and projectile fragments are both assumed to approach

limiting values in the target and projectile rest frame respectively.

Feynman (1969) considers a hadron to consist of a large number of

constituents or partons (virtual particles) which have small internal

momentum and hence the total parton momentum is simply a fraction

of the hadron momentum $x = \dfrac{P_n}{E_c}$. In a high energy collision the

hadron is broken into its virtual constituents and it is assumed

that on becoming 'real' the momentum is not affected. Hence the

produced particle momentum spectrum depends only on the ratio of the parton and
hadron momentum $x = \dfrac{P_n}{E_c}$ rather than both separately. The multiplicity of produced

particles is predicted to grow logarithmically with laboratory

energy (Van Hove (1971)). Furthermore, although scaling allows the

momentum distribution of produced particles to be any universal

function of x, the number of particles shown in the centre

of mass are not expected to increase with energy as they are

from the two fireball model. At low energies scaling is not

expected to be applicable and it is therefore reasonable that the

experimental evidence supports CKP. However, impressive evidence

has been produced (Albrow et al. (1973)) to support the idea of

scaling from 20 GeV up to the ISR energies ($\sim$ 1500 GeV). The

possibility of scaling may be incorporated into the fireball

model by allowing the fireballs to be produced along a multiperipheral

chain (see Fig. 3-1 (b)). In this model the number of fireballs

would increase logarithmically with energy and the momentum distribution

would on average scale.

In summary, the relatively low energy nucleon-nucleon collision

data is best accommodated by the semi empirical two-fireball

model. The model may be extended to higher energies and incorporate

scaling by multiperipheral production of several fireballs. The

most recent data from accelerators precludes the possibility of a

simple two fireball model at high energies. A detailed review of

multiple production of hadrons at cosmic ray energies has been

made by Feinburg (1972)

3-4   Experimental and Theoretical Considerations Involved in the

Choice of Parameters for the 'Normal' Model

3-4.1 Multiplicities

There is a great deal of controversy about the form of the

relation between the energy of interaction, E_p, and the number of

secondary particles produced, n_s. The scaling hypothesis

(Feynman (1969)) predicts a logarithmic rise of n_s with increasing

E_o and indeed as far as accelerator data is concerned there is

little to contradict this. The double fireball model (Cocconi

(1958)) indicates an $E_p^{\frac{1}{4}}$ law and a simple form of single fireball

or thermodynamic model predicts an $E_p^{\frac{1}{2}}$ multiplicity law.

Fig. 3-2 shows a review of the data on multiplicities of

charged mesons produced in proton-proton interactions that have

become available in the last fifteen years; the compilation was made
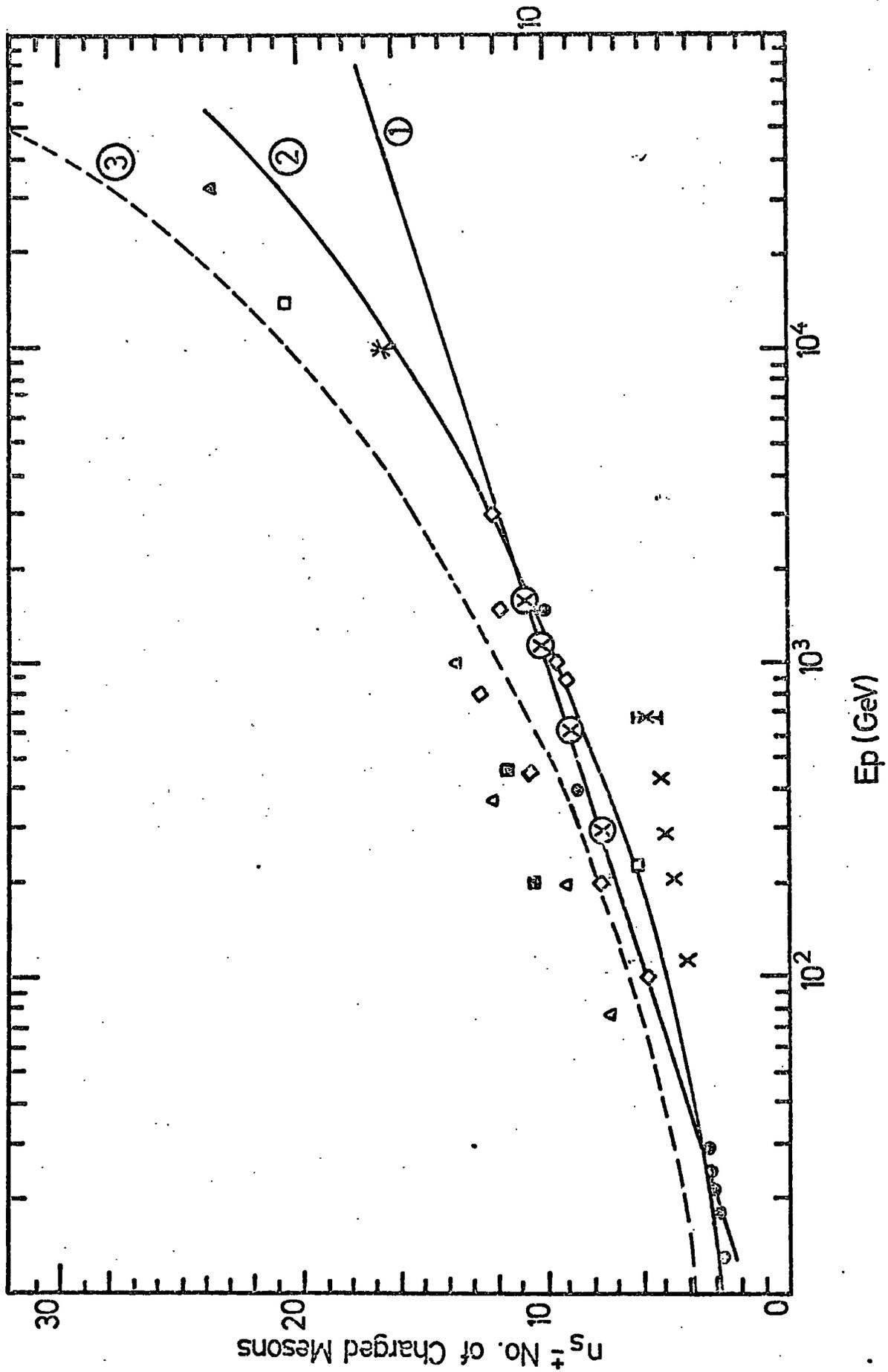
Fig. 3·2

by Grieder (1971) and recent data have been added. The data from

the Echo Lake experiment (Jones et al. (1970)) shown in this diagram

have recently been revised (Jones et al. (1973)) and are now in

agreement with the data from the I.S.R. experiment (Antinucci et al.

(1973)). The highest energy for which data from accelerator experiments

available is 1500 GeV in the laboratory system.

Since the data are widely scattered it is difficult to discount

any of the multiplicity laws mentioned above. A logarithmic law

has been fitted to the data of Antinucci et al. $(n_s^{+-0}=4.60 \ln E_p - 4.61)$.

and this is denoted by line ① (The revised data from the Echo Lake

experiment are fitted by this multiplicity law). Line ② shows an

$E_p^{\frac{1}{4}}$ law fit of the data for p-p interactions and line ③ corresponds

to a simple picture of the multiplicities expected for p-Air interactions

on the basis of line ②. Line ③ has been used for the 'normal'

model and corresponds to

$$n_s^{+-0} = 3.2 \ E_p^{\frac{1}{4}} \text{ for p-Air interactions}$$

the assumption is incorporated that the increase in multiplicity

when nucleus, rather than nucleon, targets are considered is $A^{0.19}$

where A is the atomic mass number of the target nucleus

i.e $n_{s_{p-N}} = n_{s_{p-p}}$ x 1.6 for the CNO group.

This assumption is discussed further in §3-4.2

There are data available at higher energies than shown in Fig. 3-2

which come from cosmic ray experiments. These could be interpreted

as suggesting a multiplicity increasing as fast as $E_p^{\frac{1}{2}}$ (Fowler (1963))

but tend to be based upon measurements of single events and therefore are

not conclusive. Further, the high energy multiplicity data originate

exclusively from emulsion experiments (where the targets are nuclei)

which poses a number of questions on the interpretation of the data.

Clearly, one of the main requirements is to determine how p-N

collisions differ from p-p collisions.

Although a dependence of the multiplicity of the form $E_p^{\frac{1}{4}}$

has been used in the 'normal' model, simulations have been made of

air showers using models incorporating different relations to

investigate the importance of this assumption; the results will be

discussed in §4-5.5.

3-4.2 The Coefficient of Inelasticity

The first statistical theory attempts of multiple production

treatment (eg.Fermi (1951), Landau (1953)) proceeded from the idea

that all the energy of colliding hadrons is spent for the generation

of new particles. However, studies of EAS at that time showed that

under collision with an air   nucleus a nucleon generally releases

only a small part of its energy, ~0.3 - 0.5. This important

characteristic - the coefficient of inelasticity has a wide

distribution but the mean value is found to be independent of energy

in the range 25 < E_L < 3000 GeV (Feinburg (1972)). Recent

estimates deduced from experiments under the supposition that the

interaction process is developing according to the two fireball

scheme give $<K>_{pp}$ = 0.43 and $<K>_{pC}$ = 0.67   (Jones et al (1970))

In the present work a value of 0.5 has been assumed for the

inelasticity of the p-N interactions and allowance has been made

for intranuclear cascading as will be described in §3-4.3. In the

Monte Carlo and Hybrid computational procedures the value of the

inelasticity was allowed to vary as described by the function:-

$$P(K)dK = -2.045 \; x(1-K)^{1.43} x\ln(1-K)$$

Brook et al,(1964). This function has a mean value of K = 0.5.

Accelerator data at lower energies and cosmic ray calorimeter

and hadron attenuation length measurements at higher energies,

indicate that the pion air nucleus inelasticity, K_π ,lies between 0.8 and 1.0. Furthermore, a value approaching unity is consistent with the experimental evidence for lack of leading pions in pion-nucleus interactions, (see §3-4.7).

3-4.3   The Relation between the Multiplicity in p-p and p-N

Interactions

The data on multiplicities at high energies from accelerators refer mainly to proton-proton interactions. In EAS simulations, however, data for proton-air nucleus interactions are more relevant. It is therefore necessary to establish a relationship between the multiplicity in p-p interactions, $n_{s(p-p)}$ and the multiplicity in p-N interactions, $n_{s(p-N)}$. One would expect intuitively the number of mesons produced in p-N interactions to be higher than the number produced in p-p interactions because of the possibility of intranuclear cascading within the nucleus. The hydrodynamical theory of Belenky and Landau (1954) indicates that for collisions of two nuclei of atomic mass, A, the dependence of the multiplicity on A is of the form $n_s \alpha\ A^{0.19}$ and one would not expect any stronger dependence in p-N interactions. A survey of multiplicites obtained from experiments using emulsions (nucleus targets) and hydrogen bubble chamber (nucleon targets) by Hough (1971) suggests agreement with such an $A^{0.19}$ dependence. Therefore for the 'normal' model the relationship

$$n_{s(p-N)} = 1.6 \times n_{s(p-p)}$$

was used and assumed to be energy independent. However, this survey was confined to energies up to 10 GeV and can be improved upon in the light of recently available data. This ratio has been considered in a recent review by Gottfried (1973) and he finds the value of $\frac{n_{s(p-N)}}{n_{s(p-p)}}$ to be 1.68 ± .06 for an incident laboratory momentum of

~200 GeV/c. At energies higher than this Gottfried has produced a value for this ratio by using $n_{s_{(p-N)}}$ measured in cosmic ray emulsions and $n_{s_{(p-p)}}$ by extrapolating from accelerator data. The values quoted at an energy of 8 TeV are

$$\frac{n_{s_{(p-N)}}}{n_{s_{(p-p)}}} = \begin{cases} 1.63 \pm .12 & \text{if } \sigma_{inel} \alpha const \\ 2.11 \pm .15 & \text{if } \sigma_{inel} \alpha \ln^2 s \end{cases}$$

Dar and Vary (1972) have made a study of the values of this ratio predicted by various multiparticle production models. They show that if an accurate measurement of it could be made at very high energies it would be useful as a simple tool for distinguishing between mechanisms for multiparticle production in elementary particle collisions. Fig. 3-3 shows the predictions of these authors for the ratio of $n_{s_{(p-N)}}/n_{s_{(p-p)}}$ as a function of energy from fireball type models. Also shown are the values (based on measurements) of this ratio given by Gottfried (1973) and Lohrmann and Teucher (1962).

3-4.4 The Mean Free Path for Proton-Nucleus Interactions, λ_p

In order to calculate the mean free path of protons in a particular medium it is necessary to know the interaction cross section, σ, since collision lengths are based upon the values of σ thus

$$\lambda_p = \frac{1}{N_o \sigma}$$

(N_o is the number of molecules per gram).

It is well known that

$$\sigma = \pi r_o^2 A^{\frac{2}{3}} \quad \text{where } r_o = 1.26 \times 10^{-13} cm \qquad 3.1$$

This value of σ is based upon measurements made by Ashmore et al. (1960) on the absorption of 24 GeV protons. It should be noted that this relationship holds only for targets with $A > \sim 4$ since the lightest nuclei exhibit a certain transparency and the true absorption cross sections are 20-40% lower than the values given by

Fig. 3.3

Eq. 3.1 . For the absorption of protons in the atmosphere $(A=14)$, one finds a value of $\sigma \sim 295$ millibarns which corresponds to a mean free path of $\sim 80g$ cm^{-2}

At the time when the parameters to be used in the 'normal' model were decided upon the evidence from accelerator and cosmic ray data pointed to an energy independent interaction cross section; a constant value of 80 g cm^{-2} was therefore adopted for the mean free path of protons in air. However, recent data obtained from accelerators indicate that the proton-proton inelastic cross-section increases with energy above ~ 300 GeV. Fig. 3-4 shows this rise which has now been established to a laboratory momentum of 1500 GeV/c (Morrison (1973)). The energy dependence of the total cross section given by Leader and Maur (1973) is of the form

$$\sigma_{tot} = 38.4 + 0.49 \times \ln^2 \left(\frac{s}{122} \right) \text{ mb} \qquad 3.2$$

where s is the cms energy in GeV. Yodh, Pal and Trefil (1972) have suggested on the basis of cosmic ray data, values in substantial agreement with this conclusion.

If we consider a primary proton of energy 10 GeV in the laboratory system then using $s = 2m_p(m_p + E_L)$ it is found that $\sigma_{tot}=38.5$ mb; for a primary proton of energy 10^8 GeV the value of σ_{tot} has risen to 87.4 mb. By making the assumptions that this rise is due to the inelastic cross section rising and that a similar rise is present in the cross section for proton-nucleus interactions, the conclusion may be reached that if

$$\lambda_{p-N} = 80 \text{ g.cm}^{-2} \text{ at } 10 \text{ GeV}$$
$$\text{then} \qquad \lambda_{p-N} = 23 \text{ g.cm}^{-2} \text{ at } 10^8 GeV$$

Fig. 3-5 shows the predicted fall of the mean free path for protons in air together with an arbitrary curve of the form

$$\lambda_{p-N} = 93.E_L^{-0.066}$$

which was used in initial simulations (Dixon et al.(1973)).
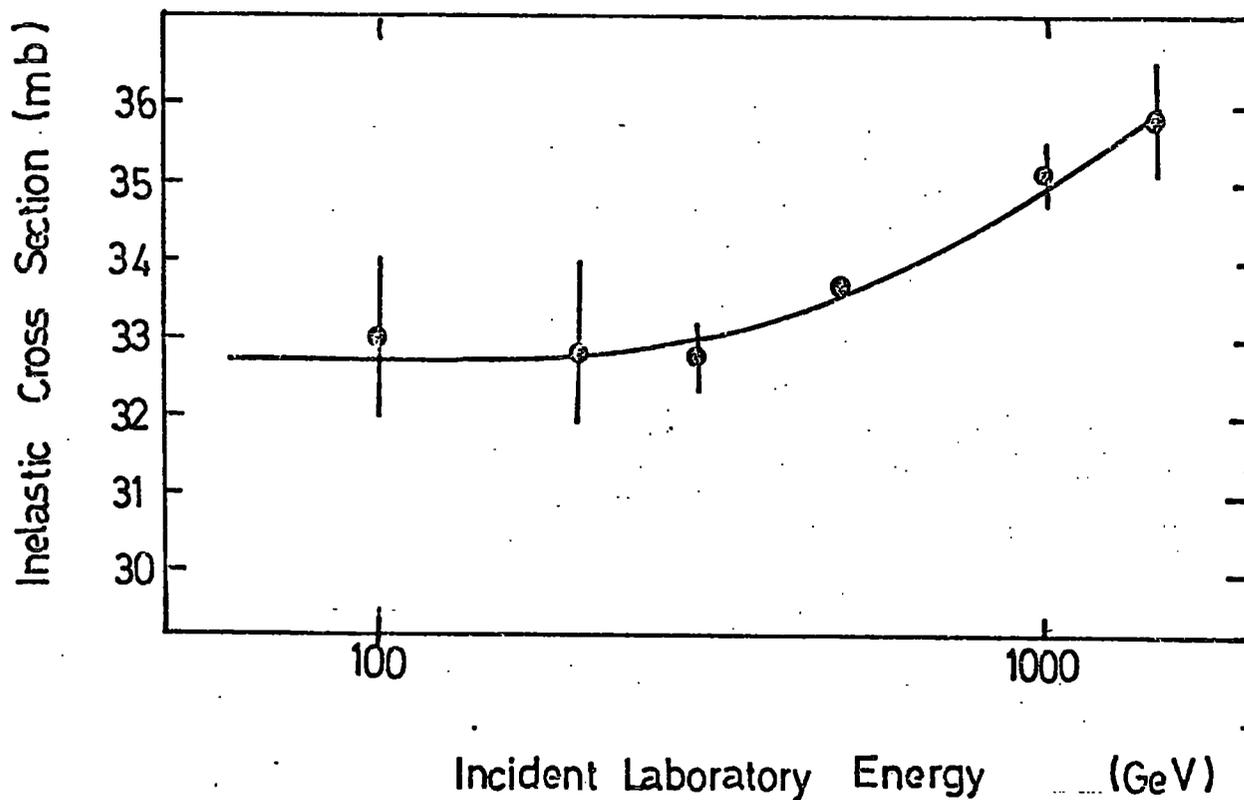
Figure 3.4

The energy dependence of the inelastic cross section for proton-proton interactions

Fig. 3·5

Ep(GeV) →

Mean Free Path, λ_p, (g cm^{-2})

$\lambda_p \propto \dfrac{1}{\ln^2(E_p)}$

$\lambda_p \propto E_p^{-0.066}$
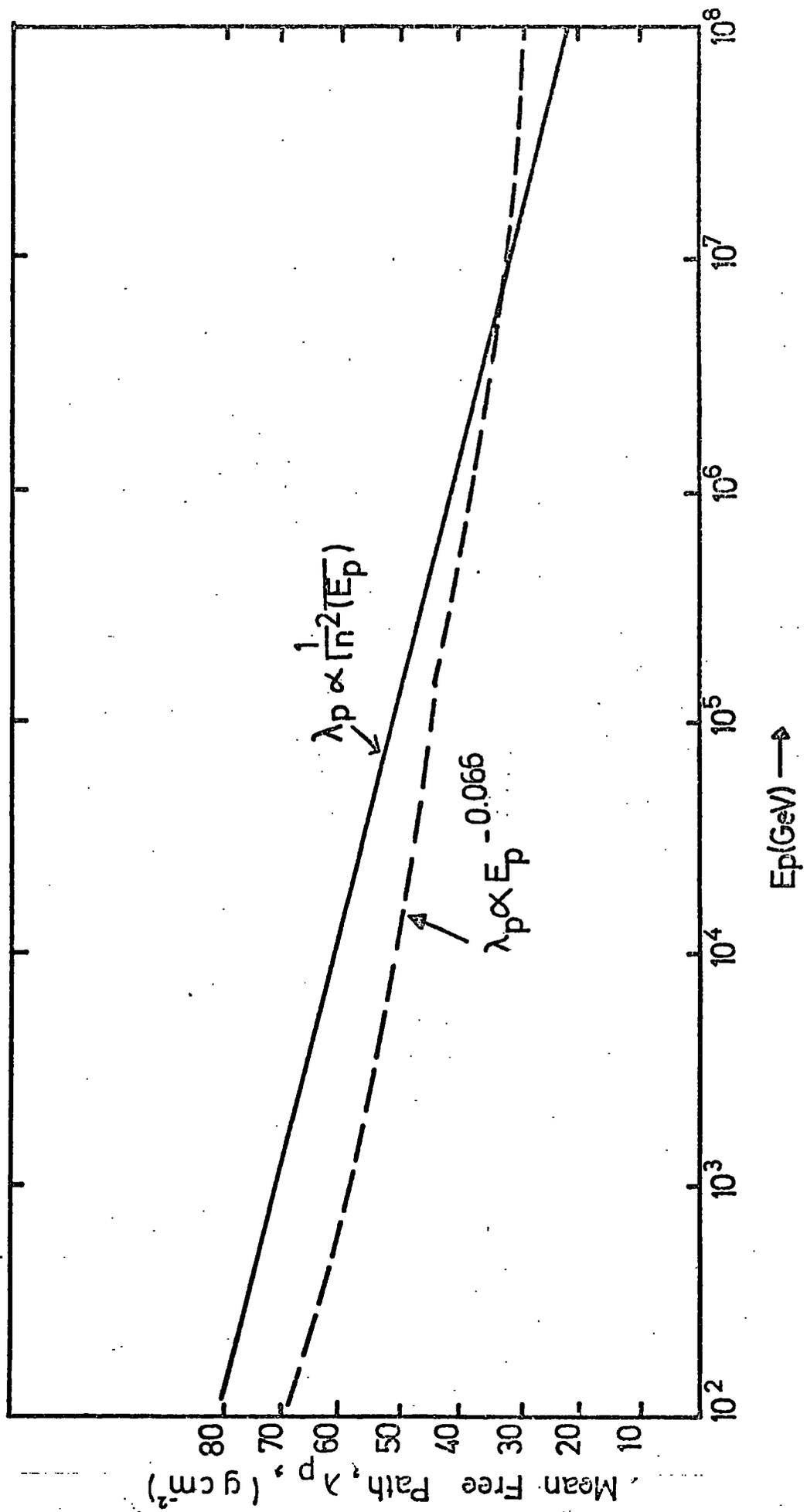
3-4.5 Pion-Nucleus Interactions

It is assumed here that pion nucleus interactions are very similar to proton-nucleus interactions except for the coefficient of inelasticity, which is taken to be unity, and the mean free path.

A value of 80 g cm^{-2} has been assumed for λ_p in the 'normal' model and a value of 120 g cm^{-2} was taken for λ_π. This mean free path was assumed to be energy independent.

Experimentally it is found that $\frac{\sigma_{\pi N}}{\sigma_{NN}}$ = 0.62 $\pm$ .02 (Giacomelli (1972)). If one assumes that $\sigma_{\pi N}^-$ and σ_{NN} are pion dominated and fractionization holds, a simple ratio model may be used to derive σ_{π^-p} :-

$$\sigma_{\pi^-p} = \tfrac{1}{2} \left(\sigma(\pi^+,p) + \sigma(\pi^-,p) \right) = 0.62 \; \sigma_{pp} \qquad 3.3$$

Although there is no firm evidence that $\sigma_{\pi p}$ shows the same rise with energy as σ_{p^-p} this is a possibility that should be considered. From equations 3-2 and 3-3 the rise in the value of σ_{π^-p} is predicted to be

$$\sigma_{\pi^-p} = 23.8 + 0.3 \; \ln^2 \left(\tfrac{s}{122} \right) \qquad 3.4$$

The consequences of σ_{π^-p} varying with energy as suggested by Eq. 3.4 are discussed in Chapter 4.

3-4.6 The Energy Distribution of Secondary Mesons

3-4.6.1 Longitudinal Momentum

The two fireball model for high energy interactions described in §3-3 predicts the production of pions in two well collimated cones, one moving forward in the centre of mass and one moving backwards;
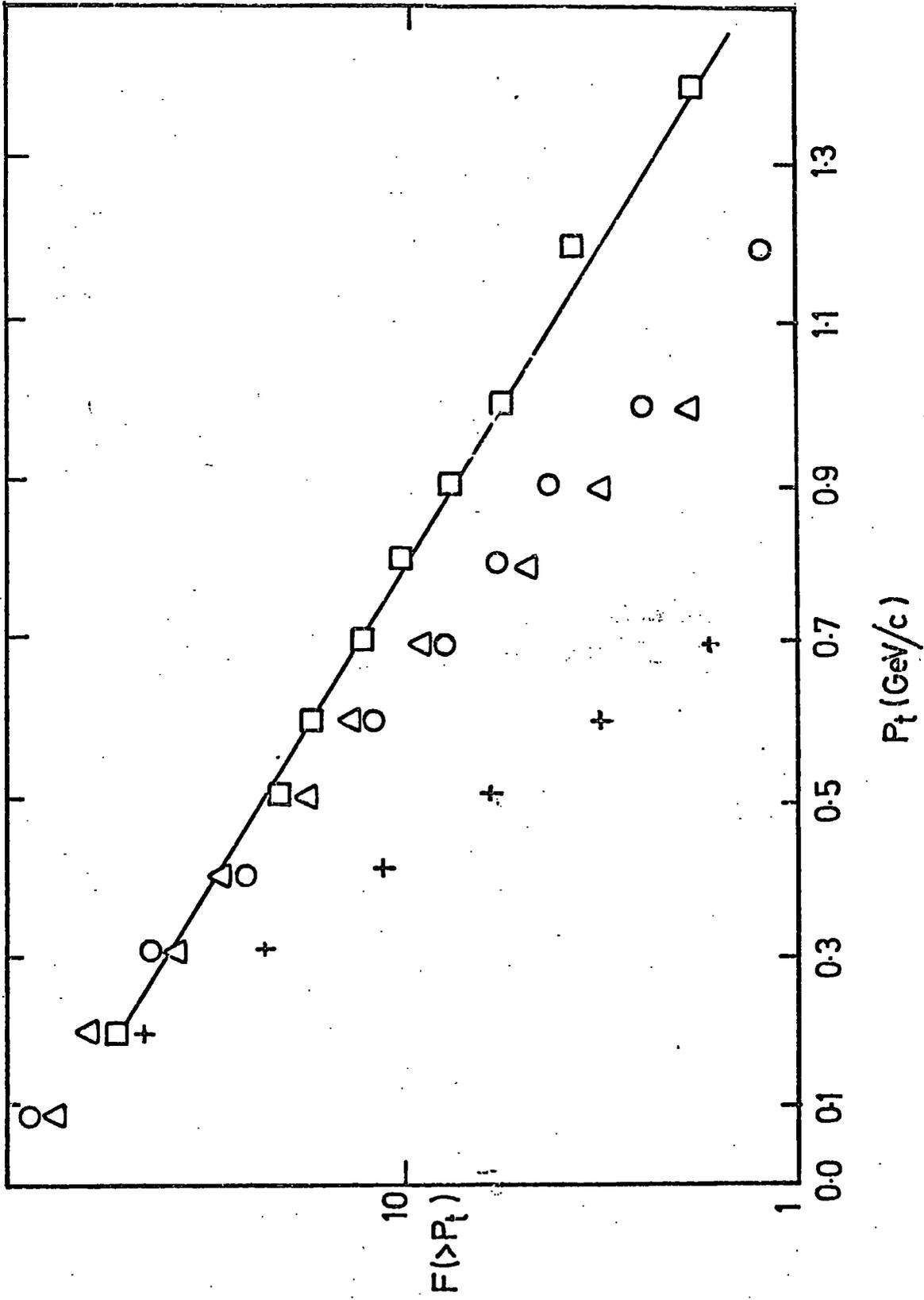
Fig. 3·6

éach cone containing approximately half of the particles produced in the interaction.

Since for speed of computation it is easier to work in the laboratory system than in the cms, one usually uses an approximation of the transformation of the momentum distribution from the centre of mass system to the laboratory system which can be expressed as the sum of two exponentials representing roughly the backward and forward moving particles (the so-called backward and forward cones). The distribution is

$$f(E_L)dE_L = C \left(\frac{1}{U} e^{-E_L/U} + \frac{1}{T} e^{-E_L/T} \right) dE_L \qquad 3.4$$

in which U and T are the mean laboratory system energies in the backward and forward cone respectively. This distribution was suggested by Cocconi Koester and Perkins (1961) and is a good fit to p-Be low energy data. At cosmic ray energies ($\sim 10^6$ GeV) there is some indirect confirmation of this from emulsion measurements of the energy of γ rays from the decay of π^0 mesons produced by collisions of cosmic ray primaries (Fowler and Perkins (1964)). To calculate the mean backward and forward cone energies the inelasticity and the number of secondaries must be known.

$$T = \gamma_s (V + \beta_s \pi) , \qquad U = \gamma_s (V - \beta_s \pi)$$

where   V = energy of particles in cms

$$\pi = p_\ell^* = V^2 - m_\pi^2 c^4$$

where E_p is the incident proton energy and E_r is the energy radiated

$$n_s \times \frac{U + T}{2} = Const. \times E_p^{\frac{1}{4}} = E_r$$

and

$$\frac{U + T}{2} = \gamma_s V$$

$$\therefore V = \frac{E_r}{n_s \gamma_s}$$

The centre of mass system has a Lorentz factor γ_s given by

$$\gamma_s = \sqrt{\frac{1}{2}\left(1 + \frac{E}{m_p c^2}\right)}$$

where $E = E_p$ in the case of an incident proton

Thus T and U may be calculated for proton nucleus interactions.

The energy spectra of secondary mesons from pion-nucleus interactions are dealt with in a similar manner. In this case, however, the system is assumed to behave kinematically as though the incident particle is a 'ghost' nucleon with energy $E = E_p/K$ where K is the coefficient of inelasticity and that E_p is radiated in the form of pionization. This follows suggestions by Saltzman and Saltzman (1960) and was also used by Hillas (1972) in his simulations. Integration of Eq. 3-4 gives an expression for the total energy radiated in the laboratory system namely $E_r = C(U + T)$ in which $C = \frac{n_s}{2}$. The discussion of recent accelerator data in §3-3 leads to the conclusion that the CKP distribution does not predict the momentum spectra of secondaries in high energy interactions correctly. However, at the time when the parameters for the 'normal' model were chosen the evidence against CKP was not strong and its ability to describe the momentum spectra observed in relatively low energy interactions le/d to its choice. The consequences of scaling will be discussed in §4-5.7.

3-4.6.2 Transverse Momentum

The mean transverse momentum $\langle p_t \rangle$ of secondaries from high energy interactions is difficult to study directly and there is some controversy about the value of this parameter and also about its energy dependence. One of the most characteristic features of collisions seen in emulsions is the collimation of the products; in the cms the produced particles move within two narrow cones i.e. with small transverse momenta. At very high energy the measurements of momenta is a difficult problem and so p_t-distributions in individual events are studied only up to $E_L \sim 10^3 - 10^6$ GeV. For higher energies the angular distribution of energetic particle fluxes in EAS is exploited. Such investigations point to a gradually

increasing value of $<p_t>$ until a constant value of ~ 0.4 GeV/c is reached.

Fig. 3-6 shows the integral p_t-distributions for four energies on a semilogarithmic scale according to Fowler and Perkins (1964). Within the interval of 0.1 $<p_t<$ 1.5 GeV/c the integral distributions are exponential with a slope decreasing as E_L increases. Thus the distribution (for a given E_L) is

$$n\ (>p_t)\ \sim\exp\ (\ -\ \text{const.}\ p_t)$$

The CKP distribution of transverse momentum as used in the normal model is:

$$dn\ (p_t)\ dp_t\ =\ (\frac{p_t}{p_o})\quad \exp\ (\ -\ \frac{p_t}{p_o})\quad \frac{dp_t}{p_o}$$

when $p_o = \frac{<p_t>}{2}$. A value of 0.4 GeV/c was adopted for $<p_t>$ at all interaction energies.

There is some evidence of high $<p_t>$ values at cosmic ray energies from Bohm et al.(1967), Matano et al.(1967),Bakich et al.(1967)and, more recently, from Hazen et al.(1973). The results were achieved by studying the structure of the core of air showers. In particular Hazen et al used a 1.5m x 2m cloud chamber to investigate EAS with more than one core. They have recorded one event which seems to indicate a $<p_t>$ of 9 GeV/c and are still analysing other similar cases. However, this evidence is by no means conclusive and since at accelerator energies most experimental data suggests a near constant value of $<p_t>$ of ~ 0.4 GeV/c (Feinburg (1972)),this is the value that has been adopted for the majority of the present work.

Elbert et al,(1968), using data from collisions of 25 GeV π^- mesons in the 80 inch Brookhaven hydrogen bubble chamber, have produced evidence for a p_t-distribution of the form

$$dn(p_t)\ =\ Bp_t^{3/2}\quad \exp\ (-bp_t)\ dp_t$$

Using this p_t distribution rather than the CKP p_t distribution is found to make negligible difference to the results by Hillas and in the present work.

3-4.7 Isbar Production

Peters (1962) suggested that nucleon isobars carry away almost the whole of the available cms energy then the subsequent decay pions carry away energy which rises linearly with primary energy. This is in contrast to the less steep rise of the energy of the pions from the pionization process. The assumption of a two fireball model does not preclude the existence of fast pions from baryon decay as shown in Fig. 3-1(a).

Although isobars have been observed readily in accelerators at low energies the production cross section appears to become quite small at high energies. For example, in the work of Bøggild et al. (1971) the pion momentum distribution fits an exponential up to the highest values of momentum and no evidence is found of a separate group of fast pions. Counter data by Allaby et al (1972) at 19.2 GeV/c also shows no evidence for strong isobar production in examining π^+ spectra. At cosmic ray energies the data is often contradictory. The Russian group (Azimov et al (1964)), using a magnet cloud chamber find a few percent of the interactions containing a high energy secondary which does not fit the main distribution of pions. However, Jones et al.(1970) in the Echo Lake experiment find no evidence of high energy pions from their angular distributions.

As a result of studying available data it was decided to omit isobar production in the 'normal' model; however, the effect on the simulation data of isobar production has been investigated and is described in §4-5.6

3-5 The Computational Procedure

3-5.1 Introduction

The present study has been made using three computational procedures for the simulations. These are:-

(i)   step-by-step technique,

(ii)   Monte-Carlo technique,

and (iii)   'hybrid' technique (involving a combination of (i) and (ii)).

In the early stages of a large programme of air shower simulation it is desirable to have at least two independent techniques for simulating EAS so that confidence in the computational accuracy may be established. Therefore at the start of the present work procedures (i) and (ii) were produced; the results were seen to be in agreement. The reason for the introduction of (iii) was to enable fluctuation studies to be made at energies $\geqslant 10^{16}$ eV. (The Monte-Carlo technique uses a great deal of computing time and because of this the primary energy of the air showers it can be used to simulate is restricted to $\sim 10^{16}$ eV).

The main facets of these simulation techniques will now be briefly described.

3-5.2 The Choice of Energy and Atmospheric Depth Intervals for the Calculations

Throughout the calculations the energy intervals employed have been quarter decades such that

$$E = 10^{(i-4)/4} \text{ GeV}$$

where E is the mid-bin energy and i is the bin number (see Fig. 3-7(a)). Certain of the initial simulations were made using 1/6 decade energy bins and the differences found between these results and results for the same showers using $\frac{1}{4}$ decade energy bins were found to be negligible (Pickersgill (1973)).

Bins →

1   2   3   4   5   6   7   8

Energy ·1778 GeV   1 GeV   1·778 GeV   10 GeV   (a)

Probability

Depth in atmosphere (gms cm^{-2})

——— 1st Interaction (i=1)

——— 2nd Interaction (i=2)

——— 3rd Interaction (i=3)

(b)

Energy →

B   A

1   Depth

p_3 p_2' $p2$ $p1$ p^1

2   (c)

p_6 p_4' p_5 p_3' p_2

3

P(s) ds

$S = \dfrac{E\mu}{E_\pi}$

(d)

·573   1

S →
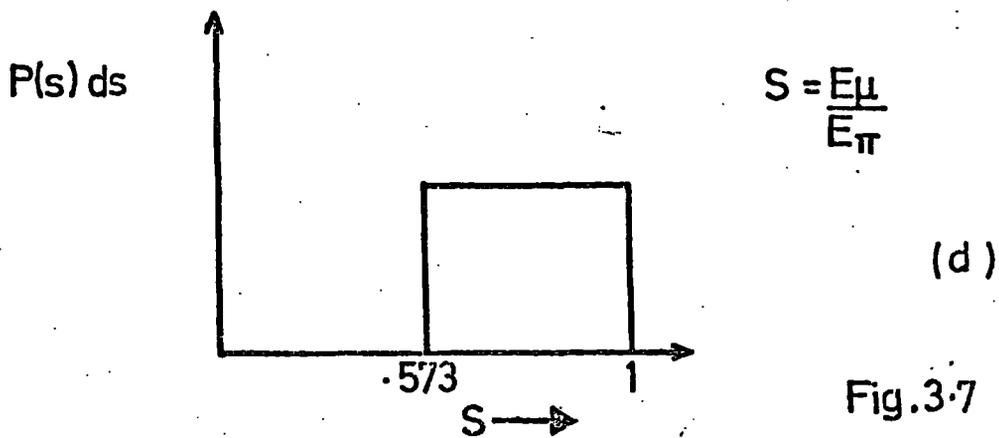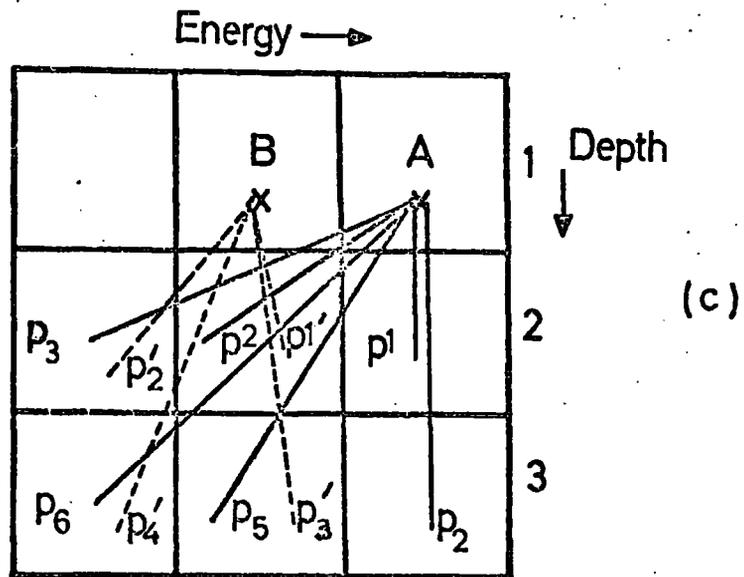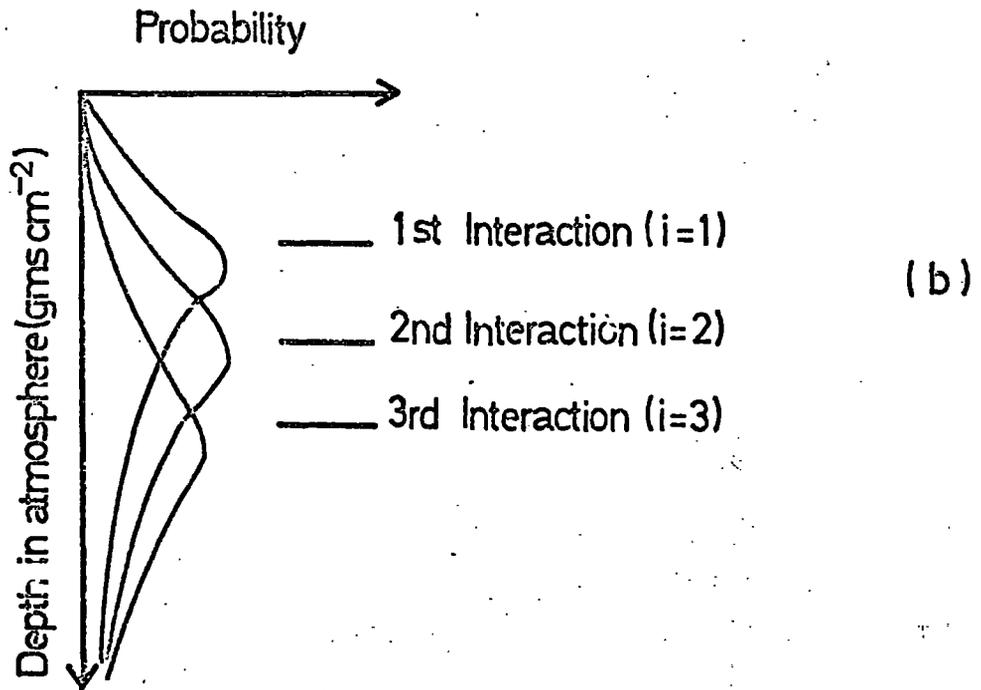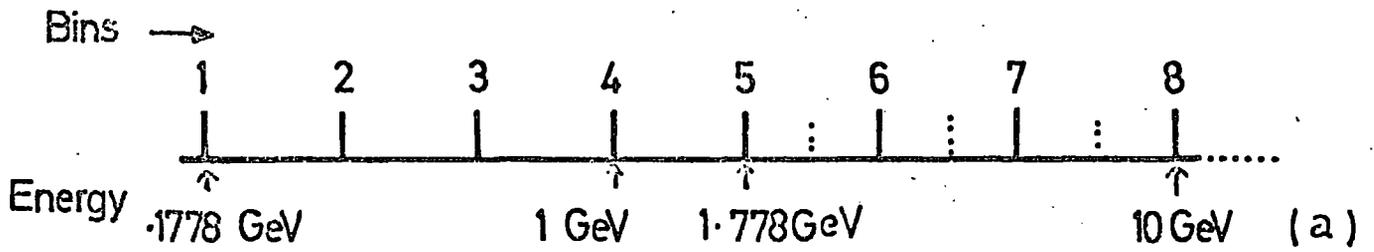
Fig. 3·7

The atmosphere was divided into 40 intervals each of 25.8 $g.cm^{-2}$, the bin corresponding to i = 1 being at the top of the atmosphere with its centre at a depth of 12.9 $g.cm^{-2}$.

The conversion from atmospheric depth in $g.cm^{-2}$ (x) to height above sea level in km (h) was made using the following equations:

when $x \geqslant 253.3/(Cos(\theta))$ ie.the troposphere

$$h = \frac{\left\{1 - (\frac{x}{1030 \times sec\,(\theta)})^{.1789}\right\}}{.0216 \times Cos\,(\theta)}$$

and for $x < 253.3/Cos\,(\theta)$

$$h = \frac{46.04 - 6.457 \times log_e\,(x.\,Cos\,\theta)}{Cos\,(\theta)}$$

This is a representation of the standard atmosphere from the United States Air Force Handbook of Geophysics (1960).

3-5.3   The Step-by-step Method

3-5.3.1   Introduction

This method of simulating air showers developed by Dedenko (1966) and Hillas (1966) was designed to predict the average development of EAS if a certain set of parameters for the nuclear interactions was assumed i.e. inelasticity, mean free path etc. The greatest value of such a method of simulation lies in its ability to test the effects of changes of values for parameters in the model. It can, of course, give no indication of the fluctuations in observables that would be expected.

3-5.3.2   The Nucleon Cascade

The calculation of the number of pions of various energies produced at different depths in the atmosphere in the nucleon

cascade was approached in the following way.

(i) An array PN(ix,i) was formed using the Monte-Carlo technique which contained the probability of a nucleon interacting with an air nucleus in the depth bin ix for the ith time. The average number of times that a nucleon will interact while traversing the atmosphere is 12 or 13 but there is a finite possibility that many more interactions may occur; the probabilities were therefore computed for up to 30 nucleon interactions. Fig. 3-7 (b) shows qualitatively the way in which the probabilities for the first three generations vary as a function of depth in the atmosphere. This array was computed assuming an energy independent mean free path of 80 g cm^{-2} for nucleons in air.

(ii) The number of pions and their energies that were produced by nucleons with energies corresponding to each interaction were computed as discussed in §3-4.5. An array $N_\pi(E_o(i),ie)$ was obtained where $E_o(i)$ was the proton energy corresponding to the ith interaction of the primary nucleon and ie was the pion energy.

$(E_o(i) = E_p \times (1-K)^{i-1}$; K = inelasticity, E_p = primary energy).

This array is obviously dependent upon primary energy and the detail of the model for interactions and therefore was computed each time a simulation was made. The number of pions of energy ie produced in depth interval ix by the nucleon cascade was given by

$$N_\pi' (ie,ix) = PN(ix,i) \times N_\pi(E_o(i),ie)$$

3-5.3.3 Successive Generations of Pions

The pions produced in the nucleon cascade could interact with air-nuclei and produce more pions which in their turn could create more pions etc. The way in which the successive generations of pions were computed was as follows.

The pions labelled A and B in Fig. 3-7(c) were produced in the nucleon cascade. The values $p_1 \rightarrow p_6$ and $p_1' \rightarrow p_4'$ associated with A and B are the numbers of pions produced by them in the depth and energy bins indicated. By starting with the pions produced in the nucleon cascade at the top of the atmosphere and working down through the depth bins, including the pions produced in the nucleon cascade, an array containing the total number of pions of each energy produced in each depth interval was obtained. It should be noted that Fig. 3-7 (c) is over simplified in that there is a probability of a pion producing more pions within the depth interval in which it was itself created; this probability was taken into account in the calculations.

The number of pions of energy ie_j produced in depth interval ix_i was given by:-

$$\Pi(ix_i, ie_j) = \sum_{i'=0}^{i'=i} \sum_{j'=j}^{j'=j \, max} N_\pi' \, (ie_{j'}, ix_{i'}). \quad P_{INT}(ie_j', ix_i', ix_i).$$

$$n_\pi (ie_j, ie_{j'})$$

$P_{INT}(ie_j', ix_i', ix_i)$ was the probability of a pion of energy ie_j' produced in depth interval ix_i' would interact in depth interval ix_i and its derivation is described in Appendix 1. $n_\pi(ie_j, ie_{j'})$ was the number of pions of energy ie_j produced as a result of a π-N interaction where the pion energy was ie_j' (see §3-4.5).

$\Pi(ix, ie)$ contained the total number of pions produced in the EAS and the approximation was made that 33% of these were neutral pions and decayed instantly $(\Gamma \sim 10^{-16} \text{secs})$ into two gamma rays, hence starting the electromagnetic cascade.

3-5.3.4 Lateral Development of Hadrons and Muons

In order to assess the lateral development of the EAS it was necessary to assume a transverse momentum distribution for pions

produced in p-N and π-N interactions. The CKP transverse momentum distribution described in §3-4.6 was assumed in the 'normal' model; Appendix 2 describes the use of the distribution.

3-5.3.5 The Muon Component

Once a charged pion was created in an interaction there were four possibilities for its subsequent behaviour

(i) It could interact and thus be removed from the simulation

(ii) It could decay to a muon which would survive to sea level

(or the observation level of interest)

(iii) It could decay to a muon which would decay to an electron before reaching the observation level

(iv) It could survive as a pion until it reached the observation level.

An array PRDEC (ix,ie) was formed by the Monte Carlo technique to give the probabilities of pions of each energy and at each depth in the atmosphere falling into catagory (ii).

The pion production spectrum π(ix, ie) was then multiplied by PRDEC(ix,ie) giving the pion production spectrum at each depth interval responsible for muons which reached sea level. These spectra were assumed to be of the form $AE^{-\gamma}$ over limited ranges of energy.

Under this assumption the muon spectrum was obtained as follows.

$$N_\mu(E_\mu)\, dE_\mu = \int_{E_\mu}^{E_\mu/0.56} \frac{A \cdot E_\pi^{-\gamma}}{0.44 E_\pi} \cdot dE_\pi$$

$$= \frac{A(1-0.56^{\gamma})\, E_\mu^{-\gamma}}{0.44\gamma}$$

(Fig. 3-7(d) shows the probability of a pion of energy E_π decaying to a muon with a particular fraction of its energy).

The value of γ was assessed separately for each energy interval. The value of E_μ at sea level was estimated by assuming a constant energy loss by ionisation of 2 MeV per $g.cm^{-2}$ for pions and muons. The contributions from all depth intervals to the muon numbers at sea level were summed.

3-5.3.6 The Pion Component

As a by-product of the generation of PRDEC (ix,ie) by the Monte-Carlo technique, an array PISURV (ix,ie) was formed containing the probabilities of pions of energy ie and created at atmospheric depth ix surviving as pions to sea level. The lateral development of the hadron component of the shower and the total pion energy spectrum was found in the same manner as for the muons except that the transformation from pion production spectrum to muon spectrum was unnecessary.

3-5.3.7 The Electron Component

Information about the electron component of EAS was derived from the pion production spectrum $\pi(ix,ie)$. It was assumed that equal numbers of π^+, π^- and π^o were created in the interactions and therefore $\Pi(ix,ie)/3$ represented the neutral pion production spectrum.

The two approaches used in order to predict the development of the electron-photon cascade through the atmosphere are outlined in §2-2.1 and described in more detail in Appendix 3.

It should be noted that the physical significance of Approximation B may be questioned. This is because the total numbers of electrons at each depth are computed and in reality Approximation B cannot give the correct number of electrons near zero energy (Rossi (1965)).

3-5.3.8 The Optical Cerenkov Response

In recent years the optical Cerenkov light emitted from large air showers has been studied (Krieger and Bradt (1968), Diminstein et al,(1971)). The possibility that this may be a sensitive measure of the longitudinal development of the shower caused the incorporation of predictions for this component in the present calculations. The treatment of the Cerenkov radiation from the shower electrons was undertaken by G.J. Smith (1973). The starting point for these calculations was once again the pion production spectrum $\pi(ix,ie)$ Typical results are described briefly in §4-2.5

3-5.3.9 Radio Emission in EAS

Calculations have been made for the radio frequency emission resulting from the separation of extensive air shower electrons and positrons in the Earth's magnetic field according to the theory of Allan (1971). This work has been reported in detail by Hough (1973).

The starting point for radio emission calculations was the pion production spectrum from which the electron photon cascade was derived using a combination of calculations under Approximation A and the numerical data of Messel and Crawford (see Appendix 3).

3-5.4 The Monte-Carlo Method

3-5.4.1 Introduction

This is a method of simulating air showers which involves following each particle produced in the cascade until it is removed by interaction or decay or reaches the observation level. Fluctuations are intorduced into the development of the shower by choosing parameters for each interaction from pseudo random distributions whose mean values correspond to those taken for the

step-by-step method. As a consequence of the detailed treatment
of each EAS such a programme is not economical of computing time
and can therefore only be used for primary energies $\leqslant 10^{15}$eV. In
order to make predictions about fluctuations and average characteristics of EAS
it is necessary to make several simulations for each set of predictions;
this is another reason for the limitation on primary energy.

3-5.4.2 Fluctuating Parameters

The parameters which were fluctuated in the Monte-Carlo
simulations were:-

(i) The mean free path of the proton; sampled from an
exponential distribution of the form $e^{-x/80}$.

(ii) The mean free path of pions, sampled from an
exponential distribution of the form $e^{-x/120}$.

(iii) The inelasticity of p-N interactions; sampled from
a distribution of the form $f(K) = (1 + \alpha)^2 (1-K)^\alpha \ln (1-K)$
where $\alpha = 1.414$ (Brook et al.(1964)).

(iv) The energies of pions produced in interactions; the
function from which the pion energies were sampled
is of the form:

$$f(E_L)dE_L = C \left(\frac{1}{U} e^{-E_L/U} + \frac{1}{T} e^{-E_L/T} \right) dE_L$$

(see §3-4.5). As each pion was generated it was randomly
placed in the forward or backward cone and its energy
chosen from the appropriate pseudo-random distribution.
The sampling continued for each interaction until all
the radiated energy had been used. In this way the number
of secondaries produced in the interaction was fluctuated
and energy was conserved.

(v) The transverse momentum; this was chosen ramdomly from
the distribution being used. eg for the 'normal' model

$$F(p_t) \, dp_t = \frac{p_t}{p_o} \exp \left(- \frac{p_t}{p_o} \right) \frac{dp_t}{p_o}$$

(vi)   The decay time for $\pi \rightarrow \mu + \nu_\mu$; this was chosen from a distribution of the form $e^{-m_\pi h / E_\pi T_\pi c}$ where h is the distance travelled, T_π the mean lifetime of the pion, m_π the rest mass of the pion and E_π the laboratory energy of the pion.

(vii) The decay time for $\mu \rightarrow e + \nu + \overline{\nu}$; the distribution from which the decay time was chosen was of the form $e^{-m_\mu h / E_\mu T_\mu c}$.

3-5.5   The Hybrid Model

In order to make predictions for fluctuations in air showers with primary energy above 10^{15} eV, the computational technique used was a combination of the step-by-step and Monte-Carlo techniques; this was known as the hybrid model. The simulation of the nuclear cascade was carried out in the same way as for the Monte Carlo technique and the step-by-step method was employed to simulate the copious pion generations. It was thought that if agreement between the magnitude of fluctuations obtained from the hybrid model and the Monte Carlo model could be established at a primary energy of 10^{15} eV, then the hybrid model could be used to predict fluctuations for EAS with higher primary energies.

C H A P T E R F O U R

RESULTS FROM PROTON INITIATED AIR SHOWERS

4-1 Introduction

The average results obtained from proton initiated EAS

simulations in the primary energy range 10^{14}-10^{19}eV from the present

study will be presented in this chapter. The results from the

'normal' model for interactions (described in Chapter 3) are

compared as far as possible with both experimental data and the

results of simulations by other authors. The sensitivity of the

results of the simulations to changes in the interaction model

assumed are investigated. The data presented in this chapter are

available in greater detail (Dixon and Turver (1973(v7))). Unless

specifically stated to the contrary, the results presented in this

chapter for the development of the one dimensional electron cascade

refer to data obtained from calculations of electron-photon cascades

under Approximation B (Greisen (1956)).

4-2 Results Obtained Using the 'Normal' Model for Interactions

4-2.1 The Electron Component

4-2.1.1 The Longitudinal Development of the Electron Cascade

The development of the electron-photon component of the EAS

simulated in the present work was calculated in two ways which are

described in Appendix 3. Both of these methods produce data for the

one dimensional electron cascades although the results are not

directly comparable since the electron size derived from the

Approximation A and Monte Carlo calculation (AAMC) refer to electrons

above a particular threshold energy (the results presented in this

chapter will be for electrons with energy >1 MeV) whereas the

electron numbers calculated from Approximation B (AB) refer to all

electrons. Fig. 4-1 shows the electron cascades produced by both
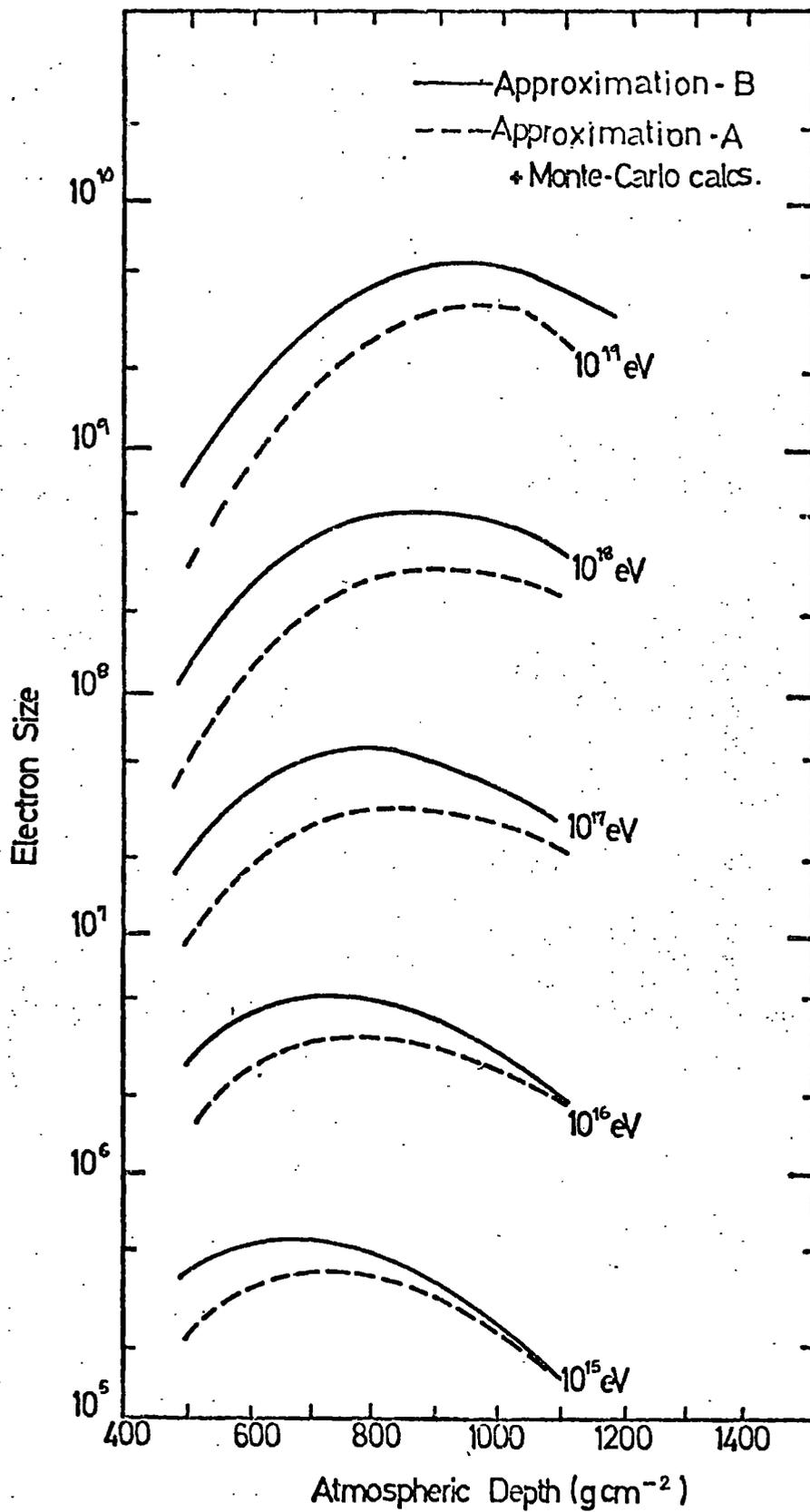
Figure 4-1

The longitudinal development of
the electron cascade of EAS
with primary energies in the
range 10^{15} – 10^{19}eV.

these methods for proton initiated EAS with primary energy in the range 10^{14}-10^{19}eV. It is clear that AAMC results in cascades having their maximum $\sim$ 50 g.cm^{-2} lower in the atmosphere and having sizes at sea level some 50% smaller than cascades derived under AB. A similar conclusion was reached by Marsden (1971) who compared cascades derived under AB with others derived using Approximation A and the numerical data of Baxter (1969).

Fig. 4-2 shows the results obtained for the one-dimensional electron cascade using Approximation B compared with the experimental data from the Mount Chacaltaya experiment (La Pointe et al.(1968)). These data were obtained by taking constant intensity cuts in the integral size spectrum at various shower zenith angles, corresponding to different atmospheric depths. The theoretical curves have been normalised at an atmospheric depth of 600 g.cm^{-2} in order to allow for differences in the threshold energy. At primary energies $> 10^{7}$ GeV the curves from the model fit the experimental points satisfactorily. However, at low primary energies the theoretical result does not predict the rapid attenuation of the electron cascade that is observed experimentally. This discrepancy between theory and experiment would clearly be worse if the comparison had been made with the results for the electron cascade from AAMC.

The absorption length of the electron cascade at an atmospheric depth of 1000 g cm^{-2} is found from the present work using electron cascades calculated under Approximation B to vary from 180 g cm^{-2} at sizes of 10^{5} particles to 295 g cm^{-2} at sizes of 10^{8} particles; this is in agreement with the results of Murthy et al.(1968). The form of the relation is:

$$\lambda_B = 25.0 \ln N_e + 95.0 \text{ g cm}^{-2}$$
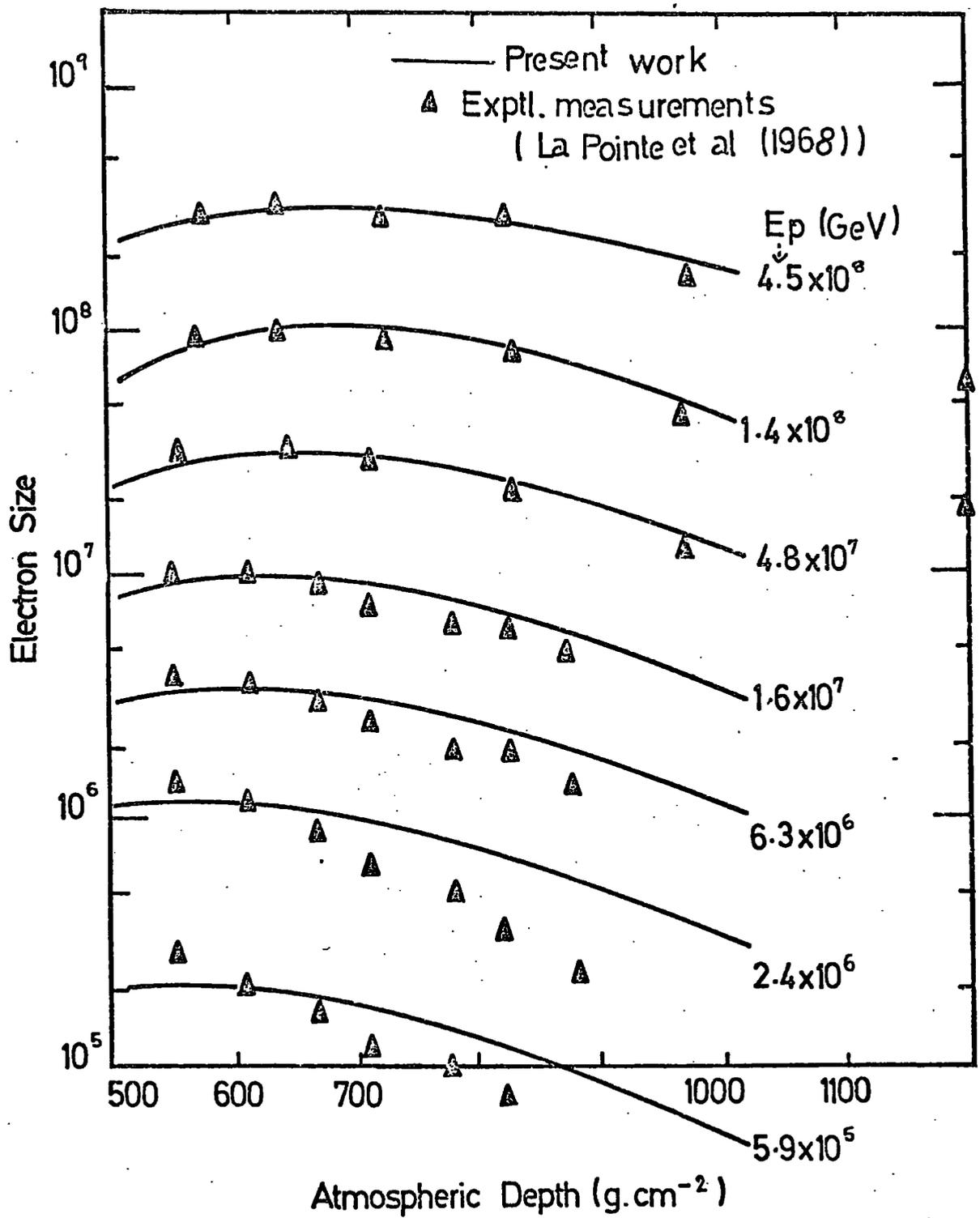
Figure 4-2

Comparison of the longitudinal
development of the electron
cascade from the present work
with experimental data

The way in which the depth of maximum development of the electron cascade varies with the primary energy of the EAS is shown in Fig. 4-3(a) and comparison is made with the results of Adcock et al.(1968), Capdeville et al.(1970) and Hillas (1972). It has often been suggested in the past (eg. Linsley (1963)) that air showers of primary energy $\sim 10^{20}$eV and zenith angle $\theta = 0^{0}$ are at about maximum development at sea level. However, these calculations, in agreement with Hillas and Capdeville et al., would require a primary energy of $\sim 10^{23}$eV to produce an electron cascade which would be at maximum at sea level. Fig. 4-3 (b) shows the way in which the sea level electron size varies with primary energy. The results from the present calculations are compared with those of Hillas (1972) and Bradt and Rappaport (1968). Also shown are the electron numbers at 530 g cm^{-2} and 830 g cm^{-2} (corresponding to the atmospheric depths of the Chacaltaya and Volcano Ranch arrays respectively).

The relationship between primary energy and the electron size at maximum development was investigated and found to be of the form

$$E_p = K N_{e_{max}}$$

The value of K from our 'normal' model was found to be 1.7 which compares with 1.9 suggested by Marsden (1971) and 2. suggested by Bradt and Rappaport (1968). The value of K from electron cascades under AAMC was found to be 2.4 for electrons above the threshold energy of 1 MeV.

4-2.1.2 The Lateral Distribution of the Electron Cascade

The use of Approximation A and the Monte Carlo data of Messel and Crawford allows the predictions of the lateral development of the electron cascade and also provides information about the energy spectra

Fig. 4·3(a)
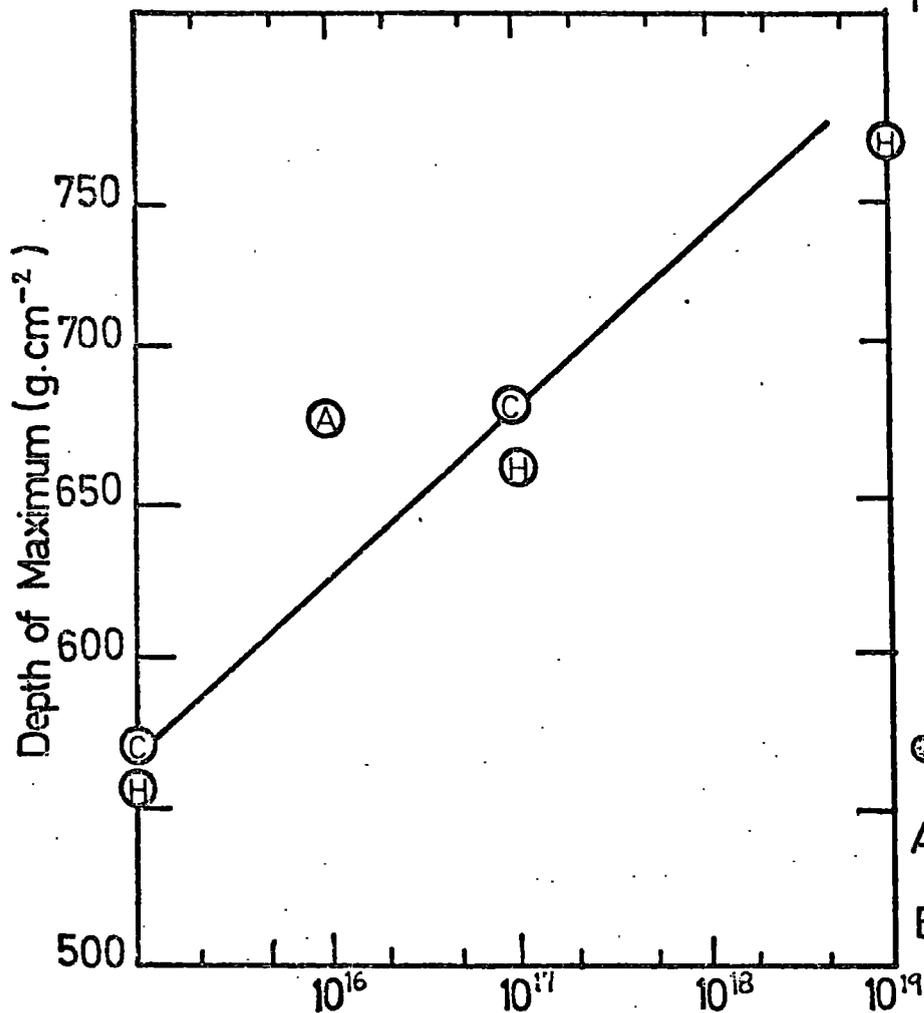
⊙ de Beer et al.(1968)

A Adcock et al. (1968)

Br Bradt and Rappaport
                    (1968)
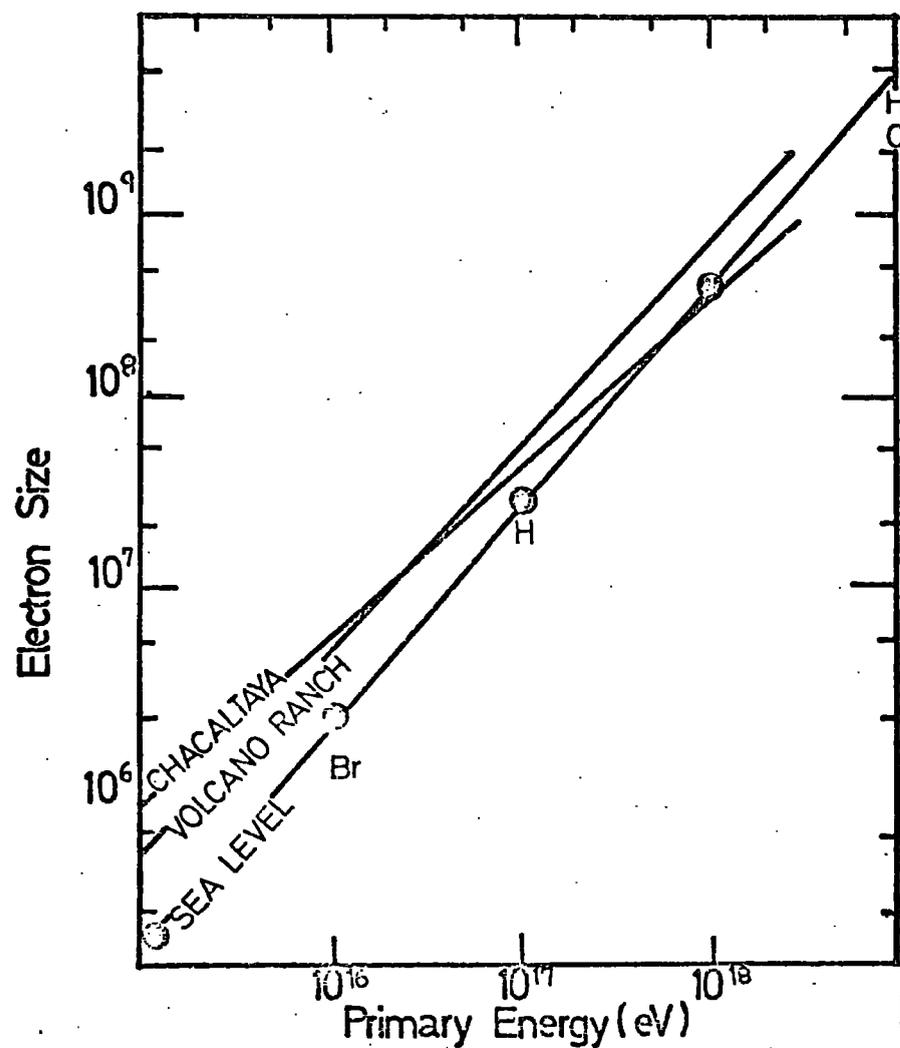
H   Hillas   (1972)

C Capdevielle et al.
                    (1970)

—— Present work

Fig. 4·3(b)

of the electrons. Data are available from Haverah Park (Armitage

(1973)), on the lateral distribution of electrons in EAS. Fig.4-4(a)

shows a comparison of the electron lateral distributions for primary

energy in the range 10^{15} - 10^{18}eV and electron threshold energy of

10 MeV ($E_e >$ 10 MeV) from the present work with the experimental

measurements of Kellerman and Towers (1970) and Armitage (1973). The

data is normalised at 500m since the threshold energies and photon

contamination make quantitative comparison uncertain.

The energy spectra of electrons at various core distances in

vertical showers initiated by protons of 10^{15}eV and 10^{17}eV are

represented by the data of Fig. 4-4 (b).

4-2.2 The Muon Component

4-2.2.1 Introduction

The 'step-by-step' and hybrid computational techniques take a

simplistic view of the muon component of EAS. Coulomb and geo-

magnetic scattering are both neglected in order to minimize computing

time. The muon component of selected air showers (using the pion

production spectrum as a starting point) has been studied in more

detail and some of the results of this work are reported here.

The two most appropriate threshold energies for comparisons

with muons detected at the Haverah Park EAS array are 0.3 GeV and

1 GeV (which correspond to the threshold energies of the Nottingham

muon detector and the Durham Magnetic Spectrograph).

4-2.2. The Total Muon Energy Spectrum

Fig. 4-5 shows the total muon number spectra for proton

initiated EAS of primary energy in the range 10^{14}-10^{18}eV resulting

from the present work. Comparison is made with the calculations

of Hillas (1972), Giler et al.(1970), Grieder (1970), Suschenko
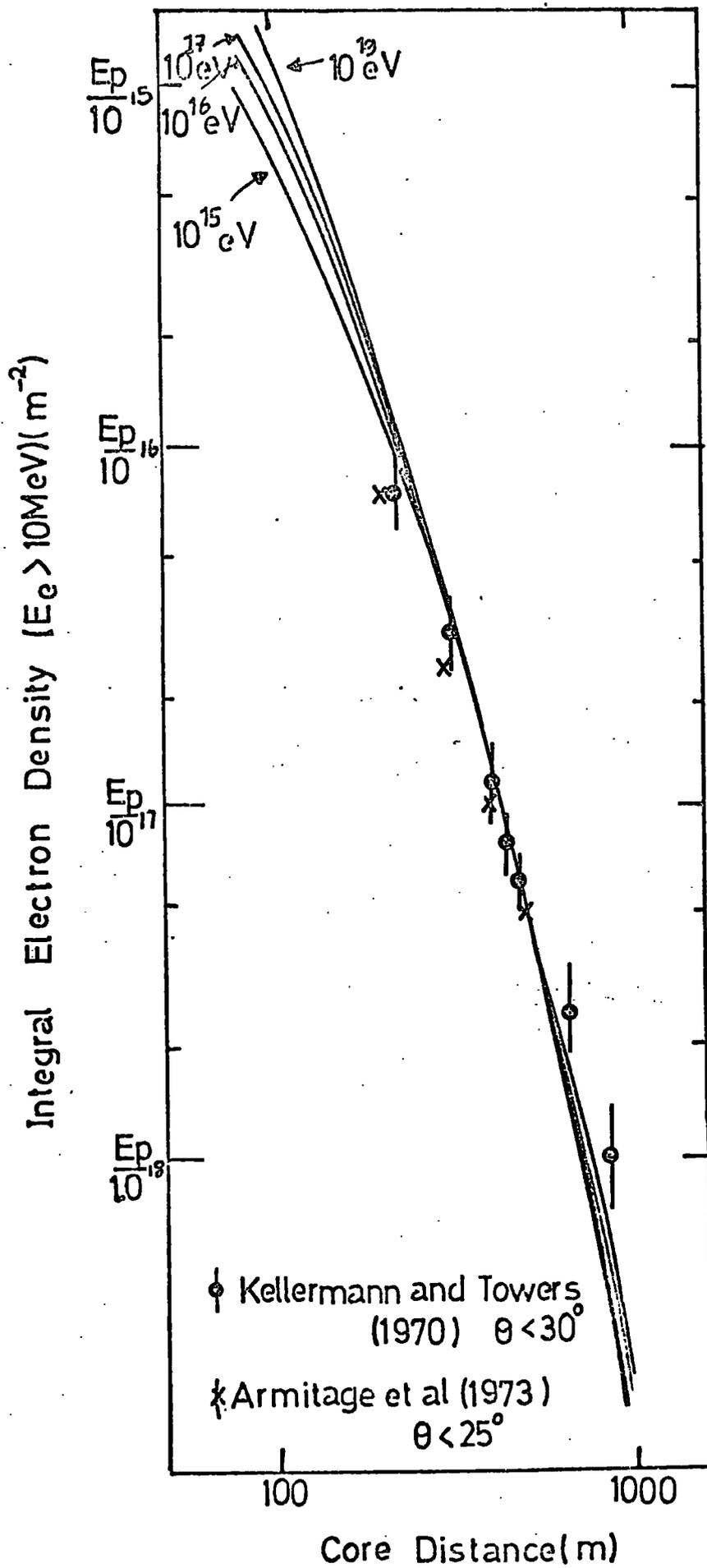
Fig 4·4(a)
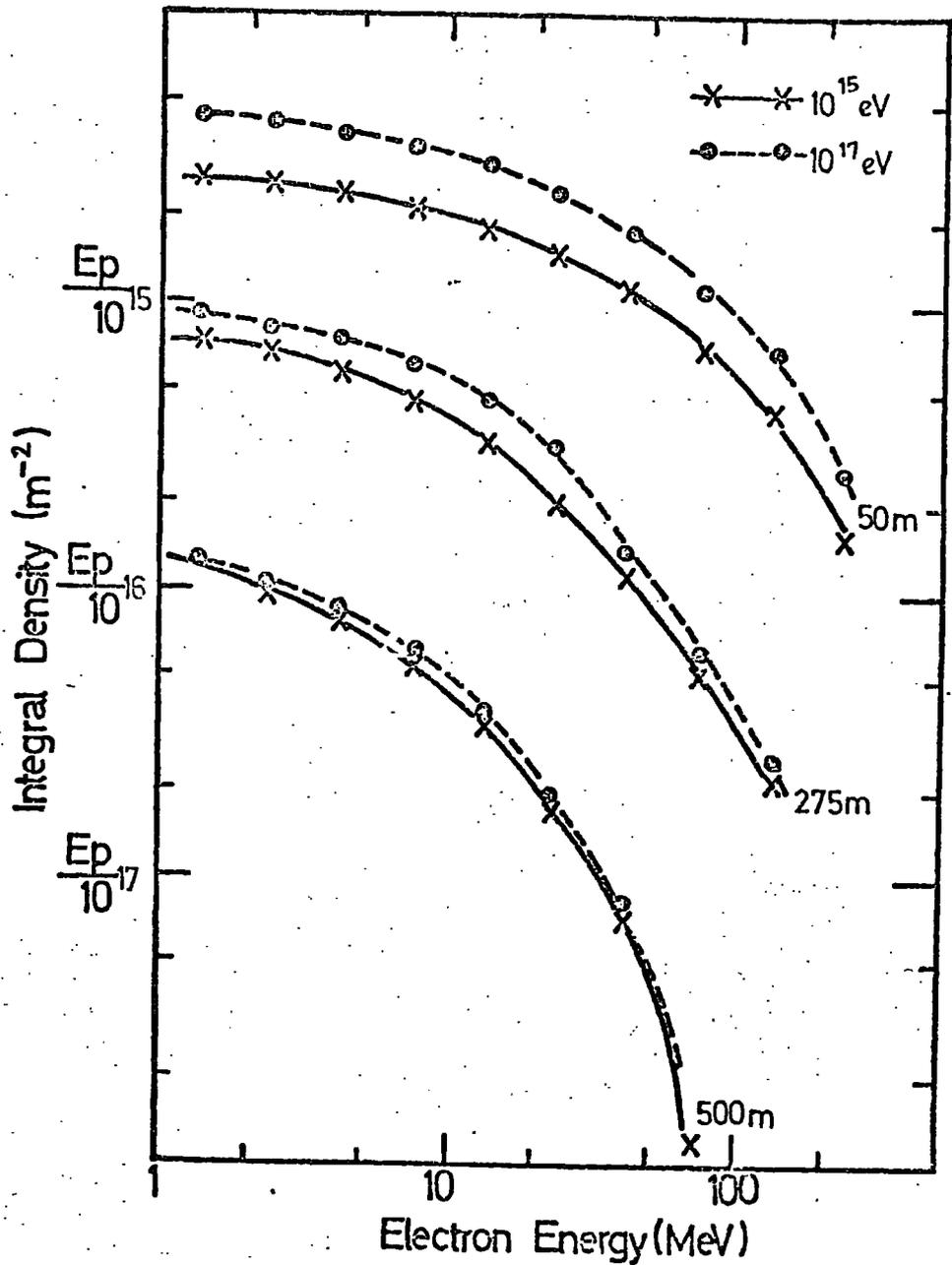
Figure 4-4(b)

The integral energy spectra of electrons in proton initiated EAS. The densities are obtained by dividing the appropriate primary energy (in eV) by the indicated figures.
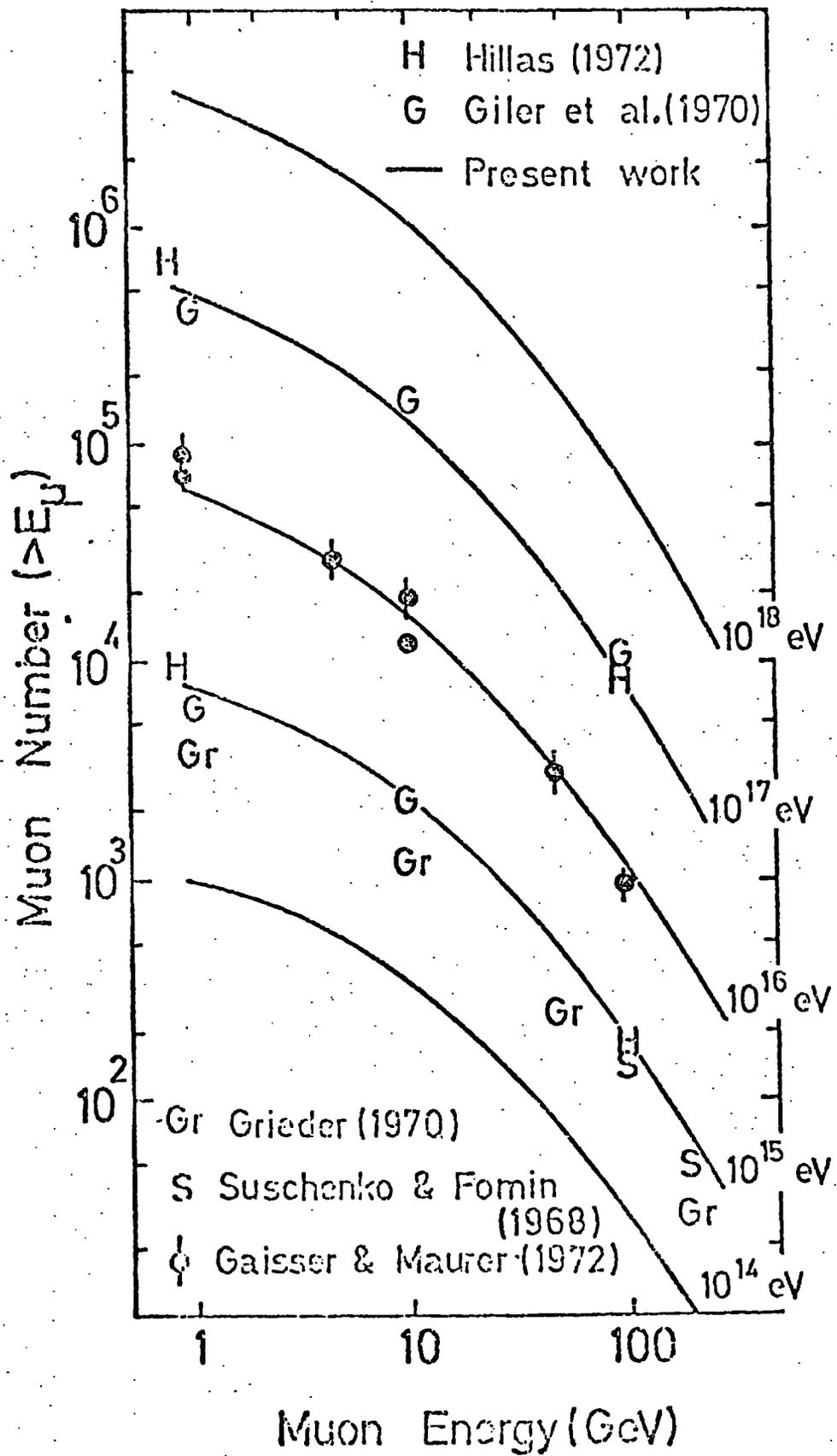
Figure 4.5

Comparison of the muon integral energy spectra for primary energies in the range 10^{14}-10^{18} eV from present work with the results of other simulations

and Fomin (1968) and Gaisser and Maurer (1972). The model of
Hillas with which comparison is made is Model E. This model is
essentially the same as our 'normal' model for interactions but
differs slightly in that the mean free path of pions is assumed to
be 100 g.cm.$^{-2}$ and the inelasticity of p-N collisions is 0.44
(as opposed to our 'normal' values of 120 g.cm.$^{-2}$ and 0.5 respectively);
the predictions of model E are made for a zenith angle of 14°. The
small difference in the results between Model E and our 'normal'
model is explicable in these terms.

Hillas defines $\alpha = d \ln (N) / d \ln (E_p)$

.(N is the number of muons and E_p is the primary energy); for Model
E the value of α is predicted to be 0.92 for a muon threshold energy
of 1 GeV. The present simulations also predict the value of α to
be 0.92.

4-2.2.3 The Lateral Distribution of Muons

Predictions of the lateral distribution of muons are more relevant
to experimental measurements than predictions of the muon total energy
spectrum since the lateral distribution is directly measurable. For
example at the Haverah Park experiment this measurement can be made
for muons with a threshold energy of 0.3 GeV using the Nottingham
detector comprising flash tubes and liquid scintillators (Armitage
(1973)) and for muons with a threshold energy of 1 GeV using the
Durham muon spectrograph (Dixon et al.(1973(a))). The lateral
distributions for muons with both these threshold energies are compared
with experimental results in Fig. 4-6. The form of the lateral
distribution found experimentally by the Durham group is

$$\Delta_\mu (>1\text{GeV},r) \quad \alpha \quad r^{-0.75} (1 + (\tfrac{r}{320}))^{-2.5} \quad m^{-2}$$

Legend:
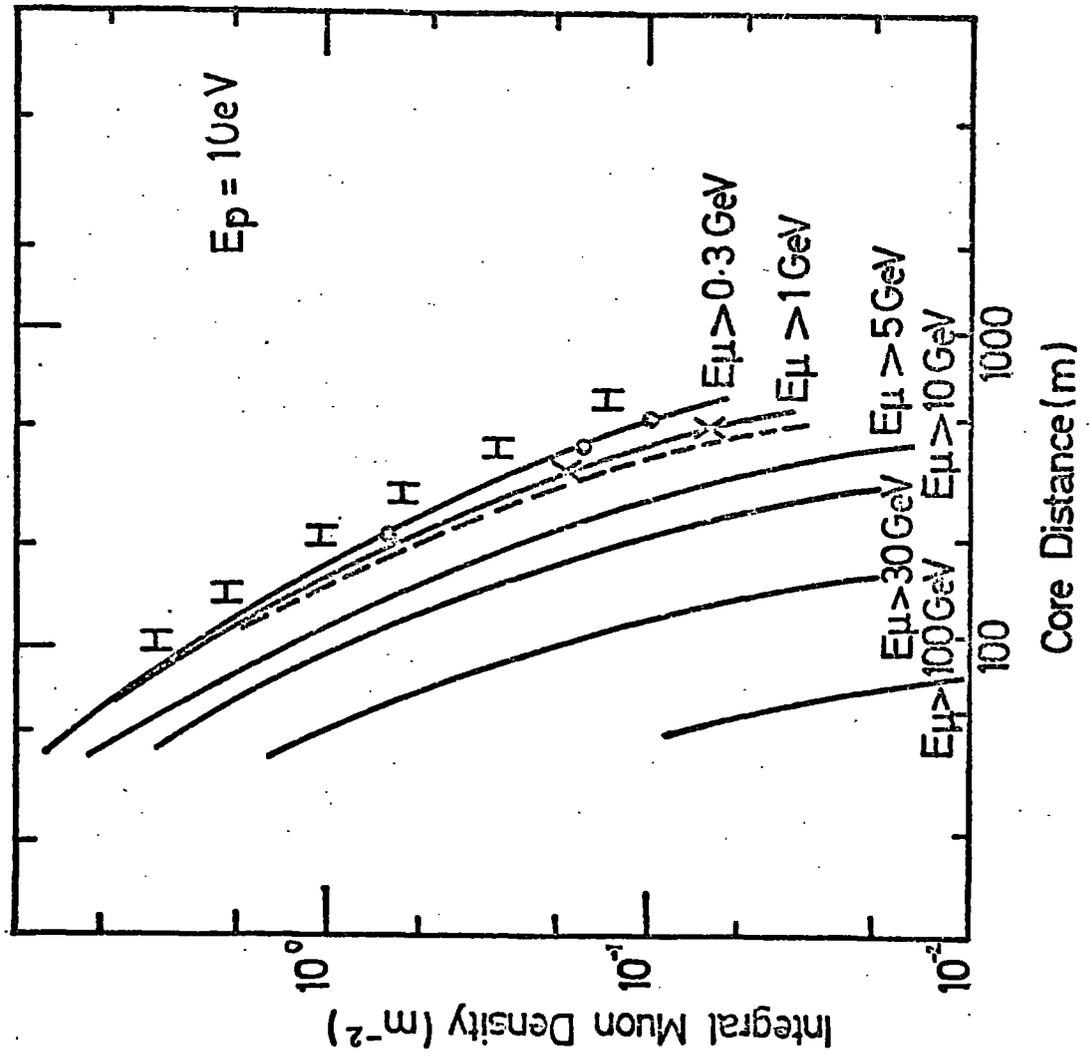
— Present work

H Hillas (1972) (>0.8 GeV)

----- de Beer et al (1966)
(Eμ>1GeV; normalised at 100m)

● Armitage et al.(1973)
(Measurement, Eμ > ·3 GeV)

X Dixon et al (1973)

(Measurement, Eμ>1GeV)

Figure 4.6

Comparison of the muon lateral
distributions for muons above
various threshold energies
from the present work with
experimental data and results
from other simulations

Plot labels:

$E_p = 10eV$

$E_\mu > 0.3$ GeV

$E_\mu > 1$ GeV

$E_\mu > 5$ GeV

$E_\mu > 10$ GeV

$E_\mu > 30$ GeV

$E_\mu > 100$ GeV

Core Distance (m)

Integral Muon Density (m^{-2})

and the Nottingham group find their data best fitted by

$$\Delta_\mu (>0.3GeV, r) \propto r^{-1} (1 + \frac{r}{276})^{-2.1} m^{-2}$$

(r is in metres in both cases).

Fig. 4-7 compares the differential momentum spectra of muons from EAS initiated by 10^{17} eV proton primaries at various zenith angles and distances from the shower core with experimental data obtained by Dixon et al. (1973(a)), and Machin et al.(1970); the experimental data refer to air showers with zenith angles less than 40°. Clearly there is good agreement between the predictions and the experimental data.

4-2.2.4 The Temporal and Spatial Characteristics of Muons in

Air Showers

The temporal and spatial characteristics of muons in air showers would be expected to reflect the longitudinal development of EAS and hence may be of use in the determination of the nature of the primary cosmic radiation. The pulse profiles of the deep water Cerenkov detectors at Haverah Park from both the muon and electron-photon components have been studied by Lapikens et al.(1973) and the angular distribution of muons with respect to the shower core direction has been measured by Earnshaw et al.(1973).

The temporal and spatial effects arising from the geometrical effects alone are considered here but work has been done as a part of the present study to find the effects of Coulomb and geomagnetic scattering upon these characteristics (Turver (1974)). As a result of this work it was found that the predictions from the 'step-by-step' and hybrid computational techniques do not differ significantly from those obtained by the more detailed computation for muon threshold energies $\geqslant 1$ GeV; for lower threshold energies the differences in
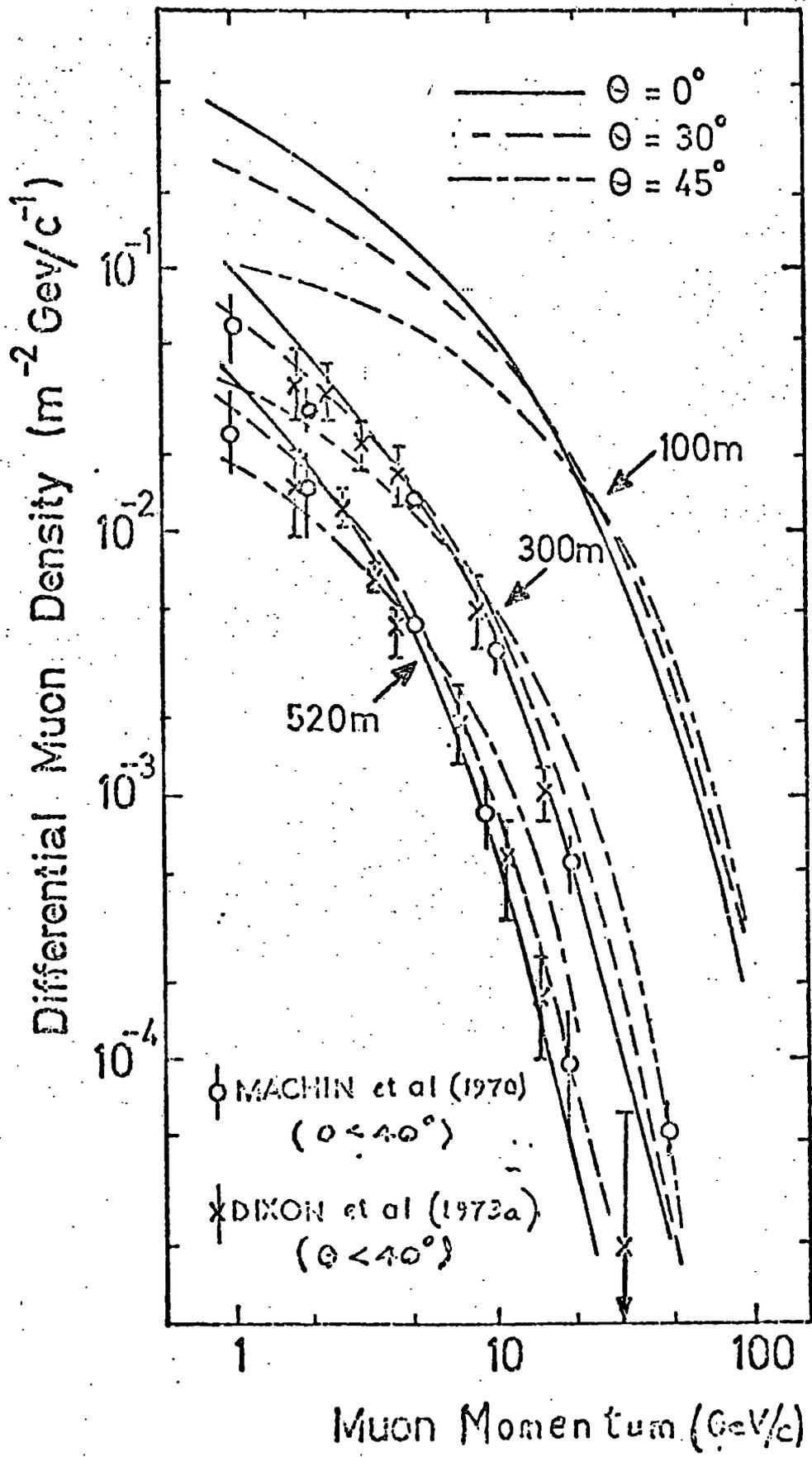
Fig. 4·7

the predictions may become very marked.

Fig. 4-8 (a) shows the way in which the median time delay and median core angle vary with primary energy, and Fig. 4-8 (b) gives the model predictions for the variation in these parameters with distance from the air shower core. Also shown in Fig. 4-8(b) is a comparison of the variation of the mean muon angle to the core found experimentally at Haverah Park with the predictions from these simulations for this parameter.

4-2.2.5   Effects of the Inclusion of Geomagnetic and Coulomb

Scattering on the shape of the Muon Lateral Distribution

The results obtained from the 'hybrid' and 'step-by-step' computational techniques for the muon lateral distribution were rather steep by comparison with experimental data, an effect noted previously in many comparisons (eg de Beer et al. (1966)).

It seemed likely on the basis of the work of Hillas (1966) that the cause of this steepness might be the absence of Coulomb and geomagnetic scattering from the model and it was decided to repeat some of the simulations dealing with the muons in detail. This work, was undertaken by W. Stephenson; the simulation techniques described in Chapter 3 were used to the point where the pion production spectrum had been formed. To have dealt in a detailed manner with all the pions produced in an EAS of primary energy of (say) 10^{17}eV would have involved excessive computing time; instead, only a fraction of the pions were followed. The way in which the selection of the pions to be followed was made was to randomly attribute an azimuth angle to each pion and only consider those pions within a particular range of azimuth angle, the geomagnetic and Coulomb scattering were calculated in each of 40 atmospheric depth intervals

Fig. 4·8(a)
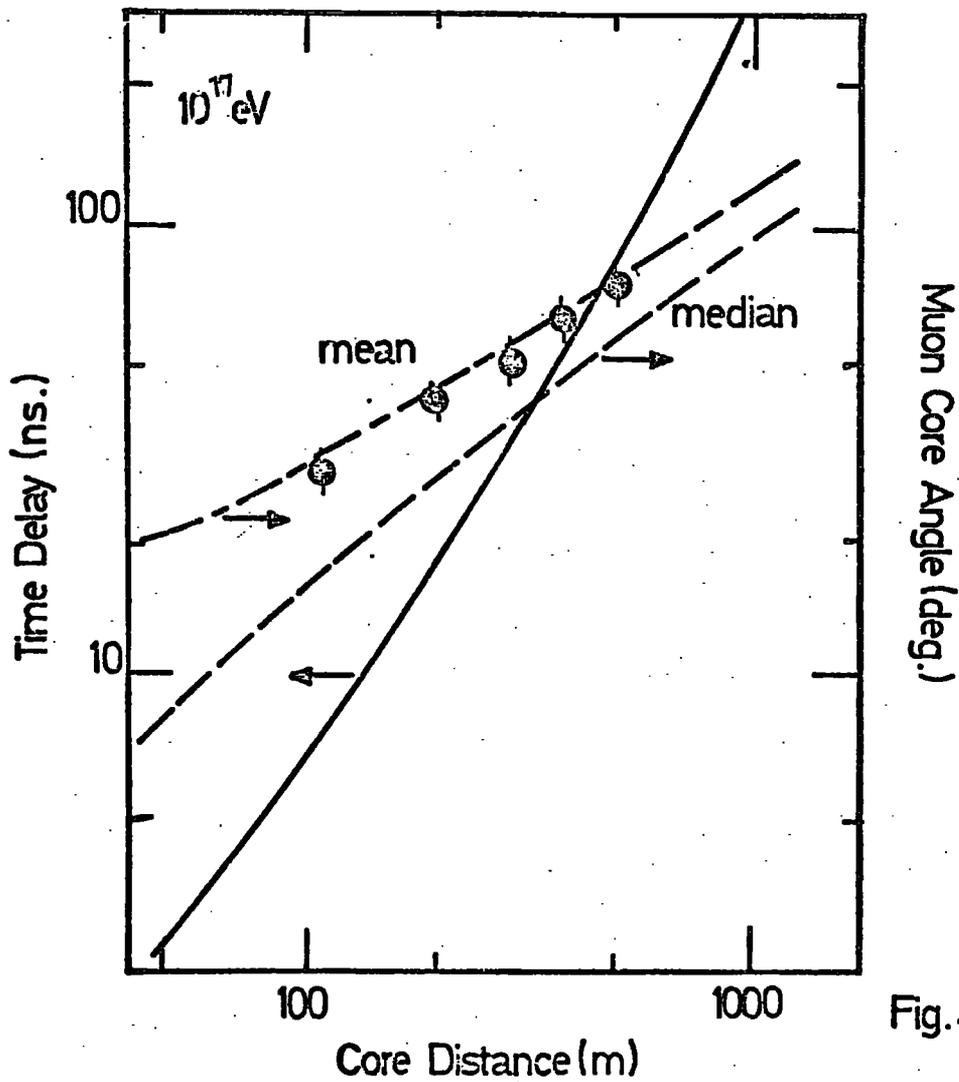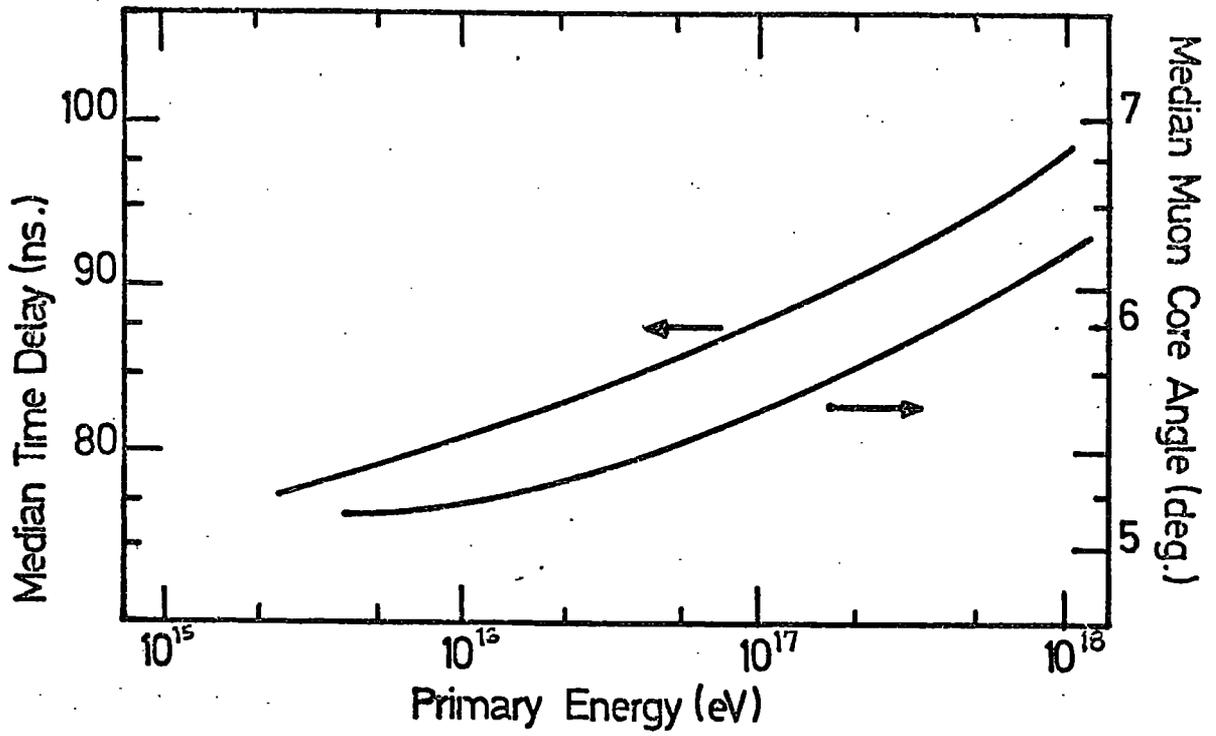
Fig. 4·8(b)

of width 25.8 g cm^{-2}. The rms Coulomb scattering angle was found by

assuming a normal distribution specified by:-

$$< \theta > = \frac{E_s}{p\beta c} \sqrt{\frac{x}{x_o}} \text{ where } E_s = \text{scattering energy}$$

~~where~~ p is momentum, x is distance travelled in g cm^{-2}, and x_o

is the radiation length in air in g cm^{-2}.

A detailed description of the method of calculation of the

geomagnetic deflection is given by Pickersgill (1973). The

predictions for the muon lateral distributions above various

threshold energies shown in Fig. 4-6 are the result of the

inclusion of coulomb and geomagnetic scattering in the calculation.

4-2.3 The Hadronic Component of EAS

The 'normal' model for nucleon-nucleus interactions does

not take into account the possible production of nucleon anti-

nucleon pairs although it is acknowledged that in high energy

interactions (E$_p > 10^7$ GeV) as many as 14% of the secondary particles

could be nucleon-antinucleon pairs (Tonwar et al (1971)). The present

work is being extended by I.S. Diggory to include predictions for

models which incorporate the production of nucleon-antinucleon pairs

in high energy interactions. For air showers simulated using the

'normal' model only one nucleon arrives at sea level in a proton

initiated EAS and this is the survivor of the primary particle. The

hadronic component therefore comprises pions and this single nucleon

(which is frequently ignored).

The predicted lateral spread of the pion component of the air

shower at sea level is shown in Fig. 4-9 for 10^{15}eV proton initiated

EAS. Comparison is made with the simulation results of Grieder

(1970) although it should be noted that the models for high energy

interactions differ considerably and that the good agreement is

perhaps fortuitous. The lateral distribution for pions in air
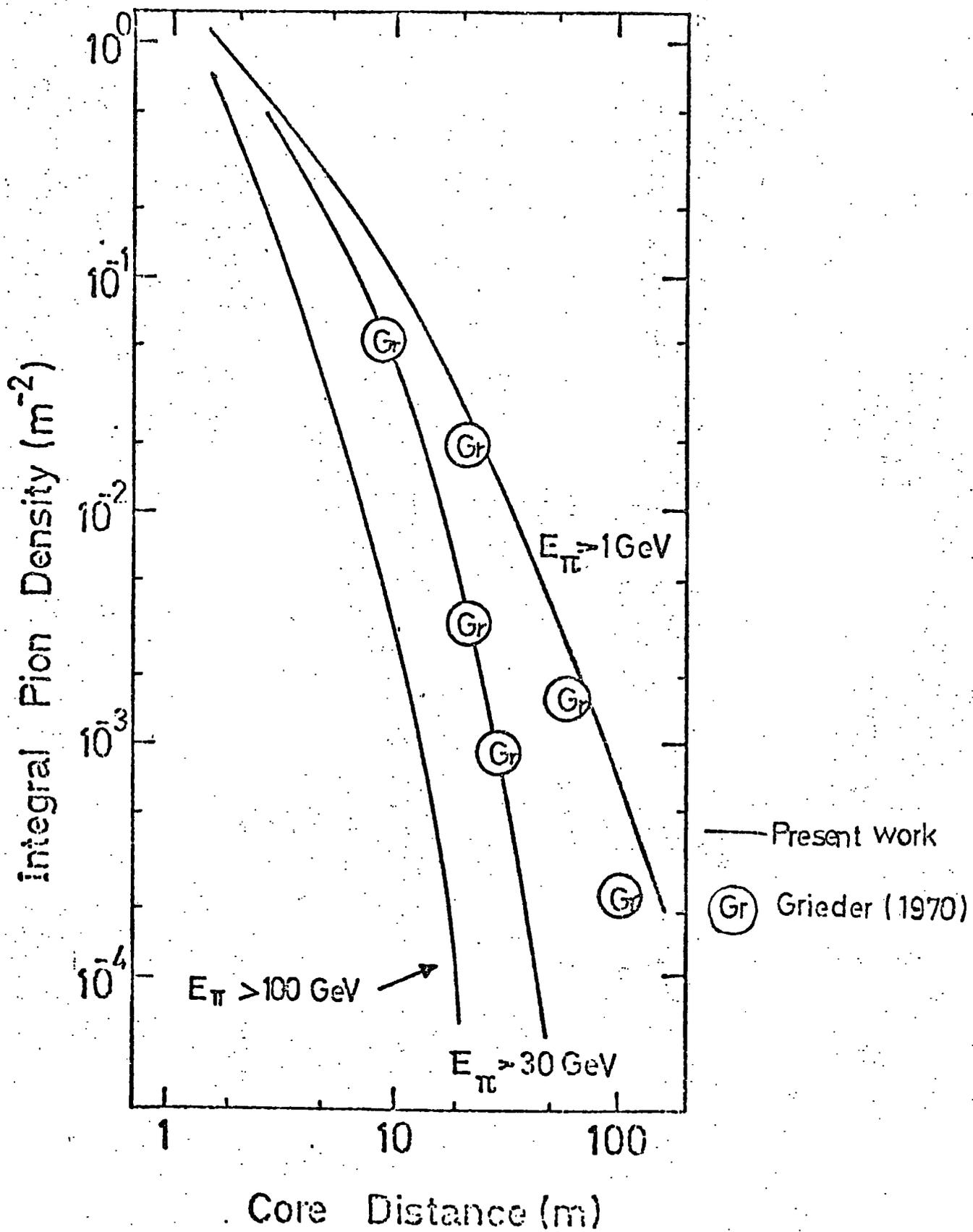
Figure 4.9

Pion lateral distribution for energy thresholds of 1 GeV, 30 GeV and 100 GeV.

showers is steeper than the lateral distribution of muons; the reason for this is that only those pions produced close to the observational level have a high probability of neither decaying nor interacting.

4-2.4 The Deep Water Cerenkov Detector Response

In order to interpret the data obtained from the Haverah Park EAS array, it is necessary to be able to predict the response of the deep water Cerenkov detectors which are characteristic of the experiment to air showers of various primary energies and core locations. The detectors respond to both muons and the 'soft' component of the showers (electrons and photons). The response is calculated in units of so-called nominal particles defined as the ratio of the detector signal corresponding to a particular event to the signal produced when a single relativistic muon traverses the detector (v.e.,µ). Marsden (1971) used a Monte Carlo electron-photon cascade program in order to describe the one-dimensional propagation in 120 cm of water of the cascade which results when an electron or photon is produced at a known height above a water filled Cerenkov detector of the type used at Haverah Park. In order to obviate the need to publish numerous tables, Marsden fitted his data to a function of the form

$$\Delta_{soft} (r,s,a) = \ln (a) \left(\frac{r}{r_o}\right)^{s-2} \left(\frac{r}{r_o} + 1\right)^{s-4.5} v.e.\mu.m^{-2}$$

where r_o = 80m at sea level; he produced tables of s and ln (a) for both initiating electrons and photons of several different energies (1, 3.16, 1C, 31.6 and 100 GeV) produced at various atmospheric heights. These results were combined directly with the solution of the electron photon cascade under approximation A (see Appendix 3) in order to allow the Cerenkov detector response to be predicted for the present work.

The results from the 'normal' model for the lateral distributions

of the deep water Cerenkov detector response are shown in Fig. 4-10

for proton initiated showers for the primary energies 10^{17}eV and

10^{18}eV.

4-2.5 The Optical Cerenkov Light and Radio Emission from EAS

Detailed accounts of the computation of the optical and radio

frequency emission from large EAS from the present study are given

by Smith and Turver (1973) and Hough (1973).Figs 4-11(a) and 4-11(b)

show the lateral distribution functions for radio frequency and

optical Cerenkov emission from air showers initiated by primary

protons of energy 10^{15}-10^{17}eV.

4-2.6 The Ratio of the Muon Density to the Cerenkov Detector Response

in EAS

One of the measurements made by the University of Nottingham

group at Haverah Park (Armitage (1973)) is the ratio of the muon

density to the Cerenkov detector response as a function of distance

from the shower core, $\frac{\Delta\mu}{\Delta c}$. In some previous comparisons of model

predictions and experimental measurements the ratio $\frac{\Delta\mu}{\Delta_c 0.75}$ has been

used (see eg. Hillas (1972), Ferguson (1971)). The reason for using

this ratio was that its dependence on the core distance at which

the measurement is made is not strong and therefore the effect of

possible core location errors is minimised. However the disadvantage

of using $\frac{\Delta\mu}{\Delta_c 0.75}$ rather than $\frac{\Delta\mu}{\Delta c}$ is that it is less sensitive to

differences in models for shower development. Armitage considered

that his experimental data had been subject to sufficiently stringent

selection criteria for the advantages of the use of the ratio $\frac{\Delta\mu}{\Delta c}$

to outweigh those of using $\frac{\Delta\mu}{\Delta_c 0.75}$. Therefore a comparison is made

here of the experiment measurements of Armitage and the predictions

of the 'normal' model for the ratio $\frac{\Delta\mu}{\Delta c}$ (Fig. 4-12). The predicted

values of this ratio are not strongly energy dependent. The results
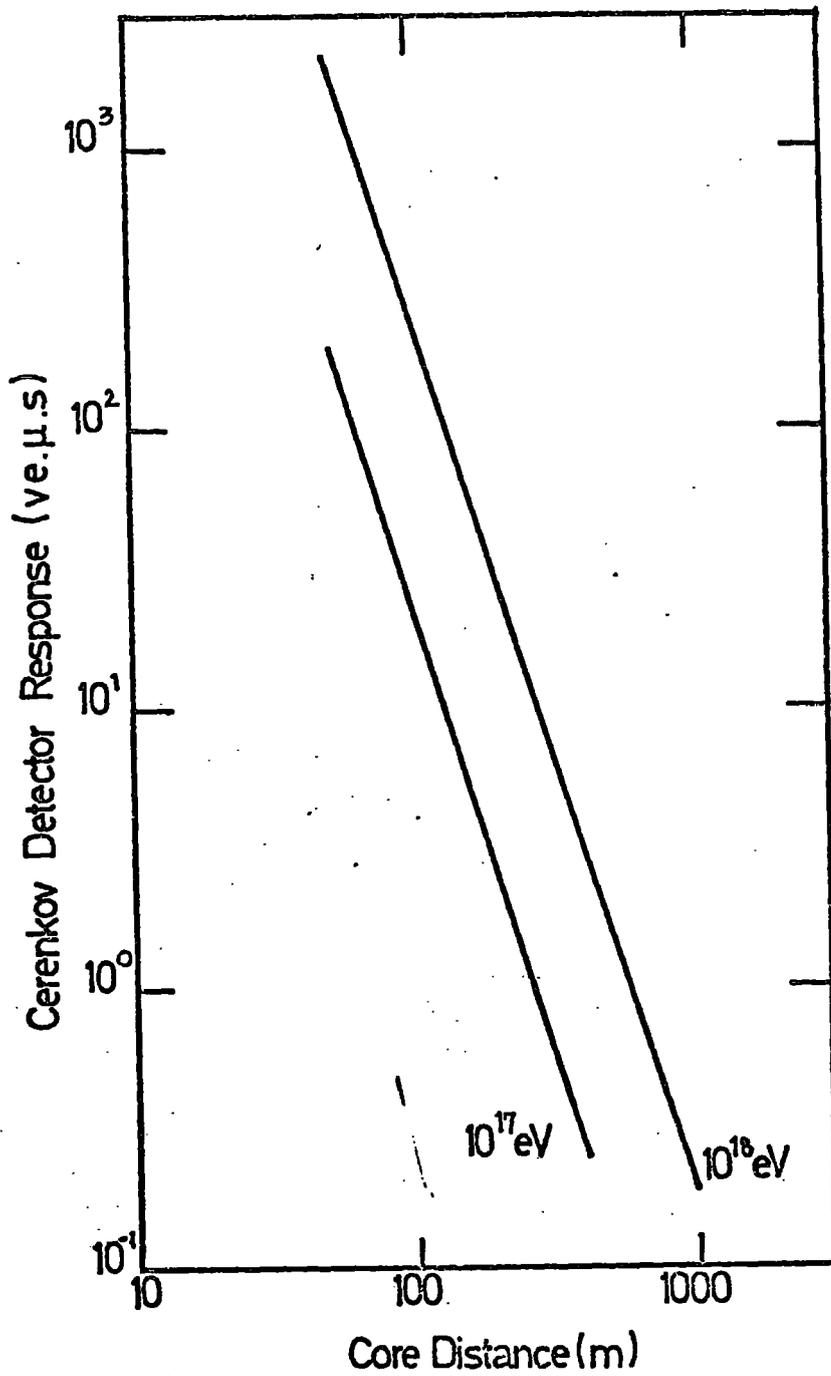
Figure 4-10

The lateral distribution of
the deep water Cerenkov
detector response
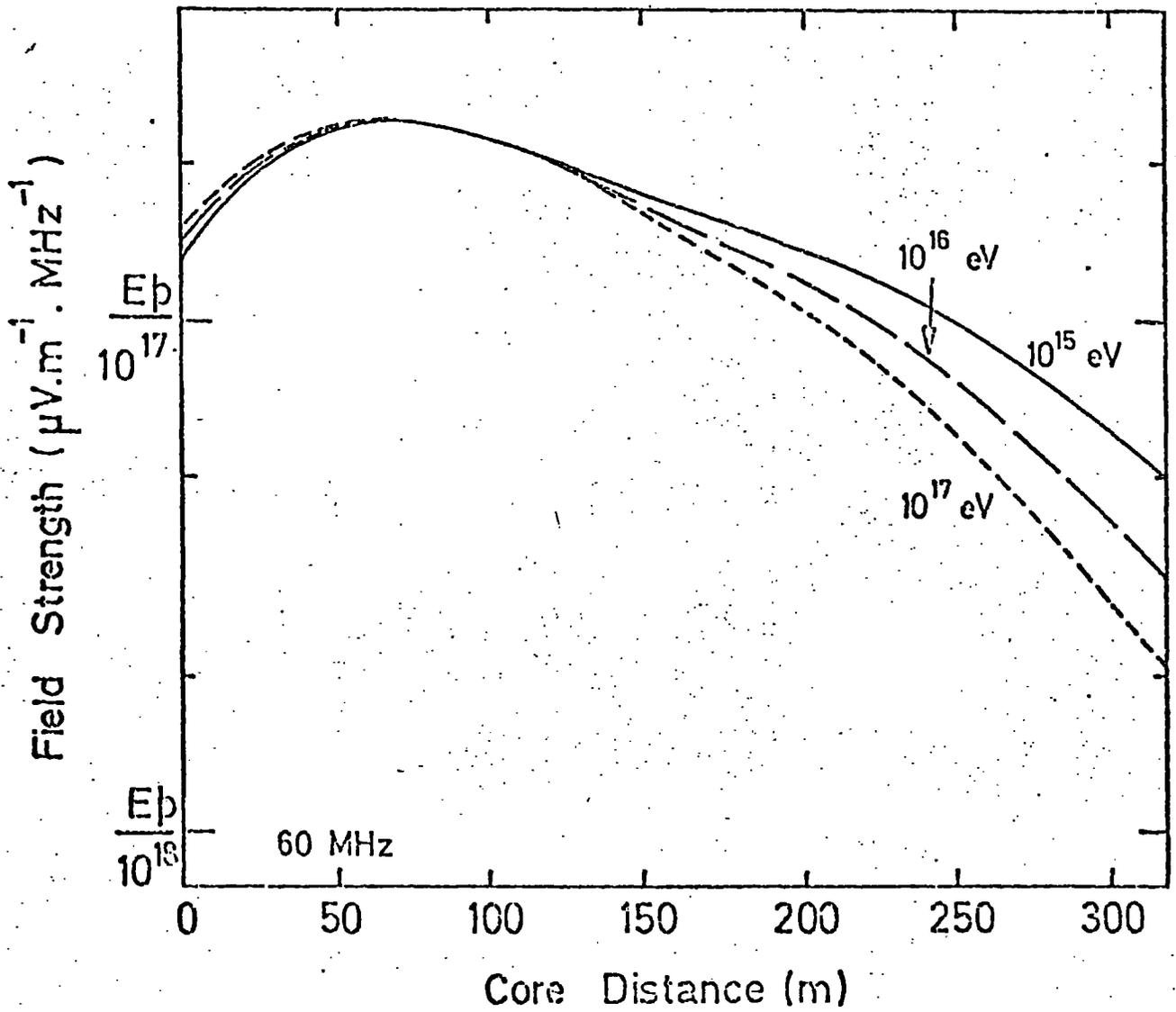
Figure 4.11(a)

The lateral distributions of
the radio emission from EAS
of the primary energy
indicated
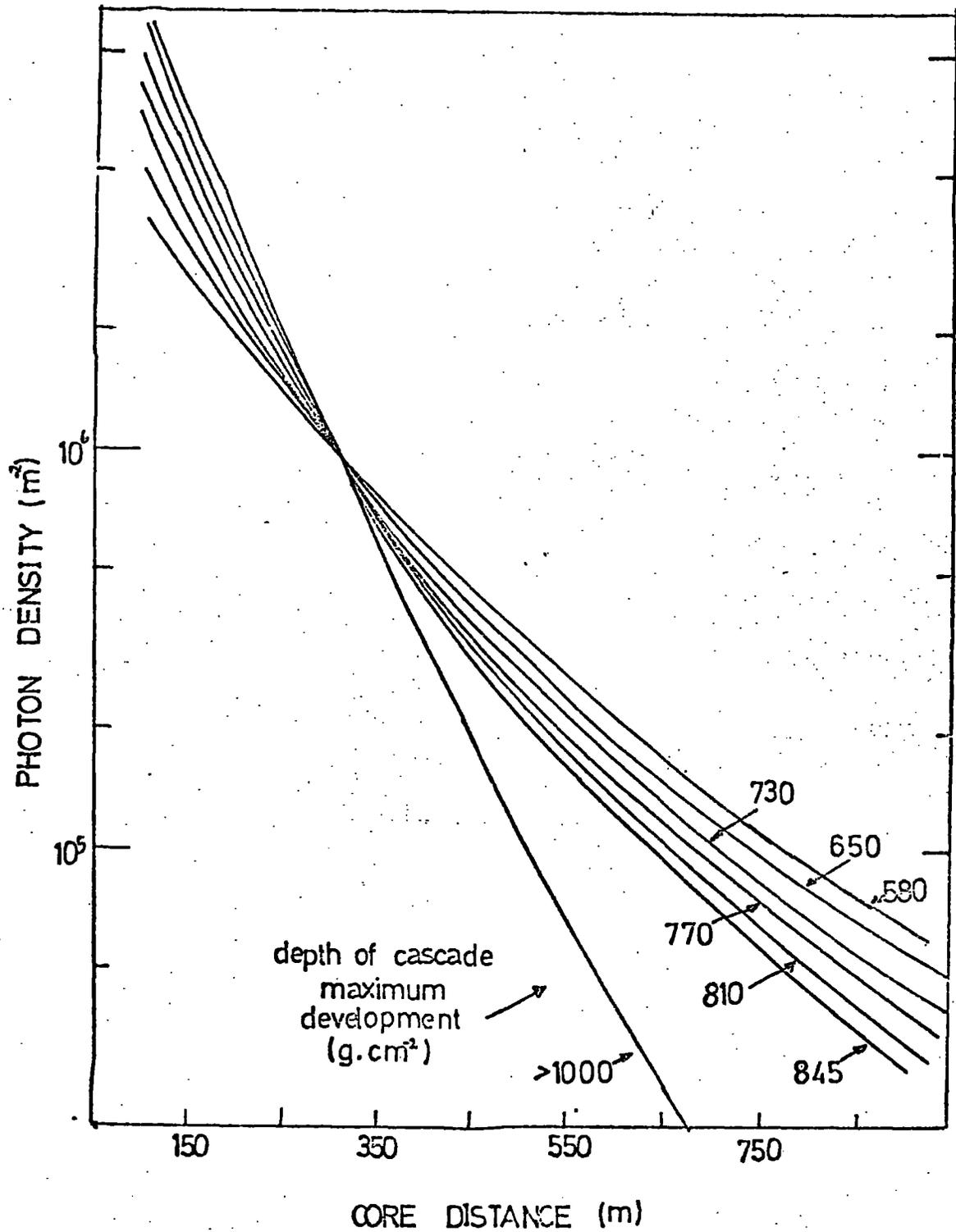
Figure 4.11(b)

The lateral distributions of the optical Cerenkov signal observed from EAS of primary energy 10^{17}eV and with the depths of maximum development indicated.
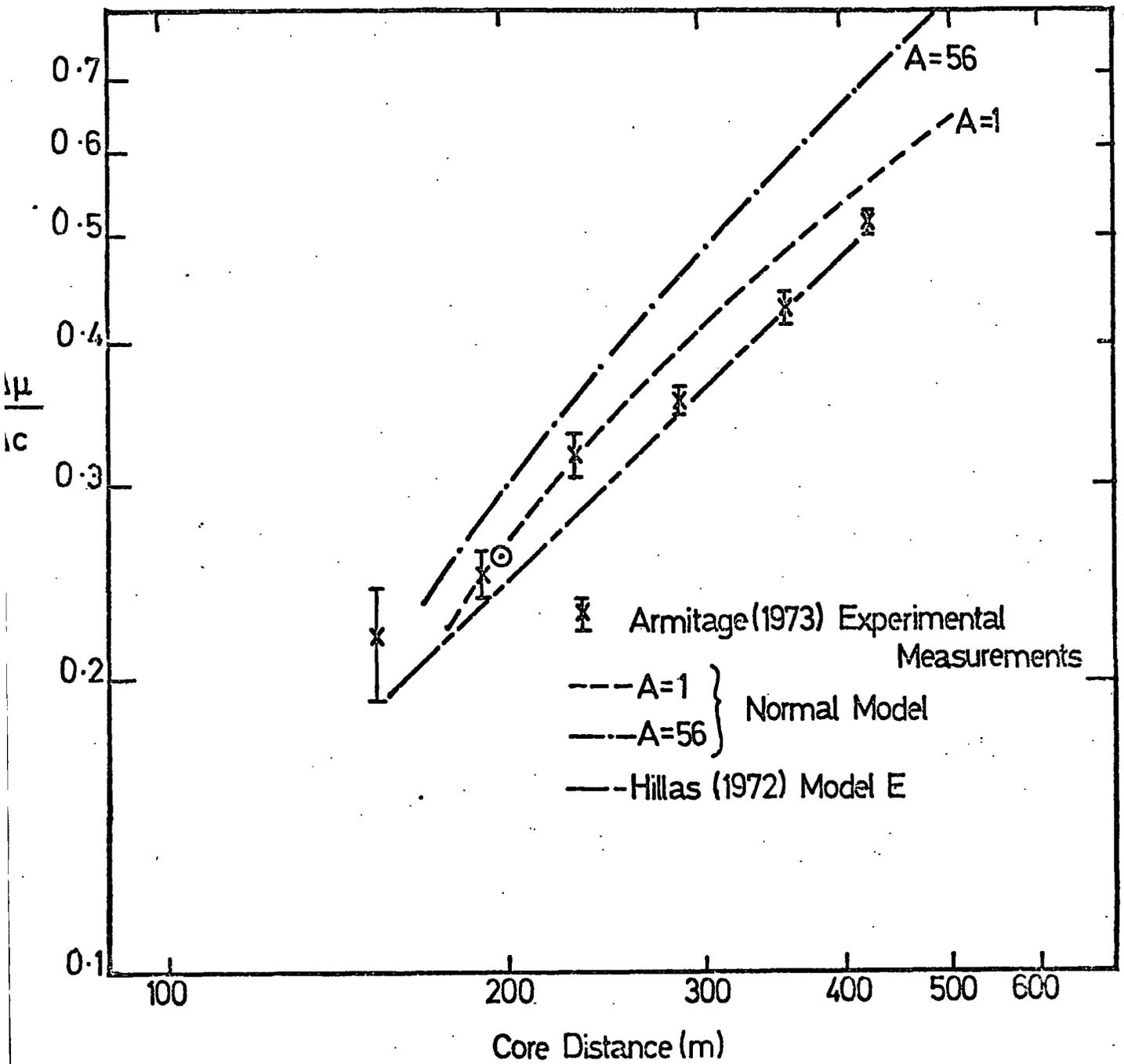
Figure 4.12

The ratio of the muon density to water Cerenkov Detector response as a function of core distance.

shown in Fig. 4-12 are from 10^{17}eV proton initiated air showers (results for 10^{17}eV iron initiated EAS and Hillas (1972) Model E are also shown).

4-3 Sensitivity to Changes in Zenith Angles

So far the results that have been presented have been for vertical air showers. However, in practice most EAS experiments measure showers in a wide range of zenith angle and therefore an investigation has been made into the effect of changing the zenith angle upon some of the shower parameters. The 'step-by-step' computational technique was used to simulate showers at various zenith angles between 0° and 60° but the results of these simulations for zenith angles $>45^{\circ}$ should be treated with caution since no correction for geomagnetic deflection, which becomes increasingly important at large zenith angles, was made.

Fig. 4-13(a) shows the way in which the total muon energy spectrum varies as the zenith angle changes. There is little difference between 0° and 15° but as the angle increases the difference in spectral shape becomes more pronounced. (The fact that the difference between 0° and 15° is small confirms the usefulness of making comparison with Hillas, Model E which considers showers incident at a zenith angle of 14.3°).

The variation of the shape of the lateral distribution of muons (>1 GeV) with zenith angle is shown in Fig. 4-13(b). The effect of increasing the zenith angle is to cause the lateral distribution to become flatter in shape.

The way in which the median muon time delay and muon-core angle vary with zenith angle are shown in Fig. 4-13 (c) for a 10^{17}eV proton initiated EAS.

4-4 The Predictions of the 'Normal' Model for Measurements Made at
Different Observational Levels

The 'step-by-step' computational techniques was used to simulate 10^{17}eV proton initiated air showers giving predictions at atmospheric depths of 530 g cm^{-2} and 830 g cm^{-2} (corresponding to the altitudes of the Mount Chacaltaya and the Volcano Ranch experiments respectively).
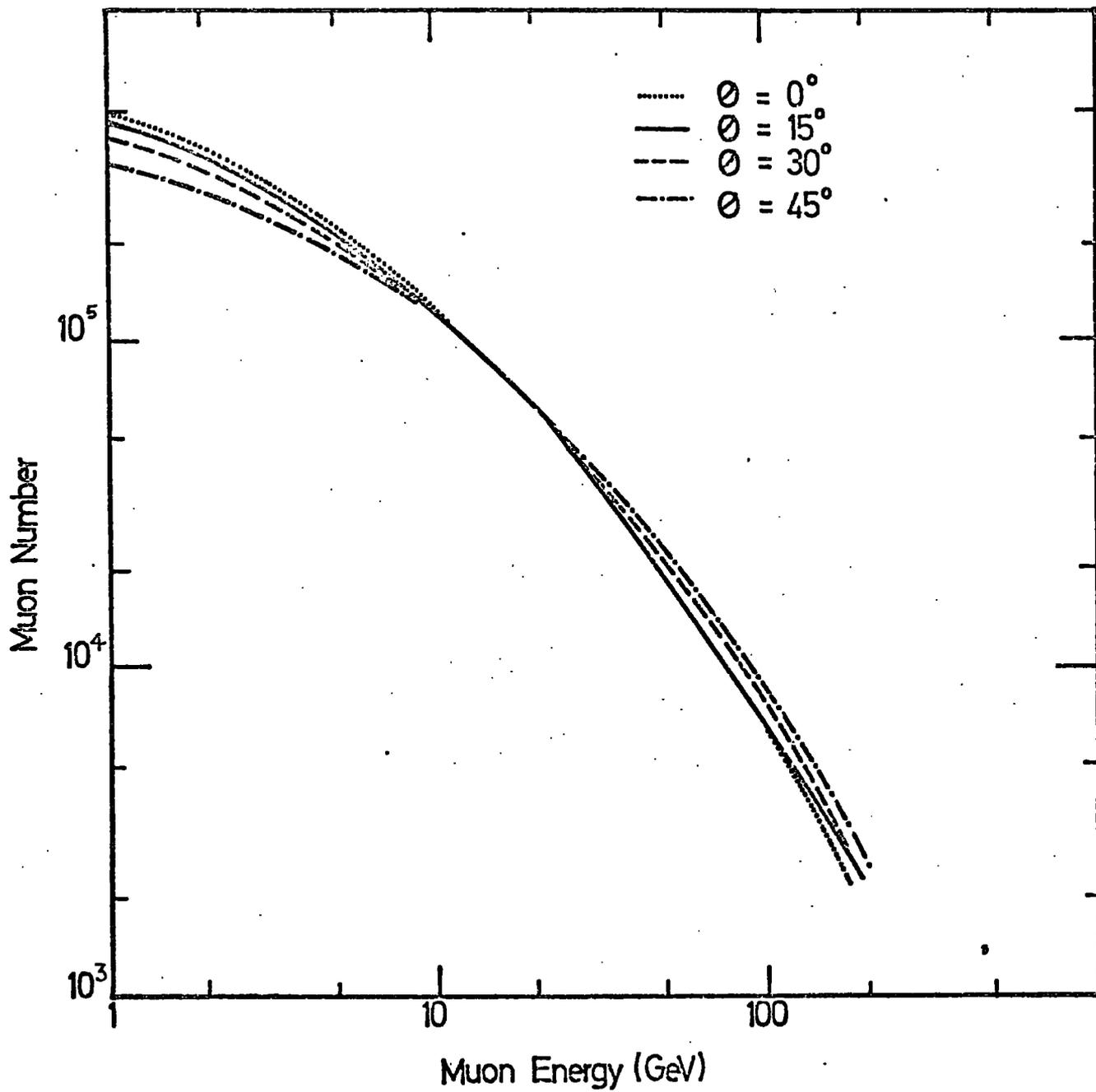
Figure 4-13(a)

Muon total energy spectra

for various zenith angles.
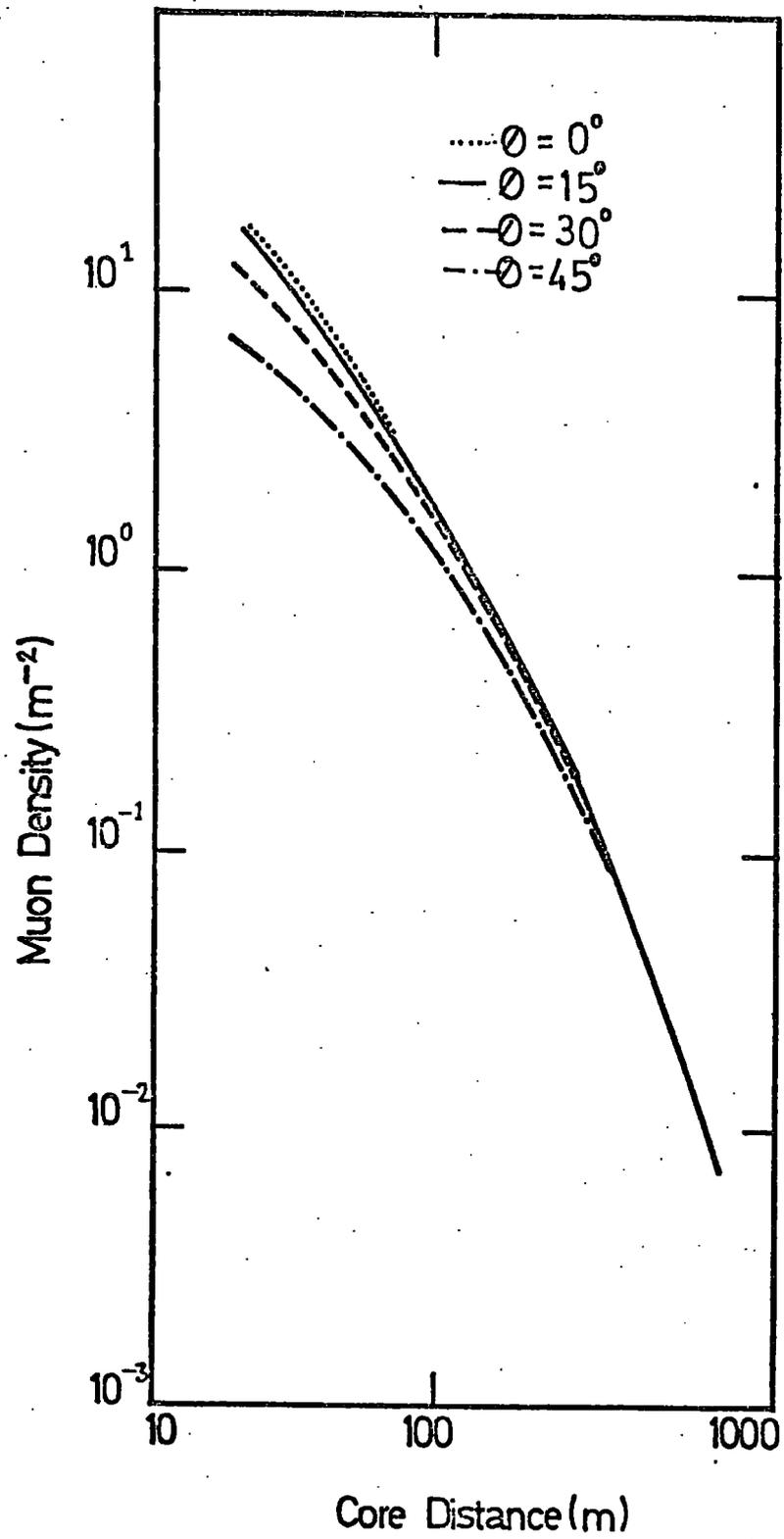
Figure 4-13(b)

Muon lateral distributions
for various zenith angles
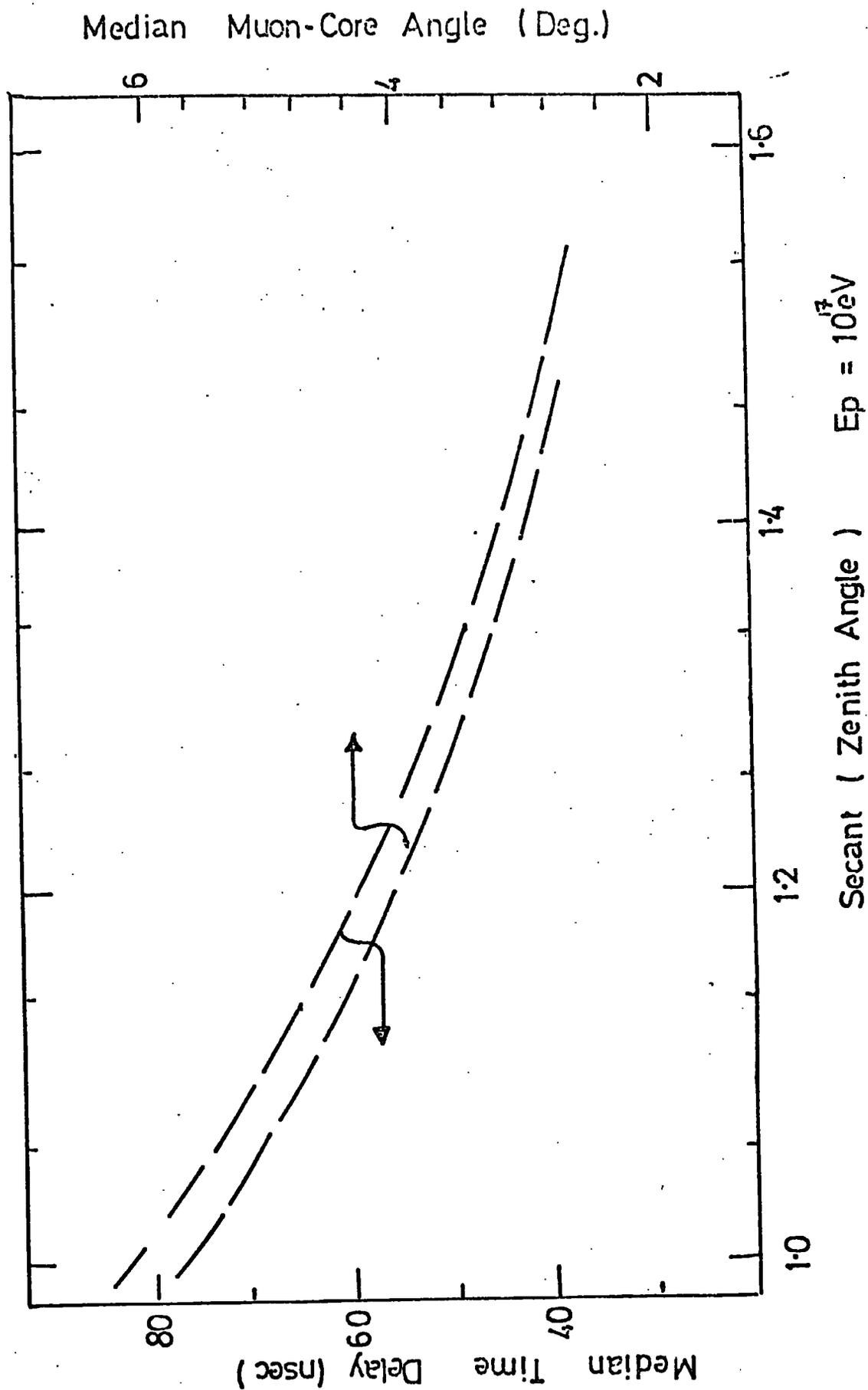
Fig. 4·13 (c)

The predictions of the model for the muon total energy spectra and the lateral distribution of muons (> 1GeV) are shown in Fig. 4-14(a) and 4-14(b). The total number of muons observed at mountain altitudes is less than the number observed lower in the atmosphere at all energies; however, the change in the number of muons (>1GeV) in going from 530 to 830 $g.cm.^{-2}$ is ~200% whereas the change in the number when the observation is made at sea level ($1030g.cm.^{-2}$) rather than at 830 $g.cm.^{-2}$ is ~25%. This results from the fact that the muon number is near maximum at sea level (see Fig. 6-9 and §6-3.2). The lateral distribution of muons steepens as the depth in the atmosphere at which observation is made increases, reflecting the smaller core distances at which those muons produced later in the shower development will be detected. Fig. 4-14(c) shows the way in which the muon number varies with atmospheric depth as a function of the threshold energy of the muons considered. The curves in the diagram refer to results obtained from proton initiated air showers of primary energy 10^{15}eV. The diagram, although not strictly relevant here, is intended to throw light upon variations in the muon component observed in the following sections.

4-5 Effects of Changes in the Model for Nuclear Interactions

4-5.1 Introduction

The reasons for the choice of the 'normal' model for interactions were described in Chapter 3 together with an account of why the choice of such a single model was necessary for the present work. However, in many cases the values taken for parameters were by no means the only reasonable choice and, because of this, simulations have been made to assess the sensitivity of the results to changes in certain
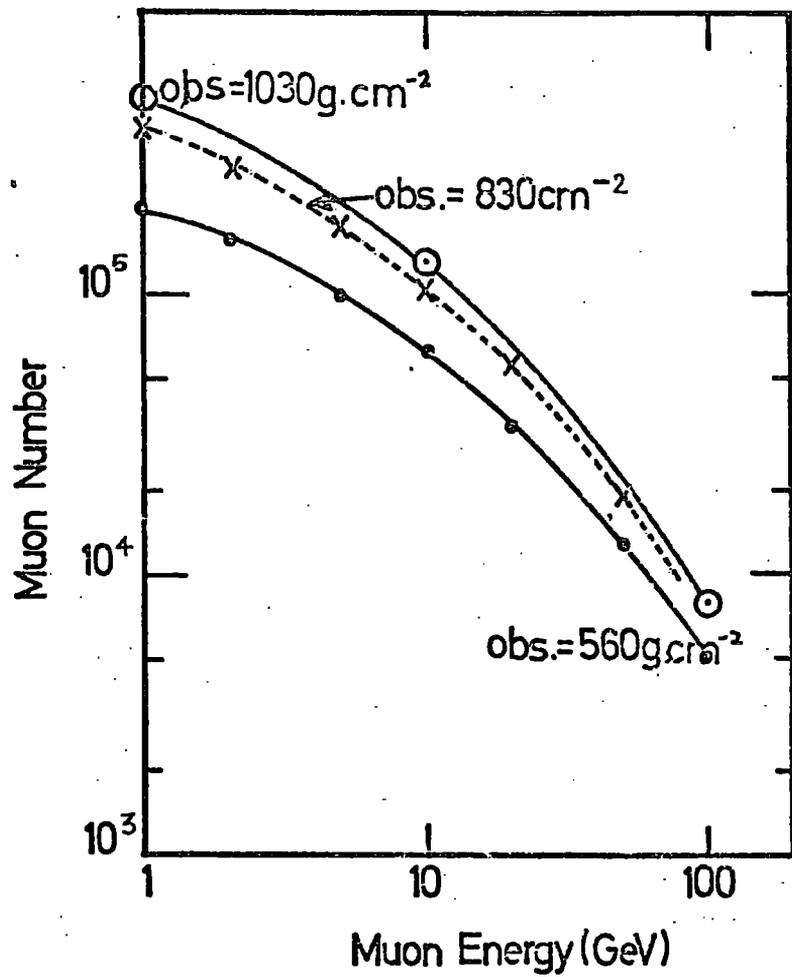
Figure 4-14(a)

Muon total energy spectra for various observation levels
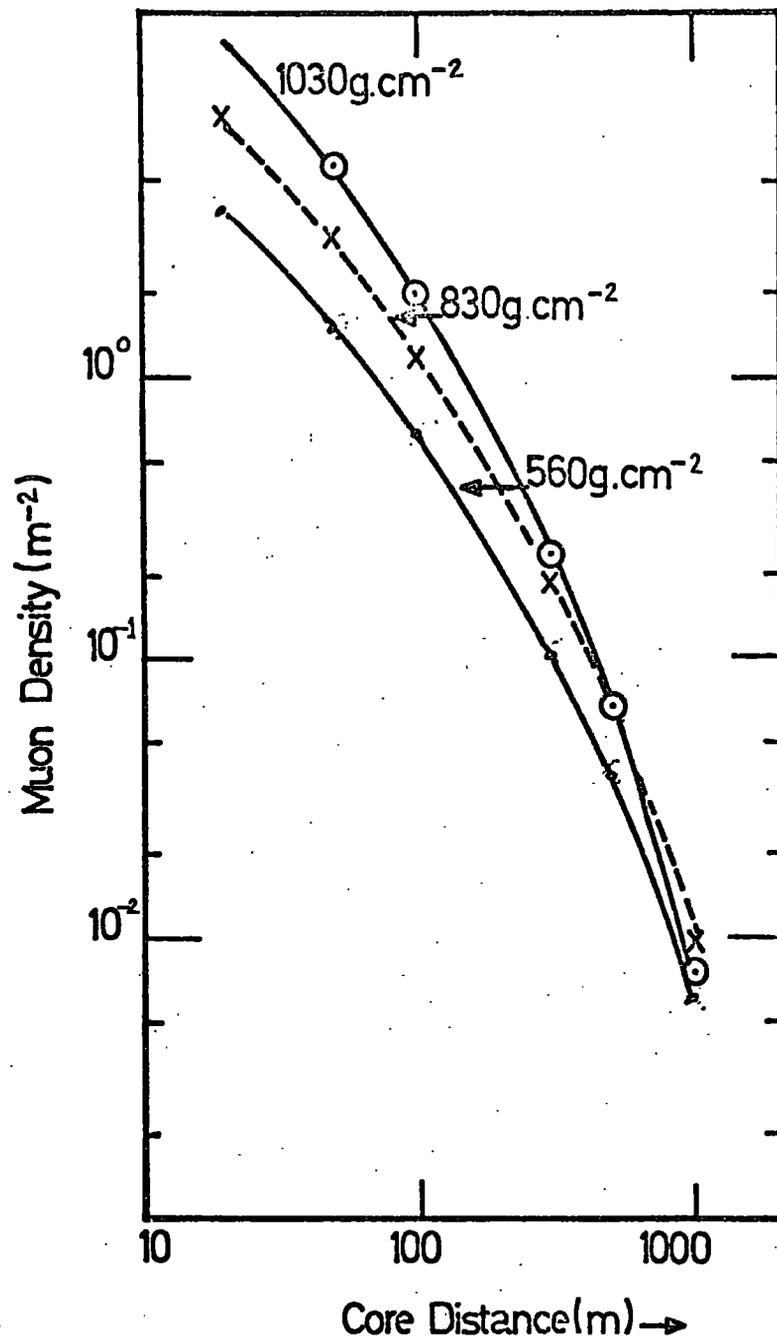
Figure 4-14(b)

Muon lateral distributions for various observation levels
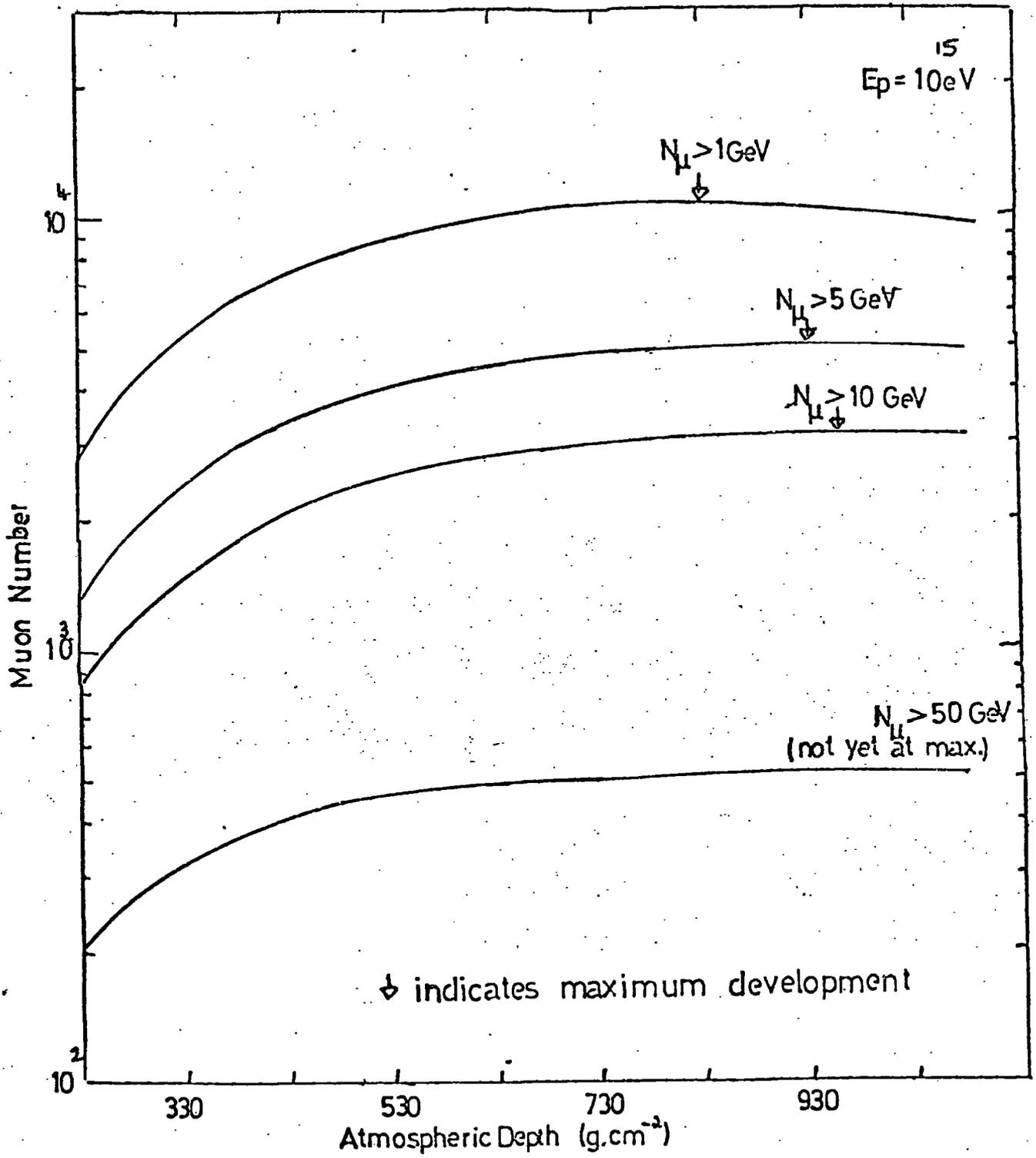
Figure 4.14(c)

The longitudinal development of the muon component in EAS indicated by a 10^{15}eV proton.

of the parameters. It should also be noted that the 'normal' model
was chosen some time ago and it was therefore interesting to see the
effects of altering the model for interactions in the light of
recent accelerator data and new ideas in hadron physics. The large
number of parameters in a shower model and choices of their values
preclude the simulation of all possible combinations; the way in
which the problem was approached therefore was to try to establish
which of the parameters caused significant changes in the way
EAS propagated when their value or distribution was altered. The
results of these investigations are briefly presented in the
following sections.

4-5.2 Variations in the Value of Inelasticity Assumed for p-p
Interactions.

The value of the coefficient of inelasticity, K, for p-p
interactions was taken for the 'normal' model to be 0.5 (see §3-4.2)
(Allowance was made for the difference between p-p and p-N
interactions by adjusting the relationship between the number of
produced particles and the energy of the interactions). The
sensitivity of the model predictions to changes in the inelasticity
were investigated by varying its value between 0.3 and 0.7 for
proton initiated EAS of primary energy $1C^{17}$eV using the 'step-by-
step' computational technique. Figs. 4-15(a) and 4-15(b) give a
comparison of the muon total energy spectra and muon lateral
distributions resulting from these simulations. It can be seen
from Fig. 4-15(a) that the difference in the total number of muons
predicted for values of K between 0.3 and 0.7 is a function of the
threshold energy of the muons. The reason for the number of low energy
muons predicted being less for an inelasticity of 0.7 than for
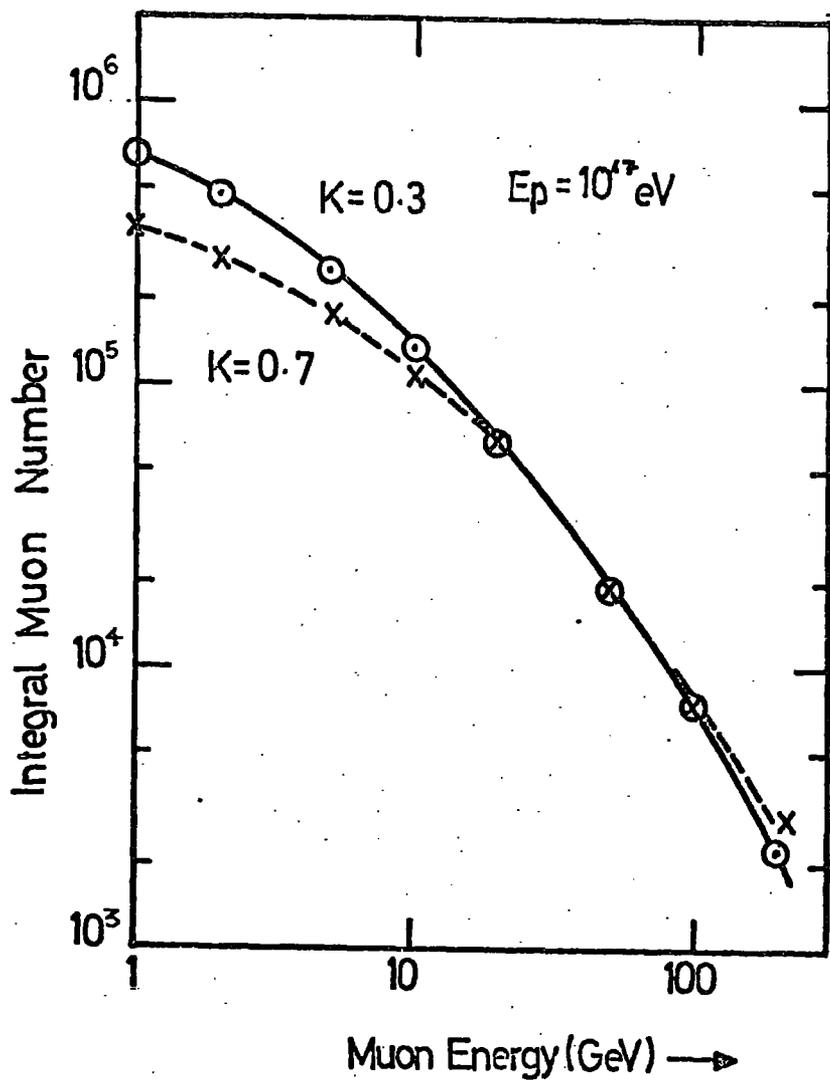
Figure 4-15(a)

The muon integral energy spectra resulting from the present work for proton initiated EAS when the inelasticity is varied from 0.3 to 0.7.
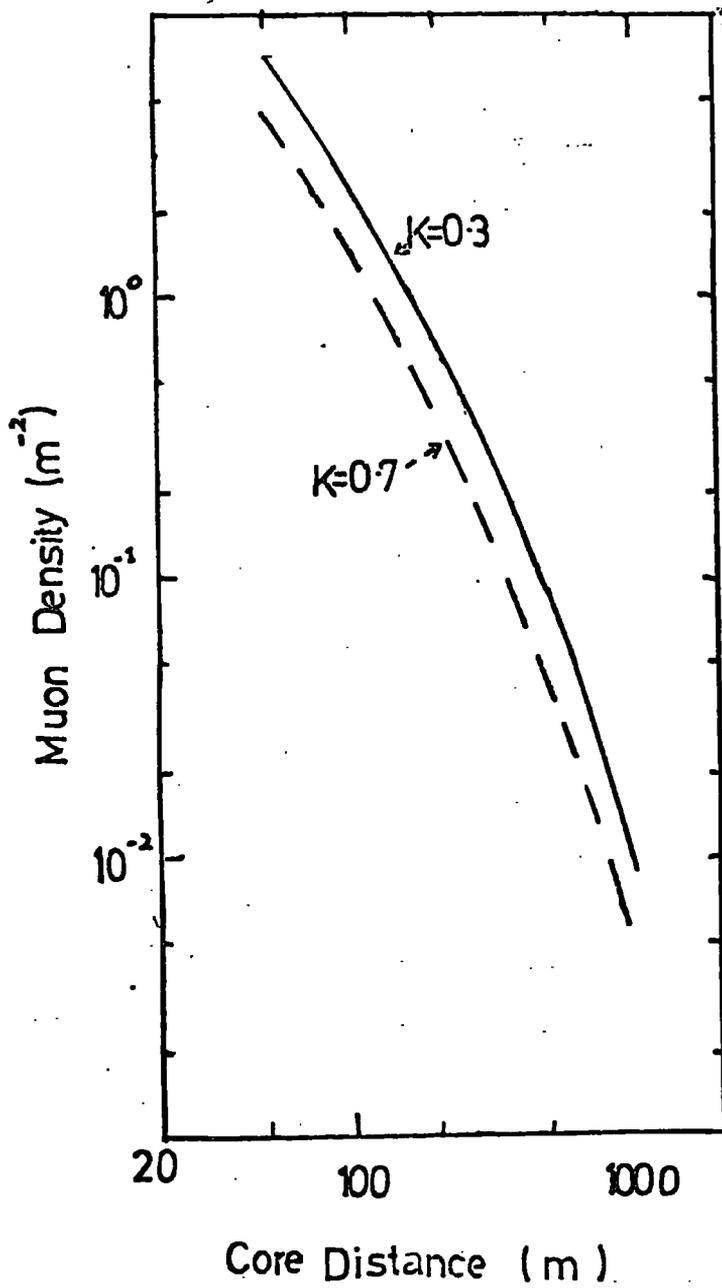
Figure 4-15(b)

Muon lateral distribution

K = 0.3 can be understood by consideration of Fig. 6-9. The result of increasing K is to cause the air shower to develop more rapidly; hence the low energy muons will be further past their maximum number when they reach sea level. Although Fig. 4-14(c) shows the development of muon numbers in 10^{15}eV showers it gives a clear indication of why the threshold energy of the muons affects the change in muon numbers predicted at sea level when K is varied. For example, for >200 GeV muons the development curve for 10^{17}eV air showers could not have reached maximum even for rapidly developing showers (K = 0.7); therefore when the value of K is increased from 0.3 to 0.7 the number of muons >200 GeV is brought closer to maximum and hence increases. The lateral distribution of muons >1GeV remains essentially the same shape when K is varied but the densities are a factor of 2 lower when K is 0.7 than when K is 0.3

Fig. 4-15(c) shows the change in the one-dimensional electron cascade when the coefficient of inelasticity is varied.

4-5.3 Changes in the Assumed Mean Free Paths for Proton-Nucleus and Pion-Nucleus Interactions

Although energy independent values of 80 g cm^{-2} and 120 g cm^{-2} were taken for the mean free paths in air of protons and pions respectively for the 'normal' model, there now exists experimental evidence to support the theory that the p-p interaction cross section rises (see §3-4.4). The consequences of such a trend are discussed in this section. In our initial simulations a variation of the proton mean free path, λ_p, with energy, E_p, of the form $\lambda_p \propto E_p^{-0.066}$ was arbitrarily assumed in view of the suggested decrease in λ_p from cosmic ray data (Yodh, Pal and Trefil (1972)).
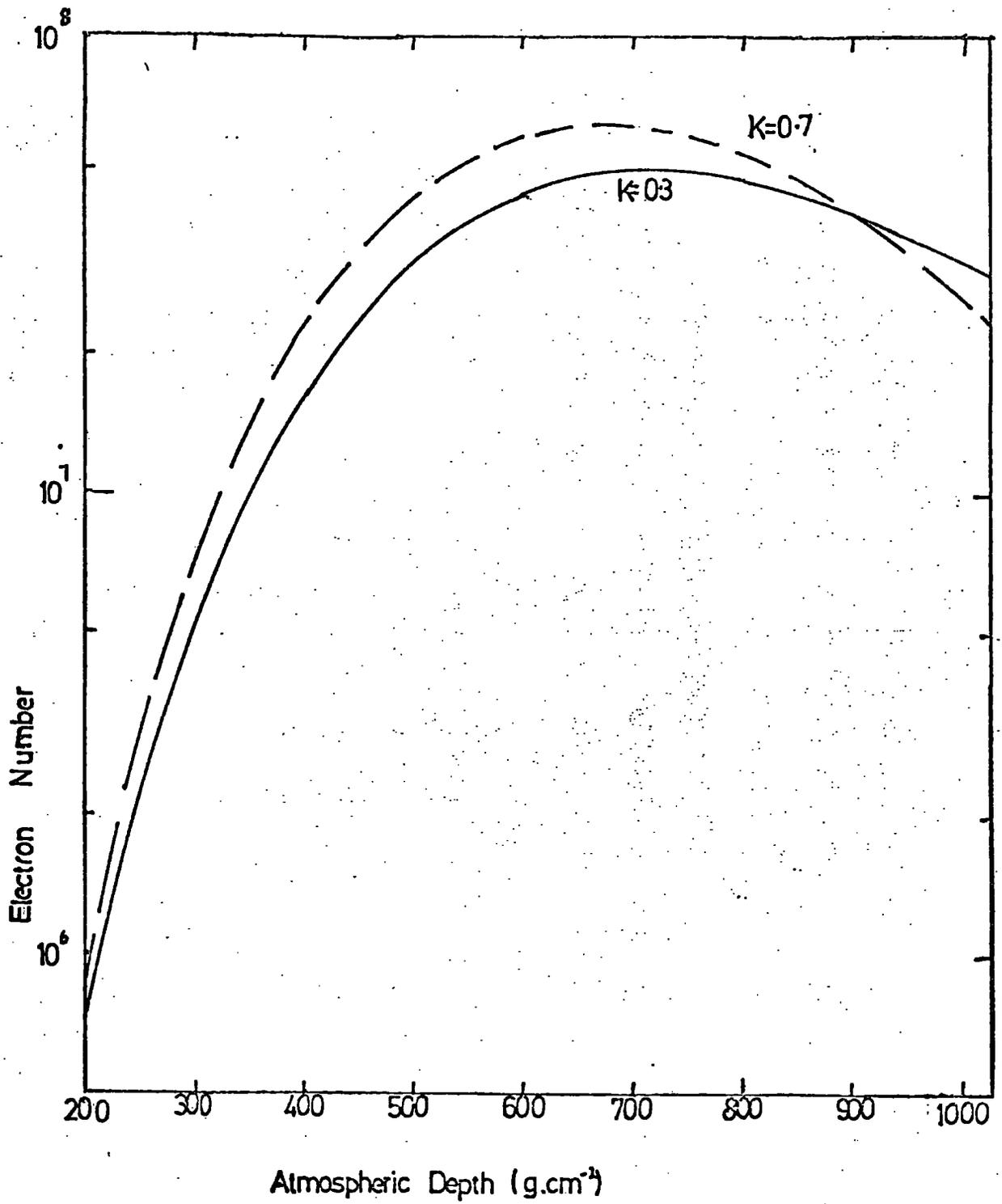
Figure 4-15 (c)

Longitudinal development of

the electron cascade.

A comparison of this relation with the more recent predictions

of Leader and Maur (1973) is shown in Fig. 3-5.

The model most closely related to the 'normal' model of the

present work is Model E employed by Hillas (1972). This model

assumes a mean free path for pions of 100 g. cm^{-2} and therefore

the effect of changing the value of λ_π from 120 g. cm^{-2} (which

is used in our 'normal' model) to 100 g.cm^{-2} was investigated.

Table 4-1 summarizes the main effects of these alterations

in the proton and pion mean free paths and makes comparison with

the results from the 'normal' model.

4-5.4   Variations in the Value of the Mean Transverse Momentum $<p_t>$

Changes in the muon lateral distribution ($E_\mu > 1$ GeV) for 10^{17}eV

proton initiated EAS which arise from varying the value of $<p_t>$

from 0.35 to 0.5 GeV/c are shown in Fig. 4-16. The effect of

increasing $<p_t>$ is (predictably) to flatten the lateral distribution.

An air shower was simulated with an energy dependent value of $<p_t>$

such that:

$$<p_t> = 0.036 \times \log_{10} (E_p) + 0.31 \qquad\qquad 4.1$$

where E_p is the energy of the incident particle in interactions.

This produces an increase of $<p_t>$ from 0.35 GeV/c at 10 GeV

to 0.60 GeV/c at 10^8 GeV. The result of this simulation was

remarkably similar to the result obtained assuming an energy

independent value of $<p_t>$ of 0.35 GeV/c; this demonstrates how

the bulk of the muons reaching sea level are produced in low energy

interactions where $<p_t>$ according to Eq. 4.1 (and direct

observation) would be ~0.35 GeV/c.

The effect of changing the shape of the transverse momentum

distribution from that suggested by Cocconi et al.(1961)

Description of Model for Interactions	Ne_{SL}	Ht_{max} $(g \cdot cm^{-2})$	Δ_μ (>1 GeV, 100m) (m^{-2})	Δ_μ (>1 GeV, 500m) (m^{-2})	N_μ (>1GeV)
'Normal' model	2.65×10^7	693	1.90	0.057	4.97×10^5
$\lambda_\pi = 100g \cdot cm^{-2}$	2.6×10^7	675	1.74	0.050	4.49×10^5
$\lambda_p \propto E_p^{-0.066}$	1.89×10^7	630	1.98	0.067	5.17×10^5

TABLE 4-1
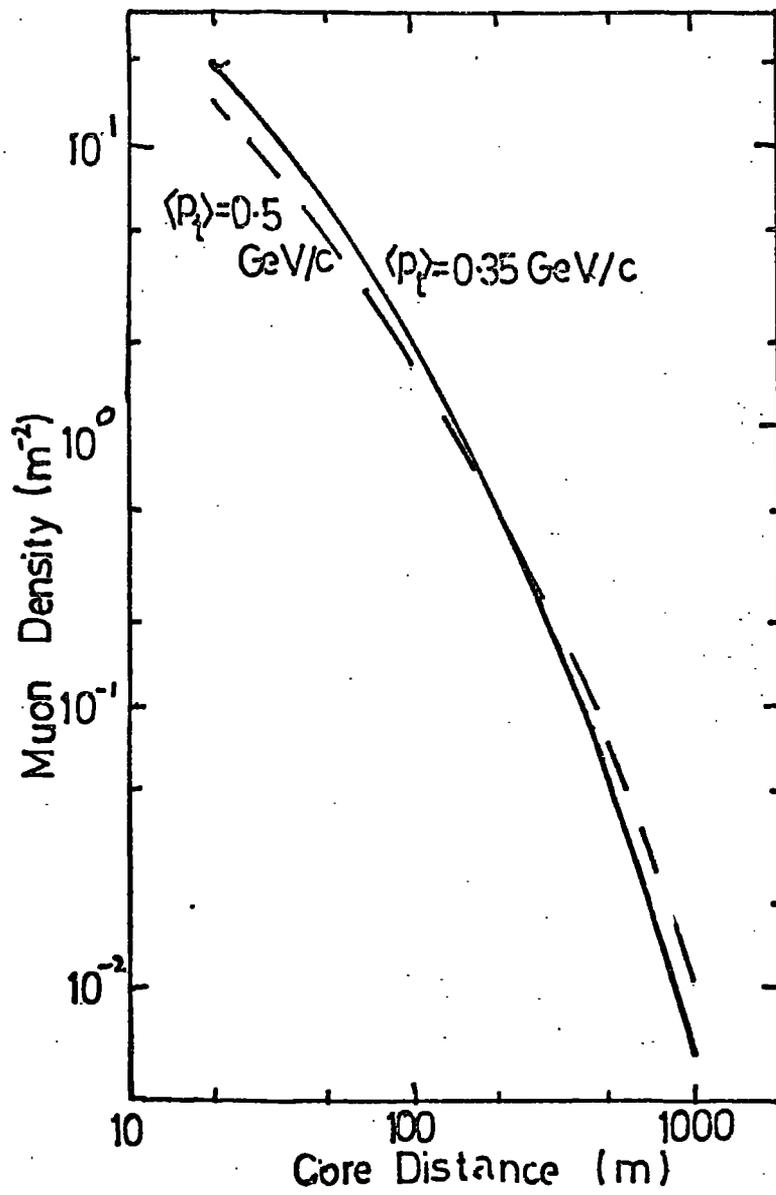
Figure 4-16

Muon lateral distribution

$$dN(p_t)\, dp_t = \frac{p_t}{p_o^2}\, \exp\left(-\frac{p_t}{p_o}\right) dp_t \quad \left(\text{where } p_o = \frac{<p_t>}{2}\right)$$

to

$$dN(p_t)\, dp_t = Bp_t^{-3/2}\, \exp\left(-bp_t\right) dp_t \text{ as}$$

suggested by Elbert et al. (1968) was found to be negligible.

4-5.5 <u>Changes in the Relationship between the Multiplicity of</u>

<u>Secondary Particles, n_s, and the Interaction Energy, E_r</u>.

The relationship between n_s and E_r is one of the most crucial

input parameters for any EAS simulations. The survey of experimental

data described in §3-4.1 lead us to choose for our 'normal' model

the relation

$$n_s^{+}\bar{o} = 3.2 \times E_r^{\frac{1}{4}} \text{ to predict the number of secondary}$$

particles produced in an interaction where the radiated energy is E_r.

However, it is essential to discover the sensitivity of the model

to changes in the multiplicity law and so a series of simulations

have been made to establish this. There is also an area of

uncertainty in the transition from p-p to p-N interactions; in the

'normal' model a value of 1.6 has been adopted for the ratio $n_{s(p-N)}/n_{s(p-p)}$ for reasons related in §3-4.3.

The range of relationships between multiplicity and energy

considered to span plausable limits were:-

(1) 'normal' multiplicity increased by a factor of 1.5

(2) 'normal' multiplicity decreased by a factor of 1.5

(3) $n_{s\pi-N}$ and n_{sp-p} both proportional to $E_r^{\frac{1}{2}}$

(4) $n_{s\pi-N} \alpha E_r^{\frac{1}{2}}$ and 'normal' multiplicities $n_{s(p-p)}$

(5) $n_s \alpha \log_e(E_r)$ (from the 'scaling' model for interactions

which will be described in §4-5.7)

Table 4-2 gives a summary of the main effects of these changes

in multiplicity law and, for comparison, the results from the 'normal'

Model for Interactions	number of electrons (S.L.)	Depth of maximum of electron cascade (g. cm^{-2})	$N_\mu > 1\text{GeV}$	$\Delta_\mu(>1\text{GeV},100\text{m})$ (m^{-2})	$\Delta_\mu(>1\text{GeV},500\text{m})$ (m^{-2})	N_e/N_μ
'Normal' model	2.65×10^7	693	4.97×10^5	1.90	0.087	50: 1
(1) 'Normal' multiplicities x 1.5	2.3×10^7	680	7.93×10^5	3.00	0.129	30: 1
(2) 'Normal' multiplicities ÷1.5	3.3×10^7	730	2.14×10^5	0.87	0.059	70: 1
(3) $n_s(\pi-N)$ and $n_s(p-N)$ both α $E_r^{\frac{1}{2}}$	1.6×10^7	580	7.4×10^5	2.86	0.10	20: 1
(4) $n_s(\pi-N)$ α $E_r^{\frac{1}{2}}$ and $n_s(p-N)$ α $E_r^{\frac{1}{4}}$	2.5×10^7	670	6.06×10^5	2.39	0.077	40: 1
(5) n_s α $\log_e(E_r)$ ('scaling law')	4.0×10^7	780	2.08×10^5	0.87	0.086	200:1

TABLE 4-2

interaction model are included. The simulations were performed for 10^{17}eV proton initiated EAS.

It is clear from this table that the logarithmic dependences of n_s upon E_r produces EAS with, according to experimental data, too many electrons and too few muons at sea level. This is also true of the multiplicity law where the 'normal' multiplicity appropriate to a certain energy is divided by 1.5. The position of the depth of maximum development of the electron cascade varies from 580 g.cm.$^{-2}$ (in the case of the multiplicity of produced particles from π-N and p-N interactions being α $E_r^{\frac{1}{2}}$) to 780 g.cm.$^{-2}$ (for the 'scaling' model).

It should be emphasised that although the results from the 'scaling' model shown in Table 4-2 are not acceptable in the light of experimental measurements this by no means excludes the model since there exist possible ways of raising the depth of maximum development and lowering the electron to muon ratio (the most obvious perhaps is to consider that the primary particle is an iron nucleus (see §4-5.7))

4-5.6 Simple Isobar Model

In order to consider the effect of allowing leading pions to be produced in interactions a simple isobar model was constructed. (It should be noted that this was a calculation based upon a simple model made in order to determine the gross features of showers produced using such an interaction model).

In π-N and p-N interactions a fraction of the energy radiated was removed to create 3 fast pions. The proportion of energy removed used in this calculation was chosen to be in the range 0.4 →0.6. The energy spectra of the secondary pions produced, in turn, by these fast pions was specified by the standard CKP

distribution.

The model was used in two ways:-

(i) when isobar production occurred only in p-N interactions and (ii) when isobar production occurred in p-N and also in π-N interactions where $E_\pi > 1000$ GeV.

Table 4-3 shows the results obtained from this model for interactions. It should be pointed out that the 'hybrid' computational technique was used for these simulations and the values in Table 4-3 were obtained by taking the mean of small samples.

4-5.7 The Consequences of Feynman Scaling

4-5.7.1 Introduction.

Feynman (1969) considered a hadron to consist of a large number of constituents or partons (virtual particles) which have small internal momentum. The total parton momentum may be expressed as a fraction of the hadron momentum $(x = P_n/E_c)$ (where E_c is the cms hadron momentum and P_n is the parton momentum). In a very high energy collision the hadron is broken into its constituents and it is assumed that on becoming 'real' the momentum is not affected. Hence the produced particle momentum spectrum depends only on the ratio $x = \dfrac{P_n}{E_c}$.

If W is the momentum of the incoming particle in the c.m.s., the spectrum of produced particles in the centre of mass should be of the form $\dfrac{d^2\sigma}{dp_z dp_t} = \dfrac{f(x,p_t)}{E}$ to fulfill the scaling law. (where p_z and p_t are the longitudinal and transverse momentum components of the pion in the centre of mass, E is the centre of mass energy of the pion and $f(x,p_t)$ is a function which is independent of W).

Model	n_e(SL)	Depth of maximum of electron cascade (g.cm^{-2})	$N_\mu > 1$ GeV	$N_\mu > 10$ GeV	$N_\mu > 100$ GeV	$\Delta_\mu > 1$ GeV, (100m) (m^{-2})
Isobars produced in n-N interactions only	3.72×10^7	760	4.47×10^5	9.9×10^4	6.25×10^3	1.78
Isobars produced in n-N interactions and π - N interactions when ($E_\pi > 100$ GeV)	2.58×10^7	656	2.84×10^5	7.9×10^4	5.00×10^3	1.11
Normal	2.65×10^7	693	4.97×10^5	1.31×10^5	7.88×10^3	1.90

TABLE 4-3

then

$$\frac{d^2\sigma}{dxdp_t} = \frac{f(x,p_t)}{(x^2 + (p_t^2 + m_\pi^2)/W^2)^{\frac{1}{2}}}$$

4-5.7.2 The Application of the Scaling Law to Present Work

In order to apply the scaling law to the present work it was necessary to find the form of the function $f(x,p_t)$. Boggild, Hansen and Suk (1971) found that the form of the function fitting data at 19 GeV/c is

$$f(x,p_t) \quad \alpha \quad \frac{\exp(-\frac{x}{0.165})}{1+\exp(-\frac{1}{.065}(x-0.62))} \cdot p_t^{1.3} \cdot \exp(\frac{-p_t}{0.155 + .1x}) \quad 4.2$$

It should be emphasised that this is an empirical fit to data on pion production from a 19 GeV/c bubble chamber study. The interactions studied were of the form

$$p + p \rightarrow \pi^- + \text{anything.}$$

In our simulations the value of p_t was chosen from the CKP distribution and a value of x was extracted at random from a distribution of the type of Eq. 4.2 The transformation to the laboratory frame of reference was made and the energy of the pion was subtracted from the interaction energy, E_r; the process was repeated until all the energy radiated had been used to produce particles. This sampling procedure was not economical in computing time and so for simulating EAS with primary energy $> 10^{15}$ eV only those interactions where the incident particle had energy in the laboratory system of ≥ 1000 GeV were 'scaled'. The lower energy interactions were treated with the 'normal' interaction procedure.

The results for 10^{17} eV proton initiated EAS simulated using the 'scaling' model as described above are shown in Table 4-2; it is obvious that many of these results for a 'pure scaling' model

are not in agreement with available experimental shower data.

4-5.7.3 The Effects of Further Modifications of the Interaction Model

when the 'Scaling' Law is Applied

Gaisser (1974) has suggested various ways in which the basic

'scaling' model for interactions may be modified in such a way as to

incorporate other contemporary interaction phenomena and to produce

better agreement with experimental measurements. These are:

(i)   use the shortened mean free path for p-N and π-N high

energy interactions suggested by Leader and Maur (1973) -

see §3-4.4 and §3-4.5

(ii) include intranuclear cascading

(iii) assume primary particles with atomic mass number $\gg 1$

(eg iron primaries).

Initially the first of these suggestions was included in our

simulations and this resulted in the depth of maximum development

of the electron cascade moving to a depth of ~ 680 g cm^{-2} and the

attenuation of the electron cascade becoming more rapid. This

constituted an improvement over the 'normal' model where the

attenuation of the electron cascade is slower than that found

experimentally. However, the numbers of muons produced were

a factor of 2 lower than those measured.

Gaisser's last suggestion was then implemented and the result

of this was to preserve the better agreement of the electron cascade

and to increase the muon numbers so that they agrée reasonably well

with experimental results. Figs. 4-17(a), 4-17(b) and 4-17(c) show

the changes in the electron component, muon energy spectrum and

muon lateral distribution resulting from these modifications;

comparison is made with the results of the 'normal' model.

Fig. 4·17 (a)

Atmospheric Depth (g.cm⁻²)

Electron Size

Fig. 4·17(b)

Muon Energy E_μ (GeV)

Muon Number $(>E_\mu)$

10^{17}eV

10^{15}eV

Muon Density (m^{-2})

Core Distance (m)

$\rho(500)=0.2$ v.e.μ.m^{-2}
$(E_\mu > 0.3GeV)$

10^{15} eV $(E_\mu > 1GeV)$
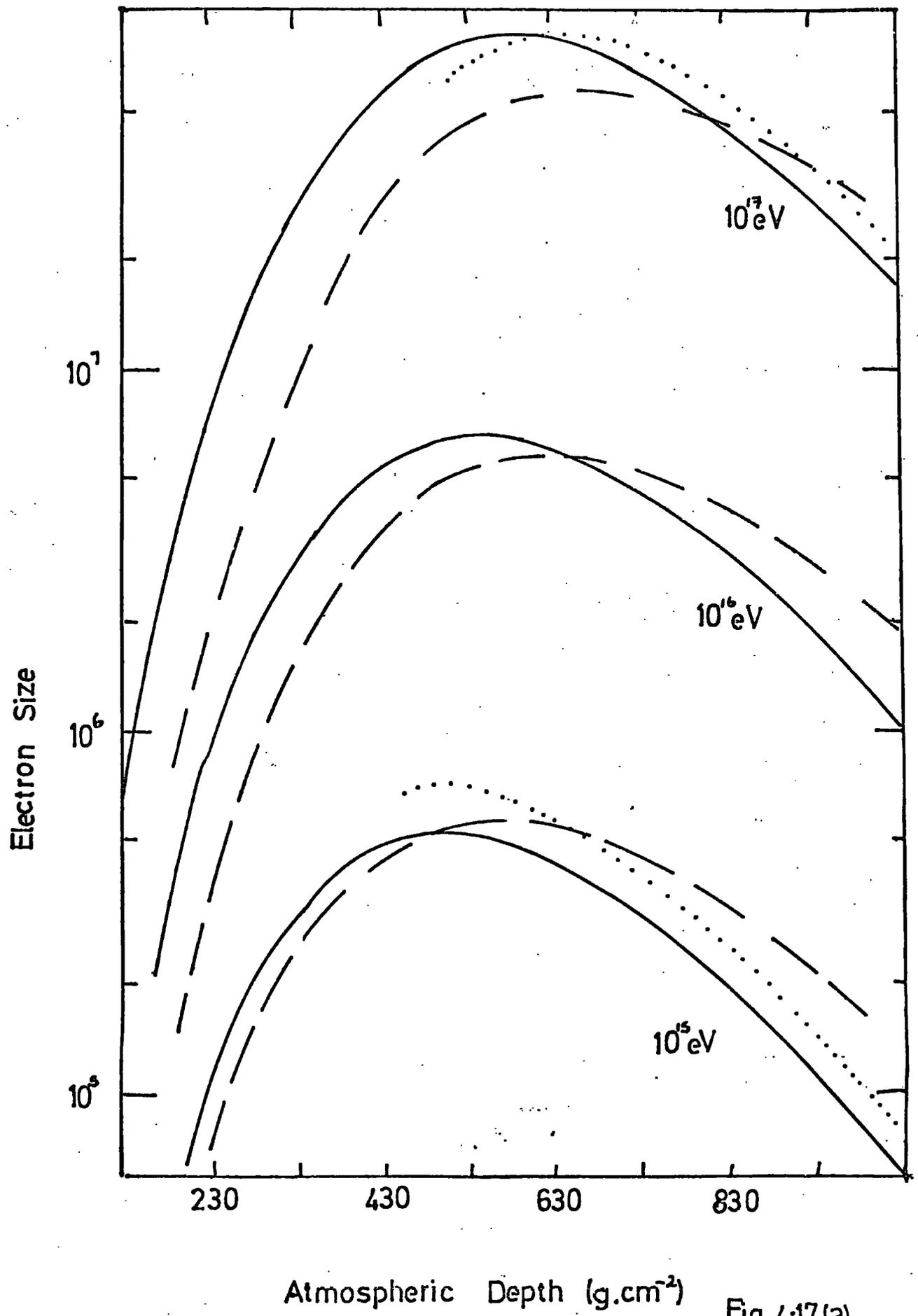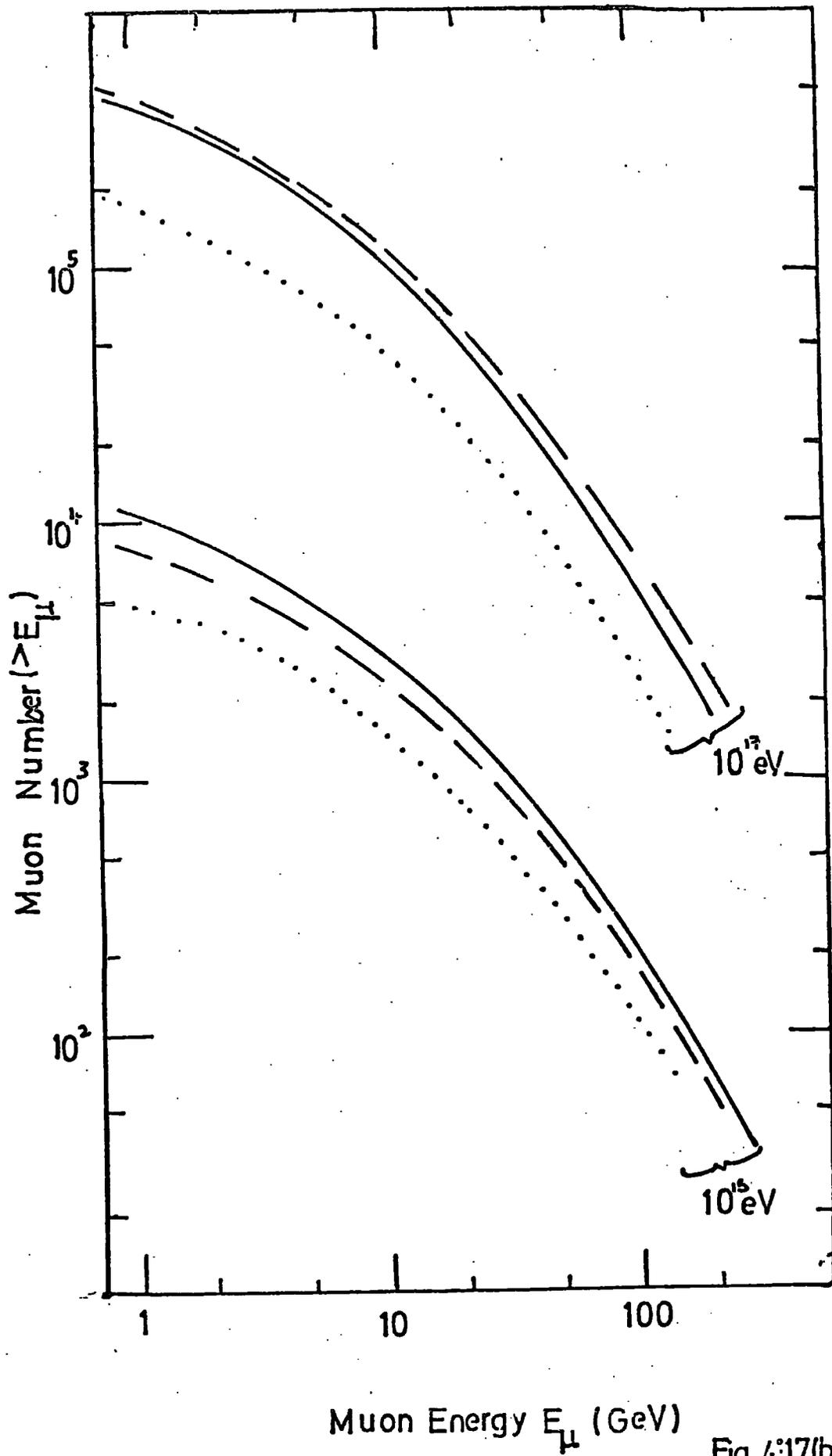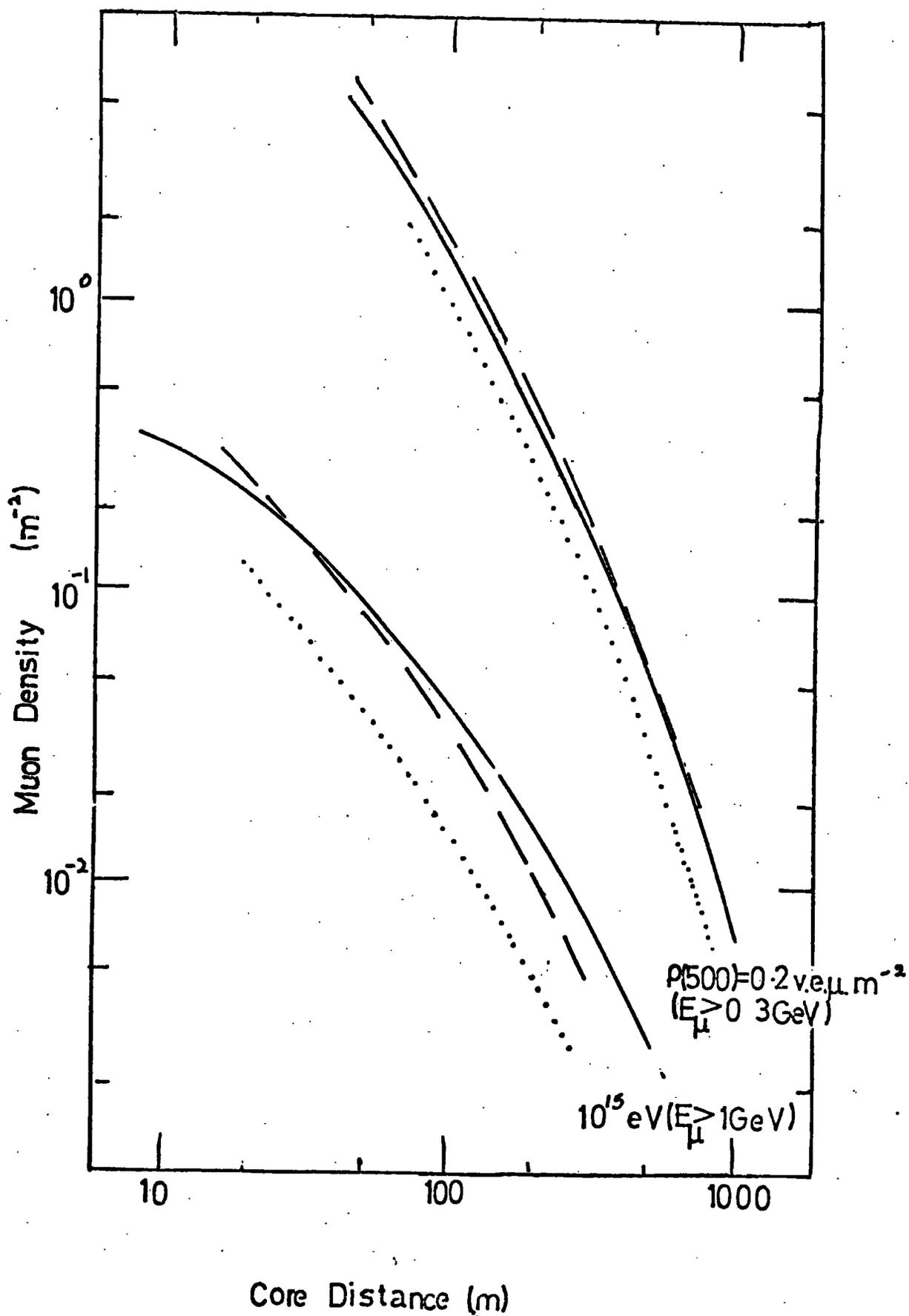
Fig. 4·17(c)

4-5.7.4 <u>Conclusion</u>

From Figs. 4-17 (a), 4-17(b) and 4-17(c) it is clear that 'scaling', when considered in addition to a shortened mean free path for protons and pions in air and the assumption of heavy primary particles, produces predictions which agree well with experimental measurement. In addition, many other observable shower parameters demonstrate this similarity of values originating from the 'normal' or this scaling model. Those experimental data which have caused the retention of the 'normal' model may now support the scaling model used by Gaisser. However, it has been shown that the assumption of iron nucleus primaries precludes large fluctuations in observables and this may be a limitation of the model. Evidence for large fluctuations in the majority of showers is not yet firm (Allan et al.(1973)) and does not at present, constitute a reason for the rejection of this model. A detailed investigation of these consequences of 'scaling' for large EAS is being undertaken by K.E. Turver.

4-5.8 <u>Summary</u>

The purpose of this chapter was to describe in detail the average characteristics of proton initiated EAS which were simulated using the 'normal' model and to assess the sensitivity of these predictions to changes in the interaction model.

The results of the 'normal' model were found to be, in many cases, in good agreement with experimental evidence and the predictions of other simulations (with the exception of the measurements of the attenuation length of the electron cascade through the atmosphere). It was found that by including the recent trend seen in accelerator data for p-p interactions of a rising

cross section with energy (and applying it to both p-N and π-N interactions) and assuming a primary particle of mass number of ∿56, good agreement can be obtained with experiemnt for the average shower characteristics if 'scaling' is used to describe the momentum distribution of secondaries in the interactions.

C H A P T E R   F I V E

FRAGMENTATION OF PRIMARY HEAVY NUCLEI

5-1   INTRODUCTION

It is essential that a realistic treatment of the break-up
of heavy nuclei in the atmosphere is used in computer simulations
of extensive air showers if useful comment on the mass composition
of the primary cosmic radiation at high energies is to be made.
An attempt has therefore been made to produce a satisfactory model
for the fragmentation of heavy nuclei on impact with air nuclei
employing data available from emulsion studies. This attempt
represents one of the major innovations of the present study.

After a brief summary of the way in which the interaction
of heavy nuclei with air nuclei has been dealt with in earlier
simulations, the fragmentation models devised for the present
work are described and the results obtained for various EAS
parameters are catalogued. Unless otherwise stated these results
have been obtained using the 'normal' model for π-N and p-N
interactions as described in Chapter 3. Finally comment is made
upon these results and the likely validity of this break-up model
for heavy nuclei.

5-2   Models of Heavy Nucleus Interactions Used in Earlier Work

5-2.1 The 'Superposition' Model

The effect of the fragmentation of heavy nuclei on entering
the atmosphere has frequently been dealt with in the past by using
what has become known as the 'super-position' model. This model
assumes that nuclei can be regarded as an unbound collection of
nucleons, each able to interact separately as a free nucleon, i.e.
a primary particle of energy E_p and atomic mass number A is
assumed to produce an EAS equivalent to the sum of A showers

each initiated by a nucleon of energy E_p/A. This approach ignores

the effective shielding of nucleons when they are in a nucleus and

is equivalent to assuming an interaction cross-section proportional

to A rather than the $A^{\frac{2}{3}}$ relationship which actually prevails. The

result is to over-estimate the rapidity with which the EAS develops

since at no stage are the nucleons bound. Furthermore, this model

must seriously underestimate the fluctuations in the development

of the nucleonic cascade, and hence the EAS as a whole, which would

arise from fluctuations in the way in which the heavy nucleus

fragments. Table 2.1 indicates those earlier simulation studies

which have incorporated the 'super-position' model for the break-

up of heavy primaries. The consequences of this model for showers

simulated using the present procedures have been considered.

5-2.2 Break-up Model used by Bradt and Rappaport

Bradt and Rappaport (1967) produced three dimensional

simulations for both proton and iron nucleus induced EAS. After

studying emulsion data (where the energies involved are of the

order of GeV/nucleon) they concluded that high energy heavy nuclei

typically survive several interactions before complete disintegration

into single nucleons. They therefore decided that the super-position

model was inappropriate and instead produced a model that they

considered to be consistent with observations at lower energies.

Each interaction of the heavy nucleus caused approximately 40%

of the matter to be detached in the form of alpha particles. In

the ensuing interaction of each alpha particle, four nucleons were

released and they in turn produced pions in their subsequent

interactions. The net affect of this break-up model was to create

a distributed source of nucleons in the upper 50-150 $g.cm^{-2}$ of the

atmosphere.

This model represented an improvement on the 'super-position' approach but was unrealistic in that no pions were produced in the fragmentation interactions of either the heavy nucleus or the alpha particles. Another criticism of the model is that no free nucleons were released during the fragmentation of the heavy primary and it seems unlikely that all the mass detached would be in the form of alpha particles. However, this development was important and indicated the possible limitations of the 'super-position' approach This model was also employed by Theilheim and his collaborators. (Theilheim and Beiresdorf, (1970)).

5-3 A Simple Fragmentation Model for Heavy Nuclei

5-3.1 Description of the Model

The successive development of a family of interactions reconstructed from data obtained in an emulsion stack flown at Brawley, California is shown in Fig. 5-1 (Abraham et al (1967)); this represents clearly the situation in the early stages of an EAS. The charge of the primary nucleus was $Z = 15$. The primary nucleus and its heavy $(Z > 2)$ fragments produced seven interactions in the stack and the analysis was consistent with these interactions being produced by nuclei carrying the same energy per nucleon. Seventeen singly charged particles were emitted from these seven heavy fragment interactions at angles smaller than 10^{-3} rad. and these particles form a 'core' which was well separated from the tracks appearing at greater angles. This feature and the multiplicity in the group, which was close to the number of protons in the primary nucleus $(Z - 15)$, strongly suggested that these tracks were due to protons emerging from successive breakups of the primary nucleus. The nucleons released in the interactions were not all expected to have the same per nucleon energy as the parent nucleus.

Fig. 5.1

1 (3+7+Mg)P
2 (11+42+Na)Mg
4 (7+8)n
5 (0+3+Na)Na
6 (0+51+Li+α)Na
7 (13+15) ?
8 (8+12)n
9 (5+13)n
10 (8+6)p
11 (2+3)n
12 (3+6)n
13 (1+4)α
14 (5+17)p
15 (0+3)p
16 (2+1)p
17 (0+13)p
18 (3+45)n
19 (0+15)n
20 (0+44)Li
21 (14+15)p
22 (2+7)p
23 (3+6)p
24 (3+40)p
25 (2+4)n
26 (4+5)n
27 (3+24)p
28 (16+23)n

The event type is described by the notation $(A+B+C)D$, where A is the number of secondaries at plateau ionization, B the number of gray and black tracks, C if any, indicates the nature of outgoing fragments of $Z \geq 2$, and D the nature of the incoming primary particle.

Approximately 150 mesons were produced in addition to the 'core' particles in the seven successive break-ups of the multiply charged fragments and it can be estimated that roughly only one-half of the nucleons composing the primary heavy nucleus did not interact. Therefore observation of the energies of the core particles should show an upper limit corresponding to the true per nucleon primary energy.

The detailed study of these data lead to the construction in 1971 of a simple fragmentation model for heavy nuclei in the atmosphere in which the fragmentation of the heavy nucleus was only partial upon each interaction. Fig. 5-2 shows the fragmentation scheme adopted together with the fluctuations allowed in the various parameters. (Further study of emulsion data to be described later suggested that these fluctuations were underestimates). This scheme of fragmentation was incorporated both into the full Monte-Carlo model and into the hybrid model (see §3-5.3 and 3-5.4).

The break-up of the alpha particles was dealt with as will be described in §5-3.3 and the mean free path used for heavy nuclei was that specified in §5-3.2 . In order to obtain the average characteristics of air showers produced by energetic heavy nuclei, the nucleon cascade was computed fifteen times and the average of these cascades was used to initiate the pion generations of a single simulated shower which provided a valid representation of an average shower.

5-3.2 The Mean Free Path for Interaction

The interaction mean free paths for heavy nuclei are found from the overlap model of nuclear interactions which gives the inelastic cross section to be

Heavy
Primary

$$MFP = \lambda_{A} = 353/(1\cdot23 + A^{\frac{1}{3}})^{2}$$
Cleghorn et al. (1969)

Sub Heavy

λA

α-particles
(15±5%)

$\lambda \alpha$

Interacting
Nucleons in
Frag. (15±5%)

Freed
Nucleons
(15±5%)

λp

2 Nucleons
Freed

2 Nucleons
interact in
Frag.

λp
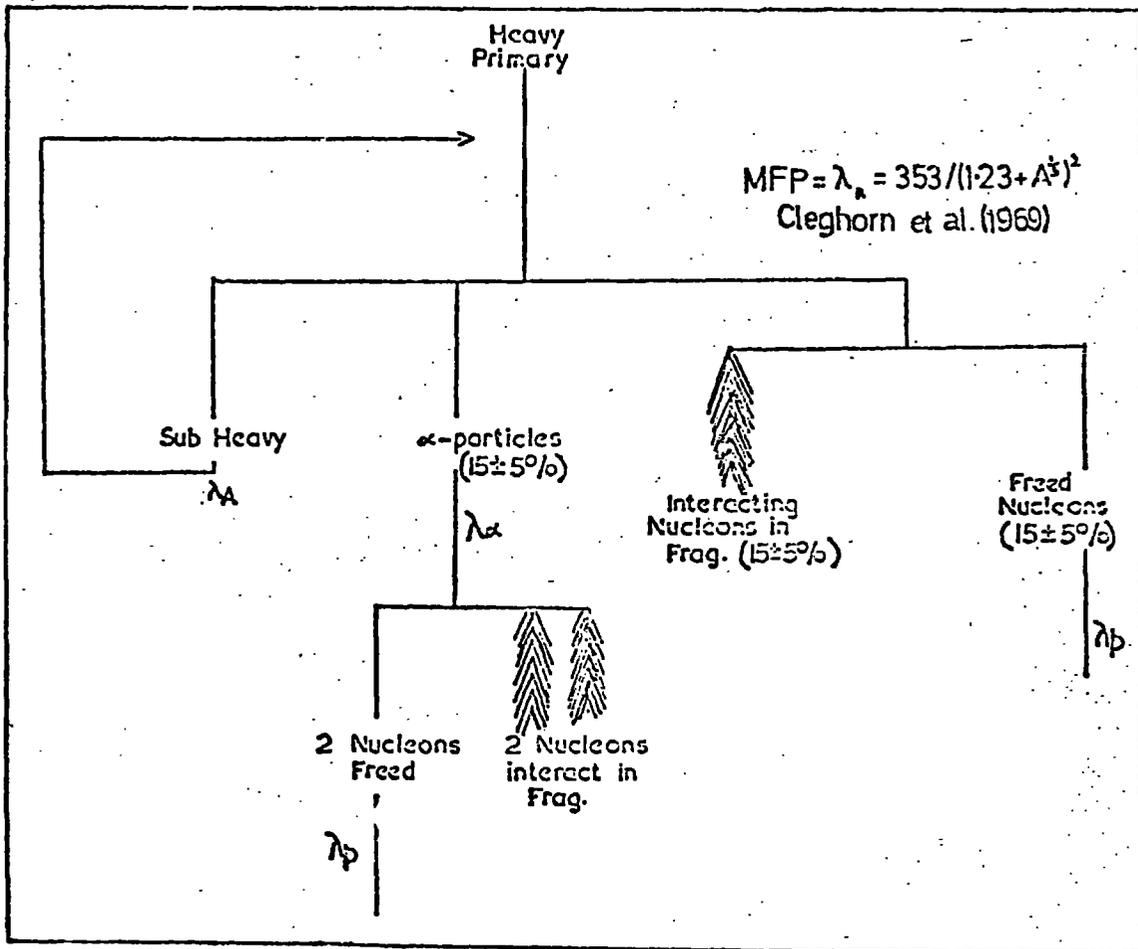
Figure 5.2

Fragmentation scheme adopted
for the simple fragmentation
model

$$\sigma_{it} = \pi r_0^2 \left(A_i^{\frac{1}{3}} + A_t^{\frac{1}{3}} - \frac{2\Delta r}{r_0} \right)$$

where the nuclear radius is given by $r = r_0 A^{\frac{1}{3}}$ and Δr is the overlap parameter. This simple model of interactions is based primarily upon geometrical considerations but when r_0 is taken to be 1.20F and Δr as 0.25F the cross sections obtained fit experimental data well (Cleghorn et al.(1967)). The mean free path for a nucleus of mass A in air is specified by:-

$$\lambda_A = \frac{353}{(1.23 + A^{\frac{1}{3}})^2}$$

The mean free paths of heavy nuclei are found experimentally to be independent of energy in the range 100 MeV/nucleon to 30 GeV/nucleon, and no energy dependence has been included in our application at higher energies.

5-3.3 <u>The Fragmentation of Alpha Particles</u>

The mean free path of alpha particles in emulsion is approximately 20 cms and this perhaps accounts for the sparse data available on their fragmentation. However, from a systematic study of disintegrations produced by alpha particles with energy >6 GeV/nucleon, Rao et al.(1956) concluded that commonly only one or two nucleons interact with the target nucleus to produce fast secondaries. Comparison is made in Table 5-1 between the effects on some of the EAS parameters of the two most likely modes of fragmentation of alpha particles in which one or two nucleons interact; the differences can be seen to be minor. In the present work we have assumed that one nucleon interacts coherently on collision with an air nucleus and the other nucleons are freed.

5-3.4 <u>Results obtained from the Simple Fragmentation Model</u>

The effect of this model is to produce a distribution of free nucleons in the atmosphere typified by the data of the histogram shown in Fig. 5-3. Also shown are the distributions resulting

FRAGMENTATION PATTERN		ELECTRON SIZE $N_e(SL)$	MUON SIZE $N_\mu(>1GeV)$	DEPTH OF MAXIMUM t_{max} $(g \cdot cm^{-2})$	MUON DENSITY $>1GeV$ $300m$ (m^{-2})
No. of Nucleons					
Interact	Free				
1	3	2.54×10^7	5.74×10^5	688	0.27
2	2	1.94×10^7	5.48×10^5	634	0.26

Table 5-1
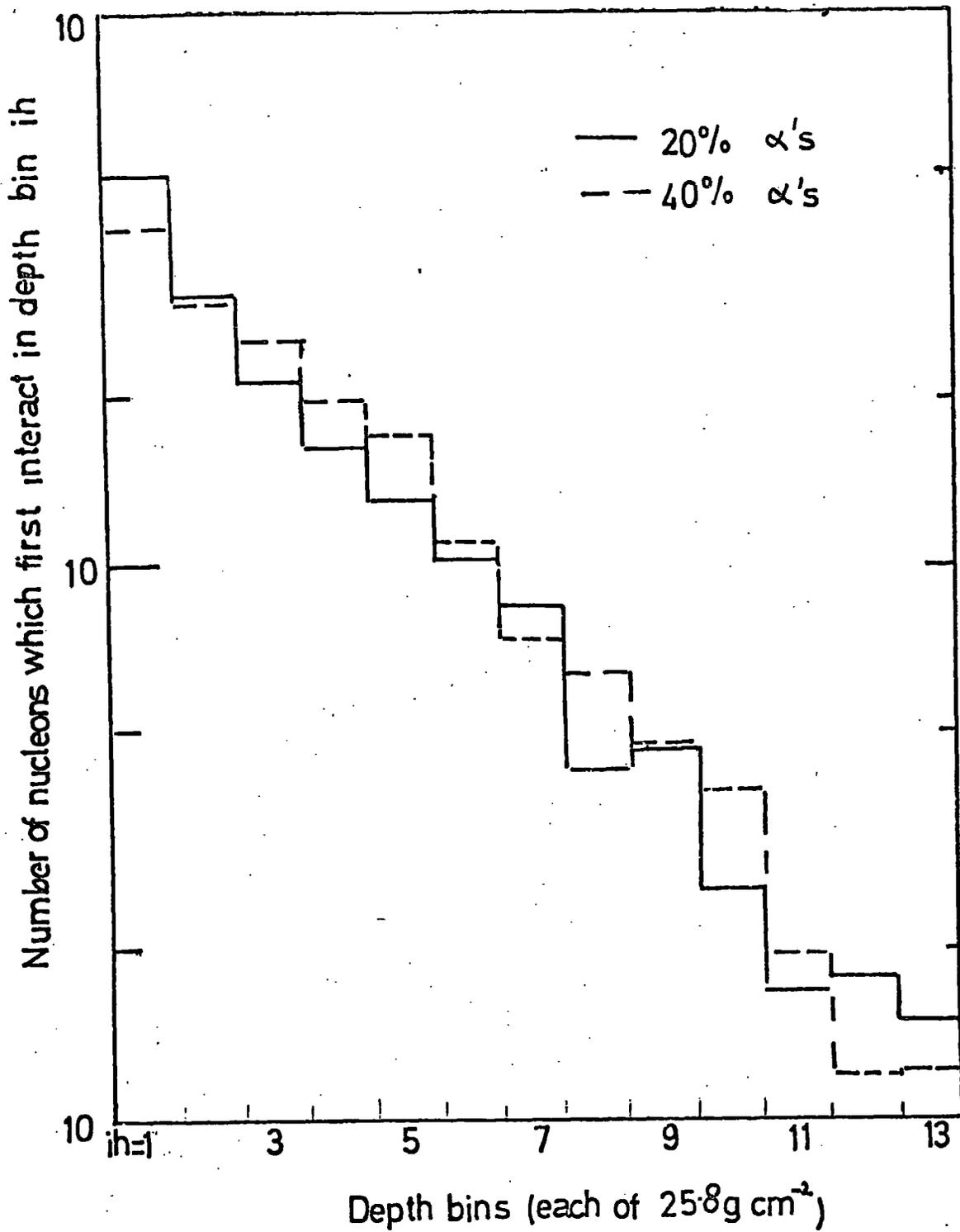
Figure 5-3

Distributions of the points in the atmosphere where the constituent nucleons of heavy primary nuclei first interact

from changing the proportion of alpha-particles produced and the percentage of the mass remaining bound as a sub-heavy.

The results achieved using this model are in broad agreement with those of 'super-position' as far as the muon component of air showers is concerned in 10^{17}eV showers. Fig. 5-4 shows a comparison of the muon total number spectrum and the lateral distribution of muons obtained from the superposition model and the simple fragmentation model for 10^{17}eV iron nucleusinitiated EAS. The electron cascade of EAS based on this model was found to develop lower in the atmosphere than that produced by the 'super-position' model. This implies that the difference between the longitudinal development of proton and heavy nucleus initiated showers is diminished if this simple fragmentation approach is adopted. Fig. 5-5 shows a comparison of electron longitudinal cascades for proton initiated EAS and for iron nucleus initiated EAS based upon 'super-position' and the simple fragmentation model. (The primary energy is 10^{17}eV in all cases).

Since the values assigned to the fluctuation parameters were based upon limited data (and subsequently shown to be underestimates), this model cannot usefully be used to give a realistic estimate of the fluctuations to be expected in observables of air showers initiated by primary particles heavier than protons.

5-4 A Realistic Partial Fragmentation Model

5-4.1 Basic Data

Emulsion data for heavy nucleus- CNO collisions at energies in the region of 5 GeV/nucleon were provided for use in these calculations by Waddington and Freier(1972),(1973)). The data consisted of details of 213 interactions in carbon and 838 in emulsion. The interactions in emulsion were considered as being with the air-like nuclei in
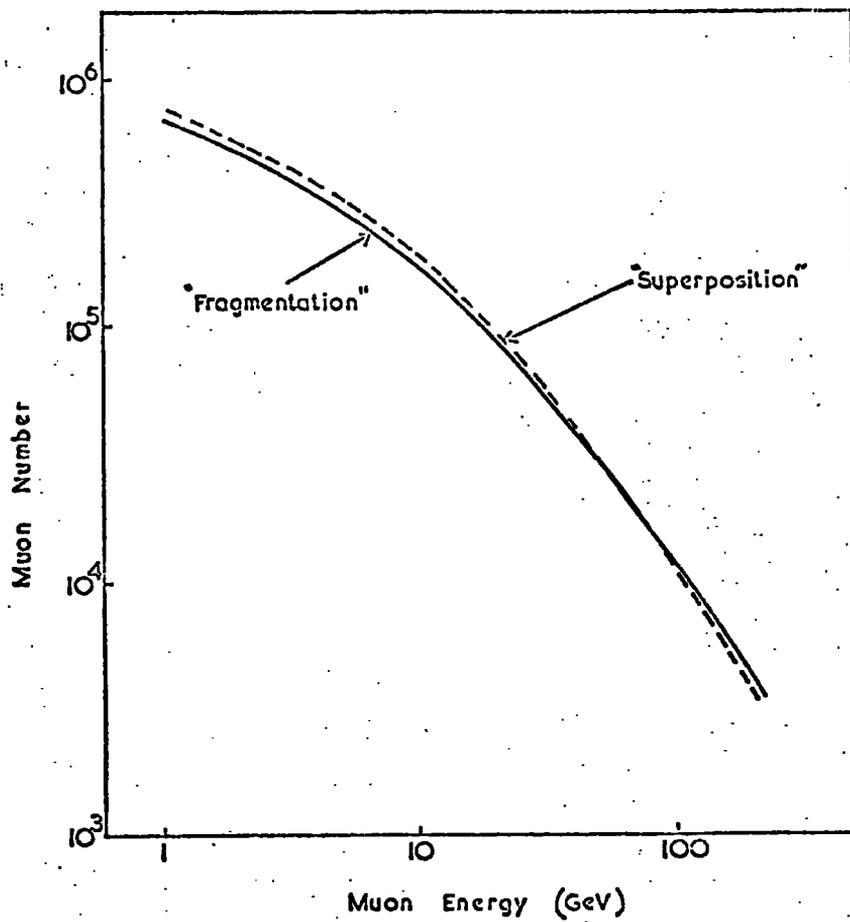
(a)
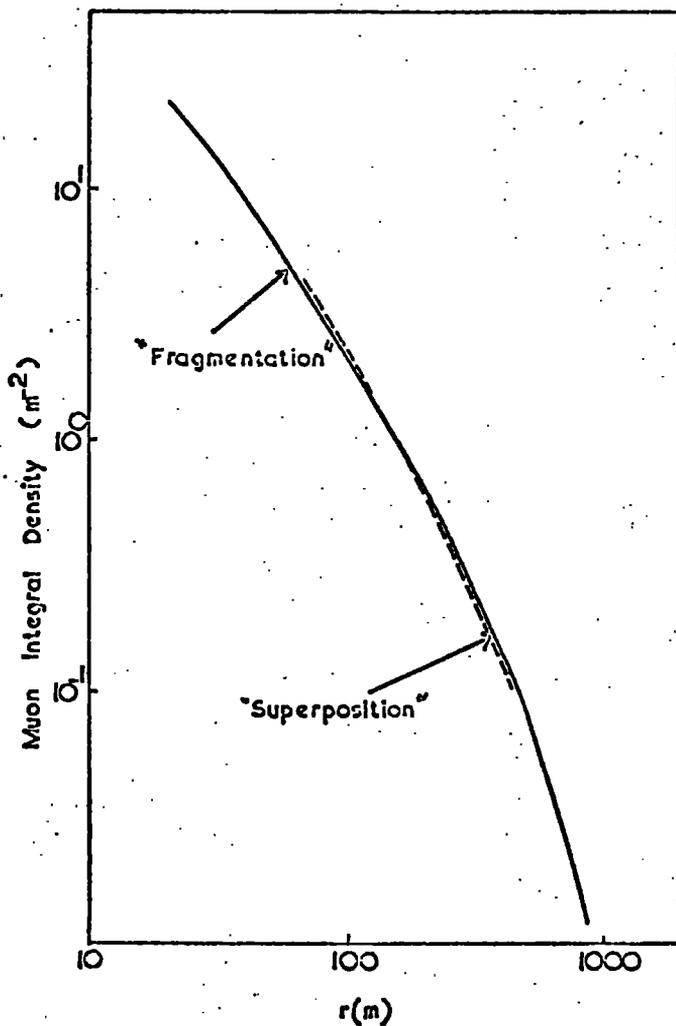
(b)

Figure 5.4

Comparison of the muon component
from simulations made using the
simple fragmentation model and
'superposition' for the break
up of heavy primary particles.
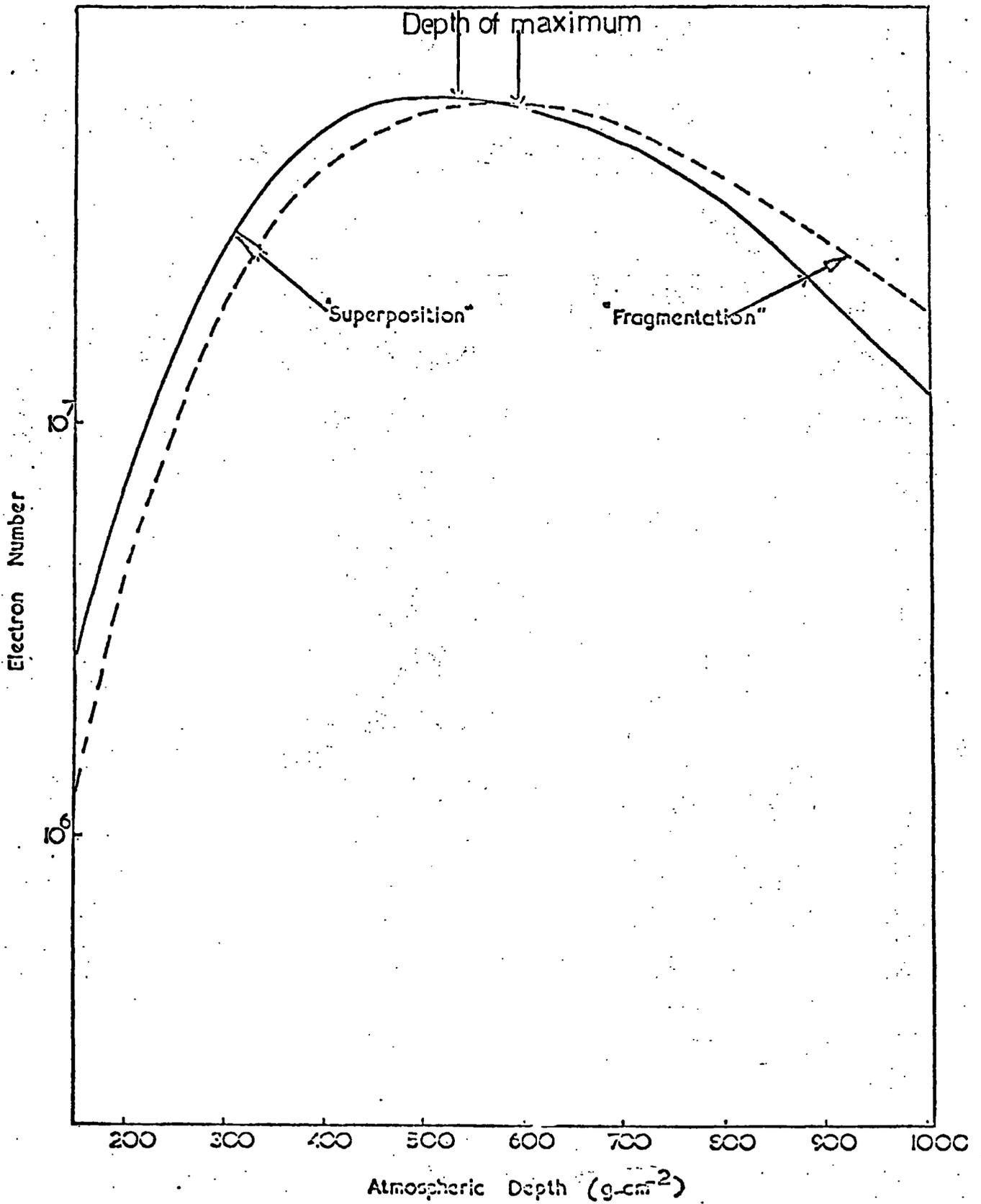
Figure 5.5

Comparison of the longitudinal development of the electron cascade from the simple fragmentation model and from 'superposition' for the breakup of heavy primary particles

emulsion, as judged on the basis of the number of particles emitted from the target nucleus. Of the total 1051 interactions, 427 were produced by VH-nuclei, $(Z \geqslant 20)$, 69 by MH-nuclei $(15 \leqslant Z \leqslant 19)$, 146 by LH - nuclei $(10 \leqslant Z \leqslant 14)$, 329 by M-nuclei $(6 \leqslant Z \leqslant 9)$ and 80 by L-nuclei $(3 < Z \leqslant 5)$. The data were believed to be all of reasonably high quality, without serious systematic errors, and internally self consistent. Although there is no guarantee that there is no slow energy dependence of the fragmentation modes that would become important when extrapolated to EAS energies, it seems that using this data is the most satisfactory approach to the problem of simulating heavy nucleon induced EAS presently available. Comment is made later on the likely validity of this approach and the consequences for it of recent discoveries in high energy physics ($§5-6$).

5-4.2 The Computational Procedure

The details of each of the 1051 interactions were stored in a data bank with the interactions grouped according to the charge of the incident particle. For each interaction the following data were available:-

(i)   the number of neutrons freed,

(ii)   the number of protons freed,

(iii) the number of alpha particles released,

(iv)   the charge of the fragment(s) produced.

To construct the pattern for the break up of a heavy nucleus in the atmosphere the following procedure was adopted. The point of interaction of the primary nucleus was chosen from a pseudo-random distribution with mean corresponding to the appropriate mean free path described in §5-2.2. An interaction of the required charge was then extracted at random from the data bank. The information available concerning the chosen 'star' describes the

interaction completely except for the number of nucleons that

interact coherently to produce pions. This quantity was chosen

from a flat distribution such that between 18% and 32% of the total

number of nucleons freed interacted coherently (Shapiro, private

communication (1973)). In cases when only a few nucleons were

freed in the interaction precautions were taken to avoid producing

too high a proportion of events with no coherently interacting

nucleons.

This information enabled the freed nucleons to be followed

to sea level, the alpha particles to be followed until interaction

and their constituent nucleons followed to sea level, and the

procedure of picking a point of interaction and an appropriate

'star' from the data bank to be repeated for each of the fragments.

In this way the cascade was followed until sea level was reached

by all the constituent nucleons. Fig. 5-6 shows the form of a

typical nucleon cascade resulting from the break-up of a silicon

nucleus in the atmosphere.

5-5 Results Obtained for Average Shower Characteristics

5-5.1 Muon Component

The results obtained from this partial fragmentation model

for the muon component of air showers initiated by iron nuclei

of 10^{17} eV are broadly in agreement with those from the 'super-

position' model. However, at 10^{15} eV the agreement between the

two models is not as good, the super-position model giving a

muon total number spectrum which is closer to the proton spectrum

than the partial fragmentation model. (See Fig. 5-7)). However,

the difference in the results from the two models is not great and

the difference between the muon numbers produced by either fragmentation

model and the muon numbers produced by proton initiated EAS is very
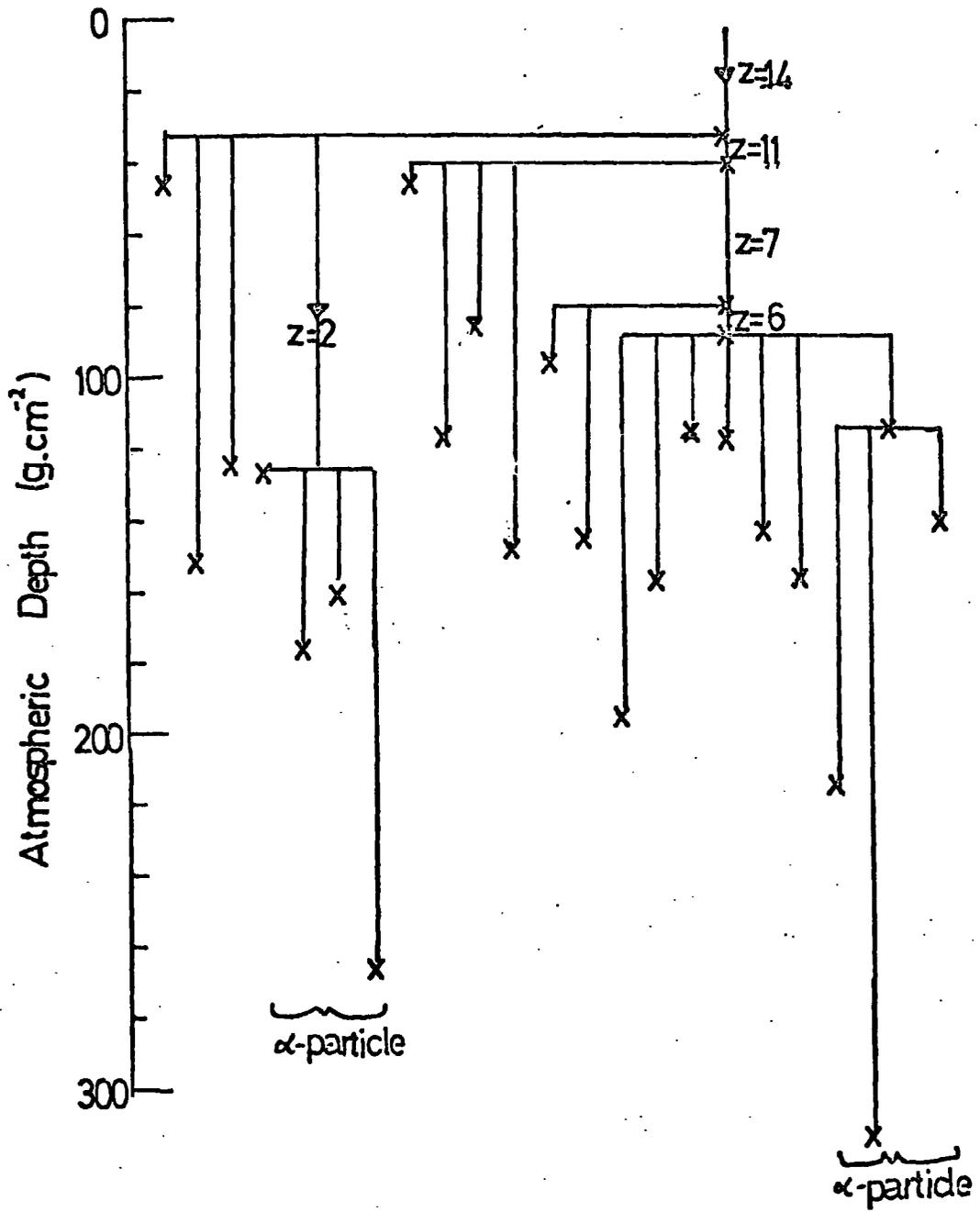
Figure 5-6

Points of initial interaction
of the nucleus in a silicon
nucleus as it fragments in the
atmosphere
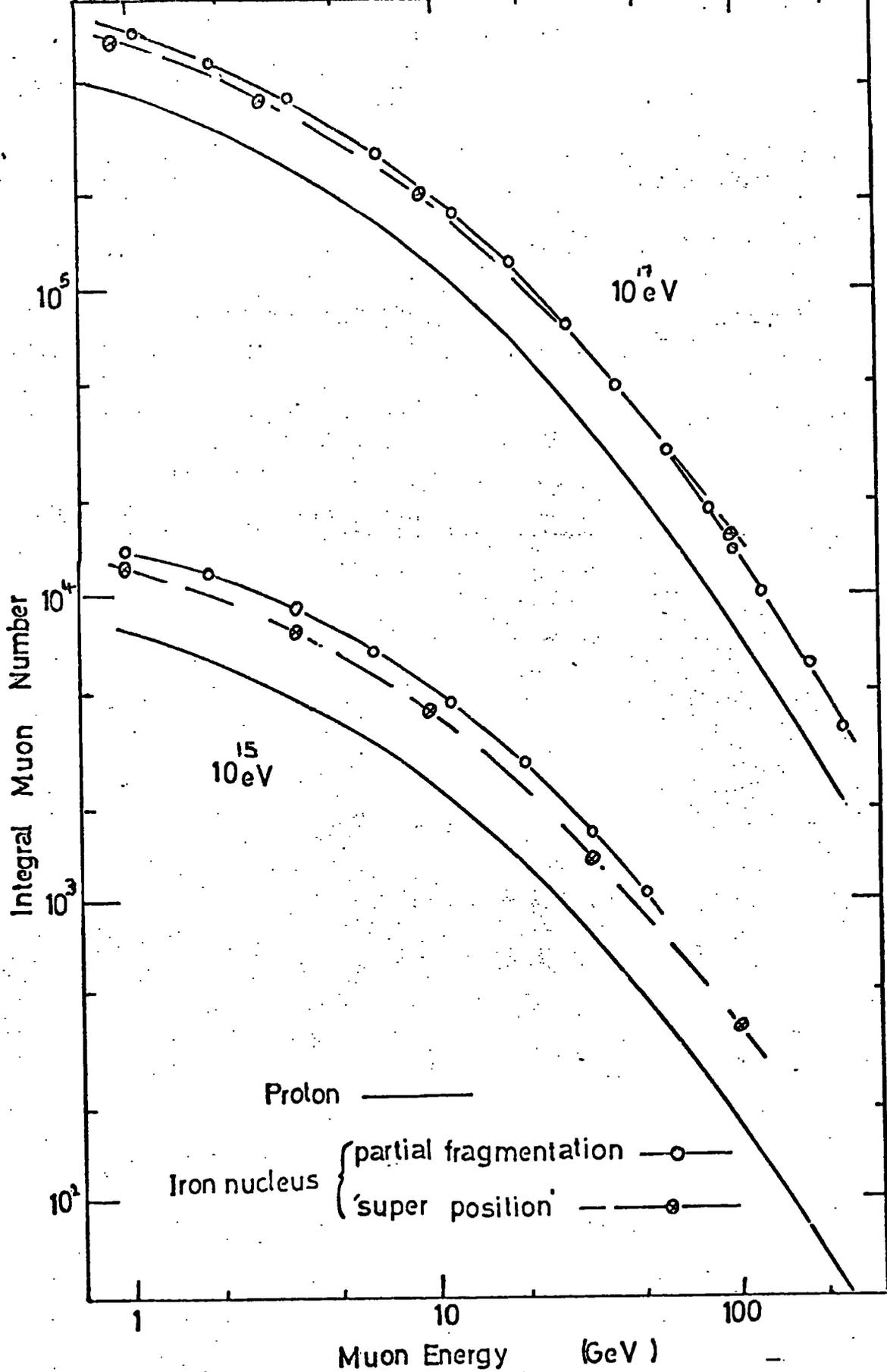
Figure 5-7

Comparison of the muon energy spectra produced by 10^{17}eV and 10^{15}eV proton and iron nucleus initiated EAS.

much greater than the difference between the numbers produced by the two fragmentation models. The iron nucleus initiated EAS is characterised by approximately 50% more muons than the proton initiated EAS in the range of muon energy 1 to 100 GeV.

5-5.2 The Electron Component

Heavy nucleus induced air showers would be expected on average to develop higher in the atmosphere than proton initiated showers regardless of the model assumed for the fragmentation. This is as a direct consequence of EAS initiated by protons developing lower in the atmosphere as the primary energy is increased (see Fig.4.3(a)) Since the super-position model assumes that the development of a shower initiated by a primary of mass A and energy E_p is equivalent to the sum of A proton showers of (lower) primary energy E_p/A the depth of maximum development of the electron cascade of such an air shower is predicted by this model to be that associated with a proton of energy E_p/A. Therefore for an iron nucleus initiated shower of primary energy 10^{17}eV the depth of maximum predicted by the super-position model is that associated with a proton of energy 1.78 10^{15}eV (ie 584 g.cm^{-2}). A 10^{17}eV proton initiated shower simulated using the 'normal' model has its depth of maximum at 694 g cm^{-2}. Therefore if one assumes the superposition model for the fragmentation of an iron nucleus the predicted difference in the depth of maximum of iron and proton initiated air showers is 110 g.cm^{-2} when the primary energy is 10^{17}eV.

The partial fragmentation model however predicts the average depth of maximum of the electron cascade of an air shower initiated by a 10^{17}eV iron nucleus to be 623 g.cm^{-2}, thus reducing the difference between an iron nucleus and proton induced shower to 71 g cm^{-2}. This has serious implications as far as attempts to measure the mass composition of the primary cosmic rays by the

determination of the average depth of maximum of EAS of known primary energy is concerned.

The average development of the electron cascades through the atmosphere predicted by both the 'super position' model and the partial fragmentation model for a 10^{17}eV iron nuclei are shown in Fig. 5-8 where they are compared with the electron cascade from a proton induced EAS.

Fig 5-9 shows a comparison of the lateral distribution of electrons of energy in excess of 10 MeV at sea level produced by an iron nucleus initiated EAS and a proton initiated EAS both of primary energy 10^{17}eV. The predictions of both the partial fragmentation model and the super-position model for the iron nucleus initiated shower are shown. A consequence of the longitudinal development of the electron cascade derived from the partial fragmentation model causes the flattening of the electron lateral distribution near the core to become less pronounced and the difference from the lateral distribution of a proton shower is thus diminished.

5-5.3   The Water Cerenkov Detector Response at Haverah Park

The average response of deep-water Cerenkov detection of the type used at the Haverah Park experiment has been calculated for simulated air showers initiated by Fe-nuclei. Fig. 5-10 shows the result of this calculation compared with the response from a proton initiated EAS of the same primary energy (10^{17}eV). The difference between the two structure functions is extremely slight which is an indication that studying the average deep water Cerenkov detector responses at Haverah Park would not yield a strong measure of the primary particle mass composition. The detector responses were calculated using the data of Marsden (1971).
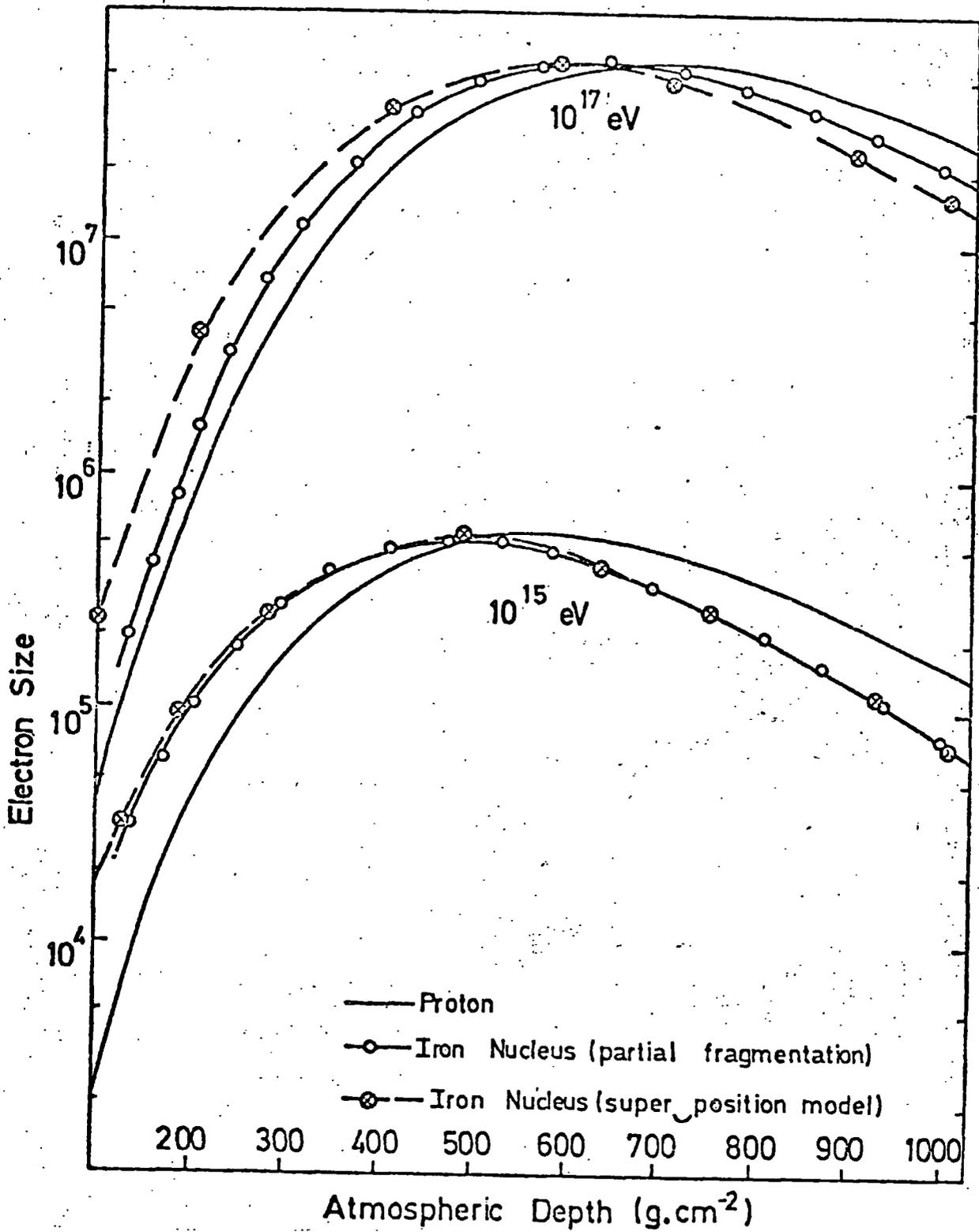
Figure 5-8

Comparison of the longitudinal development of the electron cascade produced by 10^{17} eV and 10^{15} eV proton and iron nucleus initiated EAS

Iron nucleus {superposition model ——⊕——
             {partial fragmentation model ——o——
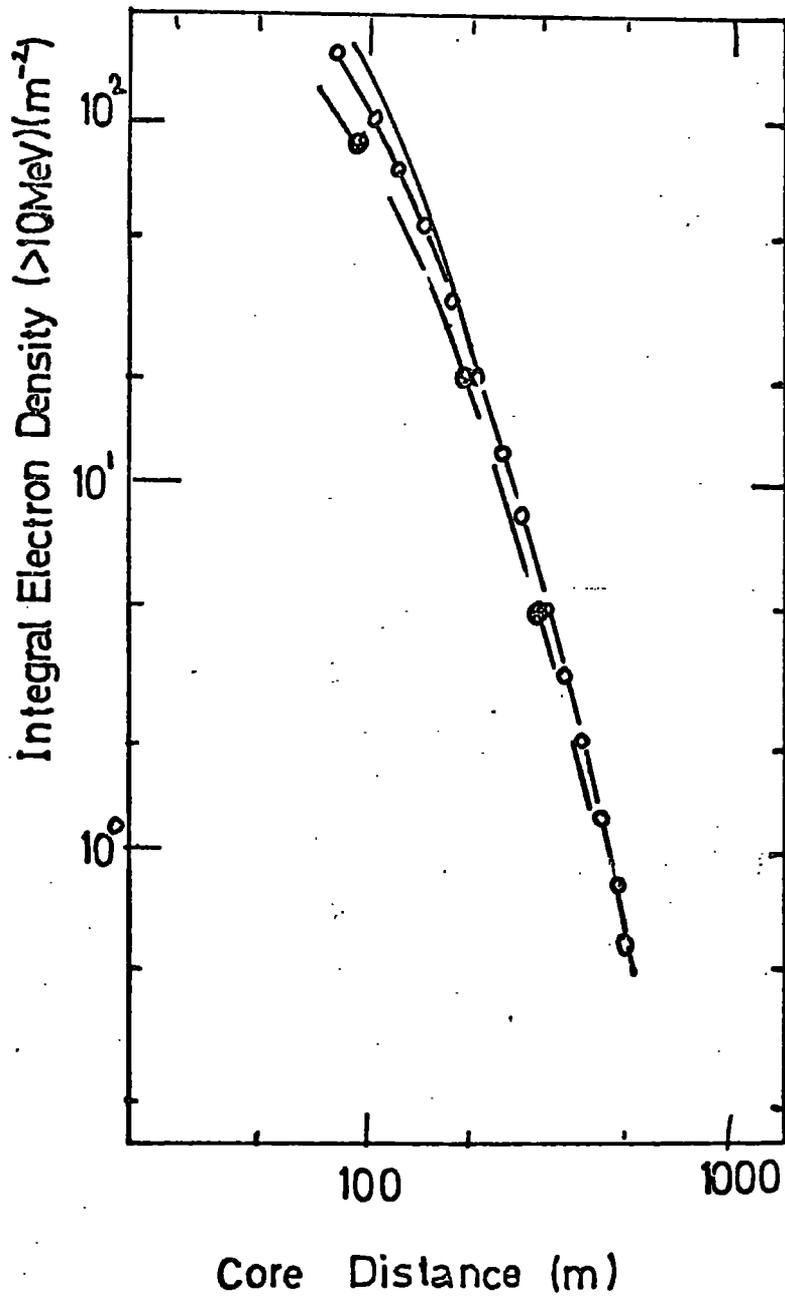
Protons ————

Figure 5-9

Comparison of the electron
lateral distributions
($E_e \geq 10$ MeV) produced by 10^{17} eV
proton and iron nucleus
initiated EAS.

Comparison of the water Cerenkov detector responses to iron nucleus and proton initiated EAS graph. Y-axis: Water Cerenkov detector responce (v.e.µ.m⁻²), X-axis: Core distance (m). Legend: proton (solid line), iron nucleus (dashed line) initiated EAS. $E_p = 10^{17} eV$
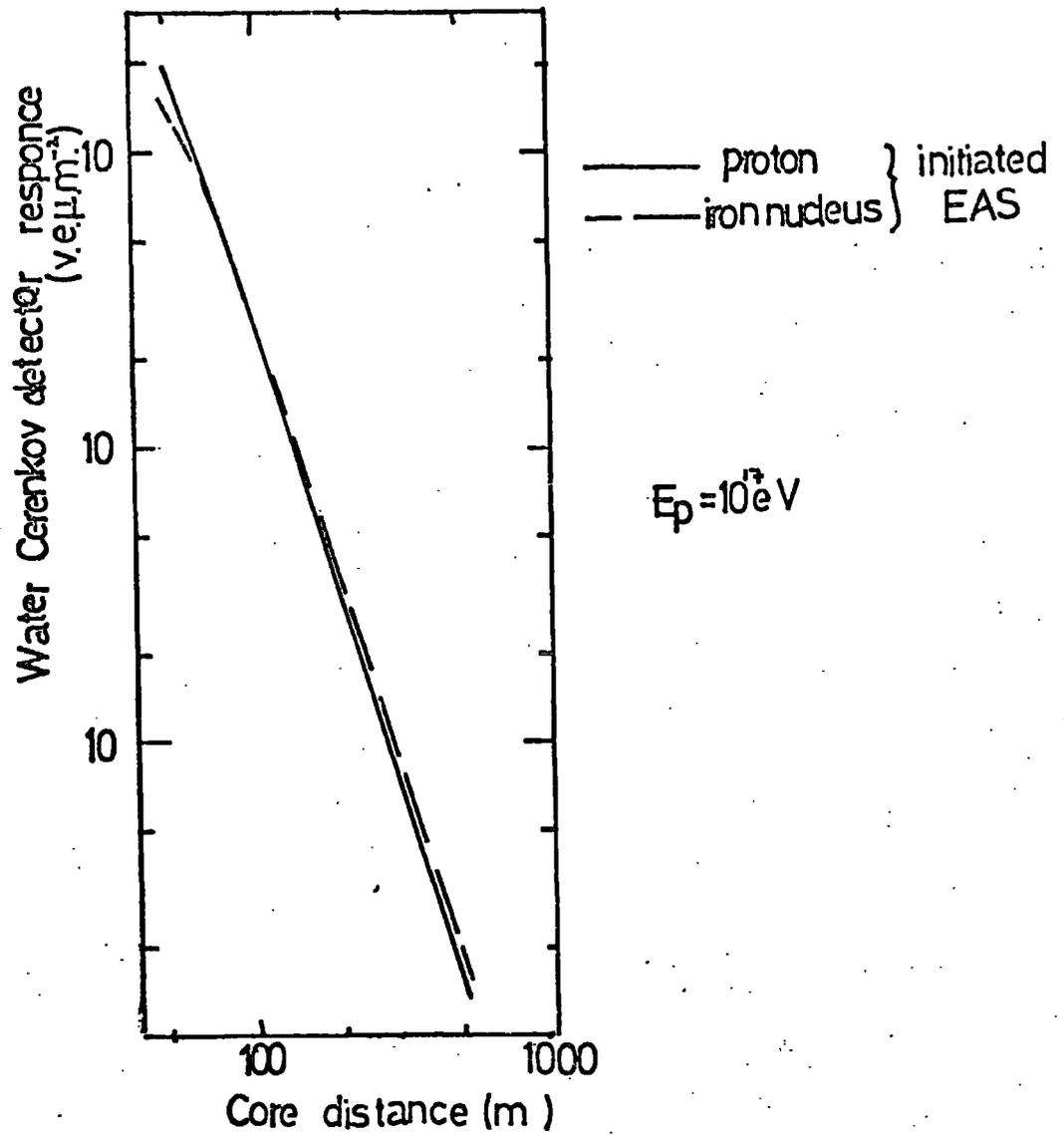
Figure 5-10

Comparison of the water
Cerenkov detector responses
to iron nucleus and proton
initiated EAS.

5-5.4 The Ratio of the Muon Density to the Response of the Deep

Water Cerenkov Detectors $\frac{\Delta\mu}{\Delta c}$.

The measurement of $\frac{\Delta\mu}{\Delta c}$ has been discussed in §4-2.6 and the

simulation results for this ratio as a function of core distance

are displayed in Fig. 4-12 for both proton and iron nucleus initiated

EAS. Comparison is made with the experimental results of Armitage

(1973). The results of the 'normal' model for interactions

together with the partial fragmentation model for iron nuclei described

in §5-4 predict values of $\frac{\Delta\mu}{\Delta c}$ which are not in good agreement with

experimental results.

5-5.5 The Optical Cerenkov Radiation Lateral Distribution

The optical Cerenkov radiation lateral distribution has been

calculated for a selection of iron initiated air showers which were

simulated using the partial fragmentation model for the break-up

of heavy nuclei described in §5-4. The result of the average of these

distributions is shown in Fig. 5-11. Comparison is made with the

lateral distribution predicted for proton initiated air showers with

the same depth of maximum development of the electron cascade. The

lateral distribution from the iron initiated EAS is rather flatter

than the distribution with which it is compared.

5-6 The Likely Validity of the Assumed Fragmentation Model

The emulsion data forming the basis for the simulations described

in this chapter were obtained from the fragmentation of heavy nuclei

of energies much lower than those associated with interactions involved

in high energy EAS. It is therefore important to recognise the possible

limitations of the model.

Recent accelerator experiments indicate that there is a rise

in the inelastic proton-proton cross sections at energies of about
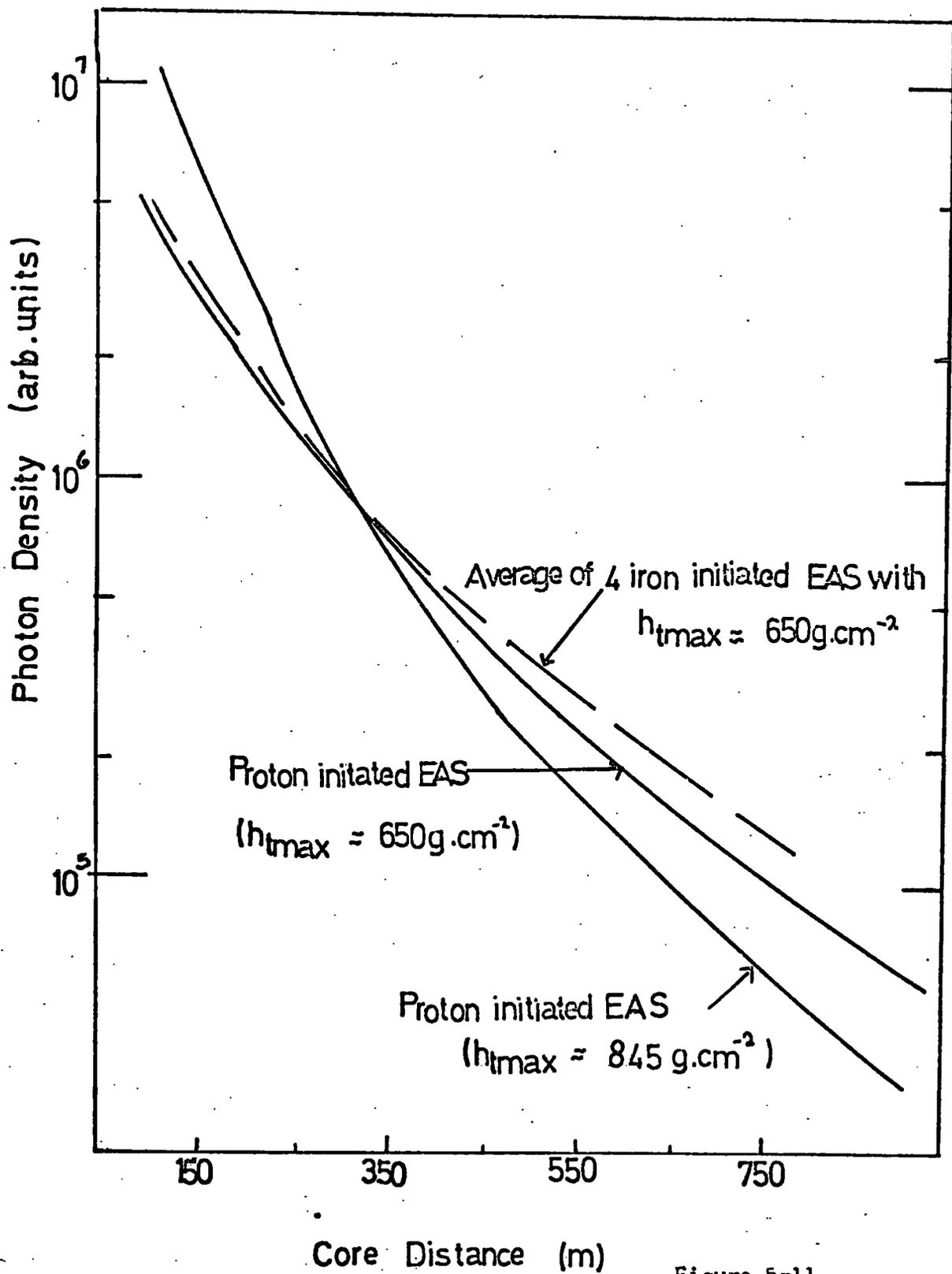
Figure 5-11

Optical Cerenkov radiation
lateral distribution

1000 GeV in the laboratory system. (Amendolia et al.(1973)). A consequence of this for heavy nucleus -air nucleus interactions may arise from the effective increase of the range of the nuclear force implied by the increased cross-section, producing greater fragmentation than in lower energy interactions. This could mean that the true representation of the fragmentation of heavy nuclei may lie somewhere between 'super-position' and the partial fragmentation described in this chapter.

On the other hand, there is also evidence that at energies above those appropriate to the emulsion data which form the basis for the partial fragmentation model secondary particles are released in a cone, the angle of which decreases with increasing energy. This might result in less disturbance to the heavy nucleus on impact with an air nucleus and would make the partial fragmentation model used here a lower estimate of the true picture.

In conclusion therefore, it must be emphasised that there is little evidence to support the use of this fragmentation model or any other at the EAS energies. However, at least the data at emulsion energies is fitted which is one of the main objectives when deciding upon the correct model for air shower simulations.

C H A P T E R   S I X

FLUCTUATIONS IN SHOWER DEVELOPMENT

6-1   Introduction.

Little is known about the mass composition of the primary

cosmic radiation at high energies ($> 10^{16}$ eV/nucleus). Indeed, there

is a lack of firm evidence to support any of the widely differing

views presently held as to the nature of the energetic primaries.

A possible method for the determination of the nature of this

radiation is based upon the study of fluctuations in the observable

parameters of EAS. The fundamental assumption upon which this

approach is based is that the fluctuations of some observables in

proton initiated air showers are very much greater than those of

the corresponding quantities in heavy nucleus initiated showers;

the large fluctuations in proton showers are thought to arise

from the relatively long mean free path for collision of the primary

with an air nucleus. The aim of this chapter is to assess as

accurately as possible the magnitude of the fluctuations of

observables in proton and heavy primary induced air showers and to

decide which observables are most likely to yield reliable

information about the longitudinal development of EAS. We shall

also consider which observables do not fluctuate and therefore

may be used to determine the primary energy regardless of the

cascade development. In order to make this assessment the 'normal'

model for shower development (described in Chapter 3) has been used

although the effects of changing the model for nuclear interactions

on the fluctuations have been investigated.

These investigations refer to the primary energy range of

$10^{15} - 10^{18}$ eV and a total of more than 650 simulations form the

basis of the work. Table 6-1 gives a summary of the simulations

Energy (eV)	Computational Technique Employed	Characteristics of Simulations	Number of Simulations
10^{15}	'hybrid'	A = 1 'normal' model	54
		A = 1, $E_p^{\frac{1}{2}}$ mult. law	25
		A = 56 normal model	25
		A = 56 'scaling'	25
		A = 1 'scaling'	25
	Monte Carlo	A = 1 'normal' model	25
		A = 56 " "	25
		A = 1 'scaling'	25
		A = 1 $E_p^{\frac{1}{2}}$ mult law	25
10^{16}	'hybrid'	A = 1 'normal' model	25
10^{17}	'hybrid'	A = 4 'normal' model	25
		A = 56 " "	25
		A = 1 " "	80
		A = 1 isobar model	20
		A = 1 $E_p^{\frac{1}{2}}$ mult. law	25
		A = 1 'scaling'	20
10^{18}	'hybrid'	A = 1 'normal' model; θ=0°	73
		A = 1 'normal' model; θ=30°	109

TABLE 6-1

Summary of Simulation Data Available for Fluctuation Studies.

made for each primary particle mass and indicates the computational procedure used. The minimum number of simulations upon which the interpretations that follow are based is 20; in the most important cases there are considerably more. For example $10^{17} - 10^{18}$ eV proton initiated showers have samples comprising more than 100 simulations each.

Table 6-2 gives a comparison of the fluctuations in various EAS parameters from 10^{15} eV iron nucleus initiated air showers produced by the 'hybrid' and the Monte Carlo computational techniques. On the basis of this comparison it was assumed that the fluctuations produced by the 'hybrid' procedure for parameters in EAS of primary energy $>10^{15}$ eV would be realistic.

The results for shower fluctuations derived from these simulations are compared as far as possible with experimental results and the results of other model calculations.

6-2 Fluctuations of the Electron Component

6-2.1 Proton Initiated EAS

The average longitudinal development of the electron cascade of proton initiated air showers is characterised by the primary energy (see Fig. 4-3(a)). As the primary energy increases, on average, the electron cascade develops deeper in the atmosphere. However, individual air showers can comprise electron cascades that differ greatly from the mean. Fig. 6-1 shows the electron cascade from a sample of ten proton initiated air showers of primary energy 10^{17} eV.

The number of electrons observed at cascade maximum, as is the case at the Chacaltaya experiment for showers of energy $\sim$ 10^{15} eV, is often used as a direct indication of the primary energy; it is interesting to note the fluctuations present in this

Parameter	Value		Relative standard deviation from the 'hybrid' technique	Relative standard deviation from the Monte Carlo technique
	'hybrid'	Monte Carlo		
Height of max. development of the electron cascade	494g cm^{-2}	482g cm^{-2}	5.6%	5.4%
Number of muons > 1 GeV	$1.40.10^4$	$1.52 \ 10^4$	4.4%	4.3%
Number of muons > 10 GeV	$4.97.10^3$	$5.00 \ 10^3$	2.2%	2.4%
Number of muons >100 GeV	$3.94.10^2$	$3.72 \ 10^2$	8.65%	12.5%
Number of Electrons at Sea Level	$7.50.10^4$	$7.15 \ 10^4$	21%	21%

<u>TABLE 6-2</u>

<u>Comparison of Fluctuations Obtained from the 'Hybrid' and full Monte-Carlo Computational</u>

<u>Techniques for 10^{15} eV Iron Nucleus Initiated EAS.</u>
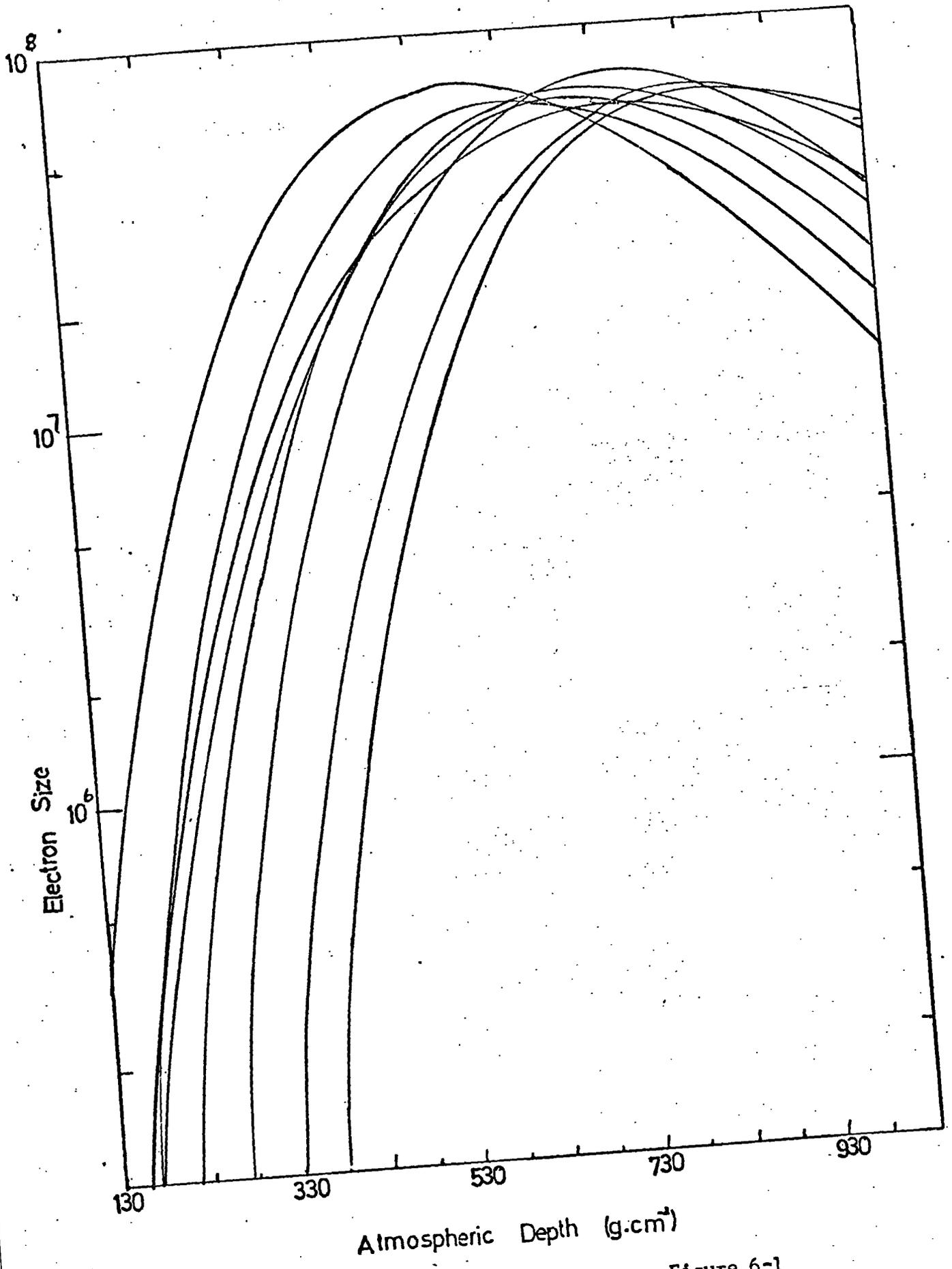
Figure 6-1

Electron longitudinal development curves

Axis labels: Electron Size (vertical), Atmospheric Depth (g.cm⁻²) (horizontal)

quantity at this and other observation depths. Fig. 6-2 shows the relative standard deviation of the electron size as a function of atmospheric depth of the observation level for proton initiated air showers with primary energies of 10^{15}eV and 10^{17}eV. It is instructive to compare the fluctuations in electron size present at an atmospheric depth of 530 g cm^{-2} for a primary energy of 10^{15}eV with the fluctuations in the Haverah Park ground parameters $\rho(600)$ at sea level for EAS of primary energy $\sim 10^{17}$eV. The Haverah Park measure of the primary energy is observed to be far less susceptable to fluctuation than is the electron size at maximum (9% as opposed to 22%).

Fig. 6-3 (a) shows the relative standard deviation for the depth of maximum cascade development as a function of energy for proton initiated air showers simulated using the 'normal' model for nuclear interactions. Comparison is made with the fluctuations obtained by Hillas et al.(1971) using their Model A.

The fluctuations in the number of electrons at sea level, Ne_{SL}, have been calculated at energies between 10^{15}-10^{18}eV and the relative standard deviations are shown in Fig. 6-3 (b). The model calculations with which these results are compared are those of Kristiansen et al.(1966), de Beer et al.(1968) and Marsden (1971).

6-2.2 Heavy Primary Initiated EAS

Intuitively one would expect the fluctuations in heavy primary initiated EAS to be smaller than those produced by proton initiated air showers. This is so because, even with the form of fragmentation described in Chapter 5, the majority of nucleons in a heavy nucleus are free by the time they reach an atmospheric depth of 150 g cm^{-2} and then they produce an overall smoothing effect on the fluctuations. The relative standard deviation of the depth of maximum development
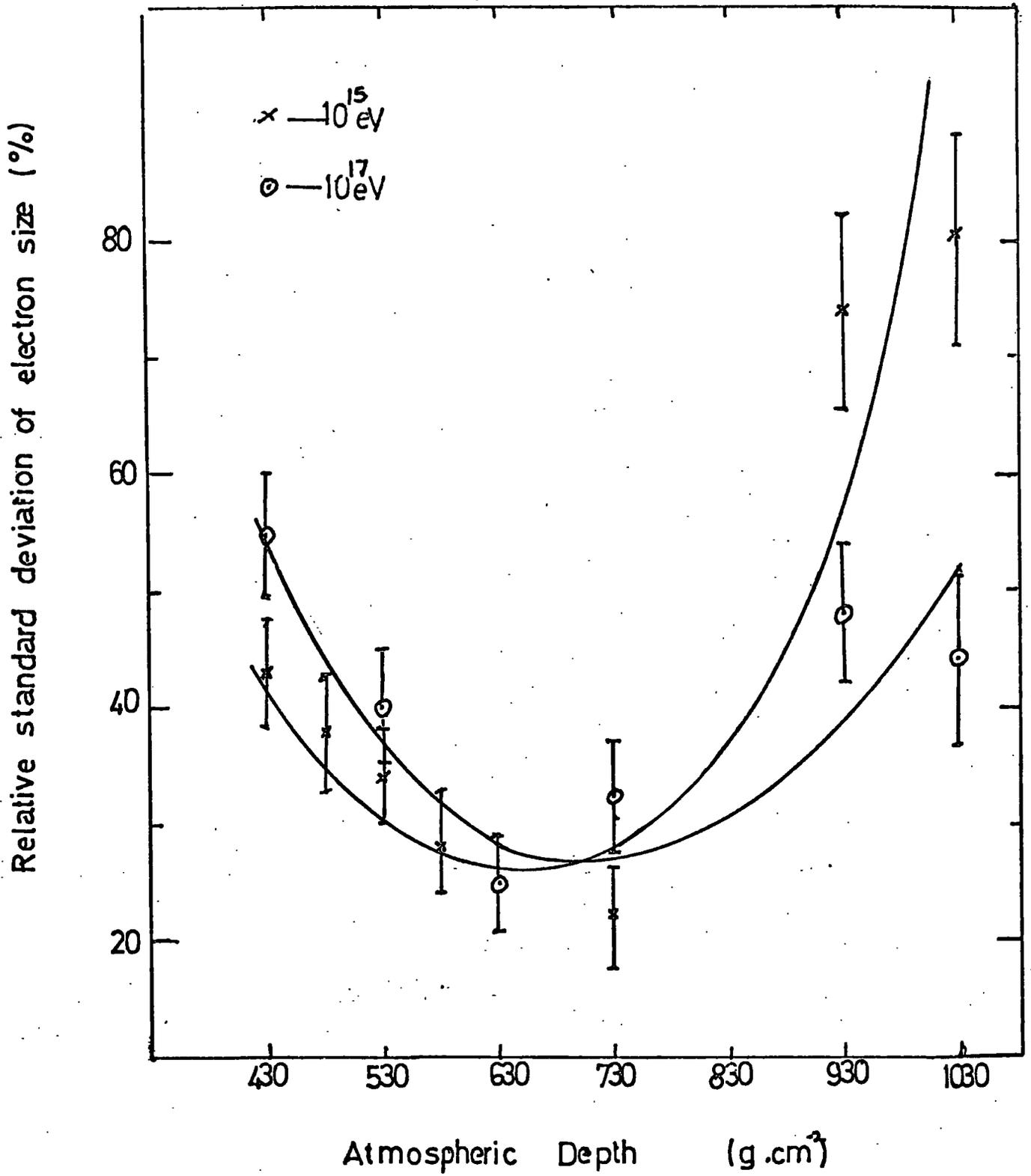
Figure 6-2

The variation of fluctuations
in electron size with
atmospheric depth.

(a)

(b)
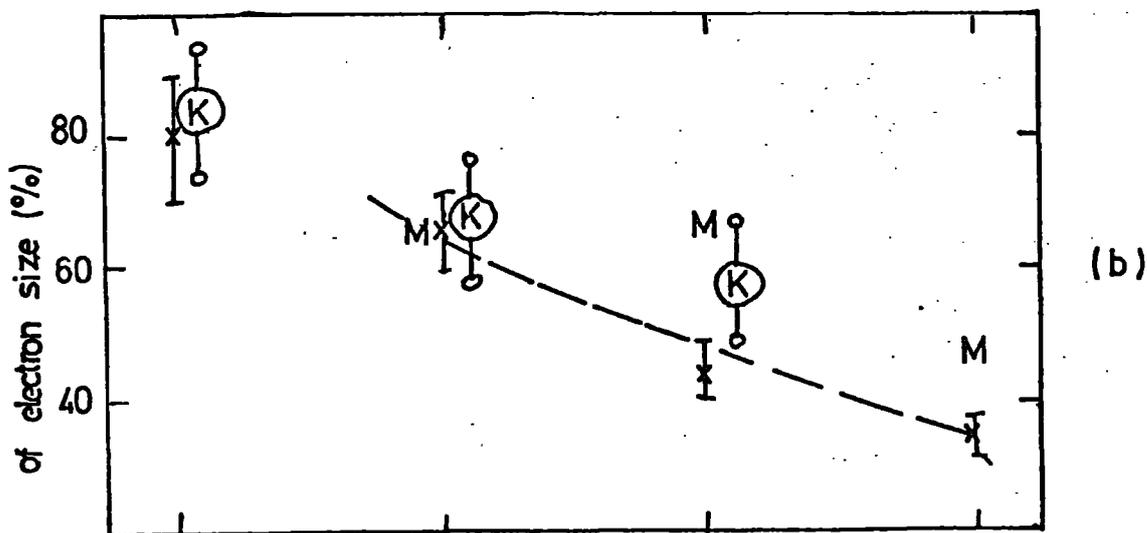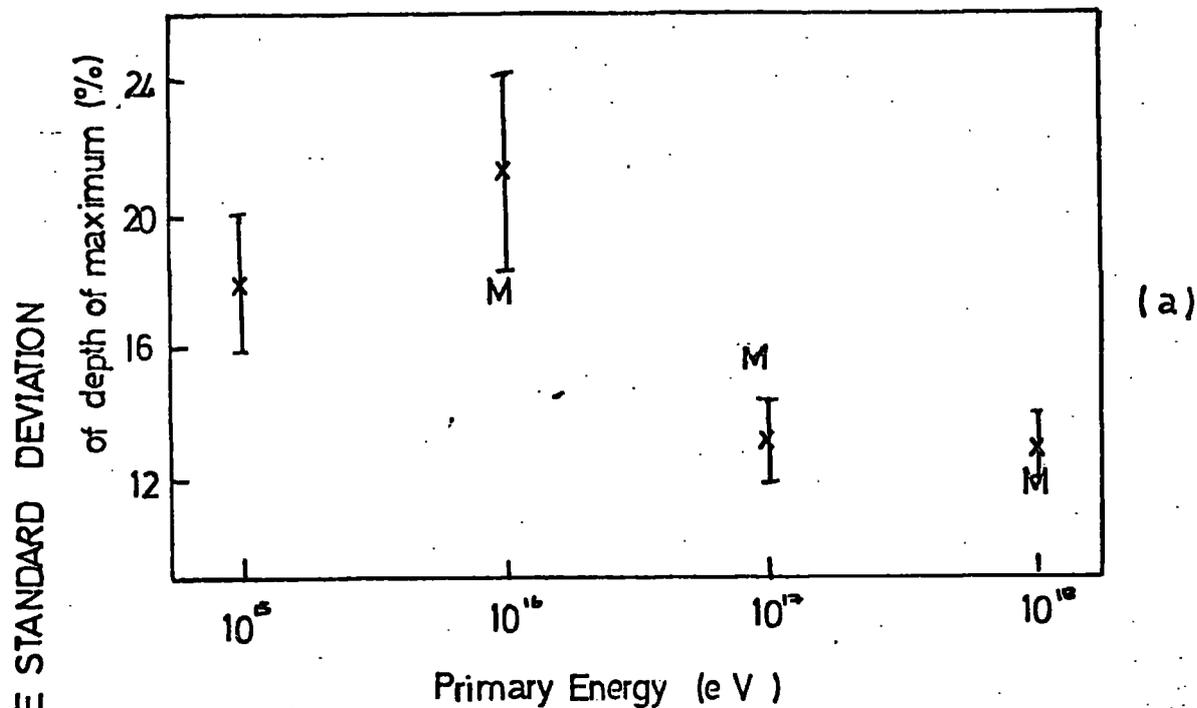
$\frac{\mathbf{I}}{\mathbf{I}}$ present work
K - Khristiansen et al (1966)
M - Marsden (1971)
— — de Beer et al (1968)

Figure 6-3

Fluctuations in the depth of
maximum development of the
electron cascade and the electron
size of proton initiated EAS as
a function of energy.

of the electron cascade and the electron number at sea level have been calculated using the partial fragmentation model described in the previous chapter and are shown as a function of energy for a primary of atomic mass number 56 in Figs. 6-4(a) and 6-4(b). The 'superposition' model predicts fluctuations in heavy nucleus initiated showers specified by a relative standard deviation which varies as:

$$\sigma_A = \frac{\sigma_P}{\sqrt{A}} \qquad (\text{Hillas et al.}(1971)).$$

The predictions of such a model based on our calculations for protons primaries are also shown. The variation in fluctuations predicted by the partial fragmentation model as a function of primary atomic mass number, A, are shown in Fig. 6-5.

6-2.3 Comparison with Experimental Data

The theoretical predictions for fluctuations in the electron cascade can be compared with experimental results by studies of the radio emission and the optical Cerenkov light from EAS, both of which may be expected to reflect the longitudinal development of the electron cascade.

It has been established that the pattern of the radio lateral distribution gives information about the longitudinal development of the shower and in particular about the height of shower maximum above the receiving antennae. Allan et al. (1973) measured the lateral distribution of the radio emission at 60 MHz for approximately 100 showers with energy $>10^{17}$ eV at varying zenith angles and on the basis of these measurements concluded that for showers recorded by the Haverah Park EAS array of the same energy and zenith angle the position of shower maximum appears to fluctuate by more than 100 g cm^{-2} about its average position. These results are supported

Figure 6-4

Fluctuations in the electron component of iron nucleus initiated EAS.

A= 56
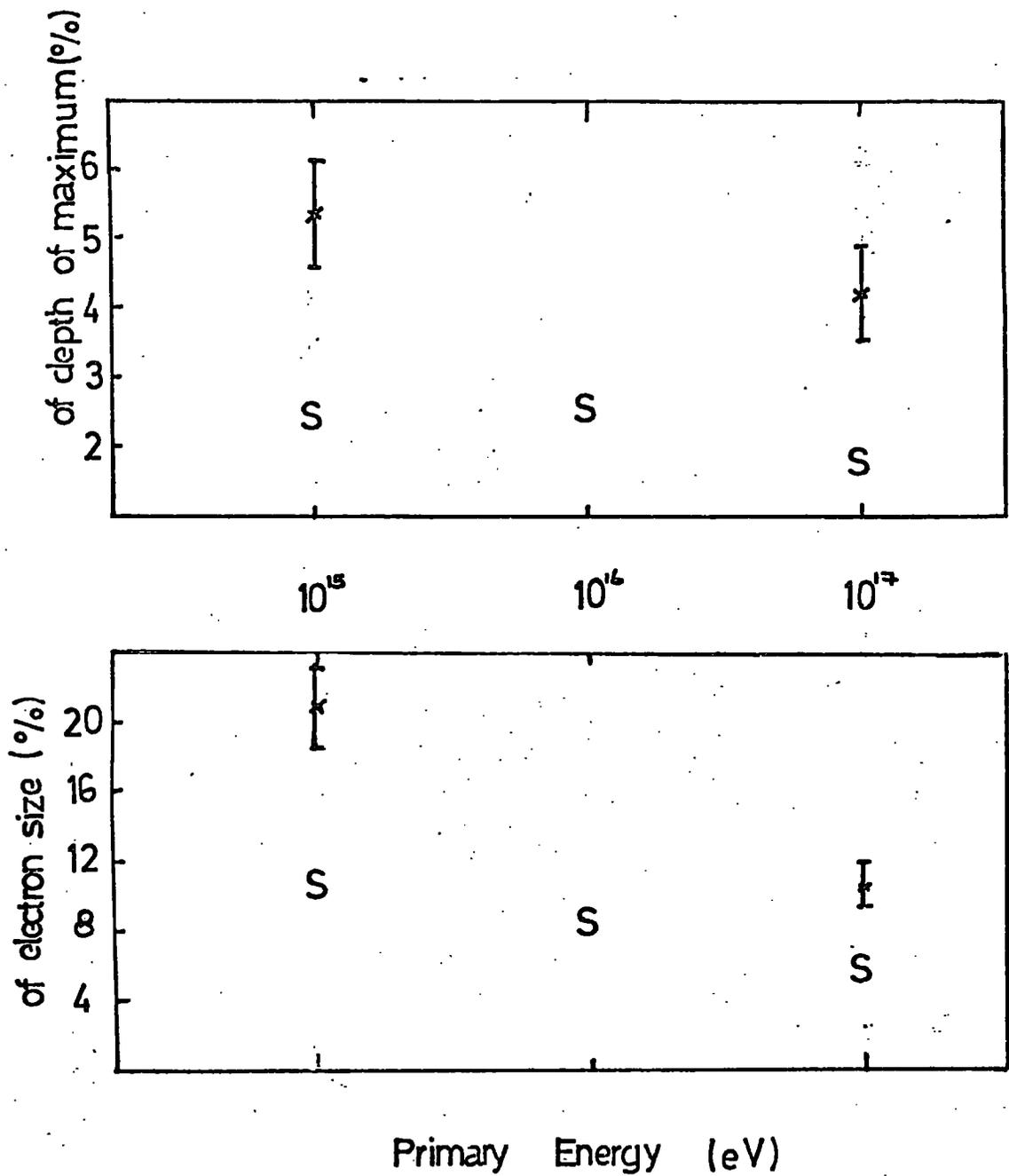
$\bar{x}$ - partial fragmentation model

S - 'superposition'
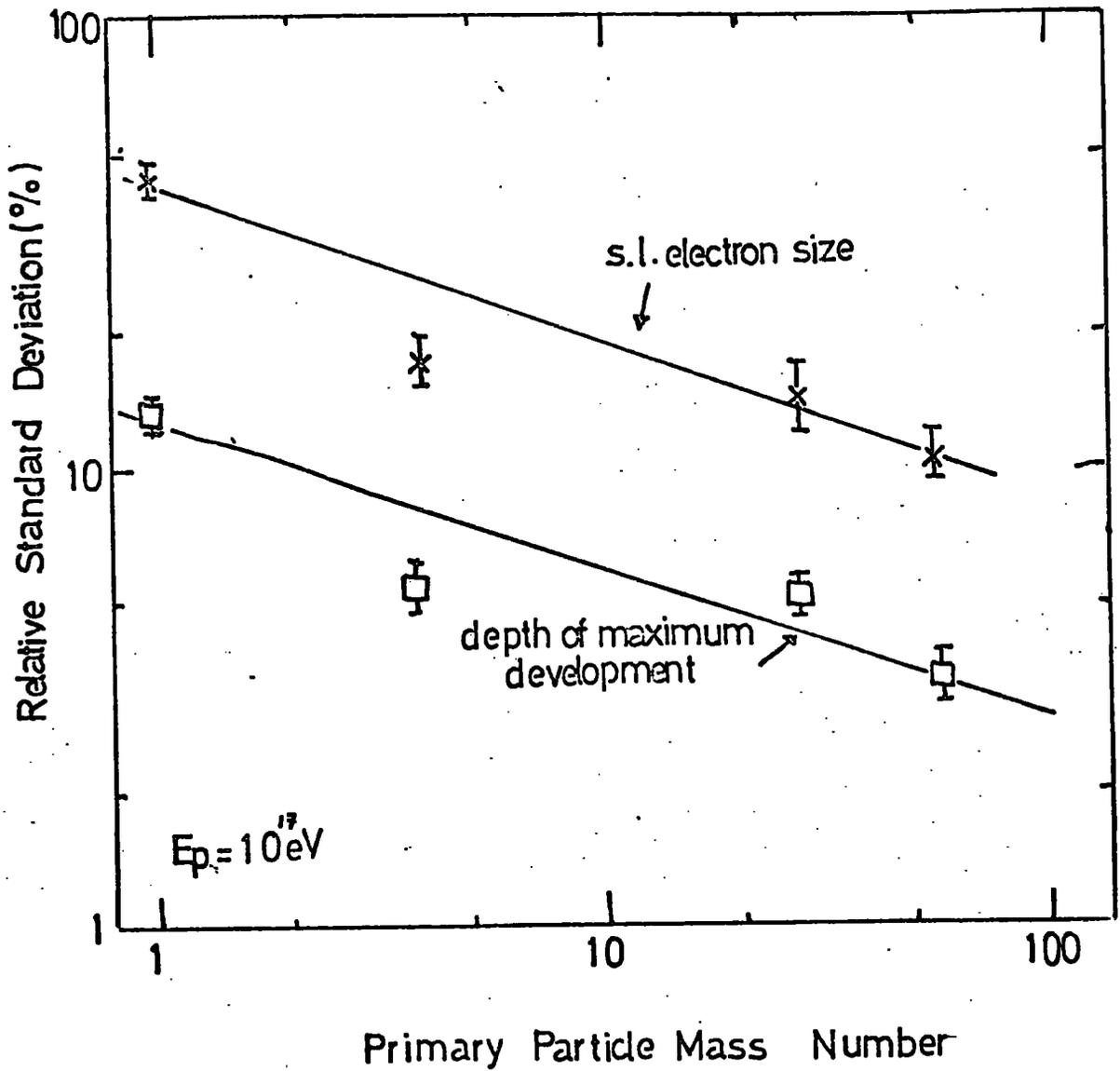
Figure 6-5

Fluctuations in the electron component of EAS.

to some extent by Mandolesi et al.(1973) who have published results from their EAS array at Bologna. The electron size range for which results are quoted is $9 \times 10^6 \to 7 \times 10^7$ particles (this corresponds to an energy range $\sim 4 \times 10^{16} \to 3 \times 10^{17} eV$). This group find a large spread in the points in their lateral distribution curve which could be caused by fluctuations in the height of maximum development of the electron cascade.

Fig. 6-6 shows a comparison of the predictions for fluctuations in the height of maximum development of the electron cascade from proton and heavy primary initiated air showers from the present work with the experimental results quoted above. It should be emphasised most strongly that the experimental data available are subject to substantial uncertainties in absolute values (Allan et al.(1973)). It will be of great interest to see whether or not the radio data are confirmed by the data on other components of the shower that will become available in the near future (eg.the optical Cerenkov signal from EAS).

Fig. 6-7 shows the extreme fluctuations of the electron cascade for air showers initiated by protons of energy $10^{17} eV$ predicted by the present work;comparison is made with data showing the same degree of fluctuation from showers initiated by iron nuclei of the same energy. This comparison confirms the validity of the fundamental assumption of fluctuation studies (ie that it is possible to uniquely distinguish wildly fluctuating proton initiated EAS) even if the more realistic partial fragmentation model for heavy nuclei (described in Chapter 5) is used.
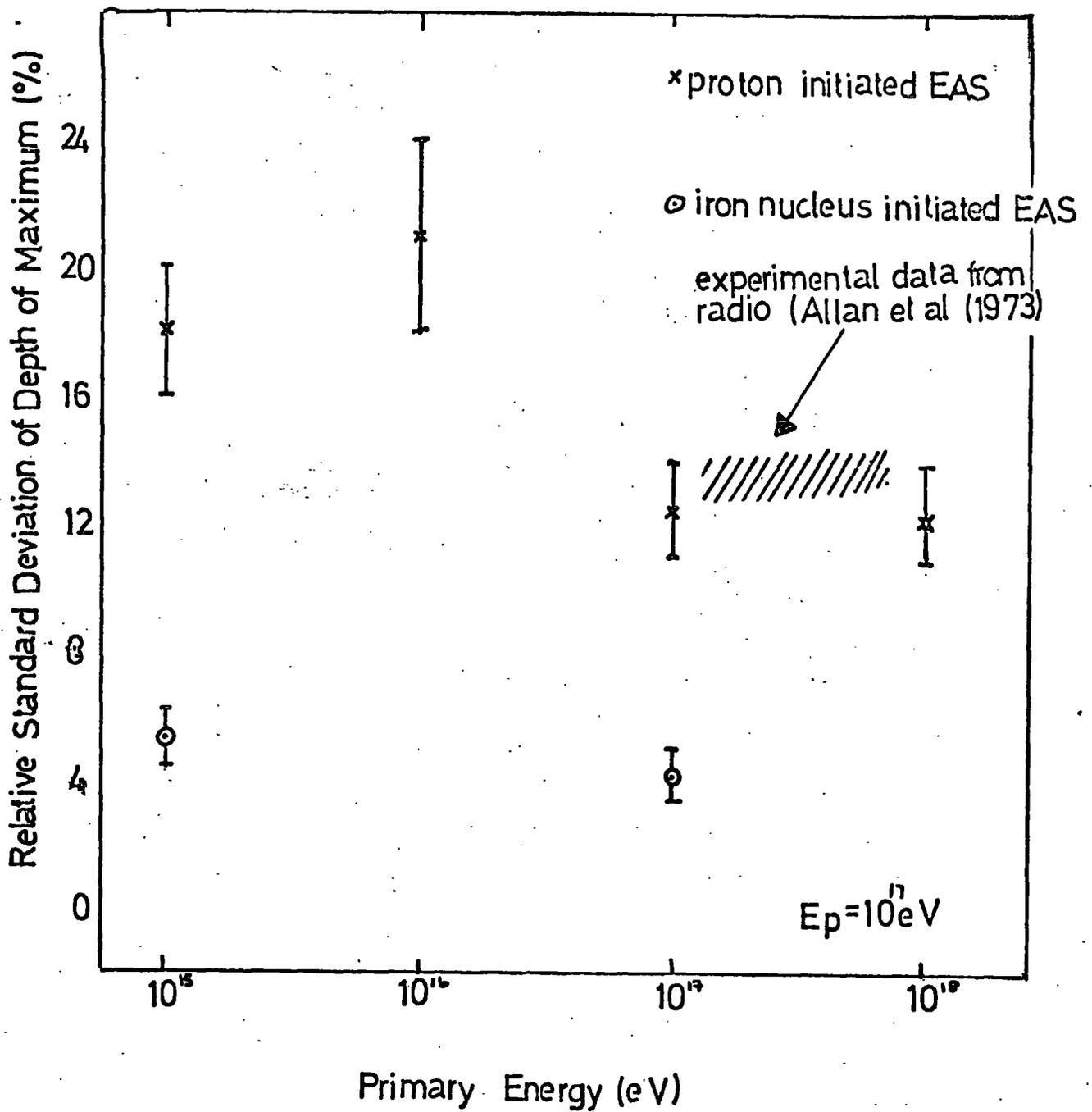
Figure 6-6

Fluctuations in the depth of maximum development of the electron cascade
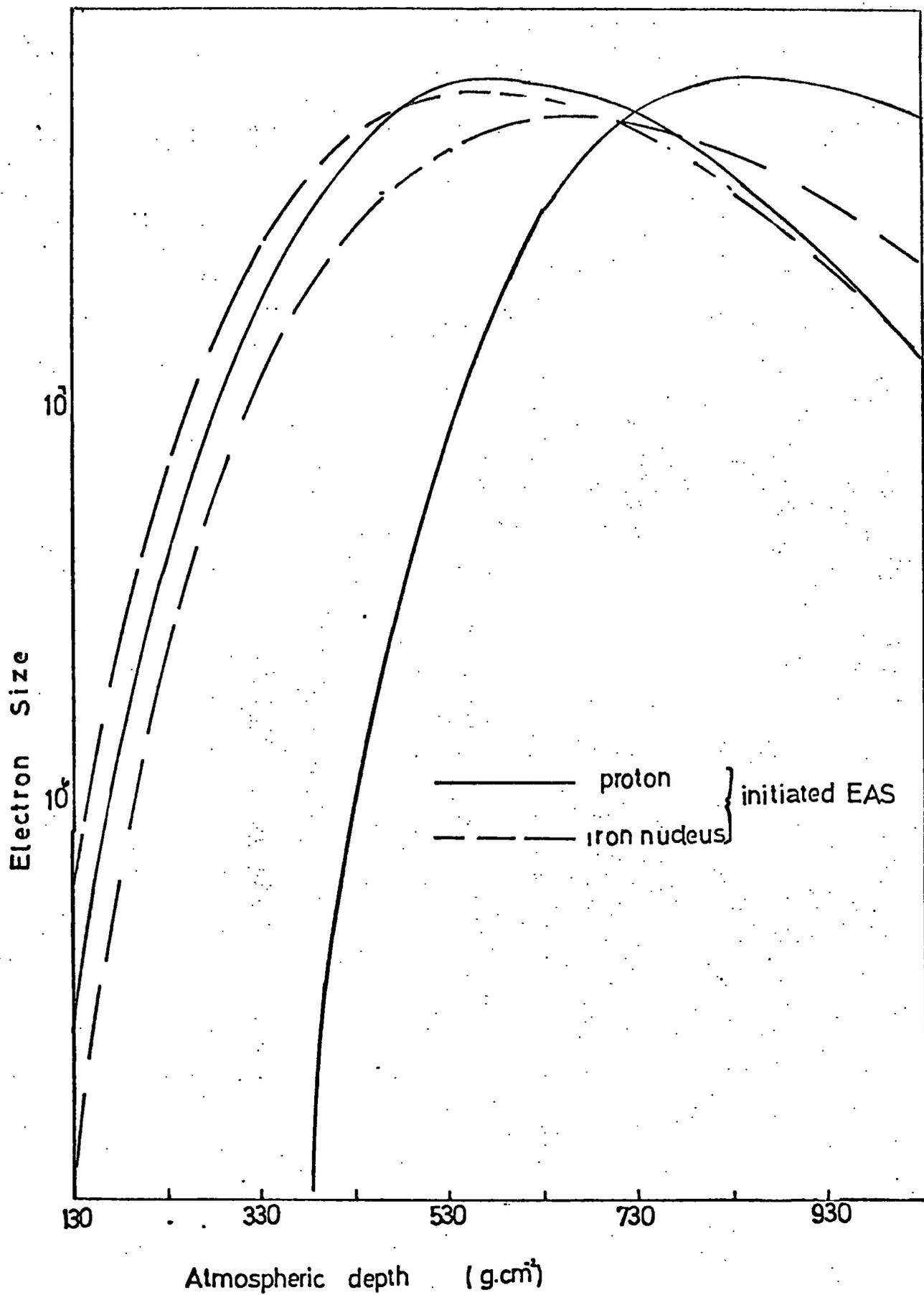
Figure 6-7

Electron cascade longitudinal
development (5% limits)

6-3 Fluctuations in the Muon Component

6-3.1 Introduction

It has been well established for some time both from experiments and from model calculations that the muon component of air showers fluctuates to a lesser extent than does the electron component. The fluctuations in various apsects .of the muon component have been calculated for the 'normal' model with particular attention being paid to those aspects that might be measurable at the Haverah Park experiment. It should be noted that the basic calculations do not include geomagnetic and coulomb scattering of the muons for EAS with primary energy $>10^{15}$ eV; Stephenson and Turver (1973) have made a more refined study of the muon component using the pion production spectrum from the present work as the starting point. It is therefore not the author's intention to make a detailed comparison of the predicted fluctuations for (say) the muon time delays with the work of other authors (eg. Lapikens (1974)).

6-3.2 Proton Initiated EAS

The fluctuations of the total muon number as a function of primary energy calculated from the present work are shown in Fig. 6-8 where they are compared with the results of Marsden (1971) and Khristiansen et al (1966). The fluctuations decrease with increasing primary energy, as do the fluctuations of the electron component but, for example, at 10^{15} eV the value of the relative standard deviation of the muon number (>1GeV) is much smaller (13%) than the relative standard deviation of the electron size (80%).

One of the reasons for the fluctuations being less for the muon component at sea level than for the electron component is that the muon cascade has a very long attenuation length and this means that the cascade is essentially at or near maximum development over a
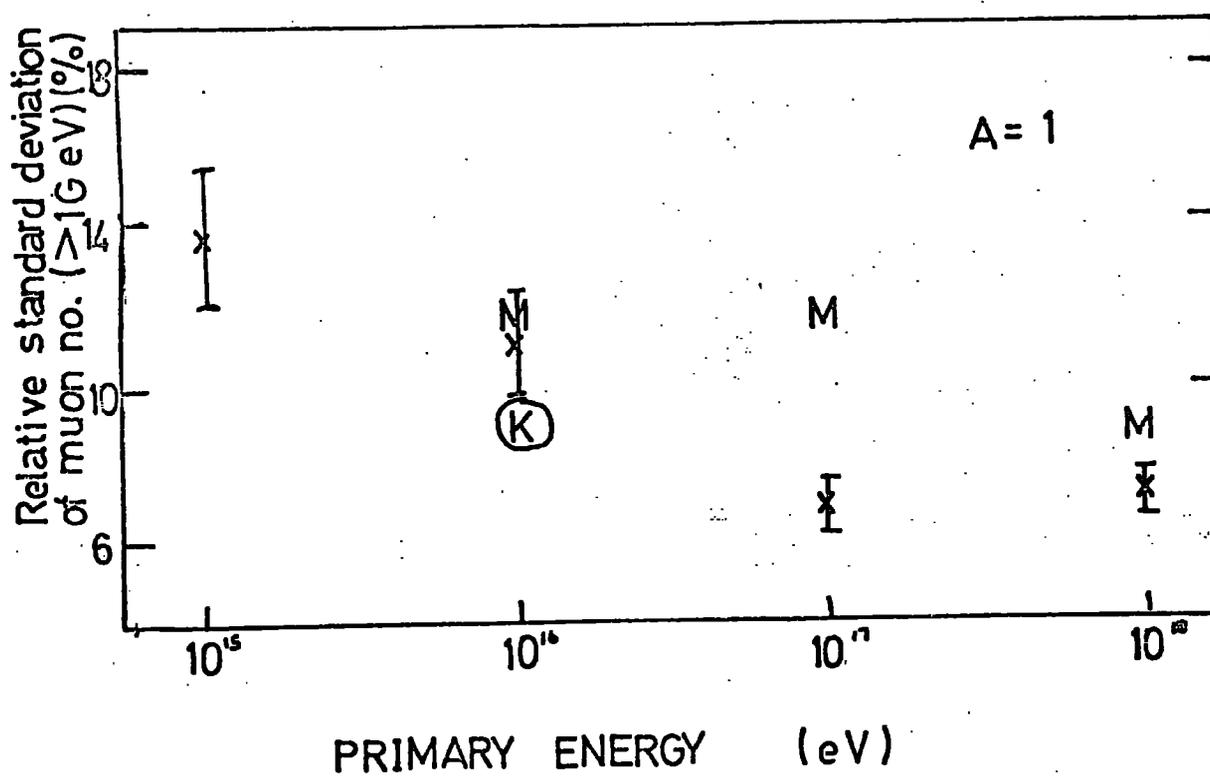
Figure 6-8

Fluctuations in the muon component

wide range of depths in the atmosphere. Fig. 6-9 shows a typical development curve for the total number of muons in EAS and a striking feature of these curves is the slow attenutation over the range considered.

The fluctuations in the density of muons with energy greater than 1 GeV at various distances from the shower core have been calculated and are displayed in Fig. 6-10. Unfortunately two problems are encountered if one considers using these fluctuations as a tool for detecting primary protons. If measurements are made near the core where the densities are greater, the core location error becomes an important factor, and unless it is very small, obscures the genuine fluctuations. On the other hand, if one moves far away from the core in order to make the measurements the density falls off rapidly and 'sampling' errors become important.

6-3.3 Heavy Primary Initiated EAS

The effect on the fluctuations in the muon component of EAS of an increase in primary mass from A = 1 to A = 56 is shown in Fig. 6-11 for 10^{17} eV primary particles. Increasing the primary mass has the effect of reducing the size of fluctuations; for example, if one considers the muon density at 50m from the shower core the relative standard deviation is 11.1% for proton initiated EAS and 3.6% for iron nucleus initiated showers. (Unfortunately both the core location error and the need for many expensive muon detectors to ensure a measurement at 50m would at present preclude the use of these fluctuations to detect protons in the primary cosmic radiation).

6-4 Fluctuations in the Deep Water Cerenkov Detector Response
        at Haverah Park

It is important when choosing a measurement to act as a primary energy estimator that it does not fluctuate much for
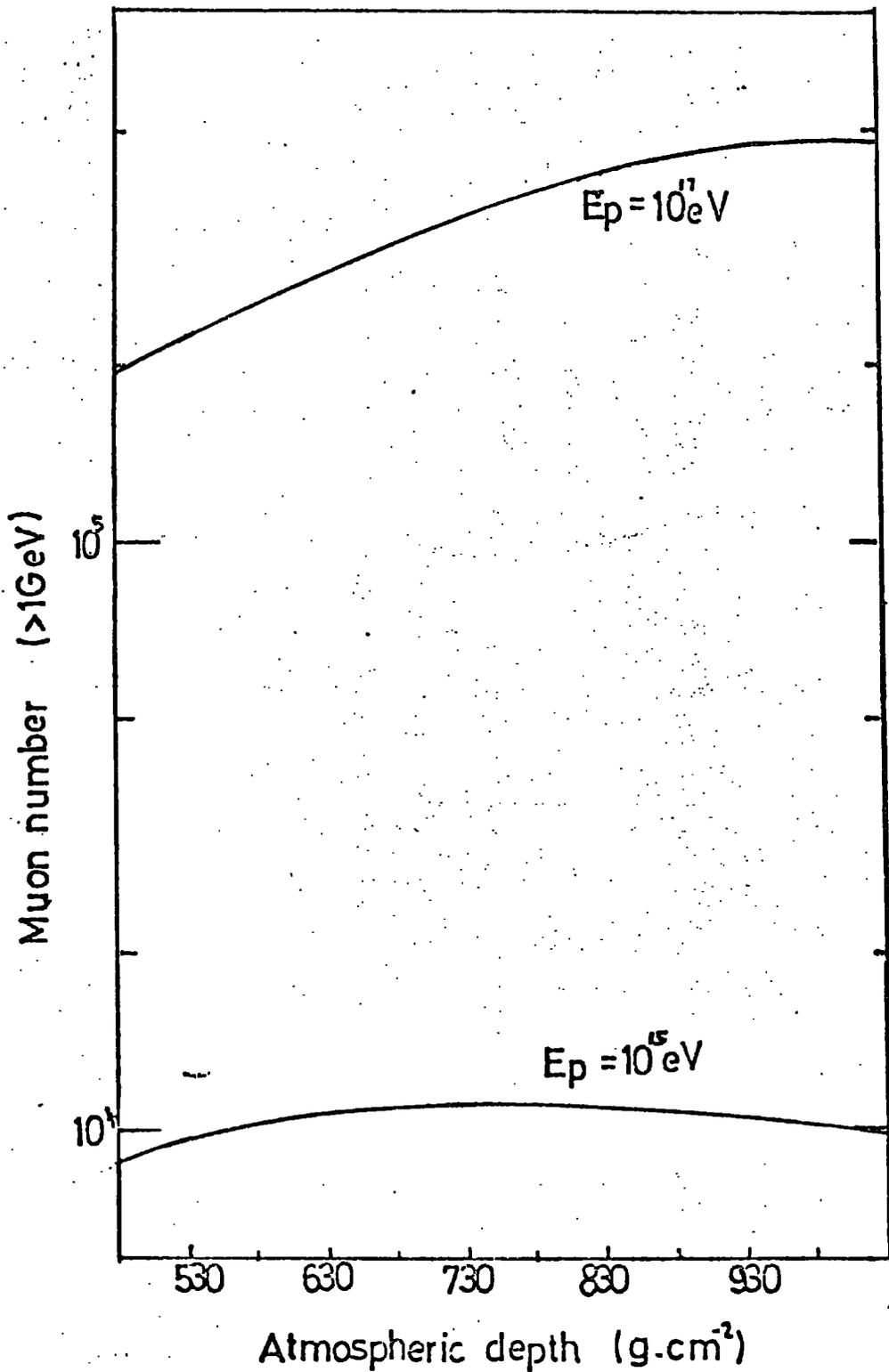
Figure 6-9

The longtidinal development of
the muon component of proton
initiated EAS of primary
energies 10^{15}eV and 10^{17}eV
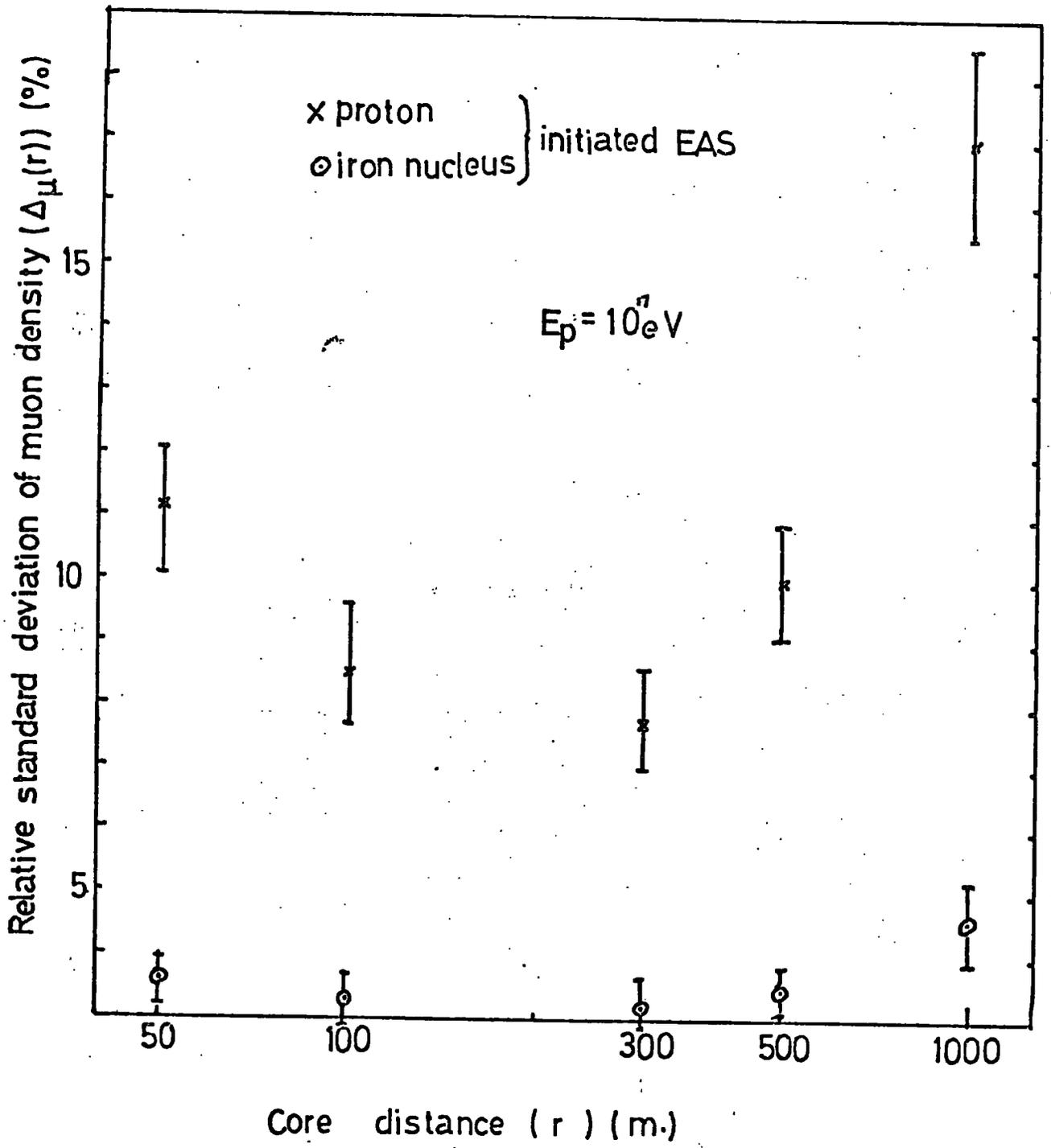
Figure 6-10

Fluctuations in muon densities
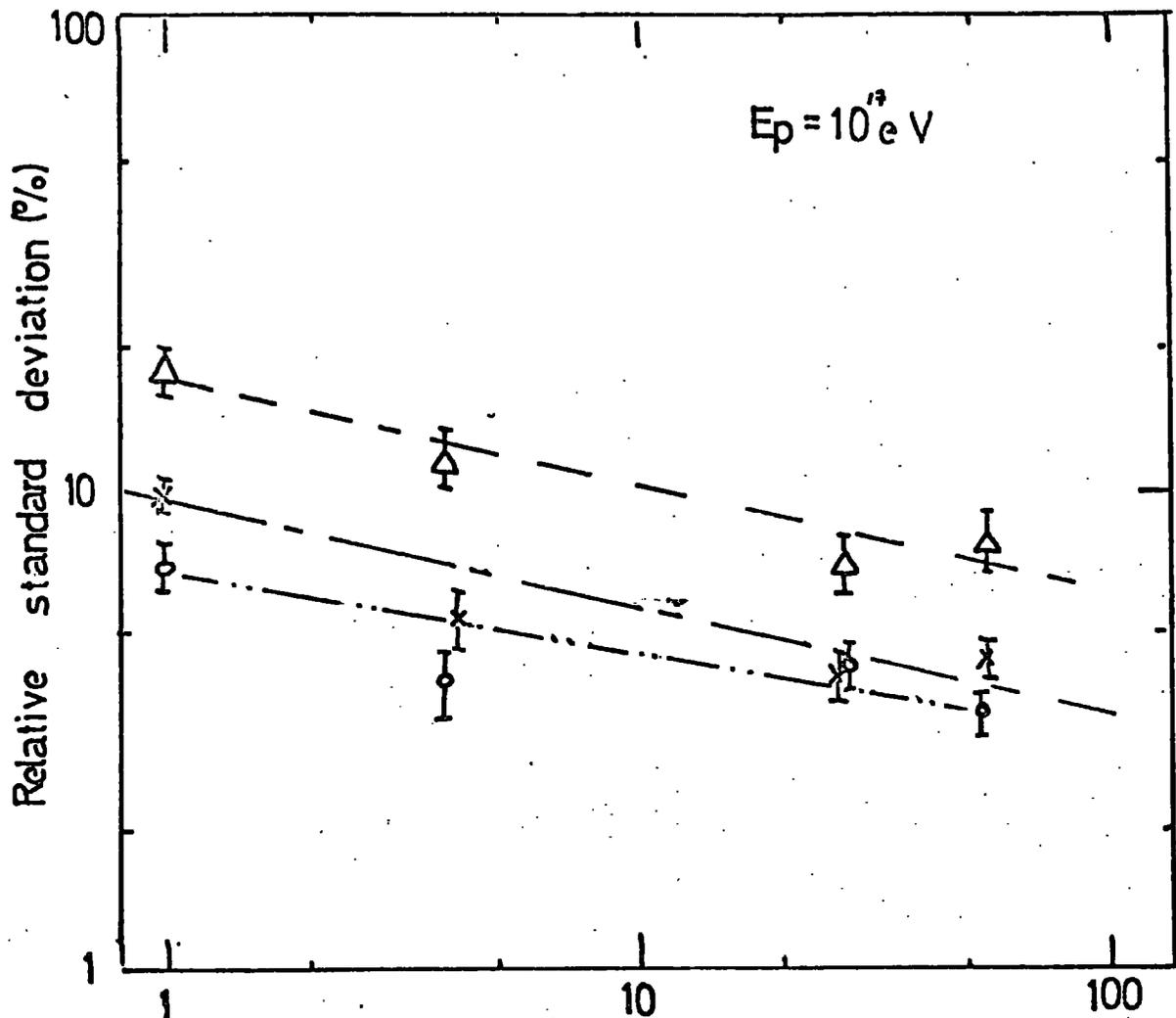
Figure 6-11

Fluctuations in muon numbers

showers of a fixed primary energy. At Haverah Park the measurement
that has been evolved for this purpose is the deep water Cerenkov
detector response at 600m from the air shower core $(\rho(600))$
(Hillas (1970)). The fluctuations in the ratio $\rho(50)/\rho(500)$ arising
from $\rho(50)$, have been suggested as a possible way of distinguishing
protons from heavier particles (Reid, (1971)). For both these
reasons it is considered important to study the fluctuations
produced in the detector response at all core distances using our
'normal' model for interactions.Fig. 6-12 shows the variation in
the fluctuation of $\rho(r)$ as a function of r for both proton and
heavy nucleus initiated air showers of primary energy 10^{17}eV.

It can be seen that the relative standard deviation of $\rho(600)$
is approximately 8% and it is therefore a very good measurement
to use as a primary energy evaluator.

The fluctuations in $\rho(50)/\rho(500)$ for proton and iron nucleus
initiated EAS have been calculated to be 23% and 12% respectively
and this would therefore seem to be a promising method for
detecting the presence of proton primaries by their extreme
fluctuations.

6-5   Effects of Changes in the Model for Interactions upon the
         Fluctuations of Air Shower Parameters

The sensitivity of the average shower characteristics to
changes in the representation of p-N and π-N interactions has
been investigated and discussed in Chapter 4. The fluctuations in
the predicted shower parameters have been studied for these
changes of the model for interactions; the results are summarized
in Table 6-3 for models involving large changes in the multiplicity
of secondaries in interactions. The 'scaling' model, which has
a multiplicity law varying as the logarithm of the radiated energy,

Model for Interactions	$\dfrac{\sigma}{Ne_{sl}}$	$\dfrac{\sigma}{N_{\mu}(>1GeV)}$	$\dfrac{\sigma}{h_{tmax}}$	$\dfrac{\sigma}{\Delta_{\mu}(>1GeV, 100m)}$
'Normal' model	$44 \pm 4\%$	$7 \pm 0.7\%$	$13.2 \pm 1.2\%$	$8.5 \pm 0.8\%$
Scaling model ($n_s \propto \ln Ep$)	$46 \pm 13\%$	$27 \pm 8\%$	$11 \pm 3\%$	$26 \pm 7\%$
High multiplicity model ($n_s \propto Ep^{\frac{1}{2}}$)	$45 \pm 7\%$	$7.7 \pm 1.2\%$	$14 \pm 2.2\%$	$10 \pm 1.6\%$

TABLE 6-3

<u>Comparison of the Fluctuations Predicted</u>

<u>for the Muon and Electron components of</u>

<u>EAS when the Multiplicity Law for the</u>

<u>Production of Secondary Particles is</u>

<u>Varied.</u>
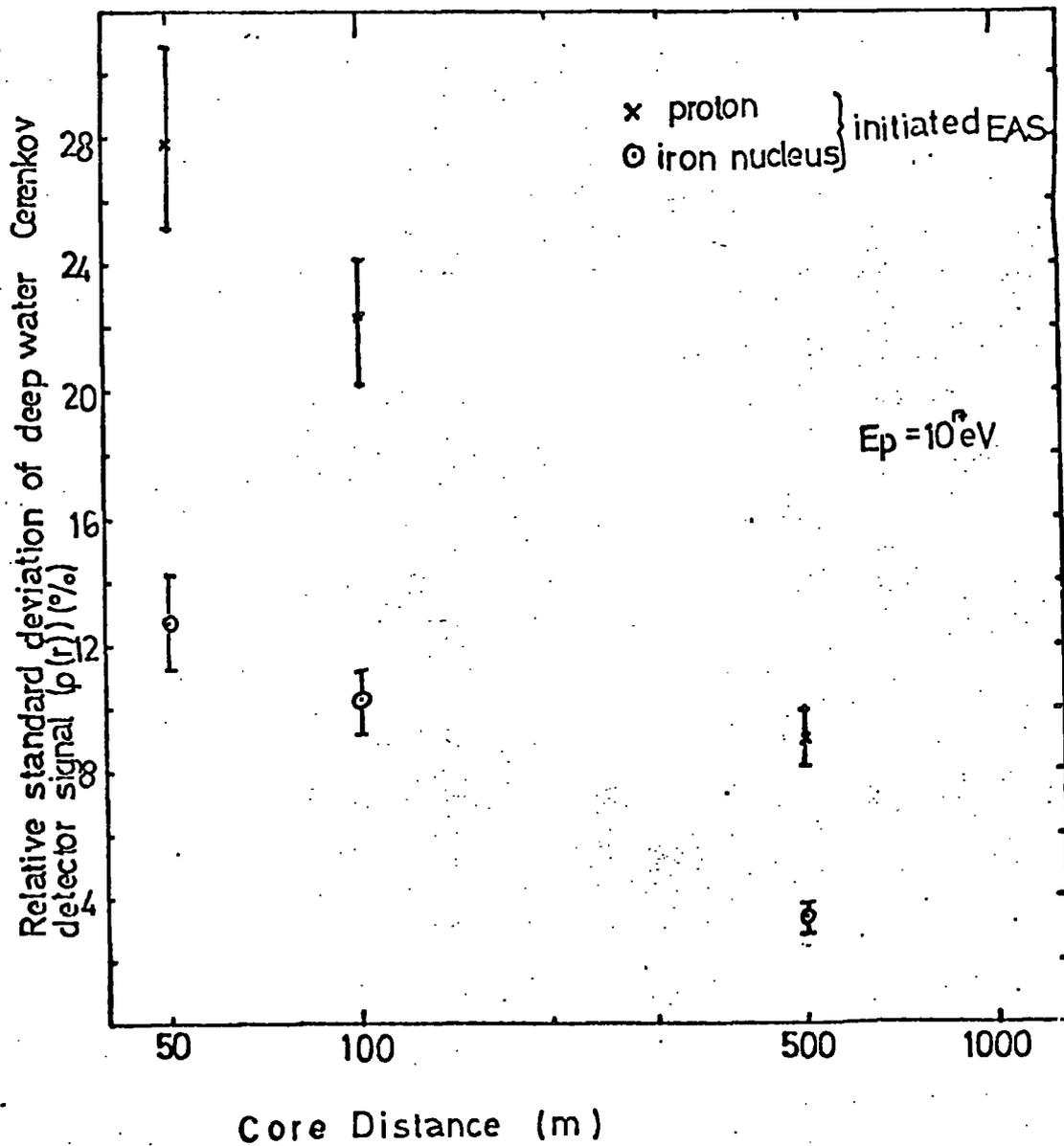
Figure 6-12

Fluctuations in the water Cerenkov detector response at various distances from the shower core

$(\ln(E_r))$ produces very much larger flucatuions in the muon numbers

than either the CKP model $(E_r^{\frac{1}{4}})$ or the high multiplicity model

$(E_r^{\frac{1}{2}})$. However, fluctuations in the electron component for all

three models are indistinguishable.

6-6   Identification of the Main Causes of Fluctuations in EAS

6-6.1   Introduction

In the following section attempts have been made to identify

the main causes of fluctuations in both proton and heavy nucleus

initiated air showers. As a tool in this search, tests of correlation

have been made using a standard statistical treatment of the data.

The procedure produces a value for the product moment coefficient

of correlation, r, for each pair of variables considered. It should

be noted that the normal quantitative interpretation of such values

is not valid because in some cases the variables are not linearly

related and also the number of values in each sample is not constant;

this makes the interpretation of r not straightforward. However,

r has been used as a qualatative guide to the correlations between

sets of variables and has proved most satisfactory in this respect.

6-6.2   Proton Initiated Air Showers

It has been suggested by authors in the past (eg Ueda and Ogita

(1957)) that the main cause of fluctuations in the air showers

initiated by protons is the point of first interaction of the

primary after it has entered the atmosphere. In order to test

the validity of this hypothesis using the present calculations, the

correlation coefficient was calculated between the point of initial

interaction, λ_1, and various fluctuating parameters in EAS. Table

6-4 shows the result of this investigation for proton primary

initiated EAS of energy 10^{16}eV, 10^{17}eV, and 10^{18} eV. The correlation

between λ_1 and the components of air showers showing large

Energy	10^{16}eV	10^{17}eV	10^{18}eV
r for λ_1 and h_{tmax}	.818	.913	0.764
r for $nsec_1$ and h_{tmax}	.205	.178	-.096
r for λ_1 and Ne_{SL}	.864	.874	.851
r for $nsec_1$ and Ne_{SL}	.314	.178	-.118
r for λ_1 and $\rho(50)$	-	.830	.825
r for $nsec_1$ and $\rho(50)$	-	.150	-.134

TABLE 6-4

r = correlation coefficient
λ_1 = point of first interaction of primary particle
$nsec_1$ = number of secondaries produced in 1st interaction
$\rho(50)$ = deep water Cerenkov detector signal at 50m
ne_{SL} = electron size at sea level.

Correlation coefficients calculated between parameters
of 10^{18}eV Proton Initiated EAS

fluctuations in this energy range (eg.electron size at sea level and depth of maximum development of the electron cascade) is high. For comparison, the values of r for the number of secondary mesons produced in the first interaction, n_{sec1}, and the same parameters are shown. It is clear that the value of n_{sec1} has very little bearing on the subsequent development of the air shower whereas the point of first interaction of the primary proton would appear to be the main cause of fluctuations.

At lower primary energies ($< 10^{15}$eV) the position of initial interaction is found to have less bearing on the development of the air shower. Since at low energies the showers are very 'old' by the time they reach the sea level this is not unexpected. Turver (1972) has established that a more appropriate variable based only upon the nucleon cascade that may be used to predict the development of an EAS is what he terms the 'shower development factor'. This is a variable which gives a measure of the dissipation of the primary energy as the primary particle traverses the atmosphere. Turver finds that the 'shower development factor' correlates very well with the fluctuating shower parameters at energies $< 10^{15}$eV; above this energy λ_1 is the major cause of fluctuations and the 'shower development factor' offers no advantage.

6-6.3 Heavy Primary Initiated Showers

6-6.3.1 Fragmentation factor F

In order to make an assessment of the correlations between the fragmentation of heavy primary nuclei and the development of the EAS it is necessary to define some measure of the fragmentation that may be calculated for each simulated heavy primary initiated EAS. The fragmentation factor, F, has therefore been defined and is the sum of a series of terms each of which is the number of nucleons

in a particular nucleus present in the cascade multiplied by the total distance that nucleus travels between the point where it was created and where it interacts. F has units of nucleons.g.cm^{-2} and represents the success of an individual cascade in carrying nucleons still shielded in a nucleus into the atmosphere. The factor is zero for the 'super-position' model for the break-up of heavy primary nuclei.

F was therefore calculated for each heavy nucleus initiated EAS that was simulated. It was hoped that if a correlation could be established between F and the longitudinal development of the shower it would be possible to use a calculation of the values of F for many fragmentation modes in order to predict the 5% probability levels for the depth of maximum of the electron cascade with good statistical accuracy. The fragmentation factor has been calculated for some 50,000 nucleon cascades of iron and silicon initiated EAS and the results are shown in Fig. 6-13.

6-6.3.2 Correlations of F with the Fluctuating Components of

Heavy Primary Initiated EAS

The correlation coefficients between F and those parameters of the simulated air showers showing large fluctuations were calculated. Table 6-5 gives a summary of these values of r for iron nucleus initiated EAS of primary energy 10^{17}eV. It can be seen that F correlates well with the depth of maximum but not as well with $\rho(50)$ and the electron size at sea level. In an attempt to find a more definite indication of the causes of fluctuations in heavy primary initiated air showers a further quantity known as the Interaction Factor, I, was calculated for each simulation. I is defined as the sum of the atmospheric depths traversed before initial interaction by all the constituent nucleons of the fragmenting nucleus. The correlation tests were repeated for I and the results
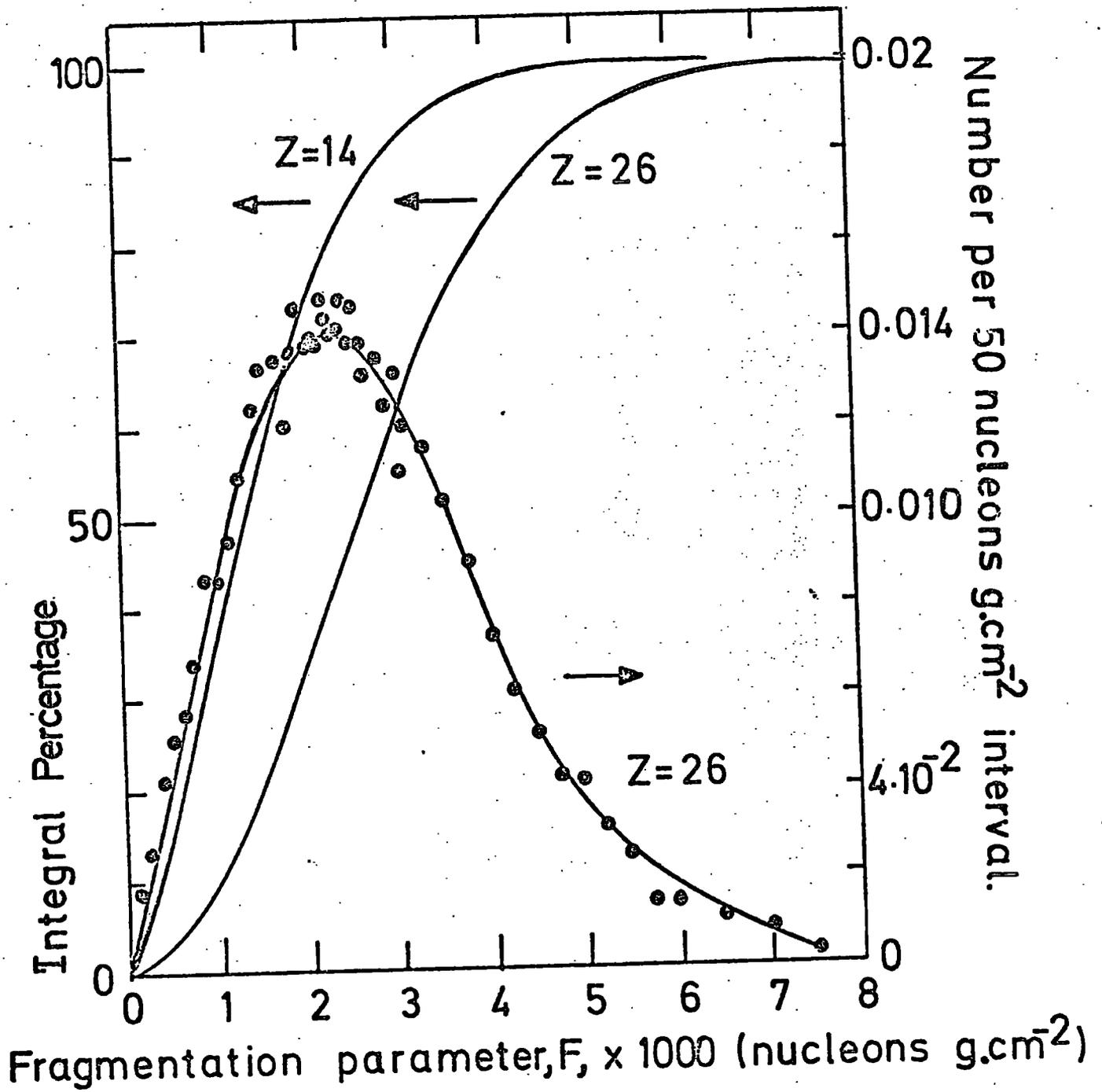
Figure 6-13

The distribution of the fragmentation parameter F from 50,000 nucleon cascades.

Parameter	Correlation Coefficient with F	Correlation Coefficient with I
Electron number at sea level ne_{SL}	0.592	0.821
The deep water Cerenkov detector response at 50m	0.386	0.665
Depth of max. development of the electron cascade	0.864	0.892

TABLE 6-5

Correlations of F and I with Fluctuating

Parameters in EAS.

are shown in Table 6-5. It is reasonable to conclude from these

results that the main cause of fluctuations in heavy primary

induced EAS is the way in which the heavy primary particle fragments.

6-7 Correlation between Parameters of EAS

6-7.1 Introduction

The simulations of the present study produce predictions

for a very wide range of parameters in EAS. In order to make

maximum use of the vast amount of available information, a

comprehensive examination of the correlations between all relevant

pairs of variables has been carried out for each catagory of simulation.

The results of this work are presented in detail by Dixon and Turver

(1973 v(iii)) but some of the main features are discussed in the following

sections.

The principal aim of the present study, as has been mentioned

previously, was to aid the design of improvements for the Haverah

Park air shower array. In this context one is searching for:-

(a) ground parameters that do not correlate with the

longitudinal development of EAS so that they may be used as a

measure of the primary energy and

(b) observables which correlate very well with the longitudinal

development of EAS so that they may be used to indicate the presence

of fluctuating protons.

It is also important to establish the degree of correlation

between various ground parameters that are likely to be measured

at Haverah Park. The following sections will present some of the

more relevant results obtained from the programme of work outlined

above.

6-7.2 <u>Correlations between Ground Parameters and the Longitudinal</u>
        <u>Development of EAS.</u>

Table 6-6 presents the values of the correlation coefficient
between various ground parameters and the depth of maximum
development of the electron cascade. The values shown in this
table were calculated from 87 simulations of 10^{18}eV proton
initiated EAS but similar values were obtained from other categories
of showers. The two parameters here that give the lowest values
for their correlation with the depth of maximum of the electron
cascade (h_{tmax}) are the muon density at 300m from the core
($\Delta_\mu(300)$) and the deep water Cerenkov detector response at 520m from
the shower core ($\rho(520)$). This indicates that these parameters
could be used as primary energy indicators. At the Haverah Park
experiment $\rho(500)$ and $\rho(600)$ are already used for this purpose
(Edge et al (1973)). The density of muons at 300m from the air
shower core is unfortunately not great (~ 2 or 3 per m^2 at a primary
energy 10^{18}eV) and therefore any attempt to use this density as an
aid to the estimation of the primary energy would necessitate the
use of very large area detectors.

An interesting point to note is the change in the value of r
between the depth of maximum development of the electron cascade
and the muon density as the distance from the core at which the
density is measured increases. This is shown in Fig. 6-14. The
correlation coefficient goes from a strongly positive value at
small core distances, through zero at ~ 300m and then becomes
strongly negative for greater core distances. The same characteristic
is shown by the deep water Cerenkov detector response, the core
distance at which r becomes zero this time being ~ 500m.

In order to detect the large fluctuations in the longitudinal
development that would be attributable to the presence of primary

104

1 Depth of maximum
2 Electron size (SL)
3 Muon density (>1GeV, 100m)
4 Muon density (>1GeV, 300m)
5 Muon density (>1GeV, 520m)
6 Deep water Cerenkov detector signal (50m)
7 Deep water detector signal (100m)
8 Deep water detector signal (520m)
9 Electron density (49m)
10 Electron density (87m)
11 Electron density (276m)
12 Muon time delay (520m)

	1 h_{tmax}	2 ne_{SL}	3 $\Delta\mu(>1)GeV$ 100m	4 $\Delta\mu(>1)GeV$ 300m	5 $\Delta\mu(>1)GeV$ 520m	6 $\rho(50)$	7 $\rho(100)$	8 $\rho(520)$	9 $\Delta_e(49)$	10 $\Delta_e(87)$	11 $\Delta_e(276)$	12 $t_{\frac{1}{2}}(520)$
1 h_{tmax}	1.00											
2 ne_{SL}	0.944	1.00										
3 $\Delta\mu(>1)GeV$ 100m	.789	.887	1.00									
4 $\Delta\mu(>1)GeV$ 300m	.116	.291	.656	1.00								
5 $\Delta\mu(>1)GeV$ 520m	-.464	-.345	.055	.789	1.00							
6 $\rho(50)$	.917	.989	.923	.399	-.233	1.00						
7 $\rho(100)$	.859	.956	.932	.511	-.096	.987	1.00					
8 $\rho(520)$	-.144	.035	.356	.898	.885	.163	.314	1.00				
9 $\Delta_e(49)$	.953	.994	.885	.253	-.391	.979	.934	-.028	1.00			
10 $\Delta_e(87)$	.936	.996	.912	.341	-.298	.997	.970	.086	.992	1.00		
11 $\Delta_e(276)$	.681	.820	.884	.697	.187	.889	.950	.586	.778	.848	1.00	
12 $t_{\frac{1}{2}}(520)$	.965	.960	.782	.085	-.053	.919	.846	-.220	.975	.947	.643	1.00

TABLE 6-6

Correlation Coefficients between Parameters in 10^{16} eV Proton Initiated EAS.
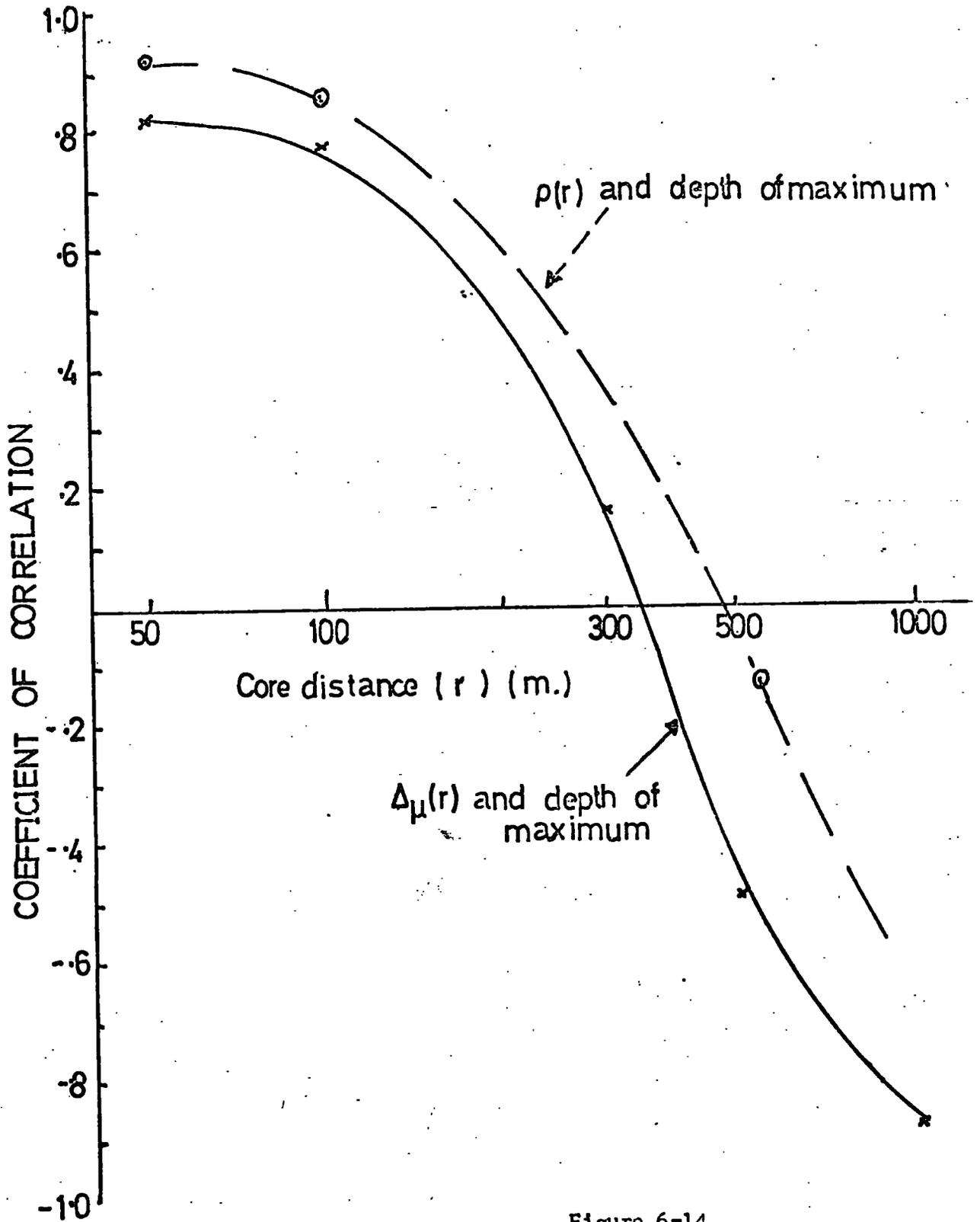
Figure 6-14

The variation in the correlation coefficients with distance from the shower core.

protons it is necessary to find observables that correlate strongly with the depth of maximum development of the electron cascade. The close core electron densities fulfil this requirement as do $\rho(50)$, $\rho(100)$ and, to a lesser extent, the muon density at 100m. Unfortunately the experiment of Blake et al.(1973) is unable to measure charged particle densities at <100m from the core because their equipment becomes saturated with the very high particle fluxes close to the core. The muon density at 100m is large enough to avoid large statistical effects in most showers falling at Haverah Park and presents one possibility for the discovery of fluctuating EAS. The deep water Cerenkov detector responses at 50m and 100m are strong possibilities since they are readily measured quantities. It should be noted that neither the radio emission nor the optical Cerenkov response have been mentioned in this section but they both essentially reflect the depth of maximum development of the electron cascade and could be used in addition to any other suggested measurements.

The predictions for the time delay measurement for muons at 300m and 500m from the core correlate well with the longitudinal development and present yet another possibility for detecting fluctuating proton initiated showers.

6-7.3 <u>Correlations Between Ground Parameters</u>

Table 6-6 also indicates the values of the correlation coefficients between the ground parameters. The close-core electron densities and the muon density at 100m from the core correlation strongly with $\rho(50)$ and $\rho(100)$. Since the majority of the deep water detector signal at 500 and 100m is due directly to the electrons one would expect the observed correlation between electron densities and deep water Cerenkov detector response at close core distances; however, it is less obvious why the correlations between the muon

density at 100m and these parameters should.be so strong. The lack of correlation between $\rho(520)$ and the muon density at 300m and any of these parameter is demonstrated. (It should be noted that the threshold energy for all the muon densities used for correlation studies is 1 GeV).

6-8 Conclusion

It has been demonstrated that, in principle, fluctuation studies of EAS could be used to detect the presence of protons in the primary cosmic radiation, in spite of the fact that the partial fragmentation model (described in Chapter 5) produces larger fluctuations in shower parameters for heavy nucleus initiated EAS than does the 'super-position' model. The Haverah Park ground parameter $\rho(600)$ has been confirmed to be almost independent of the longitudinal development of the shower and therefore a good estimator of primary energy showing fluctuations less than electron size at maximum. The ratio $\rho(50)/\rho(500)$ is predicted to be a particularly good measure of extreme fluctuations in the longitudinal development of showers.

The main cause of fluctuations in proton initiated air showers $(E_p >10^{15}eV)$ is found to be the point of initial interaction in the atmosphere, the fluctuations in observables in heavy-nucleus initiated EAS are shown to arise from the way in which the primary particle breaks up.

C H A P T E R   S E V E N

THE RELEVANCE OF THE PRESENT STUDY TO THE HAVERAH

PARK EAS

7-1 Introduction

The main purpose of this work was to aid the design of improvements

to the Haverah Park EAS array which would increase the sensitivity

of the experiment to the mass composition of high energy cosmic radiation.

The conclusion drawn from the data presented in Chapter 5 was that the

average characteristics of EAS do not offer scope for the determination

of the primary particle mass. This was particularly so since the

partial fragmentation model for the break up of heavy primaries adopted

for the present study (which we consider to be a more realistic treatment

of the break up of heavy primary particles than the 'superposition' model

which has often been used in the past) reduces the difference in the
longitudinal development of air showers initiated by protons and
heavy nuclei, (See 5-5.2).

There appears to be more likelihood of detecting the presence

of protons in the primary cosmic radiation from studies of extreme fluct-

uations in the longitudinal development. This possibility was discussed

in some detail in Chapter 6 and the suggestion of Dr. R.J.O. Reid that the

ratio of $\rho(50)/\rho(500)$ would be a useful measure of these fluctuations was

confirmed. The measurement of the time structure of incidence of air shower

particles on the deep water Cerenkov detectors at Haverah Park has been

refined independently of model simulation data by Watson and Wilson (1974)

and now offers itself as a measurement which yields an indication of

fluctuations of development among showers. The present calculations show that

the time taken for a muon detector to record between 10% and 80% of its total

signal $(t_{\mu 10} - t_{\mu 80})$ is indeed strongly correlated with the longitudinal

development of the air shower and this quantity is closely related to the parameter employed by Watson and Wilson 't$_\frac{1}{2}$', (the time over which the recorded Cereknov detector signal increases from 10% to 50% of its final amplitude).

Our computer simulations have demonstrated the sensitivity of the lateral spread of the Optical Cerenkov signal from EAS to fluctuations in longitudinal development. This measurement has the disadvantage of being available for a small number of EAS (it is estimated that conditions of limited moonlight and periods of clear sky will allow the measurement to be made for 4% of the time at Haverah Park (Smith and Turver (1973)). However, the technique involves only relatively inexpensive and simple equipment and it has already been shown by the exploratory measurements of Smith (1974) that this technique is a valuable addition to existing shower measurements.

7-1.1 The Modifications Planned for the Haverah Park Air Shower Array

The Haverah Park EAS array is shown in Fig. 1-1 as it was when the present study was commenced. Modifications are now in the process of being implémented which will enable comment to be made upon the composition of high energy primary cosmic radiation. One of the main requirements of the improved array is that it measures the detector response $\rho(r)$ at close core distances to a high degree of accuracy so that the ratio $\rho(50)/\rho(500)$ may be determined with confidence. In order to do this, additional water Cerenkov detectors are being installed. A proposed layout of the modified array is shown in Figure 7-1. There are 25 additional water Cerenkov detectors each of area $1m^2$ and the distance between them is 150m. As well as providing an accurate value of $\rho(50)$, this arrangement will also
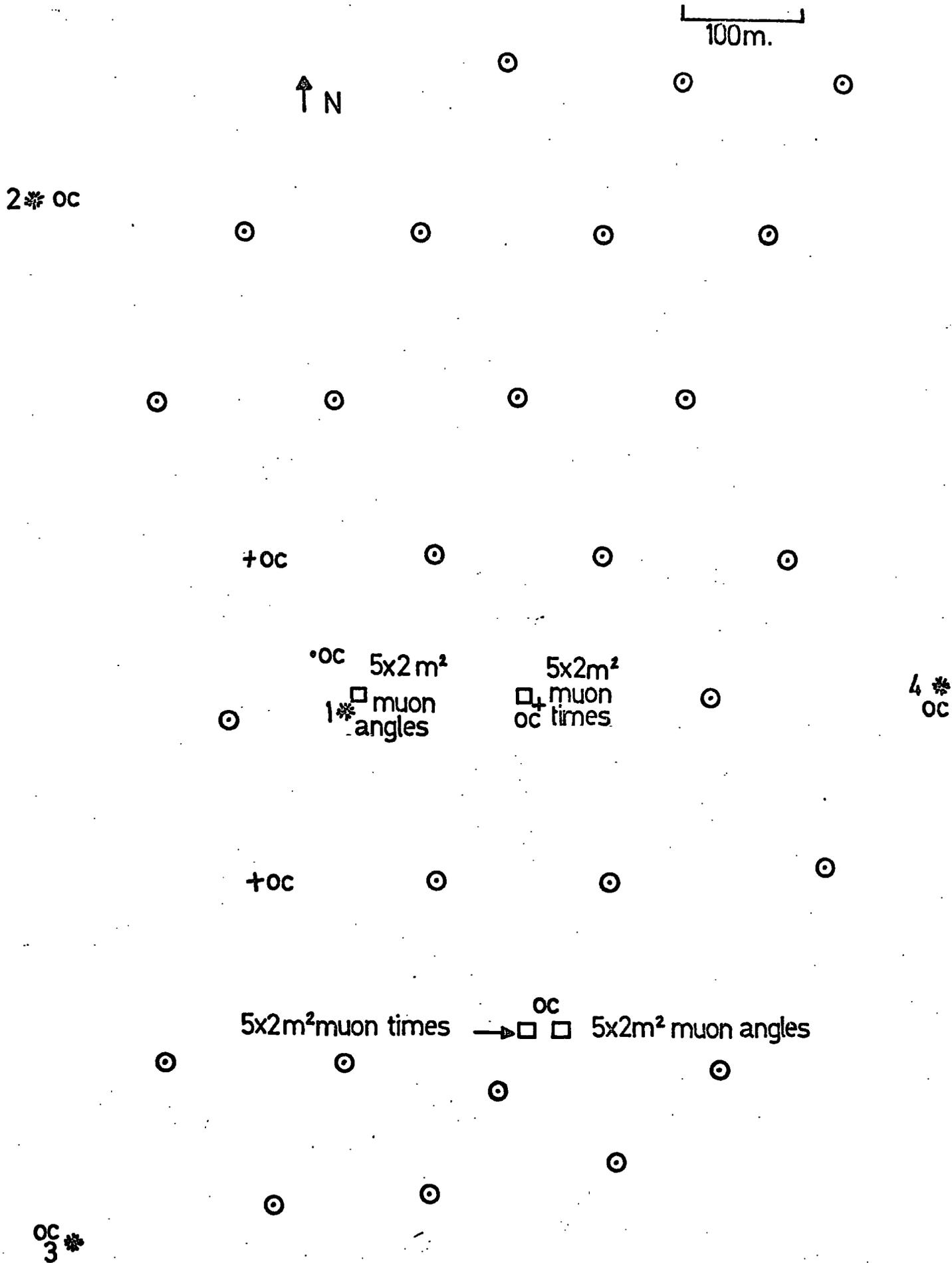
100m.

N

2 ✳ oc

4 ✳ oc

+oc

•oc   5x2 m²
   1✳□ muon
      angles

5x2m²
□₊ muon
oc times

+oc

5x2m²muon times ——▷□ □ 5x2m² muon angles
                    oc

oc
3 ✳

Fig. 7·1

improve the accuracy of the core location, in turn enhancing many other measurements.

In addition to this "infilling" of the array with water Cerenkov detectors, 9 detectors will be installed to observe the optical Cerenkov light flux emitted from air showers and its temporal characteristic. The positions of these detectors are also shown in Fig. 7-1.

The studies of Watson and Wilson of the temporal structure of the deep water Cerenkov response will be continued, work already having started to develop a system of additional records for this particular application; to date they have based their work upon the existing records of the four large ($34m^2$) detectors which from the central unit of the main shower array at a separation of 500m.

Two new muon experiments are planned. The University of Nottingham group have designed an experiment to measure the arrival times of muons in EAS using two $10m^2$ detectors and the University of Durham group are going to measure the angles of muons in EAS also using two $10m^2$ detectors. The situation of these detectors is shown in Fig. 7-1. The measurements of the radio signal from EAS will continue as described by Allan et al. (1973), providing additional information about the longitudinal development of the air showers recorded at Haverah Park.

7-2 **Cluster Analysis of Simulation Data**

7-2.1 **Introduction**

As the experimental facilities at Haverah Park become more refined there becomes available more information concerning each air shower that is recorded by the array. An attempt has been made here to investigate the feasibility of using multidimensional cluster analysis of the experimental data to divide the recorded showers into groups, hopefully characterised by the atomic mass number of the primary particle.

The way in which the study was made will be described briefly.
A set of parameters representative of measurable quantities at Haverah
Park were selected from each simulated shower; the values of these
parameters were noted for a set of simulated air showers initiated
by 10^{17}eV primary particles of varying atomic mass number. A
cluster analysis programme devised by Wishart (1969) was used to explore
the possibility of recovering,with the aid of this limited amount of
data for measurable quantities,the nature of the primary particle
for each shower in the set.

7-2.2 The Cluster Analysis Programme

The cluster analysis programme by Wishart (1969) was used for
the purpose of this investigation in its most simple mode of operation.
The computer programme allowed for the use of a maximum of 20 parameters
to describe the measurable quantities in each EAS. Initially the set
of parameters for each event were assigned to an arbitrary cluster.
The number of final clusters required and the minimum size of a cluster
were input variables. The parameters describing each air shower
were reduced to a set of standard scores by the programme and the
distances in multiparametric space between each event and its cluster
centre was calculated. Tests were made on each event to see if it was
more similar to any other cluster and if it was it was transferred.
New cluster centres were established by taking the 'centre of gravity'
of these clusters and the procedures repeated until stable clusters
were formed. The option of varying the threshold of similarity beyond
which an event could not be accepted into a cluster was available.

7-2.3 Data Used for Cluster Analysis

Shower data obtained from the 'hybrid' computational technique
were used for this study. For each simulated event in the set the

following predicted quantities were noted:

(i)   the deep water Cerenkov detector response at 50m ($\rho(50)$),

(ii)   the deep water Cerenkov detector response at 500m ($\rho(500)$),

(iii) the muon density at 100m from the shower core (Δ_μ (>1 GeV, 100m),

(iv)   the muon density at 300m from the shower core (Δ_μ (>1 GeV, 300m),

(v)   the time for a muon detector signal to increase from 10%
       to 80% of its final value (this is a parameter closely
       related to the value of '$t_{\frac{1}{2}}$' measured experimentally
       by Wilson and Watson).

and (vi)   the ratio of the optical Cerenkov signal recorded at 100m
       to that recorded at 600m from the shower core ($\phi(100)/
       \phi(600)$).

The study was based upon such simulations data from air showers
initiated by primary particles of energy 10^{17}eV/nucleus comprising:-

        20 proton initiated EAS (A = 1); p

        6 α -particle initiated EAS (A=4); α

        6 silicon nucleus initiated EAS (A=28); Si

        6 Iron nucleus initiated EAS (A=56); Fe

7-2.4 Results of the Cluster Analyses

7-2.4.1 Cluster Analysis of Simulation Data with no Allowance for Errors
         of Measurement

Initially the analysis was made for simulation data with no
allowance made for experimental errors. The shower data were normalised
to a fixed value of $\rho(500)$ (since this is the measure of primary energy
to be used experimentally) and each event was randomly assigned
to one of three groups. These groups were taken as the initial
clusters. The other five measurable parameters were

used as input data for the cluster analysis programme. The result

of this analysis is shown in Table 7-1.

TABLE 7-1

Cluster Number	Contents of Cluster
1	$10p + 6\alpha$
2	$9p$
3	$6Si + 6Fe$

(There was one proton shower showing extreme fluctuations which the

programme was unable to assign to any of the clusters). It would

therefore be possible to separate EAS of fixed ground parameters

$\rho(500)$ into groups according to the atomic mass number of the primary

particle, provided no experimental errors featured in the basic data.

7-2.4.2 The Effect of Inclusion of Experimental Errors

The analysis of simulation data described in §7-2.4.1 is clearly

not a realistic test of the feasability of using cluster analysis for

real observational data and therefore likely experimental errors were

assigned to the parameters. The relative standard deviations of the

errors assigned to the parameter initially were:

$\rho(50)$: 8% (typical of error if using a $1m^2$ detector)

$\rho(500)$: 15% (typical of present measurement)

$\Delta_{\mu}(>1 \text{ GeV}, 100m)$:20% (appropriate to a

$\Delta_{\mu}(>1 \text{ GeV}, 300m)$:30% muon detector of $\sim 20m^2$)

$t_{10\%} \rightarrow t_{80\%}$: 6%

$\dfrac{\phi_{(100)}}{\phi_{(600)}}$:15%

The values for parameters in individual showers used in the cluster analysis were sampled from normal distributions with means corresponding to the computed parameter values and the standard deviations quoted above.

The result of repeating the cluster analysis of the data for the 38 simulated EAS with these experimental errors applied to the parameters is shown in Table 7-2

TABLE 7-2

Number of Cluster	Contents of Cluster
1	14p, 3α, 3Si, 3Fe
2	4p, 3α, 3Si, 1Fe
3	1p, 2Fe

Again there was one proton initiated shower which the programme was unable to assign to any of the clusters. An investigation was made into the effect of altering the threshold of similarity value that was specified in the analysis. The range of values allowed for this quantity were 1.0 → 0.1 (the larger the value the less similarity was required in order for events to form a cluster). The value adopted for the previous runs was 0.9. By lowering the value of the threshold of similarity so that more events were excluded from all clusters it was hoped to restore some ordered clustering. However, this resulted in (smaller) mixed clusters and those events excluded from the cluster- the residue - were also mixed. Clearly with these experimental errors applied to the simulation data the cluster analysis programme is unable to sort the EAS into groups according to their primary mass number.

7-2.4.3   The Effect of Improving the Accuracy of Experimental Measurements

Possible improvements in the measurement techniques were next

considered and the error on the parameter $\rho(500)$(which features in

the normalisation of all the data) was lowered to 10%.   This resulted

in a limited amount of ordered clustering as can be seen from the

data of Table 7-3.

TABLE 7-3

Number of Clusters	Contents of Clusters
1	13p, 3α, 6Si, 4Fe
2	4p
3	1p, 2Fe

Residue: 2 protons

Cluster No.2 contains only protons as does the residue and it can

therefore be concluded that if the primary energy can be estimated

to an accuracy of 10% and the other parameters to the indicated

accuracies, cluster analysis may be used to aid the determination

of the primary mass of selected air showers. Lowering the experimental

error on $\rho(500)$ further to 5% and then removing it completely did

not result in any further ordering of the clusters.

The standard deviation on $\rho(500)$ was set at 10% and the result

of removing the errors imposed upon the other parameters (the optimum

case) was investigated.   The result is shown in Table 7-4.

TABLE 7-4

Number of Cluster	Contents of Cluster
1	6p, 4Si, 1Fe, 4α
2	2Si, 5Fe
3	12p, 2α

Residue: 2 protons

The cluster analysis in this case has succeeded in producing one cluster composed of heavy nuclei (cluster number 2) and one of protons and light nuclei (cluster number 3). Cluster number 1, however, remains a mixture of all the primary masses.

A measure of success has therefore been demonstrated, even with the inclusion of some experimental errors, in the use of cluster analysis of measurable parameters to categorize the individual showers in terms of the primary mass.

7-3 Conclusion

The present work indicates that the improvements now being implemented at the Haverah Park Air Shower Array should, on the basis of fluctuation studies, allow comment to be made upon the mass composition of the primary cosmic radiation at high energies ($>10^{17}$eV).

The cluster analysis technique for the classification of EAS by primary mass number outlined in §7-2 warrants further investigation. On the basis of the work done to date it may be concluded that if the primary energy indicator is known to an experimental accuracy of ∿ 10% it may be possible to achieve some success. It should be noted that this may be made possible by using, in addition to $\rho(500)$ the value $\phi(300)$ (the optical Cerenkov response at 300m from the shower core) in order to normalise the data for each air shower. $\phi(300)$ has been shown to be a good indicator of primary energy. Measurements of this quantity in selected showers should soon be available to an accuracy of ∿15% (G.J. Smith, Ph.D Thesis in preparation). Thus a reduction in the experimental uncertainty in the primary energy on the basis of improvements in $\rho(500)$ or the inclusion of the $\phi(300)$ value should be investigated. The errors quoted in §7-2.4.2

for the other measurable parameters are for EAS with primary energy $\sim 10^{17}$eV. These errors may be reduced when measurements of the less frequent higher energy EAS are considered. The possible use of this technique in the analysis of specially selected air showers recorded at Haverah Park may be worthwhile in the near future.

The inclusion in the simulations of the latest trends seen in nucleon-nucleon interactions from accelerator data were discussed in §4-5.7 The conclusions drawn from this investigation are that simulations made using models incorporating Feynman scaling in addition to a shortened interaction mean free path for high energy protons and pions in air and making the assumption of heavy primary particles produce predictions that fit the observed data well. (In fact the fit is better than that of the 'normal' model in the case of the longitudinal development of the electron cascade in small showers). However, the satisfactory representation of the average shower characteristics by the predictions of this model requires that the cosmic ray beam be substantially composed of iron nuclei at energies $\geqslant 10^{17}$eV; it follows that the fluctuations would be small. Thus if on the basis of the search for fluctuations at Haverah Park a large proportion of the primaries are proved to be protons, these predictions would no longer be valid. The predictions for proton initiated showers simulated using this model are not in such good agreement with experimental data. A requirement would then exist for further alterations to the representation of energetic interactions.

A P P E N D I X   O N E

Probability of Interaction of Pions
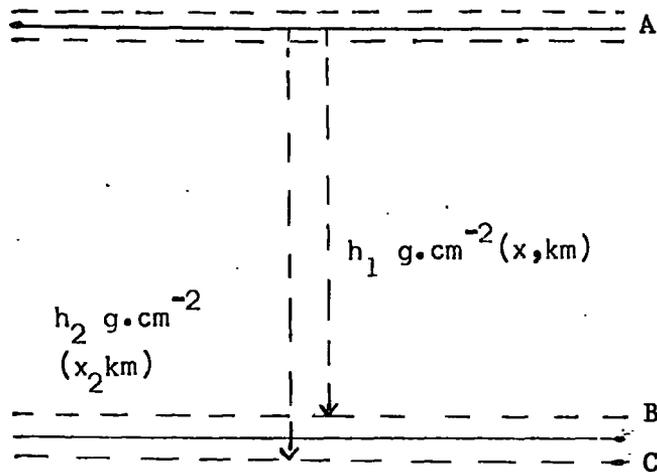
Probability of interaction between B and C

= Prob. of survival to B x (Prob. of interaction in dist. AC

− prob. of interaction in dist. AB)

$$= e^{-m\,h_1/E\tau_\pi\,c}\left[e^{-x_1/\lambda} - e^{-x_2/\lambda}\right]$$

where   m = mass of pion

τ_π = mean life of pion

E = energy of pion

λ = mean free path in air.

APPENDIX TWO

USE OF THE CKP TRANSVERSE MOMENTUM DISTRIBUTION

The transverse momentum distribution suggested by Cocconi et al

(1961) is:-

$$dn\,(p_t)\,dp_t = \frac{p_t}{p_o^2} \cdot e^{-p_t/p_o} \cdot dp_t$$

where $p_o = \dfrac{<p_t>}{2}$
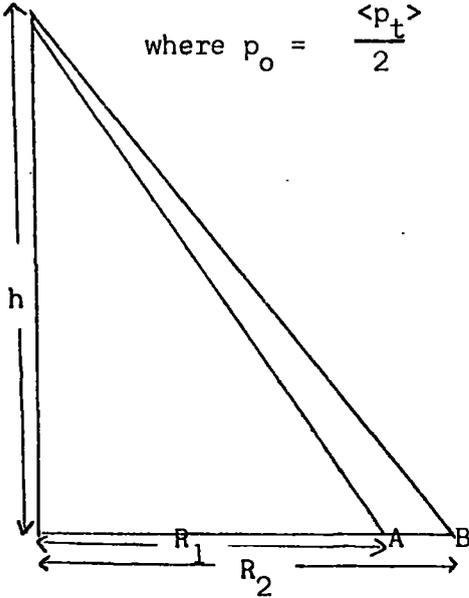
We wish to identify those pions which will be deflected such that they will fall in the annulus between A and B
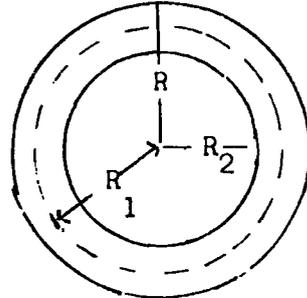
Consider pions produced in an energy bin whose upper bound is E_2 and lower bound E_1:

Since $\dfrac{p_t}{p_\ell} = \dfrac{R}{h}$ and, $p_t = \dfrac{p_\ell R}{h}$

∴ The limits of transverse momentum which will cause a pion to fall in the required annulus are:-

$$p_{t_1} = \frac{R_1\,p_\ell}{h} \quad \text{and} \quad p_{t_2} = \frac{R_2 p_\ell}{h}$$

The number of pions falling at a mean distance R from the core per unit area in the energy range $E_1 \rightarrow E_2$ is then

$$I = \frac{\displaystyle\int_{p_{t_1}}^{p_{t_2}} dn(p_t)\,dp_t}{\pi(R_2^2 - R_1^2)(E_2 - E_1)}$$

$$I = \int_{p_{t_1}}^{p_{t_2}} \frac{p_t}{p_o^2} \, e^{-p_t/p_o} \, dp_t = \int_{\frac{R_1 p_\ell}{hp_o}}^{\frac{R_2 p_\ell}{hp_o}} x \cdot e^{-x} \, dx$$

putting $x = \dfrac{p_t}{p_o}$. $dp_t = p_o \, dx$.

$$I = e^{-R_1 p_\ell/hp_\ell} \left[\frac{R_1 p_\ell}{hp_o} + 1 \right] - e^{-R_2 p_1/hp} \left[\frac{R_1 p_\ell}{hp_o} + 1 \right]$$

Assuming that $p_\ell \approx E$, we may write:-

$$I = \frac{e^{\frac{-R_1 E}{hp_o}} \left[\frac{R_1 E}{hp_o} + 1 \right] - e^{\frac{-R_2 E}{hp_o}} \left[\frac{R_2 E}{hp_o} + 1 \right]}{\pi \times (R_2^2 - R_1^2) \times (E_2 - E_1)}$$

A P P E N D I X   T H R E E

ELECTRON PHOTON CASCADING IN THE ATMOSPHERE

A3-1   The Cascade under Approximation A

The treatment under Approximation A involves the solution to
the diffusion equations for electromagnetic cascading for high energy
particles (energy in excess of the critical energy - 84 MeV for air)
and takes account only of bremsstrahlung and pair production
(the Compton effect and ionization loss by electrons are thus
ignored).

Bremsstrahlung is the emission of photons by charged particles
when their trajectories are deflected in the electric fields of
nuclei. Pair production is the phenomenon of electron positron
pairs materialising from photons as they pass through the electric
fields of nuclei.

In order to compute the development of the electromagnetic
cascade from a photon production spectrum which is specified at
discrete height intervals, one needs to obtain operators associated
with the production of electrons from gamma rays, the production
of gamma rays from electrons and the survival of electrons and
gamma rays. Therefore ge can be defined so that it is an
operator associated with pair production which, when applied to
photons in a given energy bin at a depth t, yields electron
secondary numbers in energy bins at depth t + dt. ee and gg
are the operators associated with electron and photon survival
respectively and eg is the operator associated with pair production

$$g_{u'} = \sum_{j=o}^{j=i-u} eg_j \times e_{u+j} + gg_j \times g_{u+j}$$

$$e_{u'} = \sum_{j=0}^{j=i-u} ee_j \times e_{u+j} + ge_j \times g_{u+j}$$

where g_u' and g_u' are the number of secondary photons and electrons at the depth t+dt, g_u and e_u are the original numbers at the depth t and the subscripts denote the energy bins of the particles; i is the subscript assigned to the maximum energy bin being considered

The operators which must be calculated are

$$gg_0, \; gg_j, \; ee_0, \; ee_j, \; ge_0, \; ge_j, \; eg_0 \text{ and } eg_j \quad (j>0)$$

where, for example, in the case of gg_0 the subscript j = 0 refers to the case where the photon remains in the same energy interval after it has traversed dt radiation lengths. Successive energy bins below that of the parent particle (j = 0) correspond to j values increasing in integer steps.

The calculations of these operators has been described in detail by Marsden (1971). The results are summarised here

ν is the fractional energy of the produced particle

ν_j represents the lower bound bin energies expressed as a
    fraction of the mean energy

$$f = \frac{\nu_{j-1}}{\nu_j} = 10^{0.25} \quad (\tfrac{1}{4} \text{ decade energy bins})$$

$\bar{E}_0 = y E_0$ where $\bar{E}_0$ is the mean bin energy, E_0 is the lower
                 bound and a dE/E^2 differential energy spectrum
                 is assumed for the contents of the bin

y = 1.150806

$$b = \left(\frac{4}{3} + \frac{1}{9 . \ln(183 . Z^{-\frac{1}{3}})} \right)$$

For bremsstrahlung

$$eg_i = ((f^2 - 1) v_j^2 / 2 + b (\ln(f) + (1 - f) v_j)) \, dt \quad j > 0$$

$$eg_0 = (\tfrac{1}{3} (1 - \tfrac{1}{y^3}) + b (\tfrac{1}{2} + \tfrac{1}{y} + \tfrac{1}{2y^2}))$$

For pair production

$$ge_j = 2 ((f - 1)_j + b ((f^3 - 1) \tfrac{v_j^3}{3} - (f^2 - 1) \tfrac{v_j^2}{2}))$$

$$ge_0 = ((1 - \tfrac{1}{y^2}) + b (\tfrac{2}{3y^3} - \tfrac{1}{2y^4} - \tfrac{1}{6})) \, dt$$

Electron survival

$$ee_j = (v_j(f-1) + (f^2-1) \tfrac{v_j^2}{2} + b (-f-1)v_j + \ln \frac{(1 - v_j)}{1-f})_j \, dt$$

$$ee_0 = 1 - (\tfrac{1}{3} + \tfrac{b}{2} + \tfrac{1}{2y^2} - \tfrac{1}{3y^3} - \tfrac{b}{y^2} \ln(1 - \tfrac{1}{y})$$

$$- \tfrac{b}{y} \ln^2 (1 - \tfrac{1}{y}) - \tfrac{b}{3} \ln^3 (1 - \tfrac{1}{y})) \, dt$$

Photon survival

$$gg_0 = 1 - (\tfrac{7}{9} - \frac{1}{54. \ln(183.Z^{-\frac{1}{3}})})$$

and clearly

$$gg_j = 0 \quad \text{if} \quad j > 0.$$

Using these operators the energy spectra of the electrons and photons in each depth interval may be obtained.

Approximation A is only valid for high energy particles and therefore whenever an electron or photon of 50 GeV or below was produced in a depth interval the information was stored in an array which was later used to determine the lateral development of the

shower in combination with the numerical data of Messel and Crawford.

The predictions of Messel and Crawford are only for specific electron and photon input energies (50, 10 and 0.5 GeV) and so it was necessary to divide the contents of the energy bins at each level into 'equivalent' 50, 10 or 0.5 GeV photons or electrons. This was done as shown in Fig. A.1.

Tests were made to check on the sensitivity of the result to changes in the proportions from each energy bin going to 0.5 GeV, 10 GeV and 50 GeV.
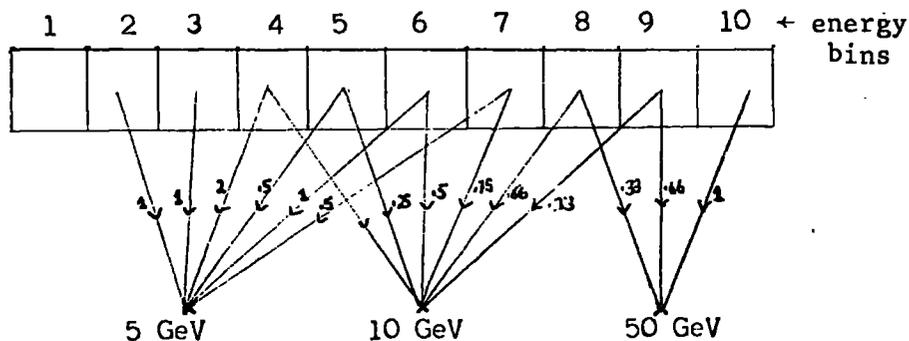
Figure A.1.

A3-2 Approximation B

'Approximation B' is a one dimensional solution of the diffusion equations for electron photon cascading which ignores the Compton effect. The solution of the diffusion equations under Approximation B was given by Snyder (1949) and is represented analytically by Greisen (1956) as:-

$$N(E_\gamma, t, > 0) \doteqdot \frac{0.31}{\left(\log_e \left(\frac{E_\gamma}{E_c}\right) \right)} e^{\left(t\left(1 - \frac{3}{2} \log_e s\right)\right)}$$

where $s = \dfrac{3t}{\left\{t + 2\ \log_e\left(\dfrac{E_\gamma}{E_c}\right)\right\}}$

This gives the number of electrons above zero energy at a depth

t (in radiation lengths) below where a gamma ray of energy

E   was produced.

REFERENCES

The following abbreviations are used for the proceedings of Cosmic Ray conferences:

Proc. Jaipur Conf.   Proceedings of the 8th International Conference on Cosmic Rays, Jaipur, 1963 (Bombay: Commerical Printing Press, 1964).

Proc. London Conf.   Proceedings of the 9th International Conference on Cosmic Rays, London, 1965 (London: Institute of Physics and the Physical Society, 1966).

Proc. Calgary Conf.   Proceedings of the 10th International Conference on Cosmic Rays, Calgary, 1967 (Canadian Journal Phys., 46, No. 10, 1968).

Proc. Budapest Conf.   Proceedings of the 11th International Conference on Cosmic Rays, Budapest, 1969 (Acta Physica Academiae Scientiarum Hungaricae 29, 1970).

Proc. Hobart Conf.   Proceedings of the 12th International Conference on Cosmic Rays, Hobart, 1971.

Proc. Denver Conf.   Proceedings of the 13th International Conference on Cosmic Rays, Denver, 1973.

There are available internal reports Dixon and Turver (1973) volumes i → vii which contain detailed information on work reported in this thesis. These are referred to as (Dixon and Turver v (i)) etc..

R E F E R E N C E S

Abraham, F., Gierdula, J., Levi Setti, R., Rybicki, K., and
Tsao, C.H., 1967, Phys. Rev., 159, 1110.

Adcock, C., de Beer, J.F., Oda, H., Wdowczyk, J., and
Wolfendale, A.W., (1968), J. Phys. A, 1, 82.

Albrow, M.G., Bagdhus, A., Barker, D.P., Bogaerts, A., Bosnjakovic, B.,
Brooks, J.R., Clegg, A.B., Erne, F.C., Gee, C.N.P., Loche, D.H.,
Loebinger, F.K., Murphy, P.G., Rudge, A., Sens, J.C. and Van der
Veen, F. (1973), Nuclear Physics B56, 333.

Allaby, J.V., Diddens, A.N., Dobinson, R.W., Klouning, A., Rochester,
L.S., Schliipmann, K., Wetherell, A.M., Amaldi, U., Biancastelli,
R., Bosio, C., and Matthiae, G., (1972), Proc. of 4th Int. Conf.
on High Energy Collisions, 2, 85.

Allan, H.R. (1971), Proc. Hobart Conf., 3, 1113.

Allan, H.R., Shutie, P.F., Sun, M.P., and Jones, J.K., (1973) Proc.
Denver Conf., 4, 2407.

Anderson, C.D. (1932), Science 76, 238

Antinucci, M., Bertin, A., Capiluppi, P., D'Agostino-Bruno, M.,
Rossi, A.M., and Vannini, G.,(1973), Nuovo Cim. Letters, 6, No. 4, 13.

Armitage, M.L., (1973), Ph.D Thesis, University of Nottingham.

Ashmore, A., Cocconi, G., Diddens, A.N., and Wetherall, A.M., (1960),
Phys. Rev. Lett., 5, 576.

Azimov, S.A., (1964), Bull. Acad. of Sci. U.S.S.R., 28, 11, 1664.

Bakich, A.M., Melley, D., McCusker, C.B.A., Nelson, D., Peak, L.S.,
Rathgerber, M.H., and Winn, M.M. (1967), Proc. Calgary Conf.,530.

Barrett, P.H., Bollinger, L.M., Cocconi, G., Eisenberg, Y., and
Greisen, K., (1952), Rev. Mod. Phys.,24, 133.

Baxter, A.J., (1969), Ph.D. Thesis, University of Leeds

Belenky, S.Z. and Landau, L.D. (1954) Uspekhi Fizichenskitch Nauk,
56, 309.

Benecke, J., Chou, T.T., Yang, L.N., and Yen, E., (1972) Phys.Rev.,188, 2159

Blake, P.R., Francis, A.H., and Nash, W.F., (1973), Proc. Denver Conf.
4, 2748.

Boggild, H., Hansen, K., and Suk, M., (1971), Nuc. Phys. B27, 1.

Boggild, H., Dahl-Jensen, E., Hansen, K.H., Johnstad, J., Lohse, E.,
Suk, M., and Vaje, L., (1971). Nuc. Phys., B27, 285.

Bohm, E., Buscher, W., Fritze, R., Roose, U.J., Samorski, M., Stanbert,
R. and Trumper, J., (1967), Proc. Calgary Conf. 550.

Bradt, H.V. and Rappaport, S.A., (1968), Phys. Rev., 164, 1567.

Brooke, G., Hayman, P.J., Kamiya, Y., and Wolfendale, A.W., (1964), Proc. Phys. Soc., 83, 853.

Capdevielle, J.N., Dupuy, J. and Cerchon, A. (1970), Proc. 6th Interamerican Seminar on Cosmic Rays, La Paz, (University of San Andras), 446.

Castagnoli, C., Picchi, P., and Vern, G., (1969), Nuovo Cimento, 61, 291.

Cleghorn, T.F., Frier, P.S. and Waddington, C.J., (1967), Proc. Calgary Conf. S572.

Cocconi, G., (1958), Phys. Rev. 111, 1699.

Cocconi, G., Koester, L.G., and Perkins, D.H., (1961), (Unpublished Lawrence Radiation Lab. Seminar 28, part 2, UCID-1444).

Cowsik, R., (1966), Proc. London Conf. 2, 656.

Dar, A. and Vary, J.,(1972), Phys. Rev. D. 9, No. 6, 2412.

de Beer, J.F., Holyoak, B., Wdowczyk, J. and Wolfendale, A.W., (1966), Proc. Phys. Soc. 89, S67.

de Beer, J.F., Holyoak, B., Oda, H., Wdowczyk, J., and Wolfendale, A.W., 1968, J. Phys. A, 1, 72.

Dedenko, L.G., (1966), Proc. London Conf. 2, 662.

Diminstein, O.S., Kaganov, L.I., Maximov, S.V., Mikhailov, A.A., Pravdin, M.I., Sokurov, V.F., and Yehmov, (1971), Private Communication.

Dixon, H.E., Earnshaw, J.C., Hook, J.R., Smith, G.J., and Turver, K.E., (1973), Proc. Denver Conf., 4, 2473.

Dixon, H.E., Machin, A.C., Pickersgill, D.R., Smith, G.J. and K.E. Turver, 1973(a), Proc. Denver Conf. 4, 2556.

Dobrotin, N.A., (1967), Proc. Calgary Conf. 4, 416.

Earnshaw, J.C., Machin, A.C., Pickersgill, D.R., and Turver, K.E. (1973) J. Phys. A, 6, 1244.

Edge, D., (1974), Ph.D thesis. University of Leeds.

Elbert, J.W., Erwin, A.R., Mikamo, S., Reeder, D., Chen, Y.Y., Walker, W.D., and Weinberg, A., (1968), Phys. Rev. Letters, 20, 124.

Feinburg, E.L., (1972), Phys. Lett. 5C, No. 5, 237.

Ferguson, H., (1971), Ph.D thesis, University of Nottingham.

Fermi, E., (1950), Prog. Theor. Phys. 5, 570.

Fermi, E., (1951), Phys. Rev., 81, 683.

Feynman., R.P.,(1969), Phys. Rev., Letters, $\underline{23}$, 1415.

Fowler, P.H., (1963), Proc. Jaipur Conf. $\underline{5}$, 182.

Fowler, P.H., and Perkins, D.H.,(1964), Proc. Royal Soc., A278, 401

Friedlander, E.M.,(1969), Proc. Budapest Conf. $\underline{A}$,445

Fukuda, H., Meda, A. and Ogita, N., (1959), Prog. Theor. Phys., $\underline{21}$, 29.

Gaisser, T.K., and Maurer, R.H., (1972), Phys. Lett. B, $\underline{42}$, 444.

Gaisser, T., (1974), Nature, 248, 122.

Giacomelli, G. (1972), Proc. of Amsterdam Int. Conf. on Elementary
    Particles, $\underline{1}$

Giler, M., Karakula, S., Kempa, J., Olejniczak, J., Popova, L., and
    Wdowczyk, J. (1970), Acta Phys. Hung., $\underline{29}$, Suppl. 3, S45.

Gottfried, K. (1973), CERN report (TH.1735-CERN).

Greisen, K. (1956), Prog. In Cosmic Ray Phys. III, Chapt. 1.

Grieder, P.K.F., (1970), Acta Phys. Hung $\underline{29}$, Suppl. 3, 563.

Grieder, P.F.K., (1971), Proc. Hobart Conf. $\underline{3}$, 970.

Grigerov, N.L., Gubin, Yu. V., Rappaport. I.D., Savenko, I.A.,
    Yokovlev, B.M., Akimov, V.V., and Nesterov, V.E., 1971, Proc.
    Hobart Conf. $\underline{5}$, 1746.

Hagedorn, R., (1965), Suppl. Nuovo Cim., $\underline{3}$, 147.

Hazen, W.E., Hodson, A.L., Winterstein, D., and Keller, O., (1973),
    Proc. Denver Conf. $\underline{4}$, 2124.

Hess, V.F., (1912) Phys. Z., $\underline{13}$, 1084.

Hillas, A.M., (1966), Proc. London Conf. $\underline{2}$, 758.

Hillas, A.M., (1970), Acta. Phys. Hung. $\underline{29}$, Suppl. 3, 355.

Hillas, A.M., Marsden, D.J., Hollows, J.D., and Hunter, H.W.,
    1971, Proc. Hobart, Conf., $\underline{3}$, 1001.

Hillas, A.M., (1972), Private Communucation.

Hollows, J., (1968), Ph.D Thesis, University of Leeds.

Hough, J.H., (1971), Private Communication.

Hough, J.H., (1973), J. Phys. A, $\underline{6}$, 892.

Jones, L.W., Bussian, A.E., de Measter, C.D., Loo, B.W., Lyon, Jr., D.E.,
Ramana Murthy, P.V., Ruth, R.F., Learned, J.G., Milly, F.E.,
Reeder, D.D., Ericson, K.N., and Cork, B., (1970), Phys. Rev.
Letters, 25, 2679.

Jones, O.W., Lion, D.E. and Vishwanath, P.P., (1973), University
of Michigan, Pre-print

Kellerman, E.W. and Towers, L., (1970), J. Phys. A, 3, 284-295.

Kolhorster, W., (1914), Ber deutsch. Phys. Ges., 16, 719.

Koshiba, M (1967), Proc. Calgary Conf. A, 525.

Krieger A.S. and Bradt, H.V., (1969), Phys. Rev., 185, 1629.

Khristiansen, G.B., Atrashkevitch, V.B., Kalmykov, N.N. and Fomin,
Yu. A.,(1966), Proc. London Conf. 2 774.

Lal, S., (1967), Nuovo Cim., 48, 466.

Landau, L.D., (1953), Izv. Acad. Nauk USSR, 17, 51.

Lapikens, J., (1974), Ph.D thesis, University of Leeds.

La Pointe, M., Kamaka, K., Gaebler, J., Escobar, I., Domingo, V.,
Suga, K., Shibata, S., (1968), Proc. Calgary Conf. S68.

Lapikens, J., Watson, A.W., Wild, P., and Wilson, J.G., (1973),
Proc. Denver Conf. 4, 2582.

Lindsley, J. (1963), Proc. Jaipur Conf. 4, 77.

Lock, W.O., (1963), Proc. Jaipur Conf. 5, 105.

Lohrmann, E., and Tencher, M.W., (1962), Nuovo Cim., 25, 957.

Machin, A.C., Orford, K.J., Pickersgill, D.R. and Turver, K.E.,(1970),
Proc. Budapest Conf. 3, 579.

Marsden, D., (1971), Ph.D Thesis, University of Leeds.

Malhotra, P.K., Shukla, P.G., Stepens, S.A., Vijayalakshmi, B.,
Boult, J., Bowler, M.G., Clapham, V.M., Fowler, P.H., Hackforth,
H.L., Keereetaveep, J. and Tovey, S.N., (1966), Nature 209, 2567.

Mandolesi, N., Morigi, G., and Palumbo, G.G.C., (1973), Proc. Denver,
Conf., 4, 2414.

Matano, T., Nagano, M., Shibata, K., Suga, K., Tanahashi, G., and
Hasegawa, H.,(1967), Proc. Calgary Conf. S56.

McCusker, C.B.A., (1967), Proc. Calgary Conf., S397.

McCusker, C.B.A., Peak, L.S., Rathgeber, M.H., Proc. Budapest Conf.,
(1969), 3, 527.

Messel, H., and Crawford, D.F., (1969), Electron-photon shower distribution function - Tables for Lead, Copper, tin and air absorbers. Pergamon Press Ltd.,

Morrison, D.R.O. (1973), CERN report (CERN/D.Ph. II/Phys. 73-11).

Murthy, G.T., Sivaprased, K., Srinivasa Rao, M.V., Tanwar, S.C., Vatcha, R.H., and Vishwanath, P.R., 1968, Proc. Calgary Conf., S147.

Nozaki, T., I.N.S., (1970), University of Tokyo Report No. SJC-P-70-3.

Oda, M., (1956), Nuovo Cim., $\underline{5}$, 615-627.

Orford, K.J.O., and Turver, K.E., (1968), Nature, $\underline{219}$, 706.

Pal. Y., and Peters, B., (1964), Kgl. Danske, Videnskab. Selskab, Mat. Fys. Medd., $\underline{33}$, No. 15. 1

Peters, B., (1962). Proc. Conf. High Energy Phys., (CERN), 623.

Pickersgill, D.R., (1973), Ph.D Thesis, University of Durham.

Rao, D and Neeklankantan, (1956), Proc. Ind. Acad. Sci. $\underline{A}$, $\underline{43}$, 181

Reid, R.J.O., (1971), Private Communication.

Rossi, B., (1965), High Energy Particles, Prentice Hall.

Rozental, I.L., (1952), Z.E.T.F., $\underline{23}$, 440.

Ryan, M.J., Balasubramanyan, V.K., and Ormes, J.F., 1971, Proc. Hobart, Conf. $\underline{1}$, 173.

Salzman, F. and Salzman, G., 1960, Phys. Rev., $\underline{120}$, 599.

Samorski, M., Staubert, R., Trumper, J., Bohm, E., Buscher, W. and Fritze, R., (1969), Proc. Budapest Conf. $\underline{3}$, 417.

Samorski, M., Staubert, R., Trumper, J., and Bohm, E., (1971), Proc. Hobart Conf. $\underline{3}$, 959.

Smith, G.J., (1973), Private Communication.

Smith, G.J. and Turver, K.E., (1973), Proc. Denver Conf. $\underline{4}$, 2369.

Smith G.J., (1974), Private Communication.

Snyder, H.S. and Serber, R., (1938), Phys. Rev.54, 317.

Sreekantan, B.V., (1972), Space Science Reviews $\underline{14}$, 103.

Stephenson W. and Turver, K.E., (1973), Private Communication

Susckenko, V.V., and Fomin, Yu. A., (1968), Preprint. University of Moscow.

Tanashashi, G., (1970), Private Communication.

Tennent, R.M., (1967), Proc. Calgary Conf., S1.

Thielheim, K.O., and Beiersdorf, R., (1970), Acta Phys. Acad. Scient. Hungaricae, 29, Suppl. 3, 519.

Tonwar, S.C., Naranan, S., and Sreekantan, B.V., (1971), Nuovo Cim., Letters, 1, 13.

Turver, K.E., (1963), Ph.D thesis, University of Leeds

Turkot, F., (1968) Proc. Topical Conf. on High Energy Collision of Hadrons, CERN 68-7, 316,

Turver, K,E. (1974), to be published

Ueda, A., and Ogita, N., (1957), Prog. Theor. Phys., 18, 209,

Van Hove, L., (1971), Phys. Reports 1C, 349.

Waddington, C.J., and Freier, P.S.,(1972) Private Communication.

Waddington, C.J. and Freier, P.S.,(1973), Proc. Denver Conf. 4, 2449.

Watson, A.A., and Wilson, J.G.,(1974), University of Leeds Preprint.

Wilson, C.T.R. (1901), Proc. Royal Soc. 68, 151.

Wishart, D., (1969) Fortran II Programs for 8 Methods of Cluster Analysis, Kans. Geol. Comp. Contr. No. 38, Kansas.

Yodh, G.B., Pal, Y. and Trefil, J.S., (1972), Phys. Rev. Letters, 28, 1005.

ACKNOWLEDGEMENTS

I would like to express my appreciation to Professor G.D. Rochester F.R.S. and Professor A.W. Wolfendale for the provision of the facilities in their laboratories that made this study possible.

I am greatly indebted to my supervisor Dr. K.E. Turver for his advice and constant encouragement throughout the whole period of this work.

I would like to thank my colleagues, Mr. I.G. Bell, Mr. J.H. Hough, Mr. C.J. Smith and Dr. P.J. Walters for many useful discussions and also members of the Durham Theory group for their help with computing.

Thanks are due to Professor C.J. Waddington for the provision of selected emulsion data for use in this work and also for his helpful discussions.

My thanks are also due to Miss J. Blackburn for her help with the diagrams and Mrs. D. Anson for her patience in typing this manuscript.